SPATIAL SCALING IN HUMAN PERIPHERAL VISION

PIA KRISTIINA MÄKELÄ

Doctor of Philosophy

THE UNIVERSITY OF ASTON IN BIRMINGHAM

March 1994

The University of Aston in Birmingham

Spatial scaling in human peripheral vision

Pia Kristiina Mäkelä
Doctor of Philosophy
1994

Summary

The observation that performance in many visual tasks can be made independent of eccentricity by increasing the size of peripheral stimuli according to the cortical magnification factor has dominated studies of peripheral vision for many years. However, it has become evident that the cortical magnification factor cannot be successfully applied to all tasks. To find out why, several tasks were studied using spatial scaling, a method which requires no pre-determined scaling factors (such as those predicted from cortical magnification) to magnify the stimulus at any eccentricity. Instead, thresholds are measured at the fovea and in the periphery using a series of stimuli, all of which are simply magnified versions of one another. Analysis of the data obtained in this way reveals the value of the parameter E_2, the eccentricity at which foveal stimulus size must double in order to maintain performance equivalent to that at the fovea.

The tasks investigated include hyperacuities (vernier acuity, bisection acuity, spatial interval discrimination, referenced displacement detection, and orientation discrimination), unreferenced instantaneous and gradual movement, flicker sensitivity, and face discrimination. In all cases tasks obeyed the principle of spatial scaling since performance in the periphery could be equated to that at the fovea by appropriate magnification. However, E_2 values found for different spatial tasks varied over a 200-fold range. In spatial tasks (e.g. bisection acuity and spatial interval discrimination) E_2 values were low, reaching about 0.075 deg, whereas in movement tasks the values could be as high as 16 deg.

Using a method of spatial scaling it has been possible to equate foveal and peripheral performance in many diverse visual tasks. The rate at which peripheral stimulus size had to be increased as a function of eccentricity was dependent upon the stimulus conditions and the task itself. Possible reasons for these findings are discussed.

Keywords: magnification, eccentricity, hyperacuity, movement, flicker.

This thesis is dedicated to my family.

Acknowledgements

This work was carried out in the Department of Vision Sciences, University of Aston during October 1990 - March 1994.

I wish to express my sincere gratitude to my supervisor, *Dr David Whitaker*, who was always available for support and discussion, and who was strongly dedicated to the successful completion of this project.

I am grateful also to *Dr Jyrki Rovamo*, who originally created the opportunity to carry out this research and was of great source of enthusiasm and optimism throughout.

My warm thanks go further to *Dr Risto Näsänen* for writing the software used in the flicker detecion and face discrimination experiments, and *Heljä Kukkonen, Keziah Latham, Olavi Luntinen, Kaisa Tiippana* and *Seija Uusinarkaus*, who kindly participated in the experiments.

The work was financially supported by the Ministry of Education, Association of Finnish Ophthalmic Opticians, the National Agency of Health and Welfare in Finland and the Trades Union of Finnish Ophthalmic Opticians. The support is highly appreciated.

Chapters and sections

List of Tables

List of Figures

Chapter 1: Introduction

The heading of this thesis "Spatial scaling in human peripheral vision" may give the impression that only the peripheral visual field has been investigated. However, all the measurements have always included the foveal region as a very important part. By definition, *fovea centralis* extends up to 0.65 deg eccentricity of the visual field measured from the very centre of the fovea. The rod free, avascular *foveola* reaches up to 2.5 deg and the yellow spot", *macula lutea*, up to 5 - 8 deg eccentricity. The visual periphery, strictly speaking, is defined as the region outside of fovea *or* macula (Millodot, 1990). However, in psychophysical studies the expression "peripheral" is often used when referring even to very small eccentricities.

When measuring visual capabilities, previous studies have usually concentrated on central vision, although normal functioning of the peripheral visual field is extremely important in everyday life. The first perimetric examinations were performed by von Graefe (1856) on patients suffering from eye diseases. From those days psychophysical techniques of measuring visual performance both at the fovea and in the periphery have developed and become increasingly defined. It has even become possible to determine the cortical sites of activity caused by a visual stimulus without any physical intervention. One non-intervening technique, mentioned in *Chapter 3*, is positron emission tomography (PET), which has permitted direct observations of visuotopic mapping. i.e. the spatial projection of the visual field onto the visual cortex (e.g. Fox, Miezin, Allman, Van Essen & Raichle, 1987).

The work of Talbot and Marshall (1941) and later Daniel and Whitteridge (1961) provided evidence supporting Polyak's (1932) original proposal that there would be a point-to-point mapping of the visual world onto the visual cortex, and the neural activity there was spatially approximately isomorphic with the image falling onto the retina. It has long been known that, in humans the visuotopic mapping from the retina onto the visual cortex is non-linear (e.g. Brindley & Levin, 1968; Rolls & Cowey, 1970; Drasdo, 1977). In relative terms, a far greater area is devoted to central vision than to the periphery, which reflects a greater functional importance of central vision under most visual conditions.

Now that more evidence has been gathered on visuotopic projections it has become clear that they are only a primary stage and a part of an extremely complex process of representation. Instead of point-to-point projection the visual information seems to be transferring as a patch-to-module projection. Each retinal patch contains receptive fields selective for orientation, movement, and size and this is represented in a three dimensional module of cortical tissue. Each module in turn contains neurons which are selectively sensitive to different stimulus attributes, and together they form a multidimensional representation of the information falling

onto the retinal patch. The findings of Hubel and Wiesel (e.g. 1974) and later others have suggested that the difference between the modules is that of scale i.e. the modules subserving the peripheral location contain cells having larger receptive fields than the cells in the foveally-connected modules, thus corresponding to a larger retinal area.

The above findings led to a series of psychophysical experiments in various tasks to test whether performance could be "scaled", or made equally good as foveal performance, by increasing stimulus size appropriately (e.g. Koenderink, Bouman, Bueno de Mesquita & Slappendel, 1978c; Rovamo, Virsu & Näsänen, 1978 etc., see *Chapter 3*). Previous scaling studies have based their scaling procedure on contemporary anatomical data or have simply used scaling factors that were found to be successful in other studies. By now it has become clear, however, that even in simple tasks the rate at which performance declines with eccentricity cannot necessarily be predicted on the basis of anatomical data. Therefore, in all experimental chapters the present study utilizes a method whereby scaling factors are based on the acquired psychophysical data.

In this thesis the eccentricity-related decline in performance will be determined for several types of acuities, from simple position and movement acuities to flicker detection and finally to face discrimination, which can be considered a relatively complex task. The scaling factor is an eccentricity-dependent value according to which the stimulus size has to be magnified in order to make peripheral and foveal performance similar in a task. Scaling factors, based on the eccentricity-related decline in performance, will be presented for each task. Determining the scaling factors with a common method enables comparison between the factors and reveals any similarities between tasks. Finding tasks that possess scaling factors of equal magnitude makes it possible to group the tasks together and maybe to find some common properties which make their processing similar. Quantifying the rate at which performance in various tasks falls with eccentricity provides useful information before embarking upon physiological explanations for differences in threshold gradients.

Chapter 2: Thresholds of vision

Findings about the limits of our visual capacities have provided a great amount of information about the structure (anatomy) and function (physiology) of the human visual system. There are countless ways to measure visual performance and several ways to define visual thresholds. In this chapter several of the most common types of visual thresholds are introduced along with the units used in that context. The concept of a threshold is defined more accurately in the General methods (*Chapter 4*). Sensitivity is, if not otherwise stated, simply the reciprocal of the threshold and both concepts are used interchangeably in this thesis.

2.1: Detection

The detection threshold (minimum visible) is a brightness threshold, and is defined as the minimum perceptible luminance difference between an object and its background. Many variables (e.g. presentation time, location in the visual field, and shape of border) influence detection thresholds. Detection is often expressed in terms of light energy, but in the context of spatial vision, another approach is possible. To simplify the situation let us consider detection of a single thin dark line against a relatively bright background. The thickness of a line is varied and the resulting retinal illuminance profiles are studied (*Figure 2.01*). The dashed line Th indicates the threshold level at which the dip in illuminance is detectable. The retinal illuminance difference between the background and the retinal image of the line (formed according to the eye's line spread function) thus determines whether the line is visible. A very thin line (a) reduces the local illuminance too little for the difference to be detected. A thicker line (b) reduces the illuminance to the threshold value and is just detectable. The thickest line (c) is clearly suprathreshold. Hecht and Mintz (1939) found that detection of the thin line is possible when the light intensity distribution in the diffracted retinal image has a dip in it's value of less than 1%. Detection thresholds are not strongly reduced by image degradation and best achieved thresholds, when measured in spatial terms, are about 0.5 sec.arc (Hecht & Mintz, 1939).

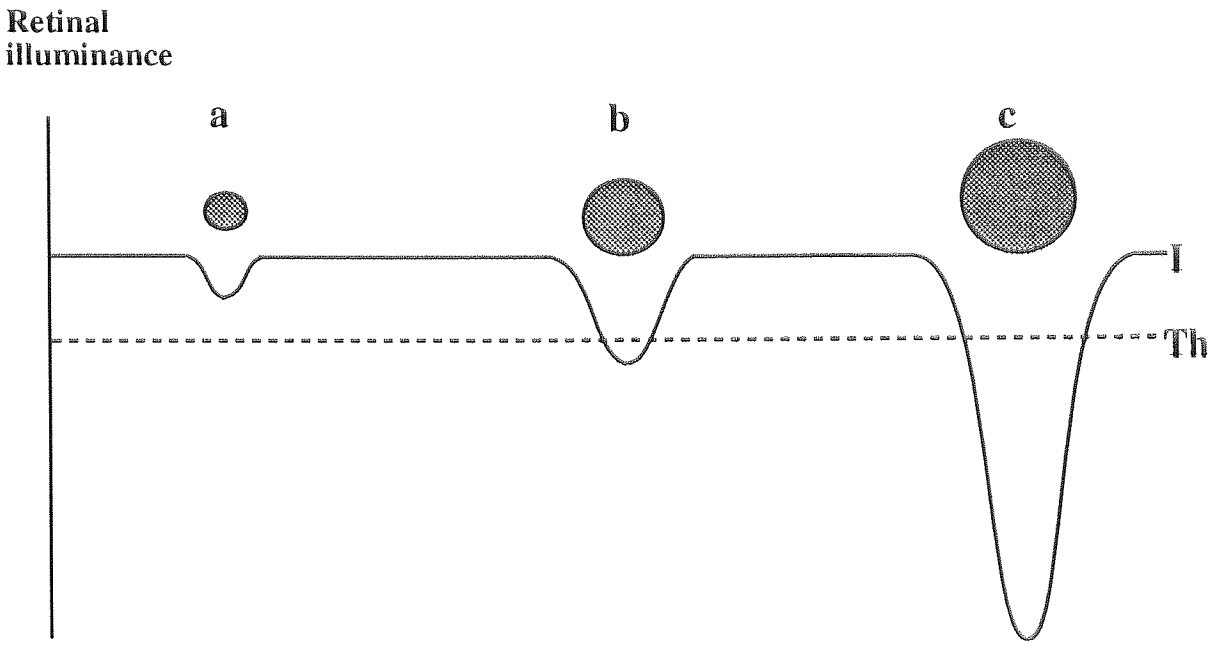

Figure 2.01: Retinal illuminance profiles of three wires of varying thickness, a-c. The dashed lines Th indicates the threshold value at which the line is detected. A very thin line (a) reduces the local illuminance too little for the difference to be detected. A thicker line (b) reduces the illuminance at the higher background intensity to the threshold value and is just detectable. The thickest line (c) is clearly suprathreshold.

The candela (cd) is the unit describing luminous intensity (I) of a point source. The units used to describe the luminance (L) of an extended source are cd m^{-2} . The size of the pupil is a determinant of the amount of light reaching the retina and this is taken into account by expressing retinal illuminance in trolands (Td). The troland is defined as the retinal stimulation provided by a source of 1 cd m^{-2} viewed through a pupil of 1 mm^2

$$Td = L\,(cd\,m^{-2}) \times A\,(mm^2) \qquad (2.01).$$

Spectral sensitivity describes the the relative detectability of lights of different wavelengths. Since the cone and rod spectral sensitivity functions are different (the most effective wavelength for a light-adapted and dark-adapted eye is 555 nm and 510 nm, respectively), two expressions exist for trolands, a photopic and a scotopic troland. The relationship between luminance, retinal illuminance and the corresponding visual function are shown in *Table 2.01.*

Table 2.01: Operating range of the visual system (after Hood & Finkelstein, 1986)

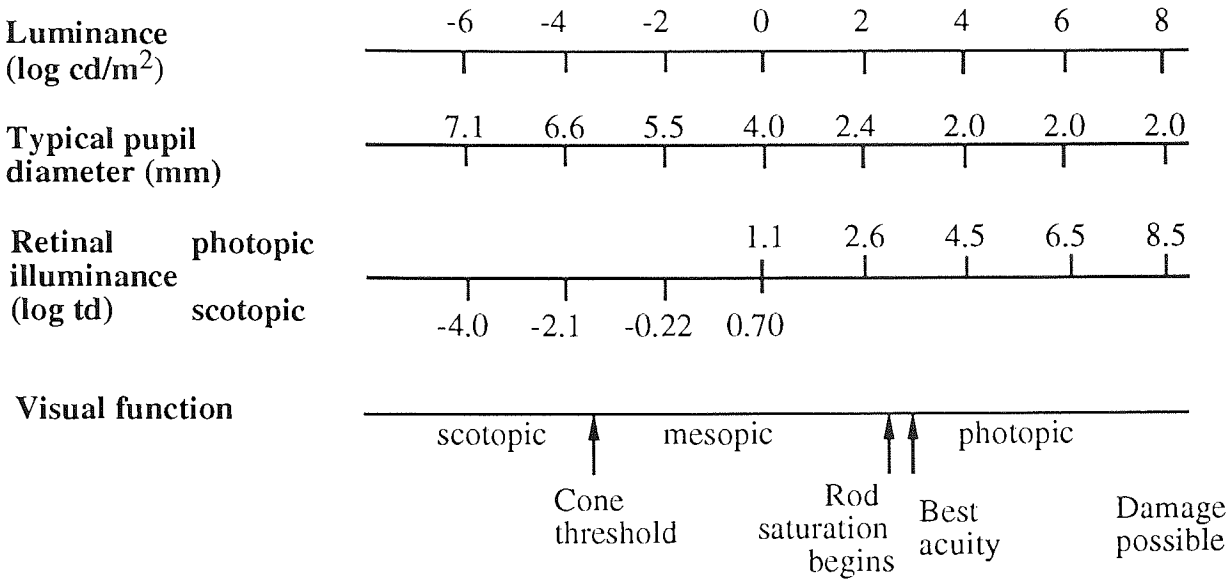

2.2: Spatial thresholds

Contrast sensitivity is a fundamental measure of our visual capability. Our ability to see is mainly based on detecting luminance differences between objects and their background. Contrast sensitivity depends, among other factors, on the spatial frequency content and eccentricity of the stimulus. This dependence is shown for a constant size grating in *Figure 2.02*.

Figure 2.02: Contrast sensitivity as a function of spatial frequency and retinal eccentricity. The target was a constant size sinusoidal grating (see *Chapter 3*, text for *Figure 3.14*). The eccentricities were as shown. From Rovamo, Virsu and Näsänen (1978).

Contrast sensitivity at the fovea usually peaks at a spatial frequency of around 5 cpd under photopic conditions. For a constant size stimulus, the maximal sensitivity, optimum frequency and highest resolvable spatial frequency all decrease towards periphery. Contrast sensitivity increases with increasing retinal illuminance up to a certain level beyond which there is no further improvement in sensitivity. This 'critical' retinal illuminance increases as a function of spatial frequency (e.g. Koenderink, Bouman, Bueno de Mesquita & Slappendel, 1978d).

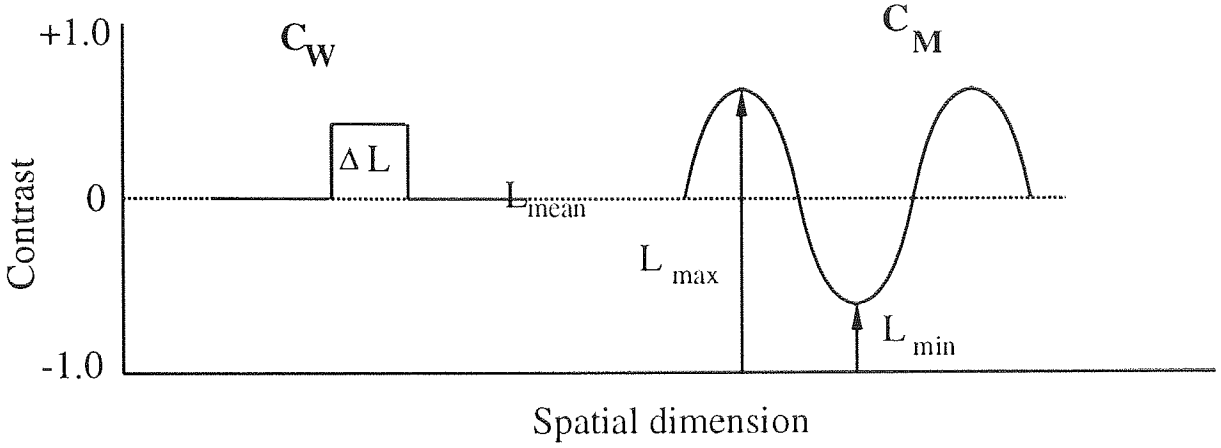

Figure 2.03: Luminance profiles for the Weber and Michelson contrasts defined in the text.

Contrast is a dimensionless, relative measure ranging from 0 to 1, as is seen from the definitions below. Contrast can be defined as a *Weber contrast* (C_W)

$$C_W = \Delta L / L_{mean} \qquad (2.02),$$

or as a *Michelson contrast* (C_M).

$$C_M = (L_{max} - L_{min}) / (L_{max} + L_{min}) \qquad (2.03),$$

where Lmax and Lmin are the maximum and minimum luminances of the region of interest (see *Figure 2.03)* . Weber contrast is preferred when expressing contrast of targets relative to a steady background. Michelson contrast is used for simple periodic patterns (e.g. gratings).

Root-mean-square contrast, r.m.s. contrast, is a definition used for complex patterns where luminance is unevenly distributed within the pattern. r.m.s. contrast is the standard deviation of the luminance distribution calculated (pixel by pixel) across the target area and divided by the average luminance.

$$c_{r.m.s.} = \left[{}^{1}/_{nm} \sum_{x=0}^{n-1} \sum_{y=0}^{m-1} c^2 (x, y) \right]^{0.5} \qquad (2.04),$$

where n and m are the number of the pixels in horizontal and vertical direction, and x and y are the coordinates of the pixels.

Resolution

Resolution is the ability to recognize two or more points in space as being separate (see *Figure 2.08*). Resolution is limited both by the optics of the eye and the spatial dimensions of the retinal cone array (see further *Chapter 3*), as well as several other factors (the optotypes used in testing, the luminance of the target and the background, the pupillary diameter, the target contrast, the adjacent contours around the target, etc.). A review on visual acuity studies has been written by Millodot (1966) in context with a study concerning foveal and extra-foveal visual acuity. Image degradation has a strong effect on the minimum angle of resolution (MAR), i.e. visual acuity, which for normal observers is about 30 sec.arc at best. The limit of resolution (which is reached at maximum contrast) can be seen in the high spatial frequency limit of the contrast sensitivity functions in *Figure 2.02*.

Resolution declines rapidly with increasing eccentricity from the point of fixation, as is shown in *Figure 2.04* from Wertheim (1891). The rate at which visual acuity declines with eccentricity varies as a function of meridian (*Figure 2.04*). This decline is faster along the vertical than the horizontal meridian.

Figure 2.04: A polar graph by Wertheim (1891) showing the distribution of visual acuity throughout the visual field. The stimulus was a grid of thin, black lines. The black dot represents the blind spot.

2.3: Spatiotemporal contrast sensitivity

Contrast sensitivity can also be measured for spatial stimuli which are modulated in contrast as a function of time. Modulation sensitivity, i.e. flicker sensitivity, is the reciprocal of the contrast needed for detection and can be considered as a parallel measure to spatial contrast sensitivity, since the lowest detectable contrast for a flickering stimulus is measured. The rate of temporal modulation is known as temporal frequency and has units of hertz (Hz), the inverse of the duration of one complete temporal cycle in seconds. Flicker sensitivity can either be measured for gratings or, as in the present thesis, for sharp-edged spots. Temporal contrast sensitivity is lowpass with respect to spatial frequency, as opposed to the bandpass shape of the static contrast sensitivity function (*Figure 2.02*). Temporal visual resolution is most often described by critical flicker frequency, CFF, the highest temporal frequency at which a maximally modulated stimulus can still be seen as flickering.

Flicker can be produced with different waveforms and the analogy with spatial luminance distributions can be seen by comparing *Figures 2.03* and *2.05*. *Figure 2.05* presents two waveforms, square and sinusoidal, as an example.

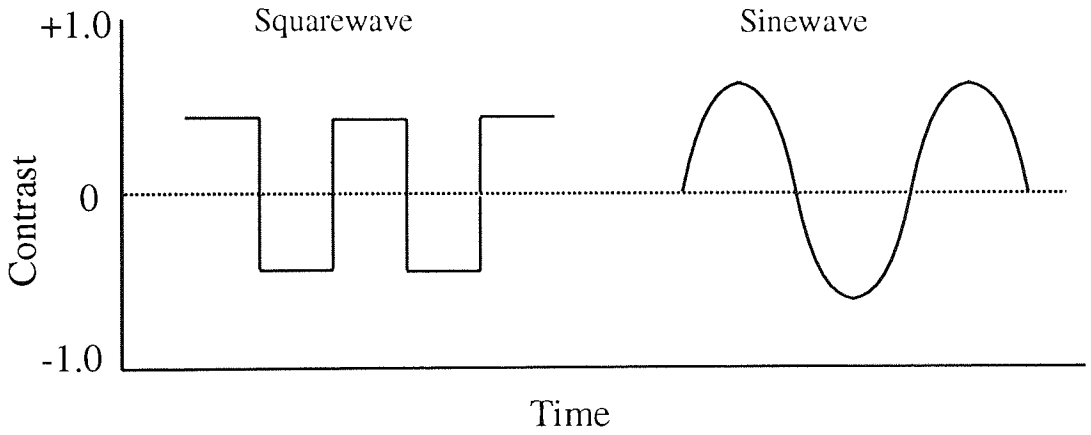

Figure 2.05: Luminance profiles for a squarewave and a sinusoidal temporal modulation.

Flicker sensitivity depends, among other factors, on the size and eccentricity of the stimulus. Flicker sensitivity for a small, constant size stimulus decreases with increasing eccentricity. At the fovea the visual system is most sensitive to low temporal and medium spatial frequency flicker, whereas in peripheral vision medium temporal and low spatial frequencies are the easiest to detect (Koenderink *et al.*, 1978a,b; Raninen & Rovamo, 1987).

Figure 2.06 shows the effect of background intensity on foveal flicker sensitivity for a 2° spot (De Lange, 1958). Peak sensitivity is achieved in bright light at about 8 Hz. At low temporal frequencies sensitivity is nearly independent of illuminance whereas sensitivity at

high temporal frequencies depends strongly on illuminance. Kelly (1961) has confirmed the results.

Figure 2.06: The dependence of flicker sensitivity function on illuminance, 2° spot (De Lange, 1958).

The criterion for detection can affect thresholds at low temporal frequencies (De Lange, 1958). Kulikowski and Tolhurst (1973) measured separately "flicker" and "pattern" thresholds for a 12 cpd grating whose contrast was modulated sinusoidally in time. At low (below 5 Hz) temporal frequencies flicker sensitivity declined but pattern sensitivity did not. Above 5 Hz pattern sensitivity became and remained inferior to flicker sensitivity. Similar results had already been presented by Tulunay-Keesey (1972). Both authors suggested a separate mechanism for flicker and pattern detection, namely *sustained* and *transient* mechanisms. This suggestion was further supported by Burbeck (1981) on the basis of the results obtained with similar stimuli.

In natural imagery temporal variations arise primarily through motion caused by the movement of the observer, the eyes, or the object.

2.4: Localization / hyperacuity

There is an important difference between resolution and localization. Consider *Figure 2.07.* If the two lines in this figure are to be *resolved* (perceived as separate) then the retinal image pattern must consist of two peaks separated by a trough, which differs in retinal illuminance from the peaks enough to exceed threshold at the eye's current adaptation level. The threshold is dependent upon the quality of the optical system as well as the luminance and separation of the objects. Further, the differential stimulation must fall within different

receptors, which sets a fundamental lower limit on resolution performance. On the other hand, *localization* is performed by weighting the responses of the receptors underlying the retinal image distribution and, because of this, it can be performed to a greater accuracy than the inter-receptor separation.

Figure 2.07: Difference between resolution and localization. If the two bright lines are to be *resolved*, conceived as separate, the retinal image pattern must consist of two peaks separated by a trough, which differs in retinal illuminance from the peaks enough to be detected. Further, the differential stimulation must fall within different receptors. Accurate *localization* is achieved by weighting the responses of the receptors underlying the retinal image distribution an can thus be considerably more accurate.

From *Figure 2.07* it can be seen that a certain amount of blurring, which spreads the image over several receptors, is necessary for hyperacuity level performance. Eye optics conveniently have a low pass filter character, the highest frequency passed by the optics is about 60 cpd (Campbell & Gubisch, 1966) This limit is also shown in *Figure 3.01.* Improving the optics of the eye would theoretically degrade positional acuities. This degradation is yet to be tested, but the aliasing phenomenon has been shown with interferometric fringes that bypass the ocular optics (e.g. Coletta, Williams & Tiana, 1990).

In *Figure 2.08* resolution and localization are illustrated in a frontal plane view. The horizontal separation between the dots in the top row decreases on moving from left to right, and resolution soon becomes impossible. The dots in the bottom row have the same horizontal separation, but their relative offset can be detected long after resolution has failed.

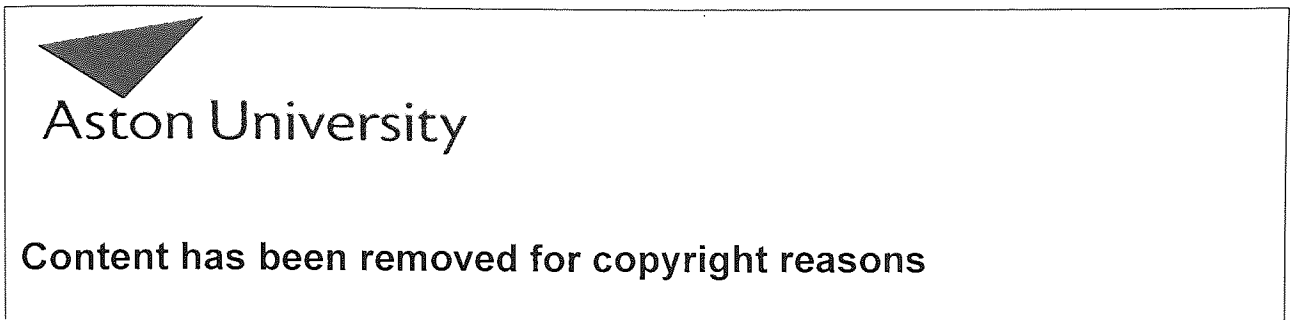

Figure 2.08: When comparing resolution (top row) and localization (bottom row) it becomes clear that localization is still possible when resolution has long failed. This occurs since for resolution the two lights must be seen as separate, whereas for localization only the relative horizontal offset of the upper and lower light needs to be determined.

Relative localization indicates the ability to determine the position of an object relative to a given reference in the visual field. Thresholds under optimal conditions may be between 4 - 10 sec.arc, which is far less than resolution limit. Due to the exceptional sensitivity of the visual system to certain thresholds, they have been coined as *hyperacuities* (Westheimer, 1975). Hyperacuity thresholds under optimal conditions may be about an order of a magnitude smaller than resolution limit set by the optical quality of the eye and receptor diameter at the retina.

Westheimer (1975) originally based his definition of hyperacuities on the magnitude of the threshold so that any task producing such threshold levels would be considered as a hyperacuity. However, the situation is not quite this simple. For example, in a vernier acuity task a subject has to detect the presence (and sometimes also the direction) of the offset of two vertical lines which are slightly offset in a direction normal to their length. Vernier acuity at the fovea measured with two abutting lines would obviously be a hyperacuity task. However, when the lines are separated by a large enough gap, or the task is performed in the peripheral visual field, thresholds can fall well over 30 sec.arc. Should the task still be

considered as a hyperacuity in this configuration? In this thesis *hyperacuity* is defined as any judgment of relative spatial position that in optimum conditions is substantially better than the resolution limit. This enables extending the term to spatial judgments made throughout the visual field.

The factor linking the numerous spatial configurations which can produce thresholds in the hyperacuity range is the need to localize two or more objects relative to each other. In the following sections different configurations for hyperacuities as well as the factors affecting thresholds are presented briefly. The effects of eccentricity on thresholds are presented in more detail in the chapters describing the experiments.

2.4.1: Vernier acuity

Vernier acuity is perhaps the most frequently cited of the all hyperacuities. In its traditional form it involves aligning two abutting vertical lines. The vernier threshold is the smallest horizontal offset which can be detected and its value is frequently found to be as little as 5 sec.arc (e.g. Westheimer & Hauske, 1975; Westheimer & McKee, 1977b), about one-sixth of the diameter of the smallest foveal cones. The lowest threshold, 2 sec.arc, has been reported by Berry (1948). In addition to lines, the vernier stimulus can also consist of separated dots (e.g. Sullivan, Oatley & Sutherland, 1972; Westheimer & McKee, 1977b), blurred bars, (Stigmar, 1971), blurred edges (Watt & Morgan, 1983), a line and chevron (Westheimer & McKee, 1977b), gaps in two parallel lines (Westheimer & McKee, 1977b), clusters of random dots (Ward, Casco & Watt 1985; Whitaker & Walker, 1988), and sinusoidal gratings (Bradley & Skottun, 1987; Whitaker & MacVeigh, 1991; Waugh & Levi, 1993). Some configurations for vernier acuity are shown in *Figure 2.09.*

Vernier acuity can also be measured without changing the position of the stimulus edges. Westheimer and McKee (1977a) formed each of the two line elements by presenting several thin light bars adjacently forming a 'ribbon' of light. Within the ribbon boundaries one of the bars was brighter than the others creating the luminance asymmetry between the top and bottom elements. Thresholds were around 5 sec.arc. Morgan and Aiba (1985) created each of the vertical vernier line components using two thin, adjacent, unresolvable bars. The apparent position of the line components was again changed by only changing the luminance asymmetry within the top and bottom components. The threshold centroid offset, about 5 sec.arc, was calculated on the basis of the threshold luminance asymmetry. In these cases vernier offset was determined solely on the basis of the 'centre of gravity' of the light distribution.

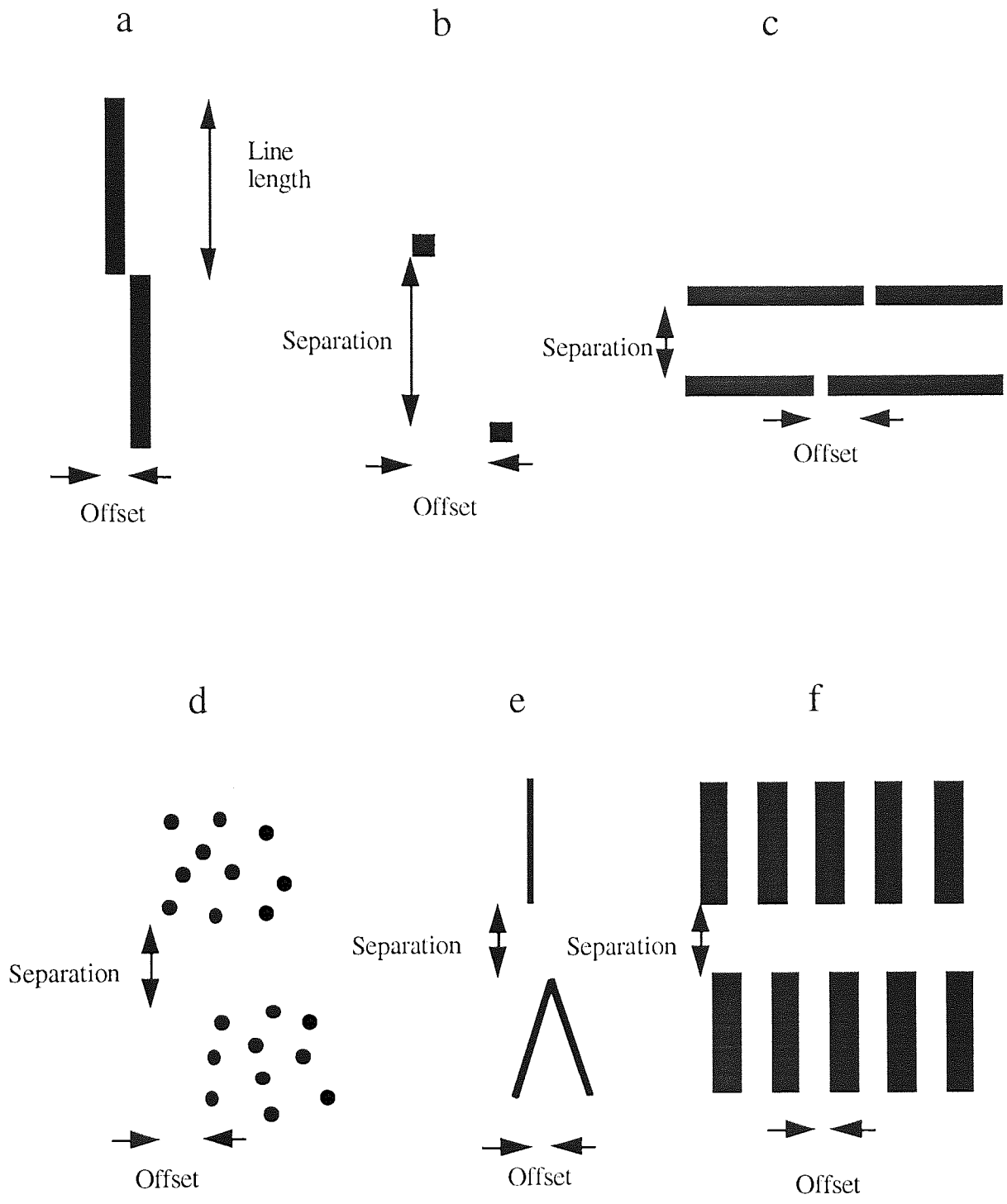

Figure 2.09: Configurations for vernier acuity: a) line stimulus; b) two-dot stimulus; c) two parallel lines with gaps; d) dot-clusters; e) a chevron; f) a grating (squarewave). The offset to be detected is marked for each configuration. The a) and b) stimulus configurations were used in the experiments in this thesis.

The spatial dimensions of the stimulus are critical. Increasing the length of the lines generally improves vernier acuity up to a certain value. Sullivan *et al.* (1972) found the optimum line length for vernier acuity at the fovea to be around 3 min.arc for abutting lines. Increasing the line length beyond this value does not improve thresholds, as is seen in *Figure 2.10* (Sullivan *et al.*, 1972; Andrews, Butcher & Buckley, 1973; Westheimer & McKee, 1977b). This has been often used to support Hering's (1899) view of averaging local signs along the vernier line elements. However, equally low thresholds can be achieved by substituting the lines with a pair of features marking their end points (Ludvigh, 1953; Sullivan *et al.*, 1972; Westheimer & McKee, 1977b). Curiously, at below about 5 min.arc dot separations thresholds actually increase if the gap has been 'filled' and the task has became a line orientation discrimination task (Westheimer, 1982).

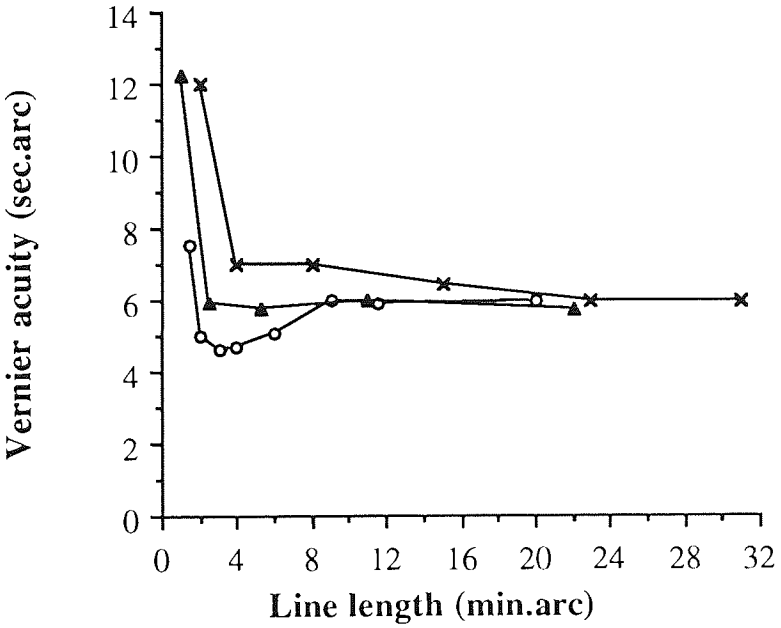

Figure 2.10: The effect of line length (plotted as the length of *one* line, not the overall length of the stimulus) on vernier acuity for abutting lines from three studies. Circles - Andrew, Butcher and Buckley (1973), horizontal lines, average of two observers. Triangles - Sullivan, Oatley and Sutherland (1972), vertical lines, 1.5 min arc gap filled in with a horizontal bar, average of two observers. Crosses - Westheimer and McKee (1977b), vertical lines, observer SM.

If a gap of 1.5 min.arc is introduced between the inner ends of the lines Sullivan *et al.* (1972) found no effect on thresholds at all for line lengths between 1.5 - 22 min.arc. Westheimer and McKee (1977b) studied the effect of line separation at three different line lengths (*Figure 2.11)* and found that increasing separations above 4 min.arc reduced accuracy considerably.

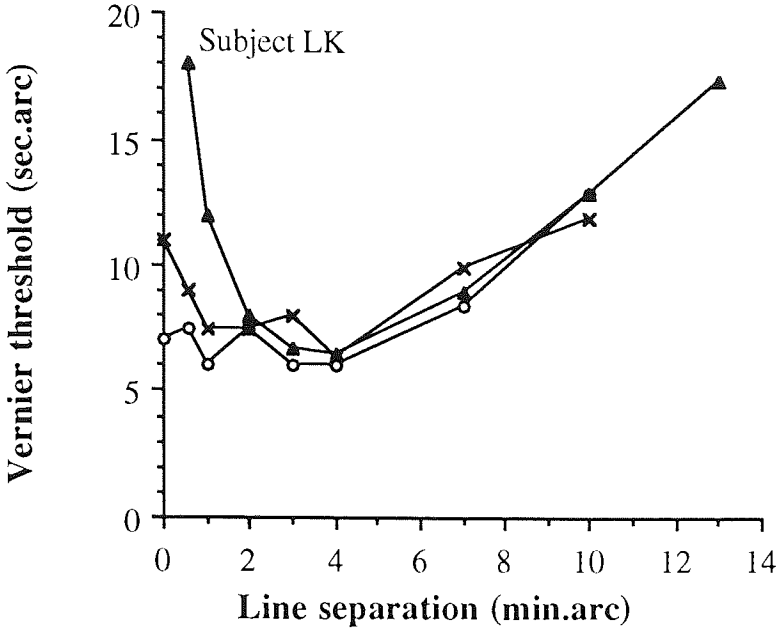

Figure 2.11: The effect of feature separation on line vernier acuity for line lengths of 0.5 min.arc (triangles), 2 min.arc (crosses), and 4 min.arc (circles). Redrawn from Westheimer and McKee (1977b).

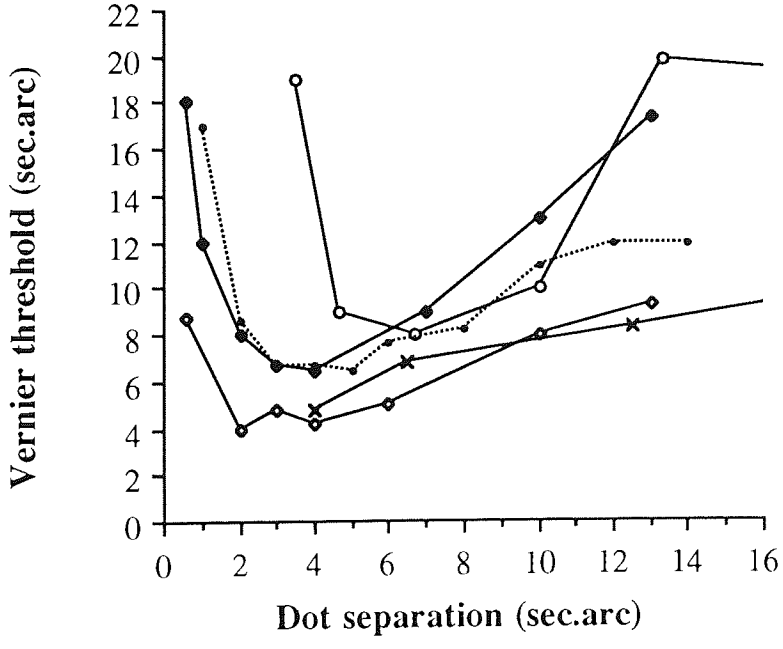

Figure 2.12: The effect of dot separation on vernier acuity. **Circles** - Virsu, Näsänen and Osmoviita (1987), subject RN. **Diamonds** - Westheimer and McKee (1977b) filled: subject LK, shown also in the previous figure, open: subject SM. **Crosses** - Sullivan, Oatley and Sutherland (1972), average of three observers. Dotted line - Westheimer (1982), average of two observers.

The optimum separation for two dots according to Westheimer and McKee (1977b) is 2 - 4 min.arc (the lines of 0.5 min.arc length were considered to represent dots). For smaller separations thresholds increase sharply whilst with greater separations thresholds increase more gradually. Earlier, Sullivan, Oatley and Sutherland (1972) had reported similar findings with increasing dot separation. *Figure 2.12* shows the above results, Westheimer's (1982) data, and the foveal measurements of Virsu, Näsänen and Osmoviita (1987).

There are temporal and spatial factors that affect thresholds in addition to the spatial dimensions of the stimulus itself. Increasing the duration of the stimulus improves vernier acuity only at low contrasts where temporal summation is needed to improve visibility (Waugh & Levi, 1993). Hyperacuity requires some period of undisturbed processing time for best performance. Westheimer and Hauske (1975) found that a stimulus exposure of as little as 50 msec was enough to allow hyperacuity thresholds as low as 6 sec.arc. However, if an interfering stimulus was presented immediately after the stimulus, thresholds increased. Presenting an interfering stimulus *before* the test stimulus had no effect on thresholds. In addition, no interference was found with stimulus exposures longer than 250 msec. Westheimer and McKee (1977a) found that onset asynchrony in presenting vernier lines started to increase thresholds above about 20 msec. The above facts underscore that hyperacuity judgment is one of relative, rather than absolute, position.

Westheimer and Hauske (1975) further found that adjacent features, horizontal and vertical lines, disturbed hyperacuity processing within a certain distance from the stimulus. The deleterious effect on thresholds peaked at 3 - 6 min.arc from the vernier stimulus. The study of Westheimer and Hauske was performed in binocular conditions. Levi, Klein and Aitsebaomo (1985) have confirmed the spatial interference result using monocular viewing.

Several studies suggest that vernier acuity improves with increasing contrast. Bradley and Skottun (1987) used abutting sinusoidal gratings of varying spatial frequency (0.25 - 10 cpd) and contrast (1 - 80%) and found that thresholds improved consistently with increasing contrast. Studies confirming these results include Bradley and Freeman (1985) using cosine gratings, Morgan and Regan (1987) who used line targets, and Watt and Morgan (1983) who used a Gaussian blurred edge.

Williams, Enoch and Essock (1984) studied the effect of retinal image degradation (blur) on line and two-dot vernier acuity at the fovea. Vernier line acuity (line length 10 min.arc) was found to be most degraded with increasing blur for the abutting lines and small gap sizes. Two-dot vernier thresholds (dots 1 × 1 min.arc) were also clearly degraded with increasing blur for the small gap sizes, but increasing the gap size to 16 - 32 min.arc nearly removed the effect of blur on thresholds. However, since the lowest hyperacuity thresholds are usually

achieved when the stimulus components are fairly close together, it is not wrong to generalise that blur degrades hyperacuity thresholds.

Practice improves vernier thresholds markedly at the fovea. According to McKee and Westheimer (1978) about 2500 trials improved performance by an average of 40%. These results were confirmed in a binocular disparity study by Fendick and Westheimer (1983), who extended their study to the peripheral visual field.

2.4.2: Spatial interval discrimination

This task measures the ability of a subject to compare the size of a test gap or spatial interval with that of a standard. The standard may be presented prior to the test gap (Westheimer, 1979; Morgan & Regan, 1987) with a possible temporal delay between the presentations. The test and a standard may also be presented simultaneously (Westheimer, 1979) or the standard may actually be internal to the observer, having been built up as the mean of the test interval over several successive presentations (Westheimer & McKee, 1977b; Westheimer, 1979; Levi & Westheimer, 1987). Under the right circumstances thresholds in the hyperacuity range can be obtained independent of the features which demarcate the spatial interval (Westheimer & McKee, 1977b).

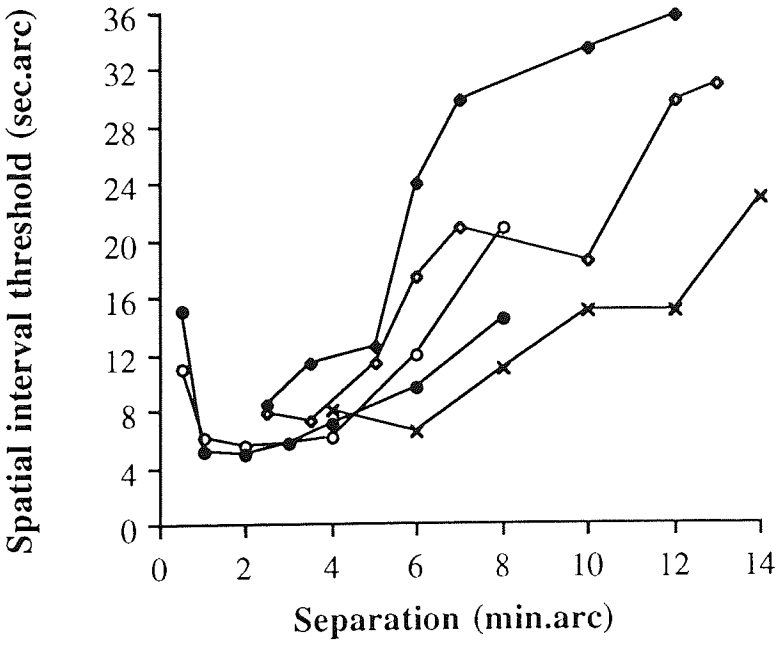

Figure 2.13: The effect of line separation on spatial interval discrimination. Circles - Westheimer and McKee (1977b) filled: subject SM, open: subject JW. Crosses - Westheimer (1979), subject GW. Diamonds - Watt and Morgan (1983) filled: subject MJM, open: subject RJW.

At the smallest separations it is natural that spatial interval thresholds are high since the task is then actually resolution-based. The optimum thresholds found are 2 - 6 min.arc, after that thresholds increase in proportion to the separation (Westheimer & McKee, 1977b; Westheimer, 1979). In *Figure 2.13* spatial interval discrimination thresholds are shown for two subjects when fixation is "traditionally" at the mid-point between the lines forming the stimulus. Whether the increase in thresholds with increasing separation is due to the increase in separation itself or whether it is a consequence of increasing the eccentricity of the two features has been the subject of several recent studies (Levi, Klein & Yap, 1988; Morgan & Watt, 1989; Levi & Klein, 1989; Levi & Klein, 1990a; McKee, Welch, Taylor & Bowne, 1990). See *Chapter 6* for further analysis on the matter.

Temporal delay between the successive interval presentations compared with simultaneous presentation causes a marked increase in threshold values (Westheimer, 1979). *Figure 2.14* shows spatial interval thresholds of subject GW for two vertical lines shown i) sequentially, each line for 0.5 sec (internal reference), ii) simultaneously for 0.5 sec (internal reference), and iii) simultaneously for 1 sec, half way of which the separation changes and the increment or decrement of the interval is to be detected, i.e. the first interval was the reference interval. The latter presentation type resembles the detection of an instantaneous displacement in the presence of references *(Chapter 8.01)*. As is seen from the data, the internal reference (in this case the mean of the ensemble of which it was a part) is far from ideal.

Figure 2.14: The effect of temporal factors on spatial interval discrimination. (Westheimer, 1979). See text above.

Unlike for vernier acuity, contrast variation between about 10 - 75% has no effect on spatial interval thresholds according to Morgan and Regan (1987), who compared the two tasks using two vertical thin bars with a Gaussian luminance profile to form the stimulus. Morgan and Regan found, as did Westheimer (1979), that apart for the lowest contrast level spatial interval thresholds increased with the separation (5 *vs* 10 min.arc) of the bars.

Burbeck (1986) found that exposure duration has a small effect on spatial interval discrimination thresholds when the two bars comprising the stimulus are separated more than about 25 min.arc. At smaller separations, where the stimulus components are closer to the fovea thresholds decrease with increasing duration up to about 400 msec. Burbeck and Yap (1990a) studied the effect of exposure duration and the presence of flanking lines on spatial interval discrimination thresholds. Thresholds for a pair of bars were independent of exposure duration 100 - 500 msec. However, when flanking lines were presented alongside the stimulus bars, thresholds increased. The increase in thresholds was considerably greater for a 100 msec than a 500 msec exposure duration.

2.4.3: Bisection acuity

Bisection acuity is the ability to bisect or judge the mid-point of the gap between two points or lines or even a midpoint of a single line. A typical experiment would present three lines side by side and the observer would be required to decide whether the centre line was to the right or the left of the middle of the stimulus defined by the position of the outer lines (see *Figure 2.15*). The visual system is extremely sensitive to this type of task, and thresholds fall well within the hyperacuity range under optimum conditions (Klein & Levi, 1985, 1987; Wilson, 1986; Yap, Levi & Klein, 1987a,b).

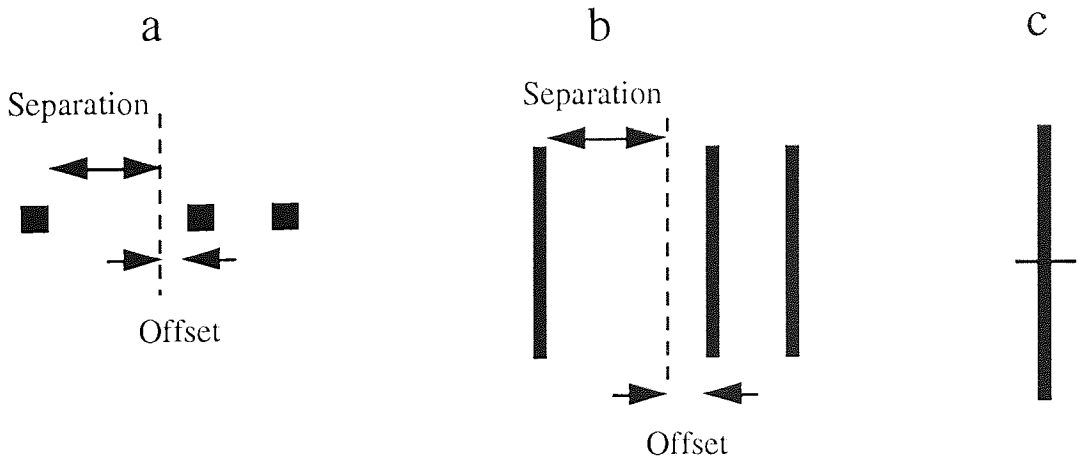

Figure 2.15: Configurations for bisection acuity: a) three-dot stimulus; b) three-line stimulus; c) single line stimulus. Three-dot stimulus was used in this thesis.

The bisection task could be performed by estimating on which side the the central component is relative to the mid-point determined by the two outer stimulus components. Alternatively, the task could be performed by comparing sequentially the size of the two gaps separating the stimulus components. The bisection task can then actually be looked on as a spatial interval task with simultaneous presentation of the two intervals. Burbeck and Yap (1990c) studied spatial interval discrimination and bisection tasks to determine their temporal and spatial limitations. When the three lines were presented simultaneously or the two intervals were presented sequentially, thresholds varied depending of the exposure duration. For short durations (33 msec) the spatial interval thresholds were lower, whereas for longer durations (500 msec) the spatial interval thresholds were higher than bisection thresholds. Burbeck and Yap proposed that the bisection task was carried out by a separation discriminator. For a short duration there was not enough time to process the task, but when the duration was increased bisection thresholds improved faster than spatial interval thresholds. The results support the suggestion that the bisection task is performed by comparing the two spatial intervals sequentially.

Above a minimum value, the relation between separation of the stimulus components and bisection thresholds is strikingly linear thus obeying Weber's law (*Figure 2.16*). Andrews and Miller (1978), Westheimer and McKee (1979) and Klein and Levi (1985) have investigated this relationship by changing the separation between the bars. The separation is here defined as half the separation of the inner edges of the two outer bars. Andrews and Miller (1978) found that increasing the separation from 20.5 to 164 min.arc changed thresholds from about 24 to 190 sec.arc. The results of Westheimer and McKee (1979) revealed a similar, approximately linear relationship between threshold and separation for separations of 3 - 12 min.arc. See *Figure 2.16* for the redrawn data. Again changes in gap size for a conventional bisection task are necessarily associated with a change in the eccentricity of the outer two stimulus components of the task. Thus, it is debatable, as in the case of spatial interval, whether the increase in thresholds with increasing separation is a direct result of separation or an indirect effect of eccentricity (Levi, Klein & Yap, 1988; Morgan & Watt, 1989; Levi & Klein, 1989, 1990a).

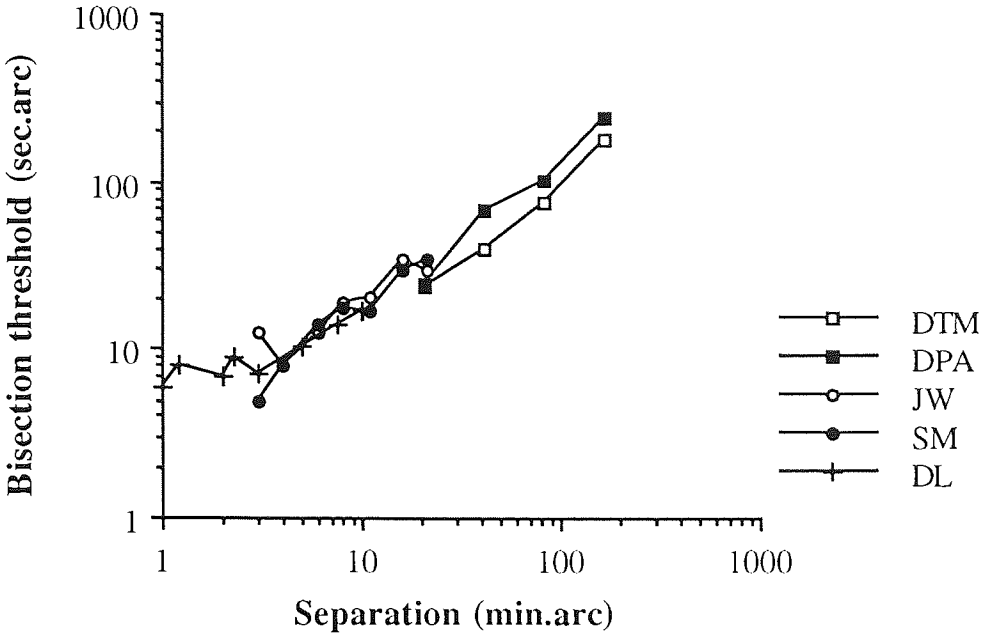

Figure 2.16: The effect of separation on bisection acuity. DTM and DPA - Andrews and Miller (1978). JW and SM - Westheimer and McKee (1979). DL - Klein and Levi (1985), the non-overlapping stimulus configuration in *Figure 2.17b.*

Klein and Levi (1985) studied separations 0.8 - 10 min.arc with two configurations (*Figure 2.17*). With an overlapping stimulus thresholds below 2.5 min.arc separation became extremely low, around 1 - 2 sec.arc. These low threshold values produced a deviation from the linear threshold *vs* separation relationship. The authors stated, however, that in this overlapping configuration there existed a strong facilitating luminance cue, which was produced by the merging luminance peaks of the bright stimulus bars (see *Chapter 2.1*). This example highlights the need to avoid producing luminance cues when choosing stimulus parameters for an experiment.

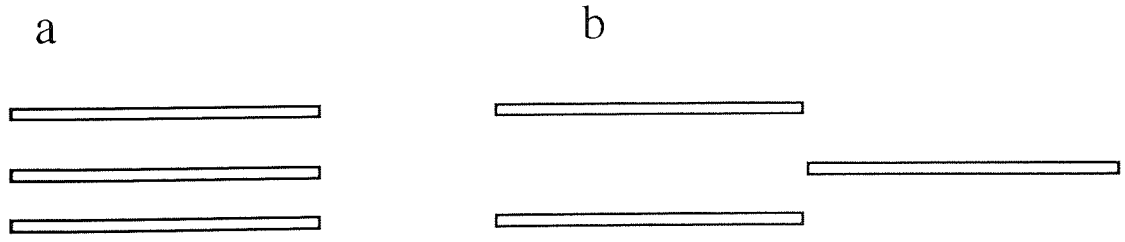

Figure 2.17: Configurations for bisection acuity task by Klein and Levi (1985). When the stimulus bars overlap (a) luminance cues become important with very small separations. Luminance cues do not occur when stimulus bars do not overlap (b).

Andrews and Miller (1978) suggested that, for line lengths below 30 min.arc, bisection thresholds were independent of line length. For longer lines thresholds improved with

increasing line length. The first finding was supported by Klein and Levi (1985) who found that for a fixed separation of 3 min.arc increasing line length from 1.3 to 32 min.arc had very little effect on thresholds.

2.4.4: Movement and displacement detection

At its simplest, the stimulus in a movement task can be a single, unidirectional object having constant velocity. Its movement is defined by three parameters, time (t), distance (d), and velocity (v) of movement. These parameters are inter-dependent according to an equation $v\ (^{m}/_{sec}) = d\ (m) / t\ (sec)$. If the duration of movement (exposure time) is held constant, threshold can be taken either as the lowest velocity *or* the smallest displacement producing the perception of movement.

Several different types of movement may be produced, three of the most commonly used types are presented in *Figure 2.18*. In *continuous movement* the stimulus appears, immediately moves with constant velocity to a new location and then disappears. In *discrete movement* the stimulus appears in one position, disappears, and then after a time interval reappears at a new position. For *stop-go-stop movement* the target appears and remains stationary for a time interval, then moves at a constant velocity to a new location and remains there for an another time interval until it disappears. In the experiments of *Chapter 8* the stop-go-stop movement is used to study unreferenced instantaneous and gradual movement and discrete movement is used the experiments of *Chapter 10*.

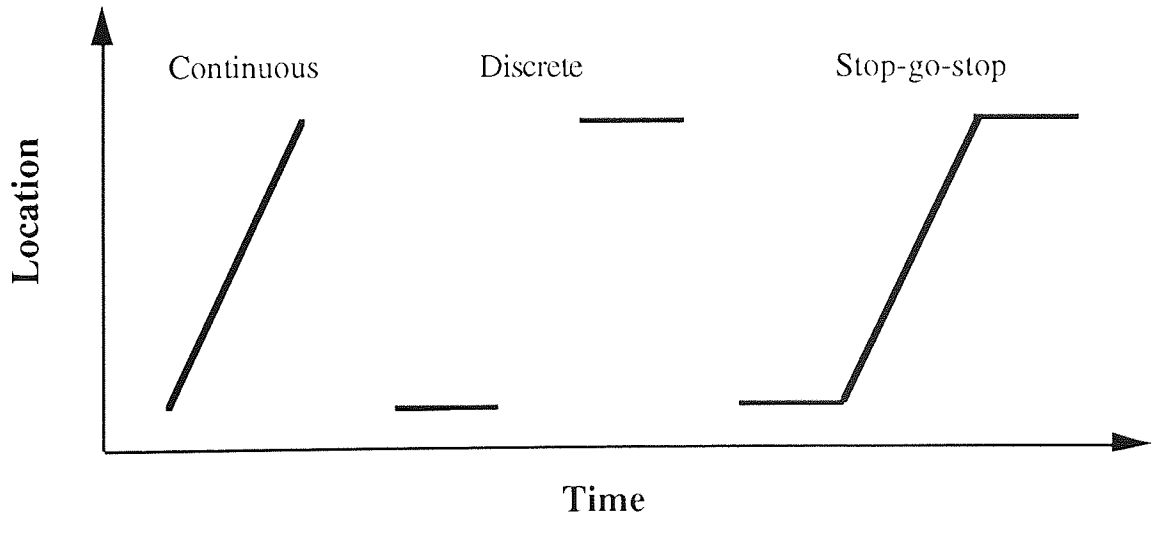

Figure 2.18: Location *vs* time representation of three types of unidirectional movement commonly used in experiments.

There has been much debate as to whether movement thresholds are detected directly or are inferred from a change of position which must always accompany any movement. As early as 1875 Exner suggested that at low velocity movement may be inferred from position changes, but perceived directly at high velocities. Boyce (1965) reached the same conclusion after studying movement in the absence of stationary references. It has long been clear that the detection of object displacement becomes easier in the presence of a stationary reference (e.g. Aubert, 1886), but there has been little agreement regarding the conditions where this holds true. Leibowitz (1955) and Tyler and Torres (1972) and Bonnet (1984) found that at the fovea a reference line has little or no effect at short durations of movement, but for long durations of movement a reference improves performance substantially. This was taken to indicate that at short durations movement is detected directly by mechanisms sensitive to stimulus velocity or displacement, whereas at long durations movement is inferred by relative position information. However, Johnson and Scobey (1982) and Whitaker and MacVeigh (1990) found that references improved thresholds for all durations.

Without a reference, displacement thresholds are proportional to the duration of movement, at least above about 100 msec. This indicates that movement detection is determined by a constant velocity prediction, since threshold distance divided by duration is constant (Leibowitz, 1955; Johnson & Scobey, 1980; Whitaker & MacVeigh, 1990). In the presence of stationary references displacement thresholds behave quite differently and are usually independent of velocity, indicating that detection is determined by the target displacement itself (Johnson & Scobey, 1980; Whitaker & MacVeigh, 1990).

Displacement detection is usually measured by presenting *two* adjacent features for a short period of time following which one of the features would suddenly change position, either making the spatial interval between them wider or narrower. The two features would then remain at this new separation for a short period before disappearing. This type of task is generally known as displacement detection, since it involves detecting the sudden displacement of one feature relative to another stationary one. Under optimum circumstances thresholds for displacement detection are very low, about 10 sec.arc (Westheimer, 1979). Interestingly, displacement detection thresholds show a very weak dependence on the separation of the two features (Westheimer, 1979; Legge & Campbell, 1981). This is opposite to the effect of separation on most other hyperacuities. However, this statement is only true if the displacement is instantaneous (Whitaker & MacVeigh, 1990).

2.4.5: Orientation discrimination

The orientation discrimination threshold is the smallest detectable change in the stimulus orientation. Orientation thresholds can be defined either in spatial terms as the distance (T) by which the end of the line is displaced from the vertical or in angular terms as the angle of tilt from the vertical (*Figure 2.19*). Depending on which way the thresholds are expressed, the optimum line length for orientation discrimination varies. In spatial terms lowest thresholds can be obtained with lines about 4 - 6 min.arc long. In angular terms longer lines (optimum 15 - 20 min.arc) may show lower thresholds (Westheimer, 1981).

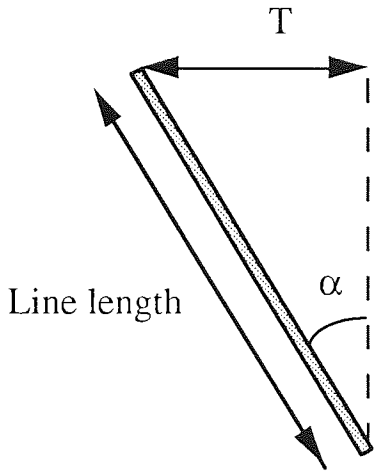

Figure 2.19: Schematic drawing of a line stimulus as viewed by the observer. Orientation thresholds can be defined in two ways. In spatial terms, threshold = T (sec.arc of visual field). In angular terms, threshold = α (deg of rotation).

At the fovea a short line suffers from optical and neural blurring and its orientation is difficult to determine. Increasing line length improves performance (measured in terms of angle of orientation) until, for sufficiently long lines, performance becomes independent of line length. This improvement with line length is shown in *Figure 2.20,* where foveal data is presented from several studies. Andrews (1967) presented the test line simultaneously alongside a long reference line. The task is inherently easy, and using an adjustment method and binocular viewing thresholds became extremely low, about 0.1 deg. Andrews, Butcher and Buckley (1973) repeated the experiment in identical conditions apart from using a method of constant stimuli and obtained somewhat higher thresholds.

Westheimer (1981, 1982) used a 75% correct level to determine thresholds, this has been converted to correspond to the 80% level used in the present study. Viewing was binocular, which usually makes a task easier, and the reference was internal. Vandenbussche, Vogels and Orban (1986) showed a 15 min.arc wide, very low luminance (0.14 cd m^{-2}) line stimulus against completely dark background, i.e. no references were given, and viewing

was monocular. The data for the vertical line stimulus is shown, the 85% correct threshold level has been equated with the present level of 80%. Minimum threshold was high, about 0.7 deg. Watt (1987) investigated several exposure durations for orientation discrimination, the 500 msec duration is presented here. Viewing was binocular, two reference lines were presented alongside the thin, bright stimulus line.

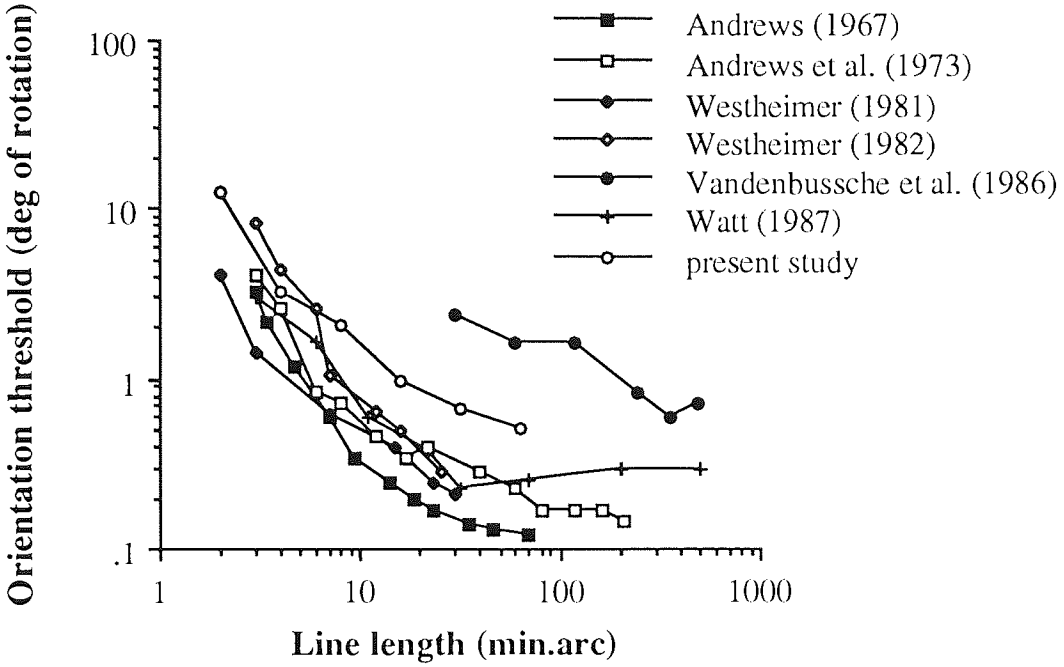

Figure 2.20: Foveal orientation thresholds (deg) shown as a function of line length. Data from several studies; Andrews (1967) subject DPA, Andrews, Butcher and Buckley, (1973) subject DPA, Westheimer (1981) subject HT, Westheimer (1982) subject GW, Vandenbussche, Vogels and Orban (1986), subject BG, Watt (1987) subject CG, and the present study, subject PM.

Westheimer, Shimamura and McKee (1976) used long lines as stimuli and reached orientation thresholds of 0.4 deg. Stimulus conditions were nearly optimal; viewing was binocular, presentation time 200 msec and vertical references were available close to the stimulus (2 deg from the stimulus). Other studies have found similar minimum thresholds; Burbeck and Regan (1983) 0.3 deg; Beck and Halloran (1985) 0.4 deg; Morgan (1986) 0.5 deg; Watt (1987) 0.22 deg; Paradiso and Carney (1988) 0.3 deg; Regan (1989) 0.3 deg; Heeley and Buchanan-Smith (1990) 0.4 deg; Skottun, Bradley and Freeman (1986) 0.5 deg; Spinelli, Bazzeo and Vicario (1984) 0.75 deg. Largest thresholds have been up to 1 - 2 deg (Vandenbussche *et al.*, 1986). These differences are not surprising considering the wide variation in stimulus characteristics used in these studies. For instance, stimuli have consisted of *lines* (Westheimer, 1981, 1982; Vandenbussche *et al.*, 1986; Watt, 1987; Paradiso & Carney, 1988; Heeley & Buchanan-Smith 1990), *dots* (Beck & Halloran, 1985), *edges* (Morgan, 1986; Heeley & Buchanan-Smith 1990), *motion-defined bars* (Regan, 1989) or

gratings (Spinelli *et al.*, 1984; Skottun, Bradley & Freeman, 1986; Heeley & Buchanan-Smith 1990). Some experimental conditions have included a reference line(s) (Morgan, 1986; Watt, 1987), some have used stimuli of very low luminance (Vandenbussche *et al.*, 1986) whilst differences in exposure duration are also known to have a dramatic effect upon orientation thresholds (Watt, 1987).

Sullivan, Oatley and Sutherland (1972) have suggested that orientation sensitivity underlies vernier acuity. This proposal was based on the finding that the two-dot vernier acuity and orientation discrimination both improve with increasing separation / line length when plotted in terms of deg of rotation until reaching an asymptote, which is similar for both tasks. According to the hypothesis, in vernier tasks subjects judge the deviation of the inner ends of the stimuli from verticality. This would explain why the thresholds elevate independent of line length when separation between vernier components is increased (*Figure 2.11*). At very small separations lower acuities are obtained when the gap between the two vernier dots is filled, thereby forming a line (Westheimer, 1982). This, however, may be due to the fact that at very small separations (in the case of Westheimer study, below 4 - 6 min.arc) filling the gap between the dots smears the already perhaps overlapping retinal spread functions. Westheimer (1981) reported that orientation recognition at the fovea was dependent of line length in a similar fashion to vernier acuity. A further similarity to vernier acuity has been found with masking studies, where flanking lines alongside the stimulus deteriorate thresholds most severely when placed about 2 min.arc on either side (Westheimer, Shimamura & McKee, 1976).

2.4.6: Other tasks

In addition to the above tasks, thresholds in the hyperacuity range are found for curvature detection (e.g. Watt & Andrews, 1982; Fahle, 1986), spatial frequency discrimination (Hirsch & Hylton, 1982, 1985) and stereoacuity tasks (e.g. Fendick & Westheimer, 1983; McKee, Welch, Taylor & Bowne, 1990). This thesis, however, does not study these tasks and so they will not be dealt with in any more detail here.

Chapter 3: Peripheral vision and cortical magnification

3.1: Anatomy and physiology

3.1.1: Overview

The visual scene is imaged on the photoreceptor layer of the retina where it is sampled and mapped via successive layers of the retina and lateral geniculate nucleus (LGN) to the striate cortex. Optical quality (Jennings & Charman, 1978), size, shape and density of the photoreceptors (Østerberg, 1935; Curcio, Sloan, Kalina & Hendrickson, 1990), convergence of cones onto retinal ganglion cells (Curcio & Allen, 1990), and the magnification of the retinocortical connections (e.g. Hubel & Wiesel, 1974) affecting visual performance vary differently with retinal eccentricity.

Optical factors that decrease the quality of the image falling onto retina include spherical and chromatic aberration, coma, oblique astigmatism, and distortion. On the optical axis, provided that the possible refractive errors are corrected and there are no media opacities, only spherical and chromatic aberration cause blur (Charman, 1983). Optical blur is the limiting factor for foveal performance, allowing the maximum of 60 cpd acuity at the fovea (e.g. Campbell & Gubisch, 1966). This acuity limit corresponds with the anatomical acuity limit determined by cone spacing (Curcio, Sloan, Packer, Hendrickson & Kalina, 1987; Curcio *et al.*, 1990).

In the periphery, as the field angle increases, coma, distortion, and oblique astigmatism cause increasing degradation of the image, and the relative effect of spherical and chromatic aberrations is small. According to Le Grand (1967) it is probable that the peripheral image retains more or less the same structure as the foveal image up to about 30 deg eccentricity beyond which a high astigmatism is manifest. Oblique astigmatism is somewhat decreased by the flattening of the curvature of the cornea and the posterior surface of the lens away from the optical axis. Correcting oblique astigmatism and all refractive errors as fully as possible does not improve peripheral visual acuity (e.g. Millodot, Johnson, Lamont & Leibowitz, 1975), demonstrating that peripheral vision is neurally, rather than optically, limited.

The average human retina contains about 4.6 million cones and about 92 million rods (Curcio *et al.*, 1990). Peak foveal cone density is about 200,000 cones /$_{mm^2}$ (Curcio *et al.*, 1990). Towards the retinal periphery cone density falls sharply (Østerberg, 1935; Curcio *et al.*, 1987). The decrease is radially asymmetrical, so that the density declines faster along the vertical than the horizontal meridian. Cones are also more densely packed in the nasal than in the temporal retina, although this *nasotemporal asymmetry* is consistently present only

beyond the optic disc (Østerberg, 1935; Curcio *et al.*, 1987, 1990). The size of individual cones grows with eccentricity and they become less polygonal in shape (Curcio *et al.*, 1990).

There is a rod-free zone in the fovea with a diameter of about 1.25 deg. Beyond this zone rod density first increases with eccentricity most rapidly along the superior and slowest along the nasal meridian. At 15 - 20 deg eccentricity the rods are packed most densely, thereafter their density again declines slowly, being highest in nasal and superior retina (Curcio *et al.*, 1990).

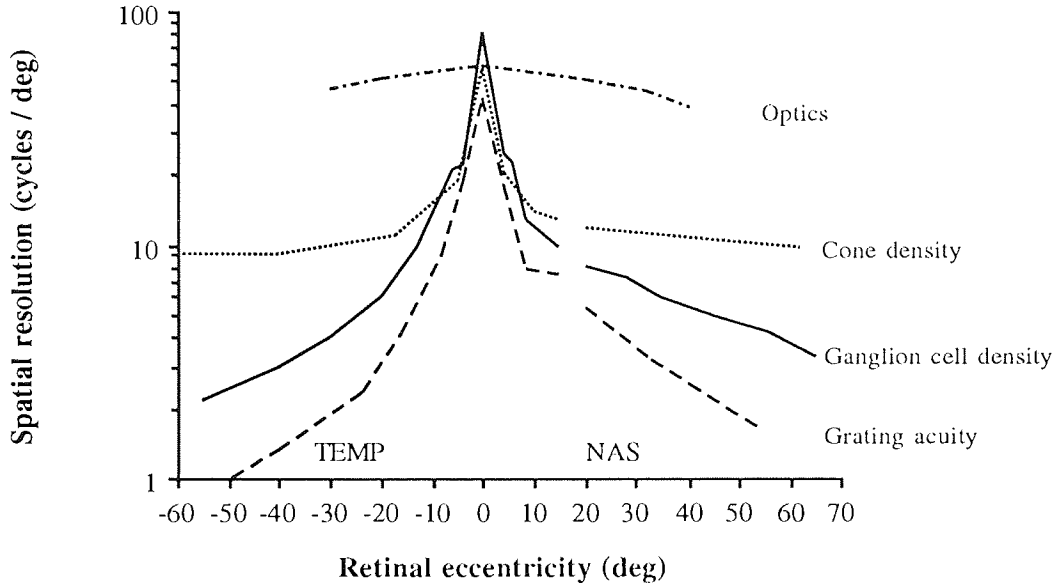

Figure 3.01: Variation of the optical quality of the eye, cone density, ganglion cell density (foveal displacement taken into account), and grating acuity with retinal eccentricity. Redrawn from Anderson, Mullen and Hess (1991).

At the fovea, the ganglion cell layer is displaced away from the centralmost area allowing as free passage as possible for the light entering the cones. In the human retina there are about 1.07 million ganglion cells on average, and their density peaks at 3.5 - 4 deg from the foveal centre. At greater eccentricities ganglion cell density falls off, and the decline is faster along the vertical than the horizontal meridian (Curcio & Allen, 1990). Retinal receptors (cones and rods) project to the ganglion cell layer, so that one or more receptors are connected to one ganglion cell forming its *receptive field.* When going towards periphery the number of receptors forming the receptive fields increases (Curcio *et al.*, 1990), the average size of the receptive fields becomes larger (Hubel & Wiesel, 1974; Perry, Oehler & Cowey, 1984; Ransom-Hogg & Spillmann, 1980) and the receptive field density decreases (Drasdo, 1977).

Unlike in foveal vision, the optical quality of the periphery theoretically exceeds the sampling frequency of the cone lattice (Jennings & Charman, 1978). Therefore, *aliasing* may occur in

the periphery. An adequate representation of a grating, for example, requires at least one cone corresponding each light bar and one cone corresponding each dark bar. Fewer cones result in undersampling of the retinal image and thus, aliasing. Consequently, a peripherally presented grating drifting at a certain velocity to the right may appear as a grating of lower spatial frequency drifting leftwards (see *Figure 3.02*). The grating is undersampled because its spatial frequency lies above the *Nyquist frequency*, $f_N = {}^1/_2$ d, where d = inter-cone distance. Nyquist frequency is the highest frequency that the cone array can reliably discriminate.

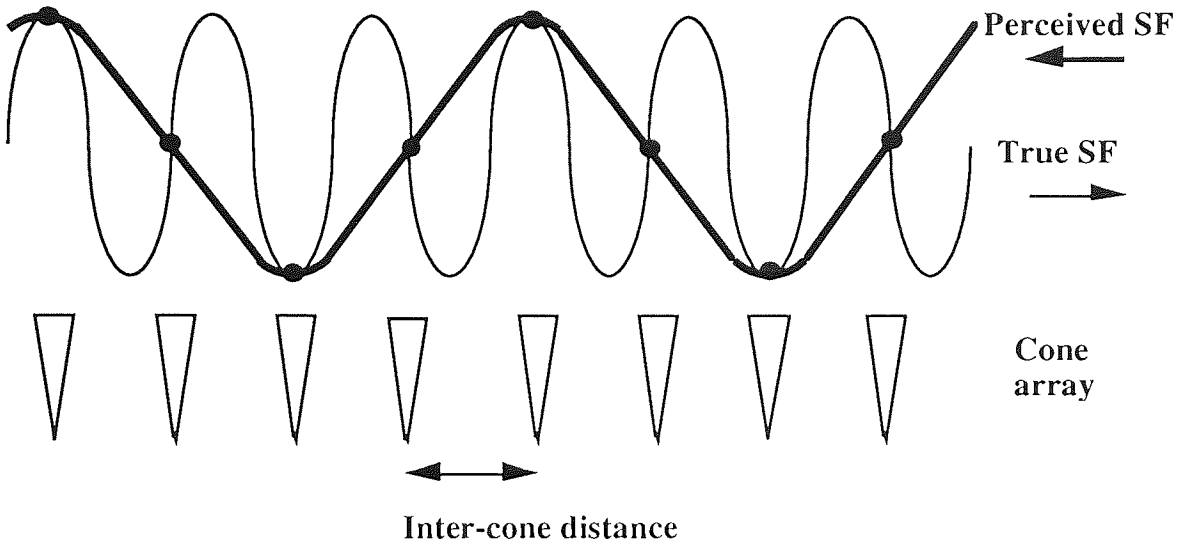

Figure 3.02: Aliasing occurs when the density of the cone lattice is inadequate to reproduce the amount of details required to perceive an image (in this case a moving grating) correctly. Aliasing may also take place when the image is stationary. Figure redrawn from Williams (1986).

Of the one million retinal ganglion cells about 90% project to the lateral geniculate nucleus, LGN (Perry & Cowey, 1984). Half of these projections come from the ipsilateral and half from the contralateral eye (Perry *et al.*, 1984). The projections originating from the foveal area are orderly mapped onto the six layers of the LGN. The layers are fused into four or fewer laminae in the area subserving the peripheral retina (Polyak, 1957; Connolly & Van Essen, 1984), which demonstrates the need for compressing information whenever possible. This compression of information is due to the finite amount of dendrites in the optic nerve and occurs already at the retinal level, where signals converge to the ganglion cells. Also in cone-ganglion cell connections more convergence takes place peripherally, as already mentioned.

Projections from the LGN arrive at the cortex where there are hundreds of cortical neurons processing the information from each retinal ganglion cell (e.g. Schein & de Monasterio, 1987). In primate vision the mapping of the visual field onto the striate cortex is

topographical although non-linear. The central 10 deg of the visual field corresponds to about half of the striate area (Daniel & Whitteridge, 1961; Connolly & Van Essen, 1984). The total striate area in one hemisphere has been estimated as 2610 mm^2 (Filimonoff, 1932) or 2134 mm^2 (Stensaas, Eddington & Dobelle, 1974).

3.1.2: Structures of the visual system

The main pathway connecting retinal receptors and cortex is the "geniculate" or "thalamic" pathway which is divided into two separate processing streams, parvocellular (P) and magnocellular (M) (*Figure 3.03*). Retinal ganglion cells mediate the visual signal to LGN from which the signal proceeds to the primary visual cortex to layer 4C. The "colliculo-tectal" or "mid-brain" pathway, where signal travels from the ganglion cells via the superior colliculus and pulvinar-lateral posterior complex to the secondary visual cortex V2 has little significance in man and higher primates (e.g. Perry *et al.*, 1984; Perry & Cowey, 1984).

Cortical neurones can be considered as "concentric", "simple", "complex" or "hypercomplex" (= end-stopped) depending on their receptive field properties. Concentric cells have receptive fields with a concentric centre-surround division resembling the retinal receptive fields and they receive input from one eye only. Concentric and simple cells' receptive fields can be mapped into on and off areas. Simple cells' receptive fields are divided into either flanking on and off region or into a central band with two parallel flanking regions on either side with the opposite excitation property. Simple cells are thus orientation selective. The majority of them are monocular and situated in layer 4 of Visual area 1 (V1). Complex cells' receptive fields can not be divided into on and off areas but they also are orientation selective, requiring, for example, an edge moving in a certain direction or a line of a certain orientation to respond maximally. Complex cells are often binocular and they are found in layers above and below layer 4. Hypercomplex cells are complex cells requiring a specific length of stimulus to respond maximally. The divisions of the cell types are not clear-cut, but there are gradations in between, so it is difficult to classify the cell types on the basis of the length specificity alone (Hubel & Wiesel, 1962, 1968).

At the cortex there is an evident columnar organization concerning ocular dominance and orientation. Ocular dominance columns reach through all cortical layers, but are most pronounced in the layer 4 of the primary visual area. When moving parallel to the cortical surface the preferred eye alternates about every 0.5 mm. Above and below layer 4 the preference changes gradually from one eye to another resulting in binocularity in about half of the cells. When moving perpendicularly deeper into the cortex the preferred eye remains unchanged (Hubel & Wiesel, 1972). The same occurrs with preferred orientation. When proceeding along the direction of the cortical surface (above or below layer 4C, which is not

orientation selective) the preferred orientation turns every 0.05 mm about 10 deg continuously clockwise or counterclockwise for 1 - 2 mm distance. When moving perpendicularly deeper into the cortex the orientation preference remains again unchanged (Hubel & Wiesel, 1977).

At any one point in the cortex there is a group of receptive fields that cluster about one point in the visual field. At the cortex this cluster of receptive fields extends a constant 1 - 2 mm, but at the retinal level the corresponding receptive fields increase in size when moving towards periphery. The cortical receptive field clusters can be thought as blocks or "modules" of 2 mm x 2 mm in size in human, containing a complete set of ocular dominance and orientation columns (hypercolumns) and all the rest of the machinery needed to analyze a region of visual field irrespective of eccentricity (Hubel & Wiesel, 1974).

3.1.3: Parallel pathways: parvocellular and magnocellular pathway

Monkey retinal ganglion cells can be divided into two main groups: M and P ganglion cells (Shapley & Perry, 1986; Schein & de Monasterio, 1987) similar to the Y and X cells originally found in cat's retina by Enroth-Cugell and Robson (1966). M and P types, amounting to 10 and 80 % of the total number of ganglion cells respectively (Perry, Oehler & Cowey, 1984), project to the LGN whilst the remaining 10% (a heterogeneous group with no structure-function relationship established) project mainly to the midbrain and superior colliculus (Perry & Cowey, 1984). The M cells have large retinal receptive fields with linear or non-linear spatial summation properties (Derrington & Lennie, 1984) and rapidly conducting axons. The P cells have smaller retinal receptive fields with linear spatial summation properties and slower conducting axons (de Monasterio, 1978; Kaplan & Shapley, 1982).

Psychophysical experiments support the idea of two main, relatively separate systems "transient" and "sustained", specialized to process different types of stimuli (Kulikowski & Tolhurst, 1973). The magnocellular (M, Y, transient) system is colour blind and more sensitive to low spatial frequencies, low contrasts and high temporal frequencies (e.g. movement). The parvocellular (P, X, sustained) system is colour selective and sensitive to high spatial and low to medium temporal frequencies (e.g. static patterns consisting of small details) (Kaplan & Shapley, 1982; Livingstone & Hubel, 1988a). Despite a separation in the P and M pathways, they do not always operate in isolation, but there is variable degree of division of labour (probably via the feedback between the visual areas) depending on the stimulus (Zeki & Shipp, 1988; DeYoe & Van Essen, 1988).

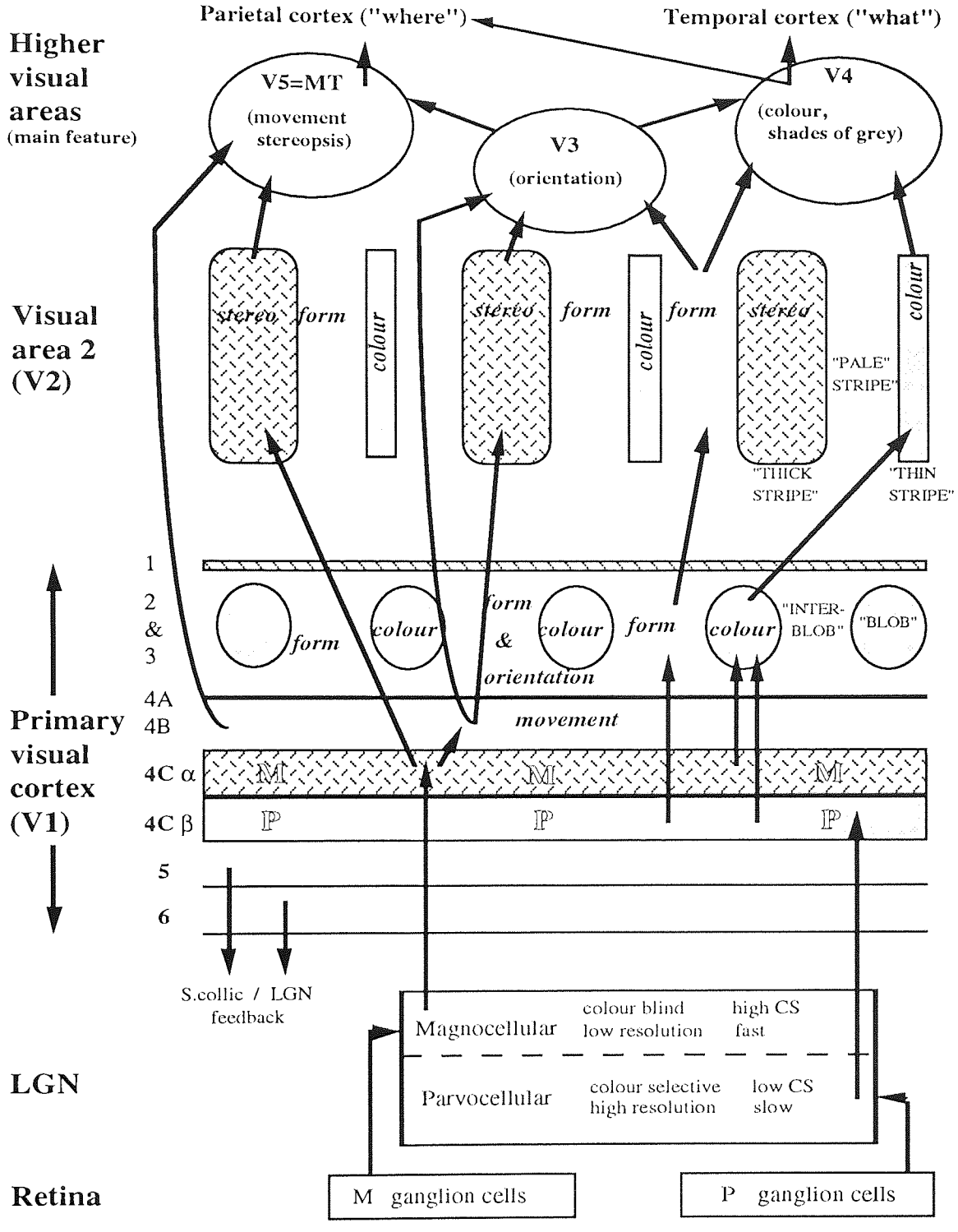

Figure 3.03: A simplified diagram of the parvocellular and magnocellular pathways, which function largely independently. All visual information enters first to V1 input layer 4. By using mitochondrial staining it has been possible to reveal "blob" and "inter-blob" areas in the primary visual cortex and stripe formations in the visual area 2. Forward and backward projections between visual areas are numerous, but only feedback to the superior colliculus and LGN is shown in the diagram. The top of the diagram indicates that the M-pathway deals mainly with localization and P pathway mainly with more accurate scrutiny of the object. The figure is mainly based on the articles of Livingstone and Hubel (1988b), Zeki and Shipp (1988) and DeYoe and Van Essen (1988).

In *Figure 3.03* the parvocellular and magnogellular pathways are presented in an simplified form. The figure is mainly based on the articles of Livingstone and Hubel (1988b), Zeki and Shipp (1988) and DeYoe and Van Essen (1988).

According to Perry and Cowey (1984) the M cells project almost exclusively to magnocellular layers of LGN, whereas the P cells project only to parvocellular layers of LGN. However, Kaplan and Shapley (1982) found that in *macaca fascicularis*' LGN there were two types of P cells; ones that project to parvocellular layers of LGN and others that project to magnocellular layers of LGN forming 75% of the cells there. These "magnocellular X-cells" had high resolution and linear summation as parvo cells, but no colour selectivity and high temporal and contrast sensitivity similar to the magno cells. It seems possible that there is no clear-cut division between M and P cells, but eventually a small amount of all gradations between will be found.

It has been suggested that at the retina the receptive field size for both P and M cells increases linearly with eccentricity, but the slope may be greater for P cells than M cells (Drasdo, 1989, 1991). This was based on findings according to which M cells are fewer and more evenly distributed, whereas more numerous P cells tend to concentrate more at the fovea (de Monasterio, 1978; Harwerth & Levi, 1978; Connolly & Van Essen, 1984; Schein & de Monasterio, 1987). Thus, the sustained system would predominate at the fovea and the transient system in the periphery. In agreement, Connolly and Van Essen found that in the LGN the ratio of cells per square-degree of visual field for the fovea to cells per square-degree of visual field for the far periphery is 20 times higher in the parvo than in the magno system. Perry *et al.* (1984), however, found that the ratio of magno type cells was a constant 10% of all the ganglion cells between 10 - 50 deg, in agreement with Livingstone and Hubel (1988b) and Perry and Silveira (1988), who have argued that mapping densities of the magno- and parvo systems do not vary with eccentricity.

Traditionally, it has been believed that there is a qualitative difference between foveal and peripheral vision, so that the fovea is specialized for discrimination and the periphery for detection. According to an alternative theory, the differences between foveal and peripheral visual performance are caused by variation in sampling density. Thus, the difference is quantitative and can be equated by providing equal cortical representations (equal amount of "modules") for foveal and peripheral stimuli by enlarging stimulus size with increasing eccentricity.

3.2: Cortical magnification (M)

3.2.1: Experiments with a constant size stimuli

Early studies of peripheral vision usually used a constant size stimulus with which to compare performance at the fovea and in the periphery. As a result, performance in most visual tasks was found to decline with increasing eccentricity, often becoming completely impossible beyond a certain limit (e.g. colour vision). This led to the assumption that the quality of peripheral vision was poorer than that at the fovea. However, the neural sampling density of the retina decreases with increasing eccentricity (Drasdo, 1977; Rovamo & Virsu, 1979), providing a plausible explanation for the decline in performance for constant size stimuli. This change in sampling density obviously makes it quite inappropriate to compare foveal and peripheral performance with stimuli of identical size at two locations of different eccentricity. When comparing performance in a task at various eccentricities, stimulus size has to be (usually) increased with eccentricity. The problem, however, is how to determine the appropriate rate of magnification.

3.2.2: Definition

As mentioned, the visual field is represented topographically in the visual cortex but the number of neurones in the visual cortex analysing a constant angle of visual space decreases rapidly from central vision towards the periphery. The scale of the topographical representation of the visual field in the striate cortex is given by the cortical magnification M. It indicates the linear extent of visual cortex in mm per degree of visual angle (Daniel & Whitteridge, 1961). Cortical magnification is greatest in central vision and declines rapidly towards the periphery. Its reciprocal increases approximately linearly with eccentricity from 0 to 10 degrees thus,

$$1/M = a + bE$$

where a and b are constants and E is eccentricity. If E = 0, then

$$1/M = a \quad \text{and thus,} \quad a = 1/M_0,$$

where M_0 = M at the fovea. Hence

$$1/M = 1/M_0 + bE \qquad (3.01),$$

which also can be expressed as (*Figure 3.04*)

$$M_0/M = 1 + bM_0E \qquad (3.02)$$

or

$$M_0/M = 1 + SE \qquad (3.03),$$

where S is the slope of the function relating M_0/M and E.

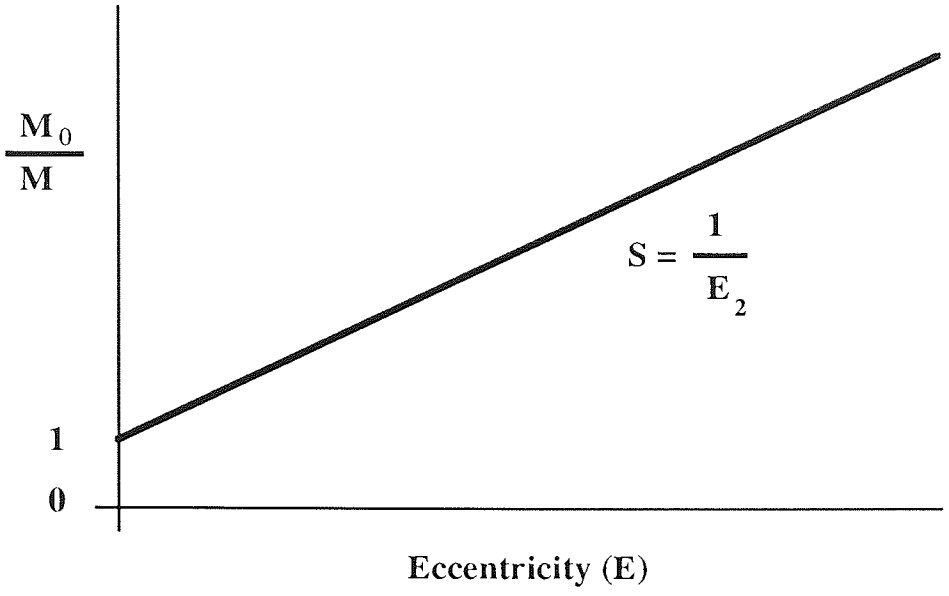

Figure 3.04: The normalized gradient for the inverse magnification as a function of eccentricity.

The background for the concept of cortical magnification is explained in the following sections.

3.2.3: E_2

E_2 indicates the eccentricity (in degrees) where $1/M$ doubles, i.e. $M_0/M = 2$. E_2 therefore also represents the eccentricity at which the stimulus needs to be doubled in size in order to produce the same cortical representation and hence the same level of visual performance. From eq. *3.03* $2 = 1 + SE_2$ or

$$S = 1/E_2 \qquad (3.04).$$

Thus,

$$M_0/M = 1 + E/E_2 \qquad (3.05)$$

E_2 represents a useful parameter with which to compare the rate at which different stimuli need to be increased in size towards the periphery to maintain equivalent performance.

3.2.4: Direct estimates of M

Direct estimates of cortical magnification in man are limited (e.g. Brindley & Lewin, 1968; Dobelle, Turkel, Henderson & Evans, 1979), but there have been several attempts to measure M directly in other primates. Spots of light are usually used as stimuli and cortical

response to the stimulus is measured via electrodes. The change in M with eccentricity can be calculated on basis of the cortical responses. It is also possible to estimate the hypothetical value of M at the very center of vision, M_0.

As early as 1932 Polyak suggested that the retina would possess a fixed projection at the cortex. Talbot and Marshall (1941) made the first report of the presence of a systematic topographic map of the visual field onto the monkey's striate cortex. The central visual field of a monkey was plotted onto the posterolateral cortical surface by measuring the cortical representation (in millimeters of cortex per angular measure of visual field) of the stimulus at different locations. Averaged results from six monkeys indicated that i) 2 min of visual angle at the fovea and ii) 18 min of visual angle at 5 deg eccentricity corresponded to 1 mm at the cortex. On this basis, $M_0 = 1\ mm/_{2min} = 30\ mm/_{deg}$ and at 5 deg eccentricity $M = 1\ mm/_{18\ min} = 3.33\ mm/_{deg}$. Using equation *3.05* we get $30/_{3.33} = 1 + {}^{5}/_{E_2}$ thus, $E_2 = 0.625$ deg.

Daniel and Whitteridge (1961) extended the mapping of the visual field representation of the central 60 - 70 deg onto the calcarine cortex using monkeys and baboons. They coined the term cortical magnification (M) and found that the inverse magnification ($1/_M$) and human visual acuity (Weymouth, 1958) varied at the same rate with eccentricity. Resolution at any eccentricity required two areas of cortical excitation separated by a distance depending on $1/_M$. At the fovea the extent of cortex per degree of visual angle is large thus, resolution is possible with a small retinal separation. In the periphery the extent of cortex per degree of visual angle is much smaller thus, a much larger retinal separation is needed for resolution. According to Daniel and Whitteridge, in order to resolve two objects their minimum cortical separation has to be 67 µm. The data from their Figure 4 (within 15 deg eccentricity only) is reanalysed in *Figure 3.05* by plotting $1/_M$ against eccentricity. The regression line drawn through the data gives y-axis intercept ($= 1/_{M_0}$) of 0.131 $deg/_{mm}$ thus, $M_0 = 7.6\ mm/_{deg}$.

In addition, from *3.05*,

$$1/_M = 1/_{M_0} + E/_{E_2 M_0} \qquad (3.06).$$

Hence, the gradient S in *Figure 3.05* $= {}^{1}/_{E_2 M_0} = 0.098$, thus $E_2 = 1.34$ deg.

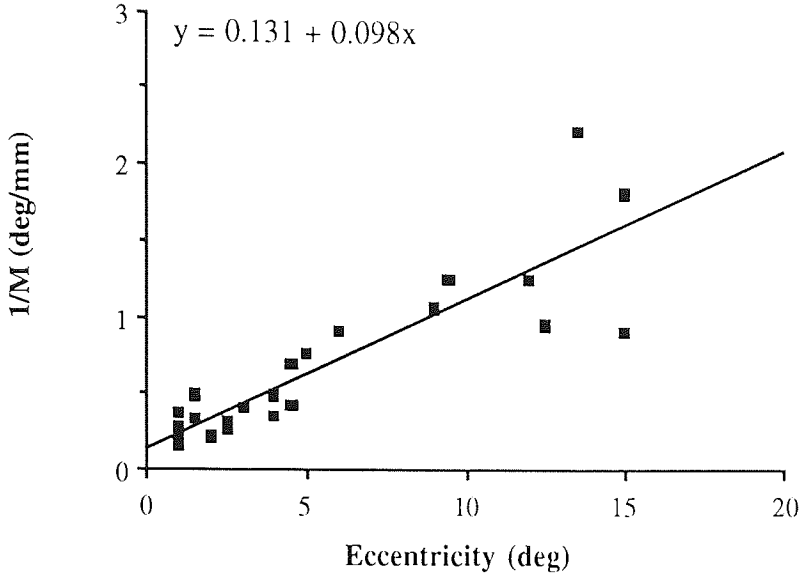

Figure 3.05: The regression line drawn through the data of Daniel and Whitteridge (1961) has a gradient of 0.098 and y-intercept ($1/_{Mo}$) of 0.131 $deg/_{mm}$.

Rolls and Cowey (1970) investigated the density of cones and ganglion cells and the magnification factors at the fovea and in the periphery in the rhesus monkey and the squirrel monkey. According to the results, the cortical magnification as well as retinal topography appeared to be closely related to the visual acuity.

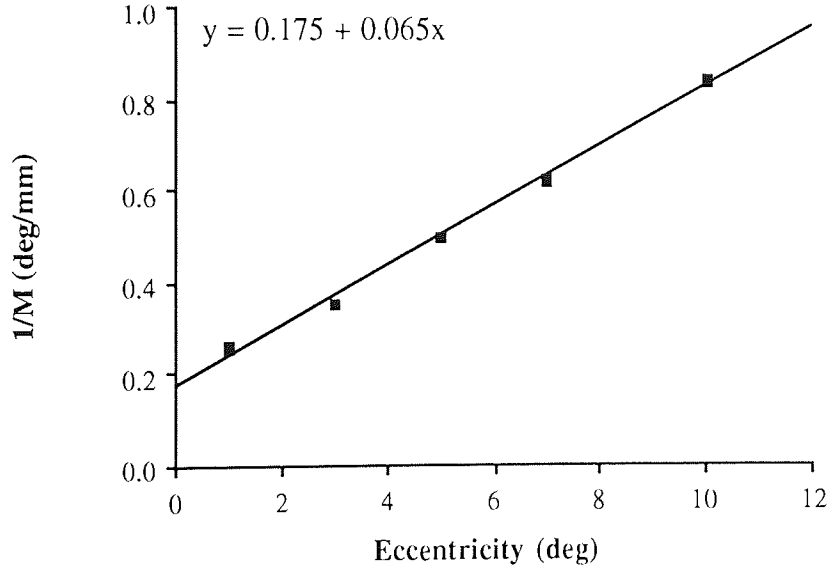

Figure 3.06: The regression line drawn through the data of Rolls and Cowey (1970) has a gradient of 0.065 and y-intercept ($1/_{Mo}$) of 0.175 $deg/_{mm}$.

The magnification factors found in the study were confirmed by estimating the total area of the visual cortex from the magnification factors and showing that this agreed with the actual area of the visual cortex. When their Figure 7 is reanalysed (in *Figure 3.06*) within 10 deg eccentricity by averaging the results from the two types of monkey, M_0 is 5.7 $mm/_{deg}$. Thus, $E_2 = 1/_{5.7 \times 0.065} = 2.69$ deg.

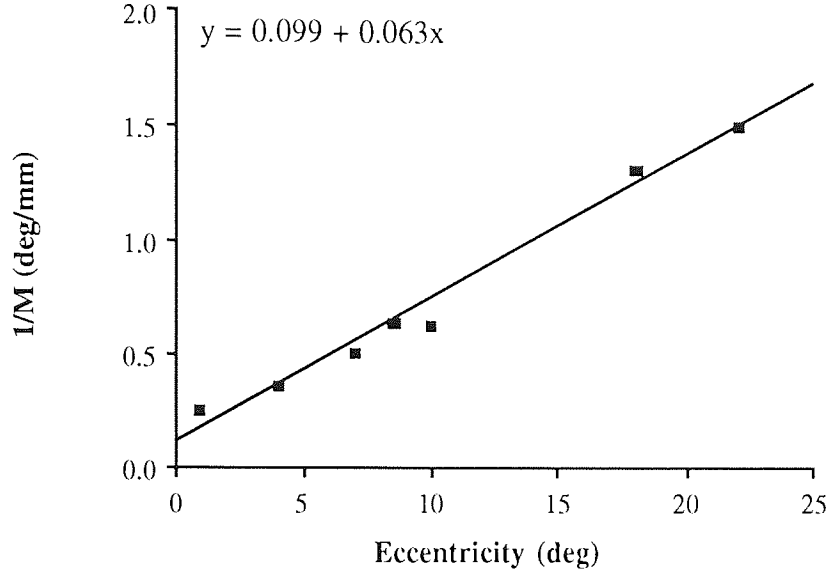

Figure 3.07: The regression line drawn through the data of Hubel and Wiesel (1974) has a gradient of 0.063 and y-intercept ($1/_{Mo}$) of 0.099 $deg/_{mm}$.

Hubel and Wiesel (1974) found modules in the rhesus monkey cortex which were about 2×2 mm in surface extent and which acted in isolation from the surrounding areas (see *Chapter 3.1.2*). For each module there was a selection of receptive fields (orientation, movement etc.) which varied in size and position in the visual field, increasing in size towards the periphery. The modules themselves were of constant size so for foveal vision they represented a much smaller area of the visual field than in the periphery. Hubel and Wiesel concluded that "...the machinery may be roughly uniform over the whole striate cortex, the differences being in the inputs. A given region of cortex simply digests what is brought to it, and the process is the same everywhere." When the cortical magnification data in their Figure 6A is replotted (*Figure 3.07*), an M_0 of 10 $mm/_{deg}$ is revealed. Thus, $E_2 = 1/_{10 \times 0.063} = 1.59$ deg.

Dow, Snyder,Vautin and Bauer (1981) measured receptive field size and magnification in the striate cortex of rhesus monkeys. They found that the cortical projection of the foveola would be about 30 $mm/_{deg}$, which was far greater than reported in other studies. This may be due to the extremely prolonged fixation to the light stimulus provided or simply to the criteria chosen when analysing the data since, according to Levi, Klein and Aitsebaomo (1985), a value of 12 - 16 $mm/_{deg}$ would describe the data better. Judging simply by the regression

line on their Figure 5 the inverse of cortical magnification would be 2.3 $min/_{mm}$ i.e. M_0 = 26 $mm/_{deg}$. The slope for their regression line is 0.12 thus, $E_2 = 1/_{26\times0.12} = 0.32$ deg.

In a later publication Dow, Vautin and Bauer (1985) presented visuotopic maps of two awake, behaving macaque monkeys. The estimated inverse magnification factors in their Table 1 are plotted in *Figure 3.08*. On the basis of the data, $M_0 = 1/_{0.04} = 25$ $mm/_{deg}$ and $E_2 = 1/_{25\times0.118} = 0.34$ deg.

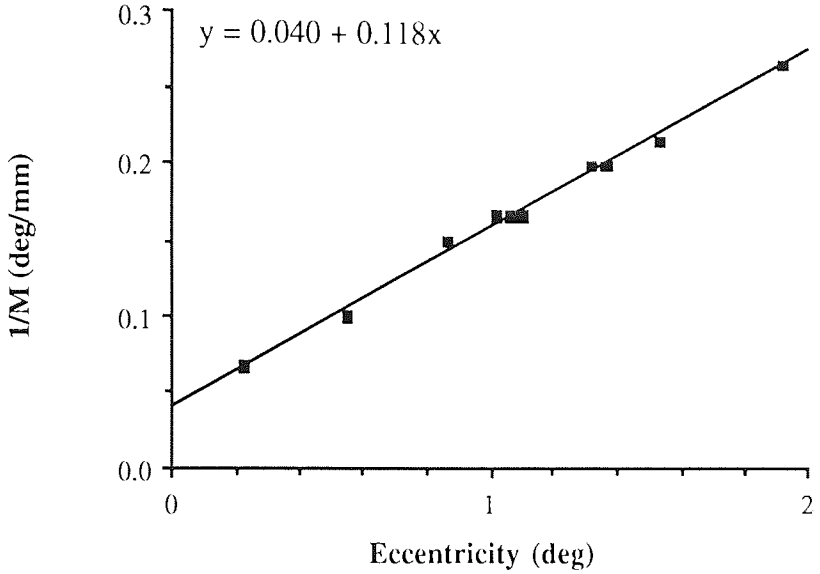

Figure 3.08: The regression line drawn through the data of Dow *et al.* (1985) has a gradient of 0.118 and y-intercept ($1/_{Mo}$) of 0.040 $deg/_{mm}$.

Tootell, Silverman, Switkes and De Valois (1982) used 2-deoxyglucose (2DG) labelling to map the foveal representation. Macacue monkeys were injected with 2DG and made to fixate a target consisting of concentric rings and spokes for 30 minutes. During this period the 2DG was concentrated at locations of peak activity in the cortex. When the cortex was investigated the staining caused by the 2DG was visible and allowed the location of activity to be plotted. The inverse cortical magnification seemed to obey the formula $1/_M = 0.077 + 0.082E$. This resembles equation *3.06* so that $M_0 = 1/_{0.077} = 13$ $mm/_{deg}$ and $E_2 = 1/_{13\times0.082} = 0.94$ deg.

In 1988, using the same method as in Tootell *et al.* (1982), Tootell, Switkes Silverman and Hamilton revised their $1/_M$, and suggested separate formulae for fitting the data in horizontal and vertical meridian. Thus, horizontal $1/_M = 0.108$ $deg/_{mm} + 0.066E/_{mm}$ and vertical $1/_M = 0.070$ $deg/_{mm} + 0.052E/_{mm}$. These result in M_0 of 9.25 $mm/_{deg}$ and $E_2 = 1.64$ deg horizontally and M_0 of 14.3 $mm/_{deg}$ and $E_2 = 1.35$ deg vertically. The differences in M_0 result from separate fitting, in reality there can only be one M_0 for one individual!

Van Essen, Newsome and Maunsell (1984) made recordings from six macaque monkeys finding an M_0 of 13.0 $mm/_{deg}$. At 1 deg eccentricity an M of 5 $mm/_{deg}$ was reported. This would result in E_2 of 0.625 deg. Taking into account the data at larger eccentricities (up to 20 deg in their Figure 6a) will produce an E_2 of 0.611 deg The cortical representation of the fovea was, according to the results, greater than that suggested by the contemporary estimates of ganglion cell density. This could indicate that the cortex emphasized the fovea more than the retina.

In *Table 3.01* are some estimates of M_0 and E_2 found for monkeys. The wide range of values may be due to inter-species variability and differences in methodology. Further, the technology available has improved progressively since 1941.

Table 3.01: Some estimates of M_0 and E_2 in monkey

Investigators	M_0 ($mm/_{deg}$)	E_2 (deg)	Monkey
Talbot and Marshall (1941)	30	0.63	rhesus
Daniel and Whitteridge (1961)	7.6	1.34	various
Rolls and Cowey (1970)	5.7	2.69	rhesus/squirrel
Hubel and Wiesel (1974)	10	1.59	rhesus
Dow, Snyder, Vautin and Bauer (1981)	26	0.32	rhesus
Tootell, Silverman, Switkes and De Valois (1982)	13	0.94	cynomolgus
Van Essen, Newsome and Maunsell (1984)	13	0.63	cynomolgus
Dow Vautin and Bauer (1985)	25	0.34	cynomolgus
Tootell, Switkes, Silverman and Hamilton (1988)	9.3-14	1.35-1.64	arctoides/cynomolgus

A few direct studies have used human volunteers (e.g. Brindley & Lewin, 1968; Dobelle, Turkel, Henderson & Evans, 1979) in connection with experiments on artificial vision for the blind. Brindley and Lewin (1968) inserted a bank of electrodes over the striate cortex of a practically blind subject and used the phosphenes generated by electrical stimulation to plot a part of her visual field. It was found that stimulation of the areas corresponding to the peripheral visual field produced a slightly larger cloud-like phosphene compared with the stimulation of the areas corresponding to the more central parts of the visual field. The rough map of the visual field on the cortex was found to agree with the contemporary maps acquired by studying trauma-induced field defects. The values derived from this report by Cowey and Rolls (1974), below, have been used in several studies when trying to determine an estimate of the values of M in man (e.g. Rovamo, Virsu & Näsänen, 1978; Virsu, Näsänen & Osmoviita, 1987; Drasdo, 1989).

Cowey and Rolls (1974) used the data of Brindley and Lewin to determine values for M_0 by relating the linear separation of an electrode pair to the angular separation (or eccentricity) of the corresponding pair of the phosphenes. For the lower visual field M was about 4 $mm/_{deg}$ at 2 deg eccentricity, then M declined monotonically to 0.5 $mm/_{deg}$ at 25 deg eccentricity. Since no strictly foveal data was available, M_0 was extrapolated.

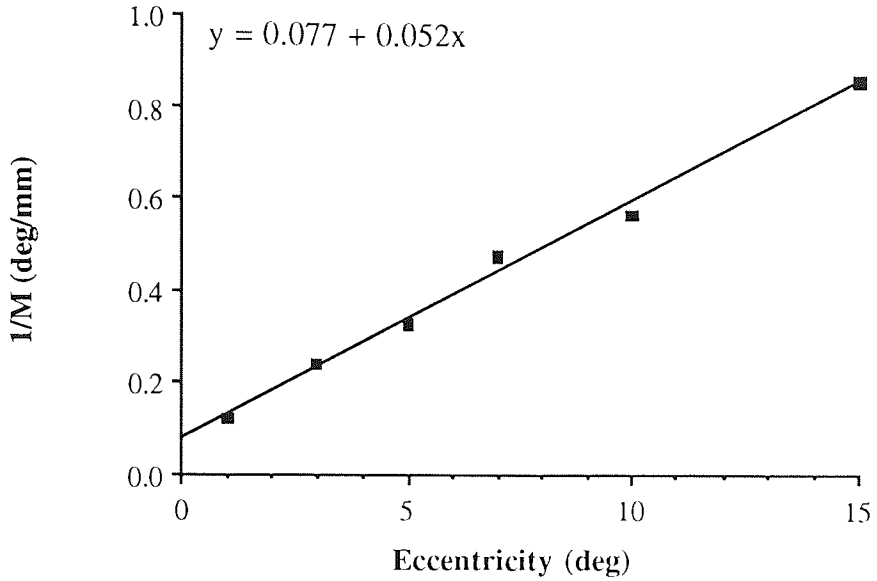

Figure 3.09: Inverse magnification factors as estimated by Cowey and Rolls (1974) from the data of Brindley and Lewin (1968) within 15 deg eccentricity. The regression line drawn through the datapoints indicates a gradient of 0.052 and y-intercept ($1/M_0$) of 0.077 $deg/_{mm}$.

Comparison with Wertheim's (1891) visual acuity data suggested that M is directly proportional to visual acuity and correspondingly, $1/M$ is directly proportional to the minimum angle of resolution in man. Thus, a constant amount of visual cortex is devoted to the minimal angle of resolution (MAR), whatever it's value. The authors' estimate for M_0 was 15.1 $mm/_{deg}$ on this one subject. Based on the data within 15 deg eccentricity only, and removing the extrapolated foveal value, M_0 decreases slightly, becoming 13.0 $mm/_{deg}$ and E_2 in this case is $1/_{0.052 \times 13.0} = 1.48$ deg.

Dobelle *et al.* (1979) performed a study similar to that of Brindley and Lewin (1968) up to 20 deg eccentricity and plotted magnification factors against the mean phosphene eccentricity. It was concluded that magnification factors corresponded with the studies of visual acuity. It is possible to determine E_2 for Dobelle *et al.*'s data by first calculating the inverse of M values, plotting them against eccentricity and drawing a least square line through the datapoints. In *Figure 3.10* the fitted line intersects y-axis at y = 0.116 $deg/_{mm}$, hence $M_0 = 1/_{0.116} = 8.62$ $mm/_{deg}$. $E_2 = 1/_{8.62 \times 0.099} = 1.17$ deg.

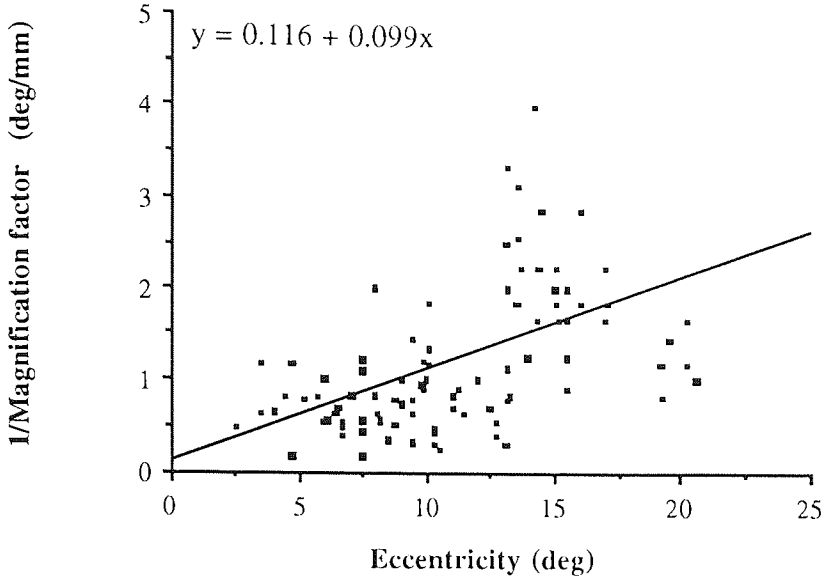

Figure 3.10: Inverse magnification factors plotted against eccentricity. The regression line drawn through the data of Dobelle *et al.* (1979) has a gradient of 0.116 and y-intercept ($1/M_o$) of 0.099 deg/mm.

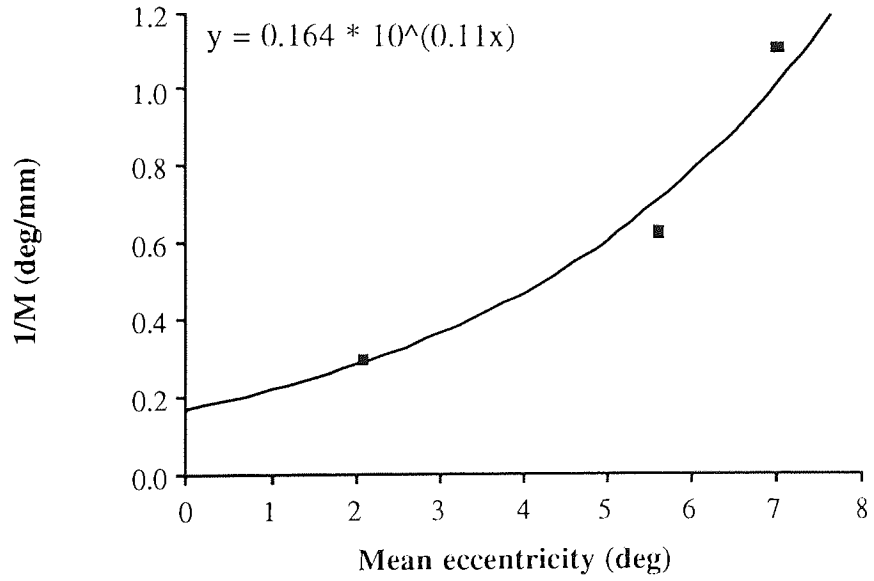

Figure 3.11: Inverse magnification factors as estimated by Fox *et al.* (1987) as a function of mean eccentricity (2.1, 5.6, and 7 deg) of the stimulus in the visual field. The linear fit would produce a negative $1/M$ thus, an exponential function is used here to find the y-intercept ($1/M_o$) of 0.164 deg/mm.

Positron-emission tomography (PET) can be used to map retinotopic organization of primary visual cortex in humans. Fox, Miezin, Allman, Van Essen and Raichle (1987) measured regional cerebral blood flow to detect locations of functional brain activation by using

oxygen-15-labeled water. Annular checkerboard stimuli extended 0.1 - 1.5, 1.5 - 5.5, and 5.5 - 15.5 deg in macular, perimacular, and peripheral stimulus conditions, respectively. Activated sites at the brain were revealed by subtracting the resting-state image of cerebral blood flow from the subject's response image. By comparing the stimulus shift in the visual field with the shift of the activated cerebral site (their Table 3) it is possible to estimate values for M. When these values are plotted against the mean stimulus eccentricity, M_0 can be determined by using an exponential fit only, since a linear fit would produce a negative $1/M$. M_0 becomes thus $1/0.164 = 6\ mm/deg$ averaged in six subjects. Due to the exponential nature of the data the E_2 will not be determined.

3.2.5: Indirect estimates of M

Richards (1971) analysed data from a specific type of migraine scotoma. In the type of scotoma which they studied, a small grey area first appeared near the centre of the visual field. It then expanded within few minutes into a horseshoe-formed arc, with bright zigzag lines at the expanding outer edge and a clear, normal central area. After about 20 minutes the arc appeared to have exceeded the limit of the visual field and the whole visual field seemed normal again. On the basis of drawings at various stages of the disturbance, Richards determined the length and width of the lines forming the outer edge of the arc. He found that line length at each eccentricity corresponded to about 1.2 mm of cortical distance.

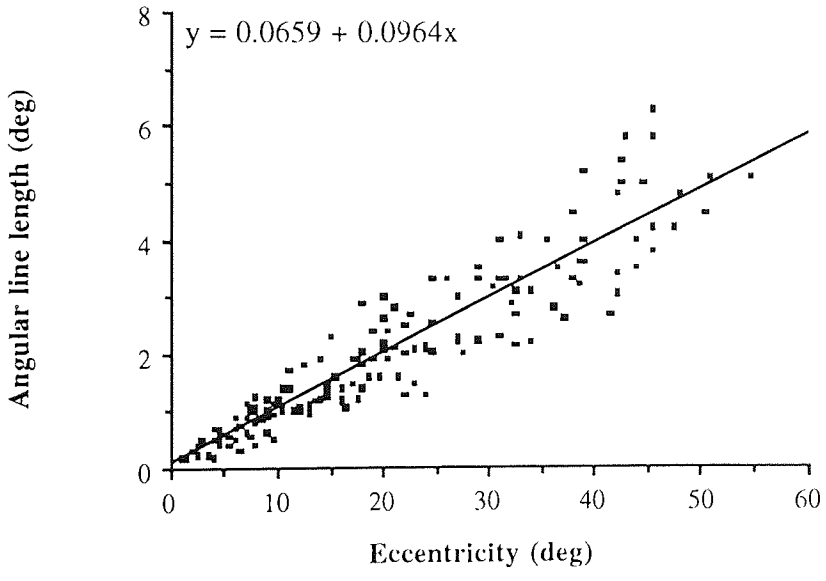

Figure 3.12: Angular line lengths plotted against eccentricity. The regression line has a gradient of 0.0964 and y-intercept ($1/M_o$) of 0.0659 deg/mm. Redrawn from Richards (1971).

The data is reanalysed in *Figure 3.12* to find an E_2 to describe the rate with which the line length increased with eccentricity. To determine the y-intercept representing the hypothetical foveal line length, data was plotted in linear coordinates, angular line length against distance from fixation point. A regression line was drawn through the data resulting in a y-intercept of 0.0659 deg. Thus, $M_0 = 1.2\text{mm}/_{0.0659\text{deg}} = 18\ \text{mm}/_{\text{deg}}$ (in slight disagreement with Drasdo's analysis, 1991, which suggested 12 $\text{mm}/_{\text{deg}}$). $E_2 = 1/_{18\times0.0964} = 0.68$ deg.

Estimates of M have been made assuming that cortical magnification varies in proportion to retinal ganglion cell density. Drasdo (1977) used ganglion cell receptive field density (D_r) and minimum angle of resolution data when determining the human M_0. He took into consideration the displacement of ganglion cells from their receptive fields at the foveola when estimating receptive fields from a selection of data on human retinal cellular topography. Drasdo formulated a general equation for cortical magnification at any eccentricity as

$$1/_M = 1/_{M0}\,(1 + SE) \qquad \text{for eccentricities smaller than 20 deg} \qquad (3.06),$$

and

$$1/_M = 1/_{M0}\,[1 + SE(1 + 3E^2 \times 10^{-5})] \qquad \text{for eccentricities smaller than 70 deg} \qquad (3.07),$$

where cortical magnification M ($\text{mm}/_{\text{deg}}$) varies as a function of eccentricity E (deg) and S is 0.59 averaged for all meridians. Drasdo found that M^2 is proportional to ganglion cell receptive field density per solid degree (D_r). In his model the foveal linear ganglion cell sampling interval and $1/_M$ double at the eccentricity of $1/_S$, i.e. 1.69 deg (= E_2). He suggested a human M_0 of 11.5 $\text{mm}/_{\text{deg}}$.

Rovamo and Virsu (1979) also used the data of Daniel and Whitterige (1961) and Hubel and Wiesel (1974) on the density of retinal ganglion cell receptive fields when estimating M. However, unlike Drasdo (1977), within the central 10 deg eccentricity they used cone density estimates instead of ganglion cell receptive field density, since within the central 10 deg eccentricity the sampling density is determined by cones and the ratio of cones to ganglion cells (according to Perry & Cowey, 1985) was estimated as 1:1. This resulted in reduced foveal representation compared with Drasdo (1977). However, in agreement with Drasdo (1977) they found that M^2 was directly proportional to ganglion cell receptive field density in primates. Since the monocular values of M are not radially symmetric, human M needed to be expressed with different equations for each of the four prime meridia.

Table 3.02: Equations of M for the principal meridia (Rovamo & Virsu, 1979)

Meridian	Equation	Valid extent	E_2 (deg)
Temporal	$M_T = M_0 (1 + 0.29E + 0.000012E^3)^{-1}$	(0 - 80°)	3.45
Nasal	$M_N = M_0 (1 + 0.33E + 0.00007E^3)^{-1}$	(0 - 60°)	3.03
Inferior	$M_I = M_0 (1 + 0.42E + 0.000055E^3)^{-1}$	(0 - 60°)	2.38
Superior	$M_S = M_0 (1 + 0.42E + 0.00012E^3)^{-1}$	(0 - 45°)	2.38

Within the central 15 deg these non-linear equations are reasonably linear, *Figure 3.13* shows the different slopes for the meridians. E_2 can be calculated from the gradients of these as 3.45 deg (temp), 3.03 deg (nas), 2.38 deg (inf), and 2.38 deg (sup).

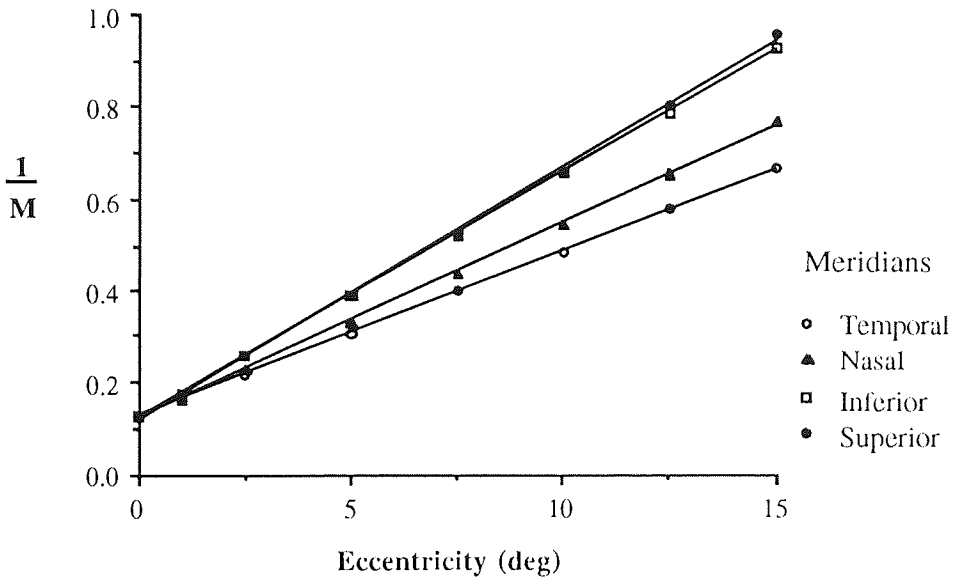

Figure 3.13: The increase of $1/M$ with eccentricity within the central 15 deg eccentricity according to the equations of Rovamo and Virsu (1979).

To stimulate the same number of ganglion cells at each eccentricity Rovamo and Virsu then scaled the retinal dimensions of sinusoidal gratings with the magnification factors obtained by the equations in *Table 3.02* and estimated the contrast sensitivity function at 25 locations across the retina. Conceivably, the scaling procedure would make it possible to reach the same peak sensitivity at each eccentricity. The results then showed that the contrast sensitivity functions could be made similar at any eccentricity by using a suitable scaling factor. According to Rovamo and Virsu (1979) a value for human M_0 was 7.99 $mm/_{deg}$ which was lower than the previous estimates in other studies.

Drasdo (1991) showed in his review article that the human M_0 can be estimated as 12.86 $mm/_{deg}$. The calculation was based on equation $M_0^2 = A_{cort}(mm^2) \times D_r(deg^{-2}) / N_g$, where A_{cort} = total cortical area (5 000 mm^2), D_r = ganglion cell receptive field density per solid degree for the geniculostriate pathway (35 720 deg^{-2}), and N_g = the number of geniculostriate ganglion cells (1 080 000). However, if *macaca fascicularis* (for which extensive data has been obtained) was accepted as a useful model for human visual system, by calculating first the macaque's M_0 as 10 $mm/_{deg}$ with the total cortical striate area of 2 400 mm^2, then applying the area of the human striate cortex would yield an M_0 of 14.4 $mm/_{deg}$. Drasdo considers the latter being the more accurate estimate of the two (verbal communication). He has further suggested E_2 values for several neural substrates: 4.76 deg for M cells, 1.29 deg for P cells, 1.36 deg for an average of all ganglion cell types and 1.14 deg for M in striate area 1 (V1).

The above values were obtained assuming that the magnification factor across the retina was equivalent to the magnification factor at the cortex. However, it has been argued that, at least in monkeys, the fovea has a much larger cortical representation than would be predicted by ganglion cell density (Dow, Snyder, Vautin & Bauer, 1981; Van Essen, Newsome & Maunsell, 1984; Perry & Cowey, 1985, 1988). The increase in representation might be due to expansion of the projections between the retina and cortex, some additional processing in the LGN or the cortex or, perhaps, an underestimate of the true retinal ganglion cell density.

Previously a 1:1 (e.g. Polyak, 1941) or 1:2 (Schein, 1988; Perry & Cowey, 1988) foveal cone to ganglion cell ratio has been suggested. Now it appears that the foveal ganglion cell density is higher than previously had been assumed, the foveal cone to ganglion cell ratio being 1:3-7 (Curcio & Allen, 1990) or 1:3-4 (Wässle, Grünert, Röhrenbeck & Boycott, 1989, 1990), making it possible that retinal and cortical magnification factors actually are equal. Further, it seems that the representation of the visual field in the striate cortex is directly proportional to the ganglion cell receptive field density as was originally suggested by Drasdo (1977).

Tolhurst and Ling (1988) reviewed the available human and monkey data. They expressed doubt about whether it was possible to extrapolate human M using assumptions based on ganglion cell density and visual acuity. M^2 may not be directly proportional to the density of retinal ganglion cells (e.g. Van Essen *et al.*, 1984 and Perry & Cowey, 1985) as has been previously proposed (e.g. Rolls & Cowey, 1970) thus, their density should not be used to determine M. Further, the minimum angle of resolution is directly proportional to the human M (Brindley & Lewin, 1968) within 1.5 and 35 deg eccentricities (Cowey & Rolls, 1974), but it has been argued (Dow *et al.*, 1981; Van Essen *et al.*, 1984) that the receptive field size,

which is related to visual acuity, is larger at the fovea than values of M would indicate. Tolhurst and Ling suggested that the human linear magnification factor should be 1.6 times greater than that in the macaque, based on the anatomical differences between human and monkey striate cortex. Human visual cortex is greater in area and has wider columnar structures. Since the writers approximated M_0 for macaque to be on average about 15 $mm/_{deg}$ (based on the results of Tootell *et al.*, 1982; Van Essen *et al.*, 1984, cited erroneously as 16 $mm/_{deg}$ instead of 13 $mm/_{deg}$, and Dow *et al.*, 1981), they estimated that the corresponding human value should be about 20 - 25 $mm/_{deg}$ rather than the widely accepted 8 - 11 $mm/_{deg}$. It was stated that M will fall by a factor of about 12 - 18 as the eccentricity is increased to 10 deg. This suggests M_{10} of about 1.5 $mm/_{deg}$ thus, E_2 becomes 0.71 deg (equation *3.05*).

Table 3.03: Some estimates of M_0 and E_2 in man

Investigators	M_0 ($mm/_{deg}$)	E_2 (deg)	based on
Richards (1971)	12	0.68	(migraine scotomas)
Cowey & Rolls (1974)	13	1.48	(Brindley & Lewin, 1968, foveal value extrapolated)
Drasdo (1977)	11.5	1.69	(data from various sources)
Rovamo, Virsu & Näsänen (1978)	7.75	2.16	(Brindley & Lewin, 1968 and cone density of the centralmost cones)
Rovamo & Virsu (1979)	7.99	2.38-3.45	(data from various sources, see text)
Dobelle *et al.* (1979)	8.62	1.17	(phosphenes)
Fox *et al.* (1986)	6	----	(PET study)
Tolhurst & Ling (1988)	20 - 25	0.71	(data in literature)
Drasdo (1991)	12.86-14.4	various	(data in literature)

3.3: Magnification scaling (M-scaling)

When applying the method of magnification scaling the sizes of peripheral stimuli are adjusted according to a pre-chosen factor in an attempt to equate thresholds in foveal and peripheral vision (Rovamo, Virsu & Näsänen, 1978). According to the theory of cortical magnification (Virsu & Rovamo, 1979) thresholds should become equal at any eccentricity when the cortical area stimulated is made equal by enlarging the peripheral stimulus by the factor M_0 / M_E (where M_E is the cortical magnification at the eccentricity E deg).

In the 1980's, after the introduction of the concept of magnification scaling, there were a large number of studies applying this method when studying foveal and peripheral performance. Some had more, some had less success in their venture. Sometimes it depends

on the reader whether the task has been considered successfully scaled or not. The most cited experiments are presented here.

3.3.1: Tasks where magnification scaling has been successful

Spatial and temporal contrast sensitivity functions:

Rovamo, Virsu and Näsänen (1978) studied contrast sensitivity as a function of spatial frequency for a stationary vertical grating when either the retinal or the cortical stimulus size was kept constant. Performance declined with constant retinal representation with eccentricity (*Figure 3.14*), but with supposedly constant cortical representation sensitivity at all eccentricities become equal (*Figure 3.15*). Eccentricities studied were 0 - 30 deg and E_2 used was 2.2 deg.

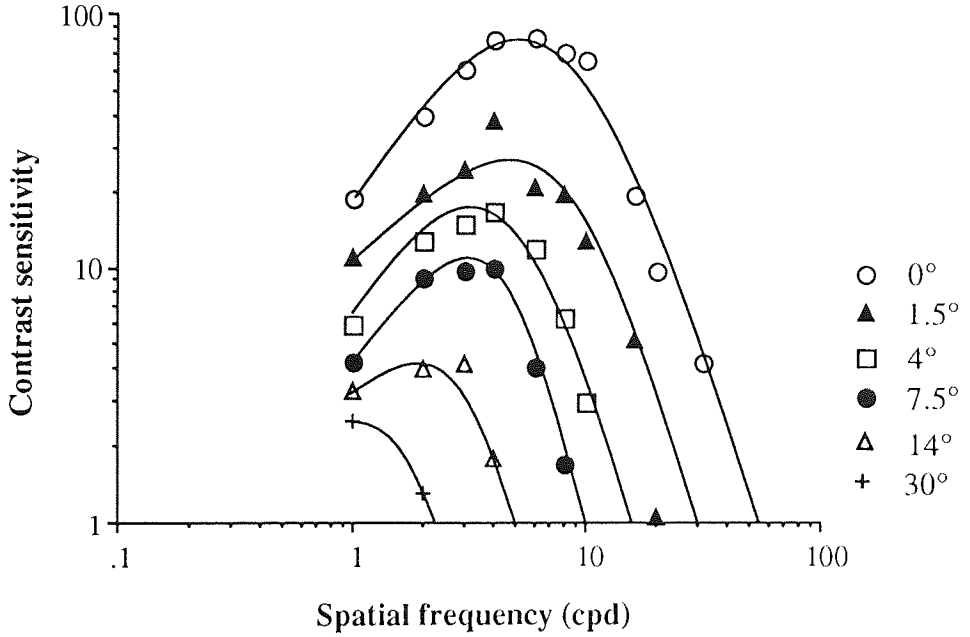

Figure 3.14: The data from Rovamo, Virsu and Näsänen (1978). Contrast sensitivity functions at various eccentricities when retinal image is constant 1 × 2 deg.

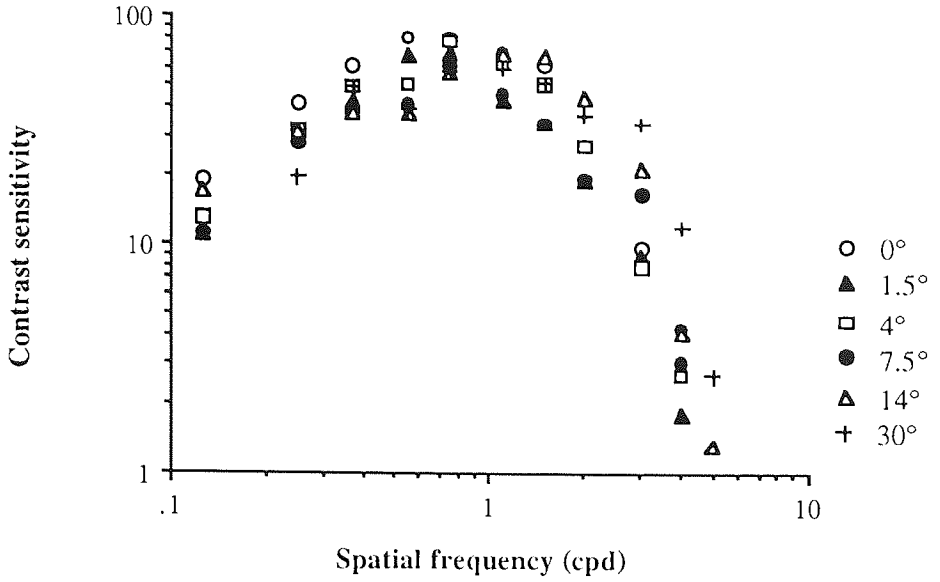

Figure 3.15: Rovamo, Virsu and Näsänen (1978), contrast sensitivity functions when retinal image is M-scaled.

Koenderink, Bouman, Bueno de Mesquita and Slappendel (1978c) used moving (4 Hz) sinusoidal gratings to study the effect of stimulus size on contrast detection thresholds at the eccentricity range of 0 - 50 deg. The sizes of the peripheral targets were increased according to the just resolvable distance at different eccentricities. At any eccentricity the target field subtended about 80 just resolvable distances (*Figure 3.16*). When expressing the spatial extent of the stimulus in units of the just resolvable distance at any eccentricity, equally high contrast sensitivities were found for the fovea and the periphery, only the sensitivity range was shifted to lower spatial frequencies in the periphery. In spite of the small systematic inferiority of the most peripheral stimuli the authors concluded that "instead of a sensitive fovea and an almost blind periphery, we have to reckon with a visual field that is more or less equally sensitive everywhere".

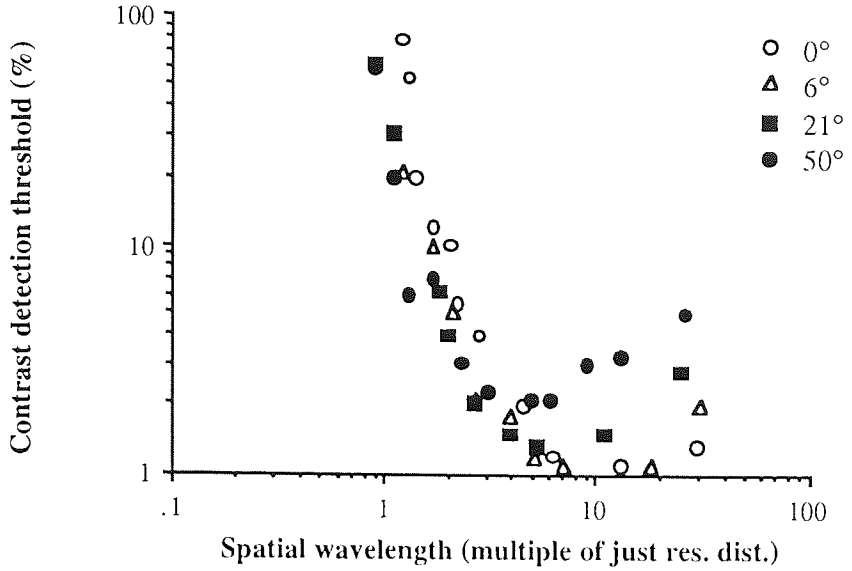

Figure 3.16: From Koenderink *et al.* (1978), their Figure 7 redrawn. Contrast detection threshold (% modulation depth) plotted against the spatial wavelength in units of just resolvable distance at any eccentricity.

Virsu and Rovamo (1979) measured the minimum contrast required for discriminating the orientation (0 deg *vs* 180 deg), or detecting steady sinusoidal gratings, as well as discriminating the direction of movement of drifting (4.1 Hz) sinusoidal gratings at the fovea and in peripheral vision. In the movement discrimination task, for instance, viewing distance was varied to change stimulus sizes according to the inverse cortical magnification (see *Table 3.02*) at the eccentricity range of 0 - 30 deg assuming $M_0 = 7.75$ mm/$_{deg}$. E_2 was thus 2.16 deg. (Estimating E_2 at the eccentricity range of 0 - 15 deg would produce a value of 2.79 deg. This difference is due to the increasing slope of the magnification curve as a function eccentricity). The foveal stimulus size was 1 deg. Spatial frequencies within the stimulus area ranged from 0.129M - 8.26M cpd at each eccentricity, corresponding, for example, to 1 - 64 cpd at the fovea. The pre-determined stimulus area for the eccentricity in question was kept constant. Sensitivity could be equated at all tasks by this scaling method. Further, acuity and resolution were found to be directly proportional to M. *Figure 3.17* shows an example of the data for contrast sensitivity as a function of spatial frequency when the task is to discriminate the direction of movement of the grating.

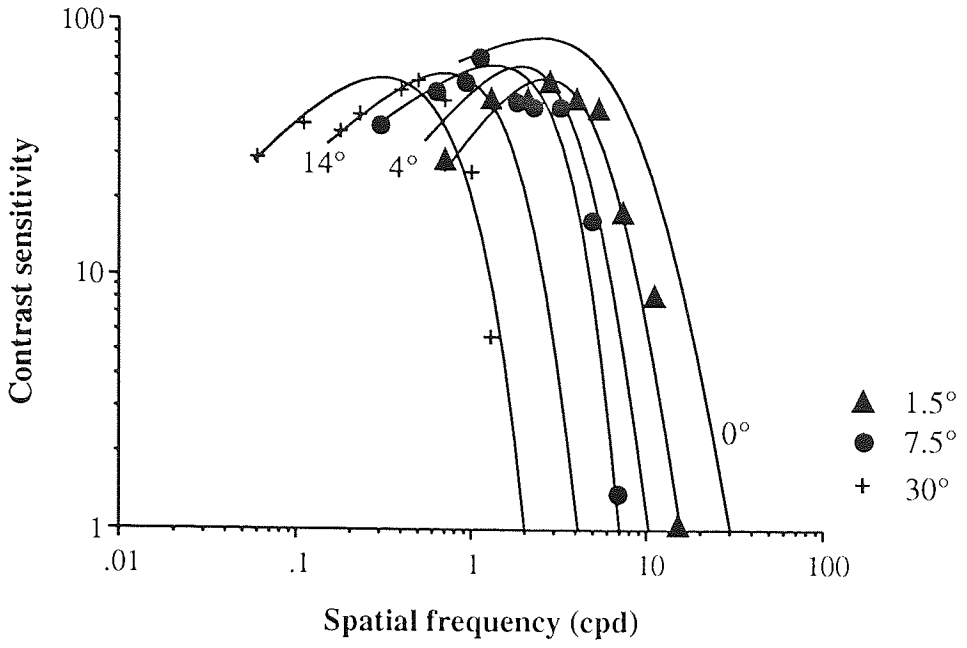

Figure 3.17: Virsu and Rovamo (1979), contrast sensitivity plotted against the spatial frequency (cpd) when the task is to discriminate the direction (left-right) of movement of the M-scaled grating in the inferior visual field. Datapoints *also in the original graph* were omitted for clarity at 0, 4 and 14 deg.

Rovamo and Virsu (1979) measured the contrast sensitivity functions for discriminating the direction of movement of sinusoidal gratings and detecting stationary gratings. Contrast sensitivity was measured in both tasks at the four principal meridians of the visual field using stimuli that were scaled according to the equations in *Table 3.02*. In all cases almost all eccentricity dependent differences in sensitivity could be equalised by scaling (multiplying) the sizes of the test gratings by the inverse of M. In *Figure 3.17* the sensitivity curves were expressed as a function of cycles per degree of visual field. *Figure 3.18* shows the grating frequencies in cortical terms, in cycles per mm of the cortex.

As is seen for the data in *Figure 3.18* the high-frequency limbs of the sensitivity functions could not be scaled adequately by this method. The authors suggested that this was due to the optical transfer function of the eye, which attenuates the high cortical spatial frequencies more for foveal than for peripheral stimuli.

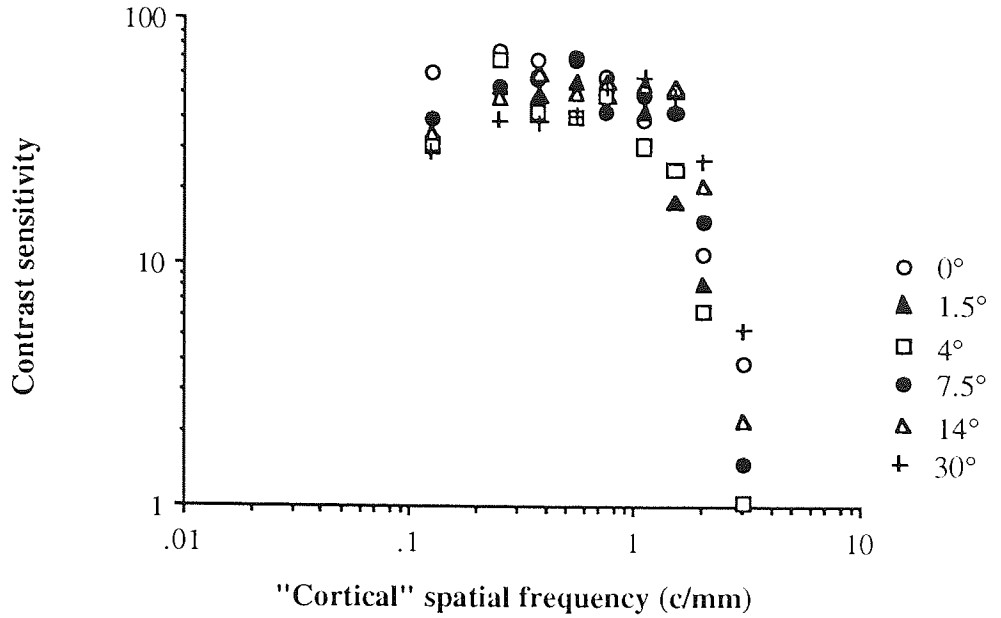

Figure 3.18: Rovamo and Virsu (1979) presented the same data for the inferior meridian (here redrawn) as in their previous article and in *Figure 3.17*, but now spatial frequency was expressed in cycles per millimeter on the cortex. The graphs from other meridians were essentially similar.

Virsu, Rovamo, Laurinen and Näsänen (1982) repeated the study of contrast sensitivity functions in the nasal visual field. This time the temporal properties of the grating were varied at various rates up to 25 Hz. Thus, the gratings were either stationary, or temporally modulated (moving, counterphase flickering or on-off flickering). The temporal contrast sensitivity functions became similar at all eccentricities when the gratings were normalized in area, spatial frequency and translation velocity so that cortical representations became equivalent (see Rovamo & Virsu, 1979). On this basis, the authors concluded that foveal and peripheral vision are qualitatively similar in spatiotemporal visual performance.

Kelly (1984) measured spatiotemporal contrast sensitivity for a circular cosine target with fixation at the centre. The stimulus extent, which was altered by changing the viewing distance, was increased first according to an E_2 of about 5 deg for the eccentricities studied (0, 3, 6 and 12 deg). *Figure 3.19* illustrates contrast sensitivity as a function of spatial frequency when the concentric grating zones flickered at 0.5 Hz. The spatial frequencies corresponding to the maximum sensitivities were estimated on the basis of the sensitivity curves as 1, 1.5, 2, and 3 cpd. Kelly presented a formula to equate the scaling functions at different eccentricities: $f_s = 3/(1 + 0.174E)$, where E = eccentricity and f_s = spatial frequency of the concentric grating in cpd. This formula has the same form as the equation *3.03*, thus 0.174 corresponds to S. E_2 therefore becomes 5.7 deg.

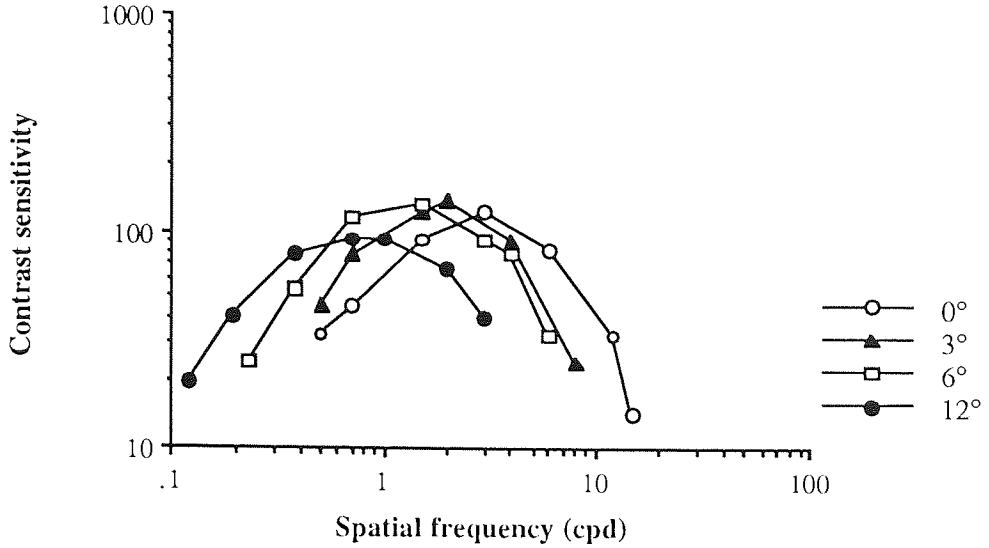

Figure 3.19: Kelly's (1984) Figure 5 redrawn. Contrast sensitivity functions (here shown unscaled) were measured at 0.5 Hz flicker rate for concentric annular zones filled with concentric cosine patterns.

When spatial frequency and stimulus extent was varied according to this formula, it was possible to equate contrast sensitivity functions of different temporal (0.5 - 30 Hz) and spatial frequencies. High spatial frequencies (3, 2, 1.5, and 1 cpd at 0, 3, 6 and 12 deg eccentricities, correspondingly) produced a lowpass sensitivity curve (not shown), whereas (in *Figure 3.20)* low spatial frequencies (0.5, 0.375, 0.25, and 0.167 cpd at 0, 3, 6 and 12 deg eccentricities, correspondingly) produced a bandpass sensitivity curve at any one eccentricity.

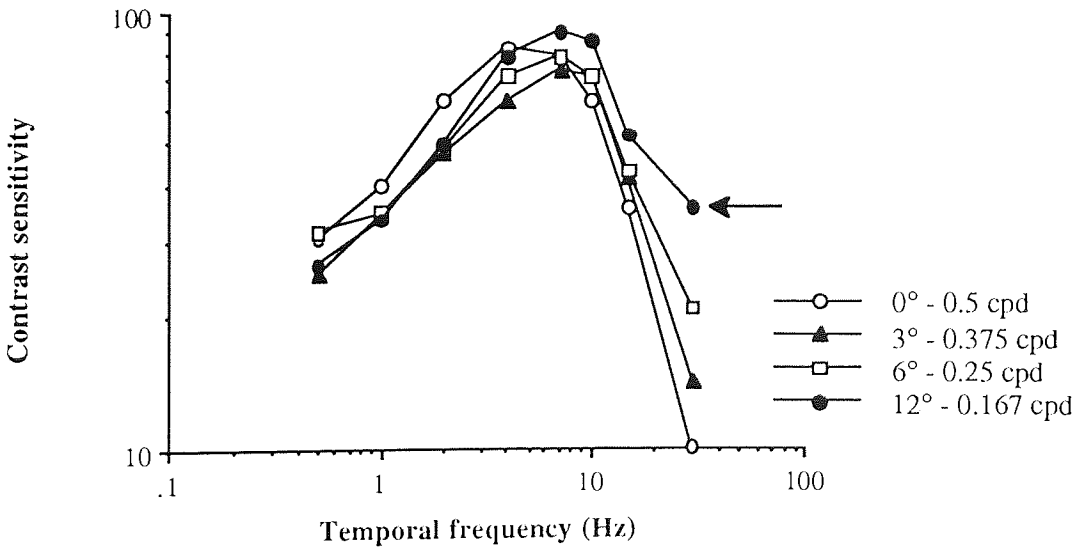

Figure 3.20: Kelly's (1984) Figure 8 redrawn. The bandpass shape of the sensitivity curves, as well as the supersensitivity at high temporal frequencies in the periphery, are visible.

According to the results, it was possible to equate flicker sensitivity at different eccentricities by varying the spatial properties of the stimulus with one exception. This exception occurred at high (above 10 Hz) temporal frequencies, where the peripheral (12 deg eccentricity) sensitivity for low spatial frequencies was systematically higher than at small eccentricities (*Figure 3.20*). Repeating the experiment with patternless flickering zones gave the same result. The supersensitivity of the periphery to large-area, high frequency flicker was suggested in the study, and will be confirmed in the flicker experiment presented in this thesis.

Colour vision:

The perceived appearance of a coloured, constant size stimulus changes and it may appear completely colourless when it is moved far enough in the visual periphery (Purkinje, 1825). The hue may change (the change depends on the wavelength) and the perceived saturation decreases towards the periphery. Moreland and Cruz (1959) found that colour vision deteriorated into dichromatism (red-green blindness) at 25 - 30 deg and to monochromatism (total colour blindness) at 40 - 50 deg eccentricity when a stimulus field subtended about 1 deg. Wooten and Wald (1973), however, showed that three colour mechanisms existed at eccentricities up to 80 deg. Gordon and Abramoff (1977) found that when stimulus size is adequate, a full range of saturated, foveal-like hues are perceived even at 45 deg eccentricity. Gordon and Abramoff (1977) concluded that ".. it is misleading to term the peripheral retina colour blind, or even colour deficient. The quality of colour vision in the periphery depends critically on stimulus size." Full saturation of the hues for even the largest stimulus sizes, however, is possible only up to 20 deg eccentricity according to Abramoff, Gordon and Chan (1991).

Noorlander, Koenderink, den Ouden and Edens (1983) determined contrast detection thresholds for spatiotemporal colour modulation and colour discrimination at several retinal locations. In the nasal retina the maximum eccentricity was 90 deg. Contrary to to the early assumptions, it was found that, with a suitable enlargement of the target size, colour discrimination in the periphery was comparable to that at the fovea. There were no colour blind areas even at the highest eccentricities measured for red-green modulation. E_2 which equated the foveal and peripheral performance in the spatiotemporal colour discrimination task was 0.81 deg.

van Esch, Koldenhof, van Doorn and Koenderink (1984) measured wavelength discrimination along the nasal retinal meridian. The stimulus size was increased according to an E_2 of 2.88 deg (based on Rovamo & Virsu, 1979). An alternating stimulation method was used, where the standard and the test field were presented to the subject alternately at 2 Hz

temporal frequency. The task was to adjust the test field until no flicker was perceived. Wavelength discrimination was found to become roughly the same from 8 to 80 deg eccentricity, although foveal wavelength discrimination was always better than peripheral wavelength discrimination.

Movement tasks :

Foster, Thorson, McIlwain and Biederman-Thorson (1981) studied the fine-grain movement illusion. In this illusion the presentation of two very closely spaced point stimuli in rapid succession causes the impression that a single dot moves over a considerable extent. The extent of the illusory distance varies from about 2 to 6 deg when the eccentricity changes from 10 to 24 deg. When mapped onto visual cortex by means of human cortical magnification factor (Cowey & Rolls, 1974), the illusion extent was found to be about 3 mm regardless of eccentricity. van de Grind, van Doorn and Koenderink (1983) studied the detection of coherent motion in stroboscopically moving random-dot patterns at the fovea and at 6 - 48 deg eccentricities. When the stimuli were size-scaled according to M (Drasdo, 1977) to obtain equivalent cortical sizes and velocities at all eccentricities, motion detection performance became roughly invariant throughout the temporal visual field.

McKee and Nakayama (1984) measured differential velocity (referenced movement) detection and velocity discrimination up to 40 deg eccentricity. When velocity was expressed as cortically scaled velocity (resolution units / sec), thresholds were rendered equal at the eccentricities studied. Baker & Braddick (1985) studied short range apparent motion using random dot arrays. d_{min}, the minimum displacement giving detectable motion, was found to increase with eccentricity according to cortical magnification. However, d_{max}, the maximum value of the displacement that still creates the perception of movement, increased more rapidly with retinal eccentricity.

Johnston and Wright (1985) investigated the lower threshold for motion of a grating as a function of eccentricity (up to 7.5 deg in the upper visual field), spatial frequency, and contrast. For grating contrasts above 0.05 foveal and peripheral lower thresholds of motion could be equated by using the values of Rovamo and Virsu (1979) and increasing the overall size of the peripheral stimulus in proportion to $1/M$. Viewing distance was reduced to increase the stimulus size with eccentricity.

Wright and Johnston (1985a) measured the threshold displacement amplitude for detecting square wave oscillatory motion of a sinusoidal grating. Threshold displacement amplitude was greater for peripheral stimuli, but when scaled inversely with the cortical magnification factor (Rovamo & Virsu, 1979), threshold displacements became equivalent in cortically

scaled units. Wright and Johnston (1985b) also studied motion after-effects for drifting gratings by varying the spatial frequency, size, temporal frequency and contrast. After adaptation to a moving grating the stimulus grating was adjusted to appear steady and this velocity was called cancellation velocity. Cancellation velocity expressed in cpd increased linearily with eccentricity and could be made approximately constant when expressed as an M-scaled velocity in cycles per mm of cortex (according to estimates of Rovamo & Virsu, 1979).

Other tasks:

Texture discrimination at different eccentricities was studied by Saarinen, Rovamo and Virsu (1987). The observer was shown a dot array whilst it appeared either i) evenly granular or ii) one half of the array appeared more granular (more unevenly distributed) than the other half. Eccentricities up to 25 deg in nasal visual field were studied. With M-scaled textures (Rovamo & Virsu, 1979) discrimination became practically independent of eccentricity.

Visually evoked potentials (VEP) are electrical potentials at the occipital cortex that occur during visual stimulation by, for example, checkerboard patterns. The check size producing the greatest amplitude for visually evoked potentials is larger in peripheral vision than at the fovea (Harter, 1970). Meredith and Celesia (1982) (also Celesia & Meredith, 1982) tested three subjects presenting a pattern reversing checkerboard stimulus monocularly at 0, 8 and 14 deg nasal retinal eccentricities. Field sizes were estimated to activate an equivalent amount of visual cortex by using the cortical magnification suggested by Cowey and Rolls (1979). The scaled stimuli produced VEPs of similar amplitude at each eccentricity tested.

Ransom-Hogg and Spillmann (1980) measured the sizes of perceptive fields at the fovea and along the horizontal meridian of the nasal retina at eccentricities up to 70 deg. They used Westheimer's paradigm, where the increment threshold for a briefly flashed small test spot is measured against several background diameters. With increasing background diameter threshold first rises, then falls, and eventually reaches a plateau. The background diameter corresponding to the highest threshold reveals the size of the perceptive field centre, whereas the background diameter corresponding to the beginning of the plateau indicates the total size of the perceptive field (Westheimer, 1965). Perceptive field size was found to correlate remarkably well with the inverse of the magnification factors calculated by Cowey and Rolls (1974). Since M is believed to be proportional to ganglion cell density, and the measured field sizes were inversely related to M, it was suggested that field sizes would also be inversely proportional to ganglion cell densities at different eccentricities.

Hampton and Kertesz (1983a) studied the extent of Panum's areas (areas of maximum

fusible disparity in deg of visual field for a target presented separately to each eye) with increasing eccentricity for eight different meridians. Panum's areas increased with eccentricity at approximately the rate predicted by cortical magnification (Rovamo & Virsu, 1979).

Tilt-aftereffect (the apparent tilt of a line or a grating following adaptation to a line or grating of a slightly different orientation) was studied by Harris and Calvert (1985) (also Calvert and Harris, 1986). For a constant size stimulus (diameter 2 deg) the effect grew larger with increasing eccentricity. When stimulus area increased with eccentricity and the spatial frequency within the area remained unchanged, tilt aftereffect still increased with eccentricity, although slower. When both the size and the spatial frequency of the gratings were made cortically equal (Rovamo & Virsu, 1979), no significant increase in tilt after-effect with eccentricity was observed.

Nothdurft (1985) investigated the ability to discriminate structured areas of different texture orientation. Line arrays consisting of 25 lines were presented in this experiment (for one subject) at temporal retinal eccentricities up to 30 deg. Line length and raster width were varied together systematically, so that the lines were always five times the length of the threshold length that had been measured previously for texture orientation detection. When the stimulus size was scaled in this manner, orientation detection threshold remained the same with increasing eccentricity. This was taken to support the concept of magnification scaling (Virsu & Rovamo, 1979).

Swanson and Wilson (1985) modelled spatial vision in peripheral vision by scaling the peak frequency of the spatial filters with eccentricity. On the basis of contrast detection data at the fovea and at 8 deg eccentricity in the temporal visual field the scaling factor at 8 deg eccentricity was estimated from the horizontal shift of the 0 and 8 deg sensitivity *vs* spatial frequency curve to be 2. Stimuli were Gaussian modulated gratings extending 1.5 × 8 deg at the fovea and 3 × 16 deg at 8 deg eccentricity. The E_2 used to increase the stimulus size with eccentricity in the experiment was thus 8 deg, which is an unusually large value for a contrast detection task. However, this factor was found to equate the foveal and 8 deg eccentricity data obtained in suprathreshold matching task.

3.3.2: Tasks where magnification scaling has not been successful

Temporal aspects of vision, as well as binocular tasks and spatially demanding tasks have been problematic when M-scaling has been attempted.

Westheimer (1983) measured temporal order detection as a function of line separation at the fovea and up to 20 deg eccentricity along the left horizontal and lower vertical meridian.

Viewing was binocular. Two adjacent vertical lines were presented in asynchrony and the order of presentation was to be detected. The length of the line stimuli used in the experiment (not a critical variable at least at the fovea, Westheimer & McKee, 1977b) was 12 min.arc at the fovea and 60 min.arc at 20 deg eccentricity. This corresponds to E_2 of 5 deg. The results indicated little difference between foveal and peripheral thresholds measured in msec, which is not surprising, since a spatial measure was not in question. A more important observation was that the optimum separation for the lines increased far more slowly with eccentricity (E_2 = 15 deg for two subjects) than visual acuity or cortical magnification would suggest.

Jamar, Kwakman and Koenderink (1984) measured the detectability of amplitude modulation and frequency modulation of suprathreshold sinusoidal gratings from 0 to 30 deg in the nasal visual field. Stimulus sizes were increased with eccentricity according to an E_2 of 2.1 deg. This scaling procedure, which had equated contrast sensitivity functions, could not produce high enough sensitivities in periphery in the case of amplitude modulation and frequency modulation.

Rovamo and Raninen (1984) were not able to equate foveal and peripheral critical flicker frequency (CFF) with M-scaling. Peripheral CFF always exceeded that at the fovea. CFF became independent of eccentricity only, when the luminance of the peripheral stimulus was reduced in inverse proportion to Ricco's area (the estimated receptive field centre) at each eccentricity.

Fendick and Westheimer (1983) found that stereoacuity up to 10 deg could not be equated with that at the fovea by scaling the sizes of the peripheral squares used as stimuli. Disparity thresholds for optimal target separation declined faster towards periphery than did the minimum angle of resolution especially between the fovea and 5 deg eccentricity. The stimulus size was increased according to an E_2 of 2.5 deg. The two squares of the foveal stimulus had a side length of 4 min.arc, the separation was varied at all eccentricities to find the optimum.

Hampton and Kertesz (1983b) determined the horizontal fusional vergence response when both the length of the line stimulus and the dichoptically produced disparity were M-scaled (Rovamo & Virsu, 1979). Eccentricities up to 20 deg were studied along eight meridians. As stimulus eccentricity increased, vergence movements compensated for a smaller portion of the disparity. Variations in vergence at different eccentricities could not be removed by M-scaling.

Stephenson and Braddick (1983) and Stephenson, Knapp and Braddick (1991) studied the discrimination of the relative phase of two grating components at the fovea and up to 10.9 deg eccentricity. When comparing contrast sensitivities for the third fundamental of the

waveform presented alone and the discrimination between two different waveform combinations (peaks add and peaks subtract condition for first and third harmonics), the discrimination task declines with eccentricity faster than the ability to detect the 3rd fundamental alone even when the grating sizes are M-scaled (Rovamo & Virsu, 1979).

Rentschler and Treutwein (1985) compared performance at the fovea and at 2 deg eccentricity using a compound grating consisting of a fundamental and its third harmonic. When the two gratings (comparison and test grating) presented sequentially at the same retinal location were mirror images with no other difference between their local contrasts, peripheral discrimination sensitivities approached chance level even when the grating was scaled in size (Rovamo & Virsu, 1979). When the fundamental and the third harmonic were presented so that the phase shift produced a difference in local contrasts between the test and the comparison grating, discrimination became nearly equal with that at the fovea when the stimulus was M-scaled. It was concluded that peripheral vision ignores the relative position of image components independently of scale.

Saarinen (1988) investigated the detection of mirror symmetry at the fovea and in the periphery. Stimulus patterns consisted of small dots and the task was to determine whether the briefly flashed stimulus pairs were mirror symmetric, or whether the dots were randomly distributed within the patterns. Detectability of mirror symmetry declined with increasing eccentricity even when the stimulus sizes were M-scaled (Rovamo & Virsu, 1979), although the decline was slower than for the constant size stimuli.

Both Westheimer (1982) and Levi, Klein and Aitsebaomo (1985) found that vernier acuity declined faster with increasing eccentricity than the estimates of M by Rovamo and Virsu (1979) would suggest. Westheimer (1982) used a constant stimulus size in his two dot vernier experiment, eccentricities studied were up to 10 deg along the left horizontal meridian, and viewing was binocular. In contrast to vernier thresholds, the dot separation which produced optimum thresholds increased relatively slowly with increasing eccentricity. Since vernier threshold and dot separation are both spatial measures, one would expect them to change at approximately the same rate, which obviously was not the case. Levi *et al.* (1985) found that vernier acuity scaled to the estimate of cortical magnification proposed by Dow *et al.* (1981), which was based on *macaque fascicularis*. This was taken to suggest that vernier acuity scaled according to *cortical* magnification whereas contrast sensitivity and visual acuity reflected the limitations in *retinal* processing caused by cone sampling, as Westheimer (1982) had already tentatively suggested.

Beck and Halloran's (1985) results indicated that, for a two dot vernier task over the limited range between 2 and 8 deg, thresholds were independent of eccentricity. However, this was

due to the use of a large foveal dot separation. This represents a classic example of how an initial choice of stimulus parameters can lead to serious distortions in the rate of change of visual performance with increasing eccentricity as will be discussed later. Virsu, Näsänen and Osmoviita (1987) succeeded in scaling a two-dot vernier task according to the estimate of cortical magnification proposed by Rovamo and Virsu (1979) based on retinal ganglion cell density using an E_2 of 3 deg.

It has been impossible to successfully apply any single factor or two factors ("retinal" and "cortical") to all types of visual tasks. Therefore, it is more sensible to determine the increase of the peripheral stimulus size on the basis of obtainable psychophysical data, a procedure which runs throughout this thesis, and which is called spatial scaling.

3.4: Spatial scaling

Because of the problems associated with the use of pre-chosen magnification factors, several authors (Johnston & Wright, 1986; Watson, 1987; Johnston, 1987; Wright, 1987; Saarinen, Rovamo & Virsu, 1989) have used an experimental procedure which avoids the need for an initial choice of a magnification factor at any eccentricity. Instead, thresholds for a sequence of stimuli which are all magnified versions of each other are measured at the fovea and at various eccentricities. Thresholds are then plotted against stimulus size for each retinal location and the amount the threshold functions are displaced relative to one another reveals the rate at which the stimulus size has to be increased with eccentricity for equivalent performance. Similar procedures have been previously used by Wilson (1970) and Lie (1980) although a scaling procedure was not consciously attempted and differences in scaling factors as a function of eccentricity were not analysed.

Wilson (1970) studied the area of complete spatial summation at 5 - 55 deg eccentricities for detection of a luminance increment against a steady background. He found that the critical area for spatial summation (representing the psychophysical measure for a receptive field centre) increases towards the periphery and spatial summation curves for different eccentricities could be superimposed along the log area axis. He suggested that, in the case of spatial summation, when the location of the stimulus is varied, only the spatial scale of the visual system changes.

Lie (1980) compared area-threshold functions for detection and resolution at various retinal eccentricities. The stimulus was a square presented randomly in two positions, as a square or a diamond. The detection threshold was reached when the observer just saw the target. For resolution threshold the observer had to discriminate between the square and the diamond. Area, contrast and eccentricity of the stimulus was varied. 23 locations were investigated

along the horizontal meridian ranging from 45 deg eccentricity in the nasal visual field to 60 deg eccentricity in the temporal visual field. The resulting threshold curves were slightly different in shape between detection and resolution tasks, but within a task the curves obtained at various eccentricities could be superimposed along the log size (in visual angle) axis.

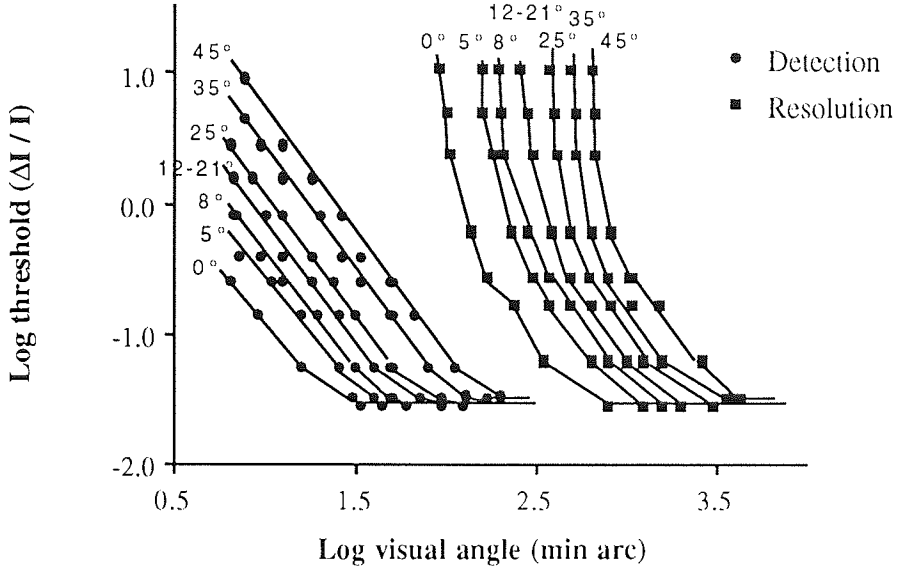

Figure 3.21: Photopic area-threshold curves redrawn from Lie (1980), temporal retina. The resolution curves are displaced 2 log units to the right along the size axis for clarity.

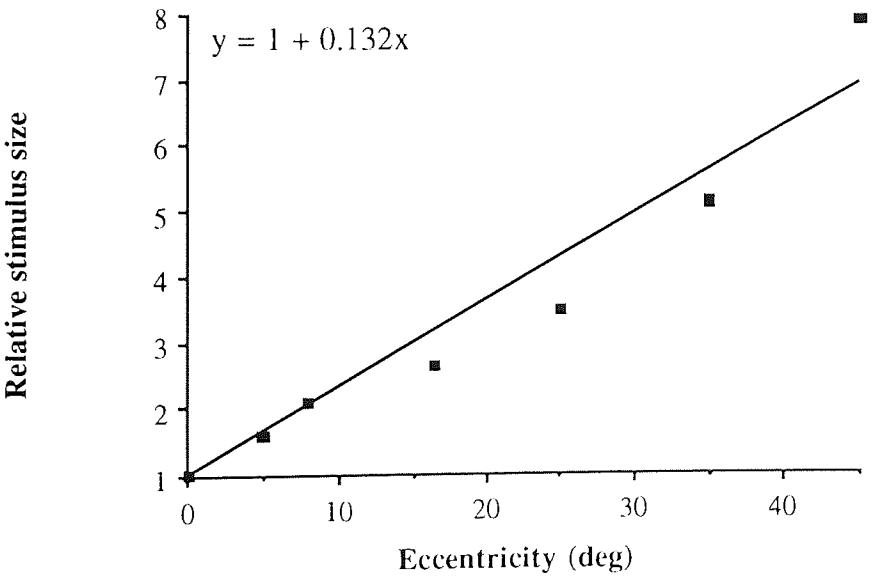

Figure 3.22: The relative stimulus sizes based on the detection data of Lie (1980) plotted against eccentricity. The regression line has a gradient (S) of 0.132 thus, E_2 = 7.58 deg.

The E_2 for the detection task can be determined by estimating the shift needed to superimpose the eccentric threshold curves onto the foveal curve. This estimate gives the relative stimulus size for equivalent performance at each eccentricity. When plotted against eccentricity (*Figure 3.22)* the regression line fitted to the data points gives the slope (S) of 0.132. Thus, E_2 becomes 7.58 deg (equation 3.04). When only the small eccentricities below 25 deg are considered, S = 0.107 thus, E_2 = 9.35 deg due to the nonlinearity of the data.

Johnston and Wright (1986) determined the apparent velocity and lower thresholds of motion for peripheral, drifting sinusoidal gratings as a function of eccentricity and viewing distance. Velocities appeared lower in the periphery. The peripheral gratings were increased in size by reducing the viewing distance. Thus, the number of cycles was constant and only spatial and temporal frequency changed between each target. Thresholds for each viewing distance were measured foveally and peripherally at 3 - 25 deg eccentricities. The log threshold functions of each eccentricity were plotted against log spatial frequency (*Figure 3.23).*

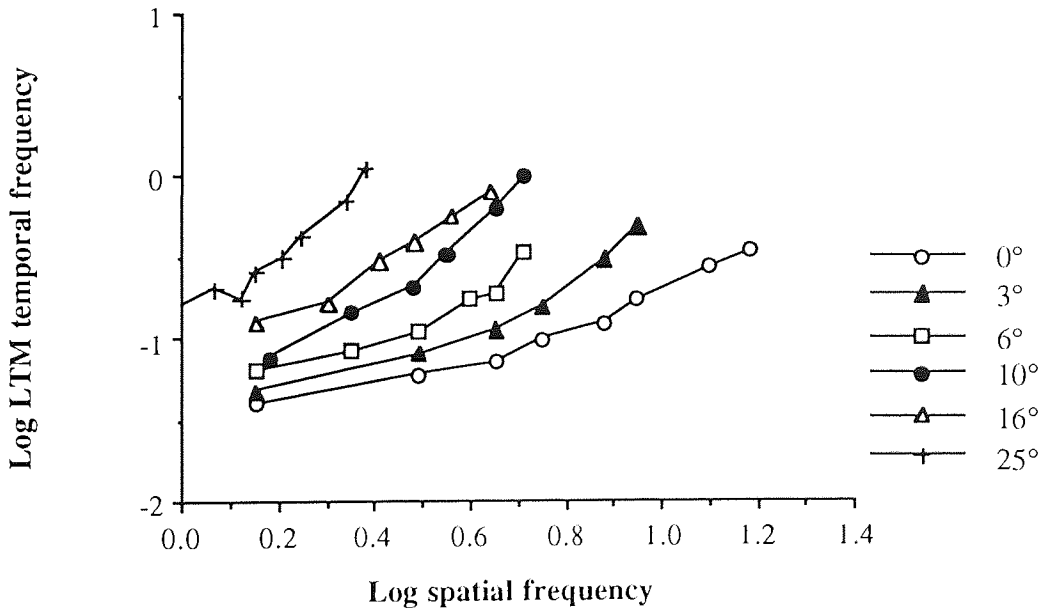

Figure 3.23: Lower thresholds of motion (LTM) plotted as a function of spatial frequency, redrawn from Johnston and Wright (1986).

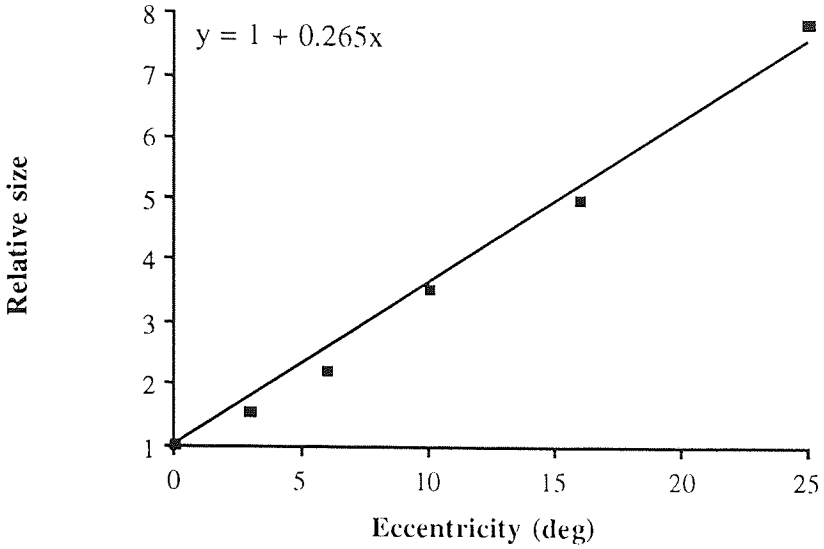

Figure 3.24: Relative stimulus sizes, based on visual inspection of the threshold functions in *Figure 3.23*, plotted against eccentricity. The regression line indicates a gradient 0.265 thus, E_2 = 3.77 deg.

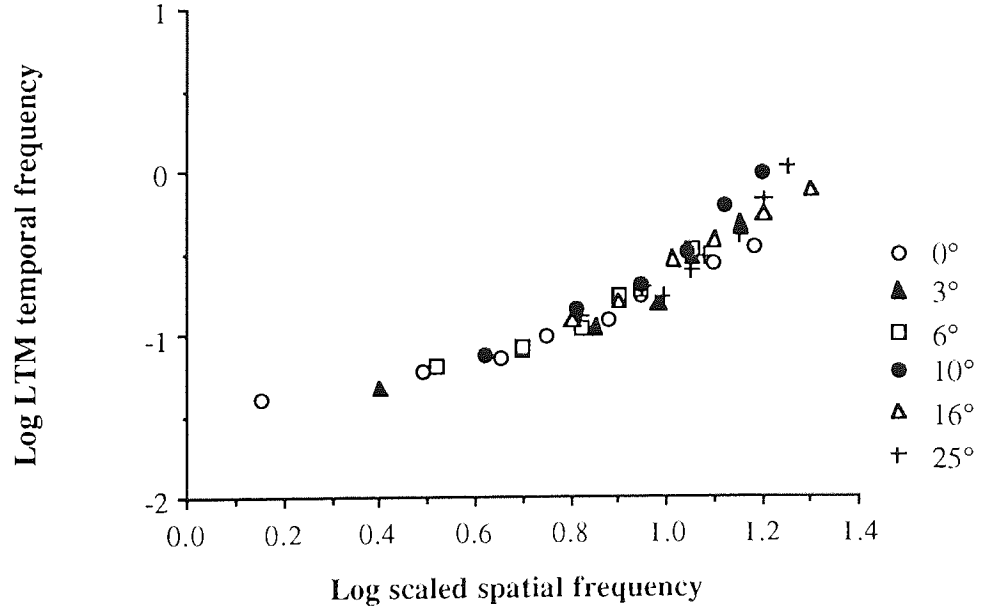

Figure 3.25: LTM plotted as a function of scaled spatial frequency.

Peripheral threshold functions could be superimposed by eye with the foveal function and the amount of transposition at each eccentricity gave the relative stimulus size, i.e. the scaling factor, for equivalent performance for the eccentricity in question. Apparent velocities at the fovea and in the periphery could thus be matched by increasing the size of the peripheral gratings. Lower thresholds of motion produced the same scaling factors as the velocity matching task, the analysis for the data of subject MW is shown in *Figures 3.23 - 3.25.*

Watson (1987) used a set of Gabor functions which were all magnified versions of each other. The size of the functions differed from each other by a factor of two. Each target, therefore, had a constant number of cycles and successive targets changed in spatial frequency by a factor of two.

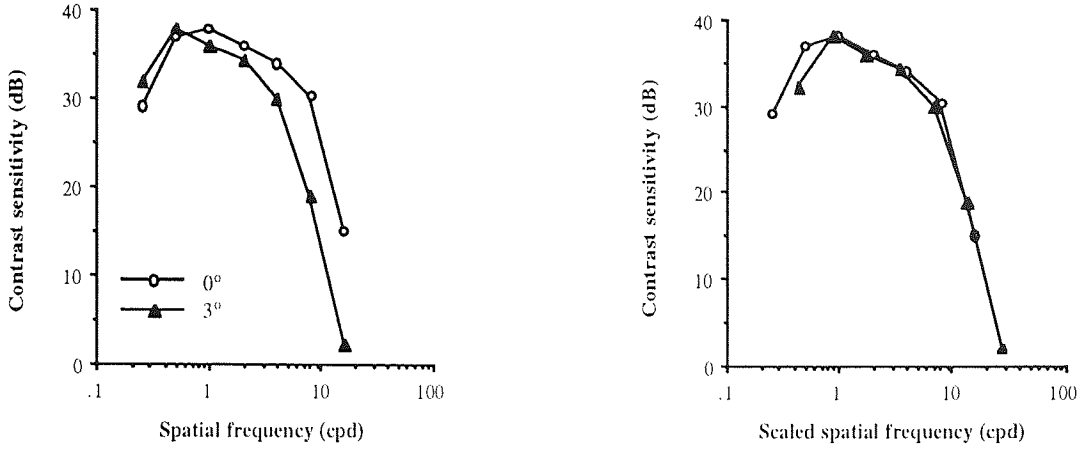

Figure 3.26: Contrast detection thresholds for size-scaled Gabor stimuli, redrawn from Watson (1987). Left panel: Contrast thresholds plotted as a function of spatial frequency. Right panel: Peripheral data is shifted to right to superimpose the foveal data.

Eccentricities of 0 and 3 deg were studied. Contrast thresholds for each target were first measured foveally to obtain a sensitivity function. The same set of targets was then used at an eccentric point to obtain another contrast sensitivity function. The scaling factor was given by the amount that was needed to shift the second sensitivity function in alignment with the first. The scaling factor for 3 deg eccentricity is 1.72. Therefore, $1.72 = 1 + E / E_2$ and E_2 becomes 4.17 deg. Although scaling was largely successful (*Figure 3.24*), the lowest spatial frequency targets failed to match properly. Watson suggested that this was due to the extended nature of the largest targets, since all parts of the stimulus were not at the same eccentricity. With a large stimulus the results do not represent the local spatial scale but some average scale across the stimulus area.

Johnston's (1987) method of scaling was similar to that of Watson (1987). Contrast sensitivity was measured as a function of spatial frequency at various eccentricities in the nasal visual field for a selection of grating sizes. In *Figure 3.27* sensitivity curves for vertical gratings for subject AJ are plotted against spatial frequency. As with Watson's data the high-frequency limbs of the functions could be superimposed by a shift along the log spatial frequency axis.

Figure 3.27: An example of the results of Johnston (1987). Contrast sensitivity for a vertical sinewave grating is plotted against spatial frequency

In *Figure 3.28* the scaling factors for *Figure 3.27* are shown as a function of eccentricity. The factors do not increase linearly so, adequate scaling of the sensitivity functions with one common factor is not successful. The E_2 within 20 deg eccentricity becomes 5.41 deg (S = 0.185) but clearly smaller (S = 0.342 thus, E_2 = 2.92 deg) within 40 deg eccentricity due to the nonlinearity of the scaling factor values. In *Figure 3.29* the sensitivity functions are presented as in Johnston (1987), simply shifted by the amount that gives the smallest deviation from the foveal curve.

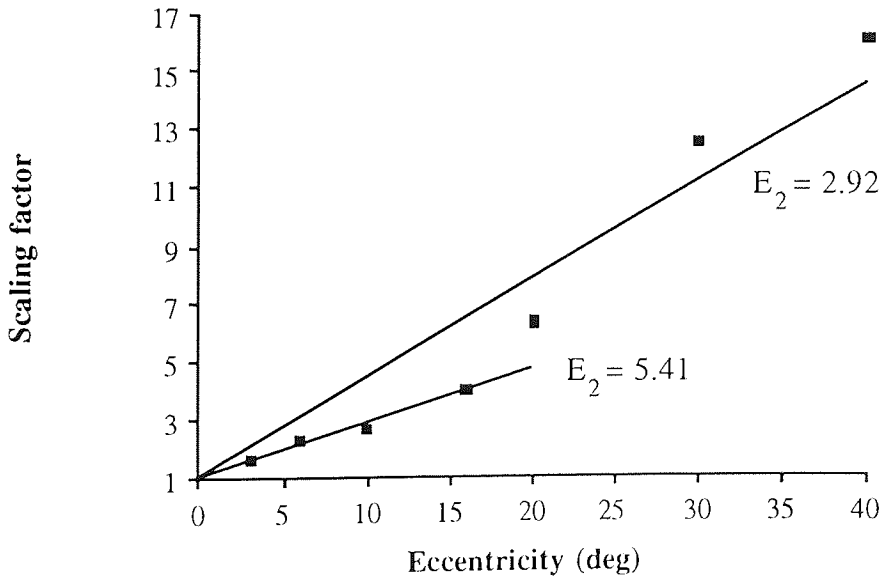

Figure 3.28: Scaling factors based on *Figure 3.27* plotted against eccentricity.

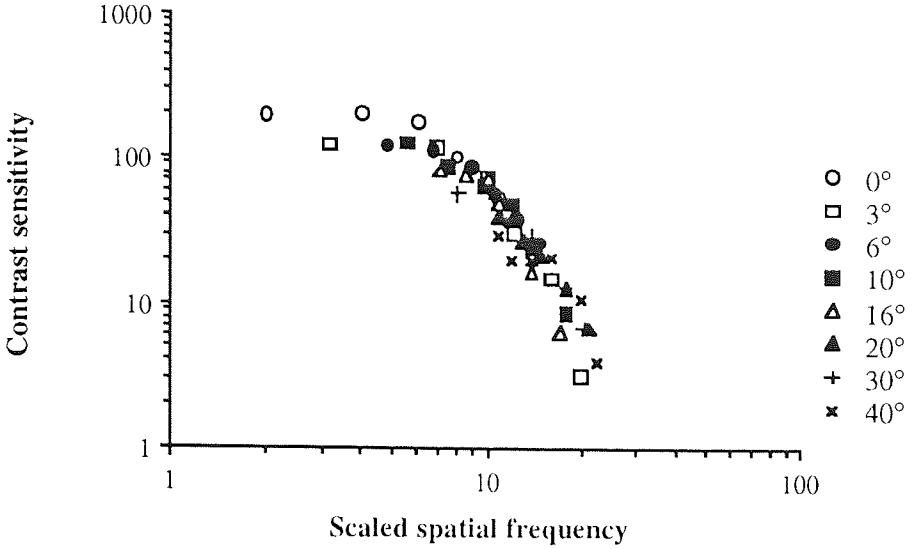

Figure 3.29: Contrast sensitivity curves from *Figure 3.27* plotted against scaled spatial frequency.

In the experiment of Saarinen, Rovamo and Virsu (1989) the subject had to decide whether two simple line patterns were identical or mirror symmetrical (*Figure 3.30*). Viewing distance was varied to obtain different stimulus sizes at each eccentricity. Separate psychometric functions for correct detection as a function of size were obtained at each eccentricity.

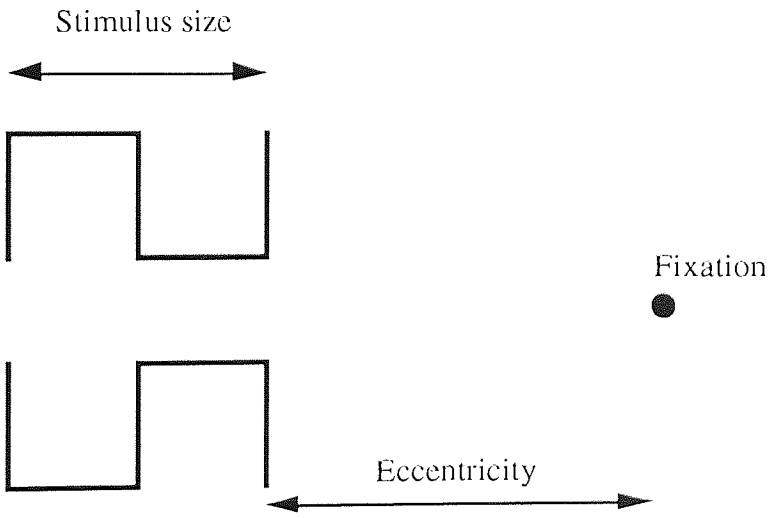

Figure 3.30: Stimulus configuration used by Saarinen, Rovamo and Virsu (1989).

The stimulus size producing 75% correct responses was plotted against eccentricity and the gradient was compared with the Rovamo and Virsu's (1979) and Levi, Klein and Aitsebaomo's (1985) predictions for the human cortical magnification factors (*Figure 3.31*). The gradient correlated well with Levi *et al.*'s prediction of rapid deterioration in performance

with eccentricity found in vernier acuity studies. This suggested that the conventional M-scaling values (Drasdo, 1977; Rovamo & Virsu, 1979) could not equate foveal and eccentric vision in this mirror symmetry task.

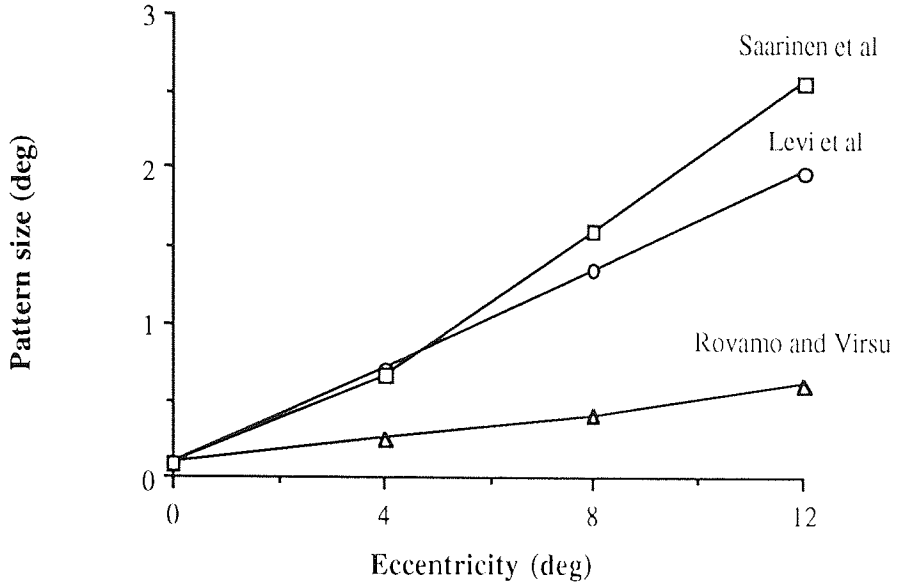

Figure 3.31: The threshold pattern size (for 75% correct) as a function of eccentricity. Also predictions for the threshold sizes applying Levi, Klein and Aitsebaomo's (1985) and Rovamo and Virsu's (1979) estimates of the human cortical magnification factor are shown. Redrawn from Saarinen, Rovamo and Virsu (1989)

3.5: Summary

This chapter has dealt briefly with human anatomy of the retina, visual pathways and the visual cortex to provide background for the concepts used when discussing magnification scaling. After defining cortical magnification, several fundamental studies have been presented, all of them aimed to determine the cortical magnification at different eccentricities. M-scaling has depended crucially on these anatomically acquired values. This dependence is unfortunate since, as has been shown, there is no clear agreement between the investigators on the actual values obtained. Several studies are presented applying M-scaling with more or less success, leading to a conclusion that just one or two magnification factors cannot possibly explain performance in all tasks. Thus, a method such as spatial scaling is preferable. The spatial scaling method is presented by describing studies that have used the method. The spatial scaling procedure is presented in more detail in *Chapter 4.8*.

Chapter 4: General methods

4.1: Threshold and the psychometric function

Were there some testing value, above which a stimulus was always seen, and below which it was never seen, that value would be considered as threshold. Unfortunately, the responses of the human visual system are not this simple. When responses to a particular stimulus are measured for differing testing values the level of response falls along a curve described by a sigmoidal function. It is called the *psychometric function* (*Figure 4.01*). The maximum information about the horizontal positioning of the curve can be obtained at the 50% point on the curve where the slope is steepest (Pentland, 1980). In psychophysics, *threshold* refers to the testing value which can be detected some pre-determined percentage (not necessarily 50%) of the times that it was presented at that value.

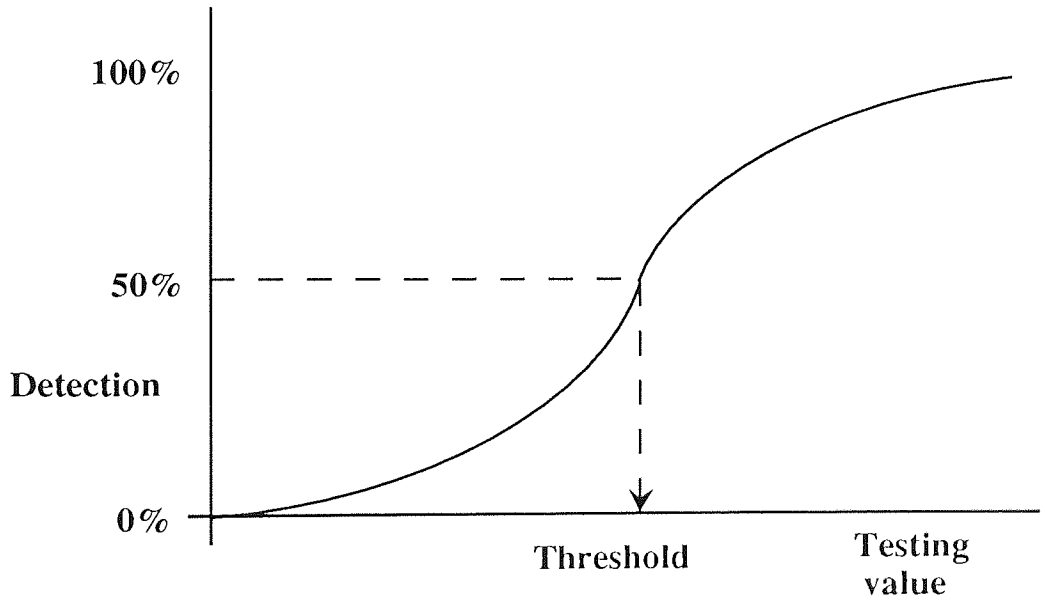

Figure 4.01: The psychometric function of a human observer.

When the testing value, e.g. contrast, of the stimulus is very low, it is never seen (detection occurs in 0% of the presentations). With high contrast the stimulus is always seen (detection 100%). At intermediate levels the stimulus is sometimes seen, and the reliability of detection increases with the stimulus contrast. At threshold the same stimulus can be seen on some presentations but not others. This is thought to be caused mainly by the variation in the resting discharge of the neurons in the visual pathways and the variation is called *internal noise* (N_i). Internal noise causes uncertainty for detection, because the visual system cannot distinguish the signal produced by the stimulus from the noise produced by spontaneous "misfire" from neurons. When summated in the visual system with the signal, the noise

element may facilitate a sub-threshold signal so that it becomes visible and a *false positive* response is elicited. Alternatively, the noise element may reduce a supra-threshold signal so that it can not be detected, thereby producing a *false negative* response.

If the experimental setting requires a judgment of, for example, whether a stimulus is present or not, it becomes possible to reach different thresholds by adopting different criteria. If the "present" response is given only when the observer is absolutely sure of having seen the stimulus, thresholds become higher than if the observer responds "present" even when there is some uncertainty. Similarly, two individuals with identical true threshold levels may exhibit different results because the more confident one gives positive responses without worrying about giving some false responses, whereas a more cautious individual responds positively only when being definitely sure of detection. In the latter case thresholds may become higher.

4.2: Two-alternative forced-choice procedure

Criterion dependency described above can be avoided by forcing the observer to make a decision between two alternatives (e.g. up/down, left/right) which are independent of the actual threshold. Whenever the testing value is below the observer's threshold, the observer is forced to make a guess based on any information available thus, criterion dependency is removed. By pure guesswork, the number of correct responses are 50% in a two-alternative forced-choice procedure. The psychometric function therefore has ordinal values from 50 to 100% and the threshold value is then often chosen to be around the 75% correct point (*Figure 4.02*).

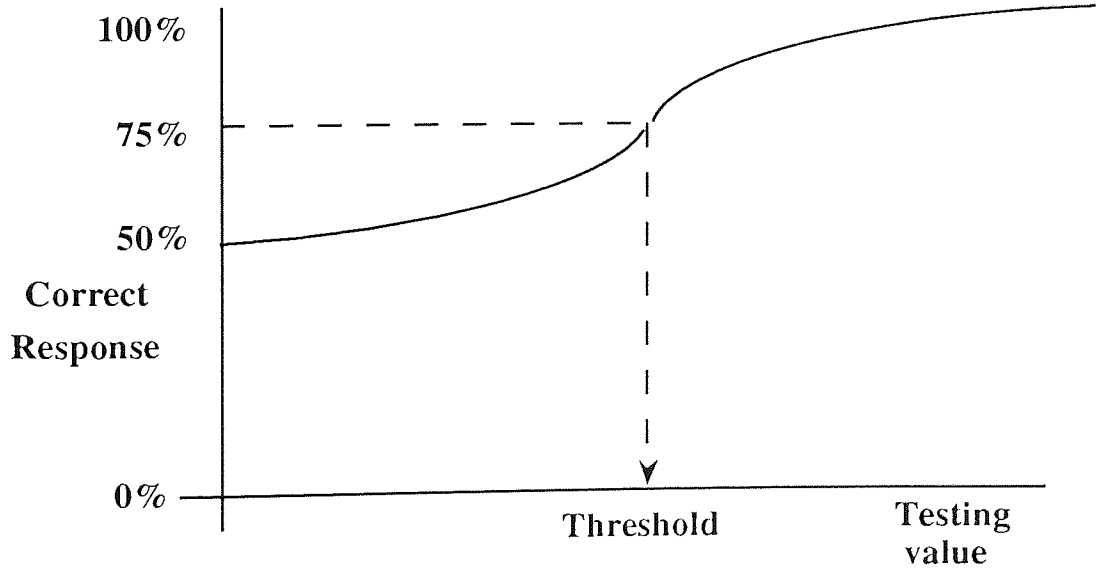

Figure 4.02: The psychometric function obtained using a two-alternative forced-choice technique. The 50% correct response can be obtained simply by guessing thus, it is taken as the lowest ordinate value. Threshold is usually taken to be around the 75% correct response level.

4.3: Staircase method (Up-Down method)

The traditional staircase method (Dixon & Mood, 1948) estimates the 50% point on the psychometric function. The testing value is either increased or decreased depending on the observer's responses. In *Figure 4.03* the black circles represent incorrect responses following which the testing value is increased. The open circles represent correct responses following which the value is reduced. Threshold is determined by noting the testing value at the points of reversal (where a correct response follows one or more incorrect responses or vice-versa), adding all these values together and taking a mean of the values.

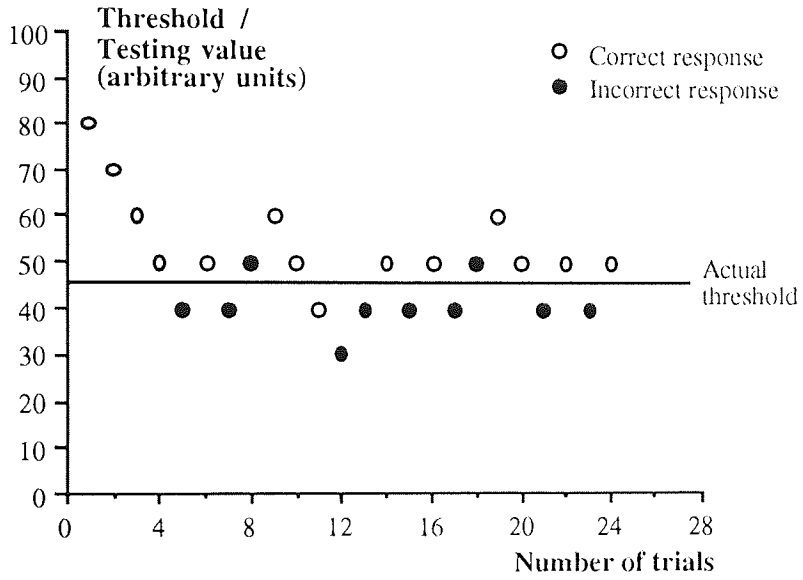

Figure 4.03: A staircase routine. In this chapter the testing value is in arbitrary units.

Some aspects of a staircase method have to be determined before starting an experiment. Preliminary estimation of the approximate threshold saves time and effort in actual experiment by making it possible to choose the *starting value* above threshold but not too far from it. Especially, inexperienced observers need to see the stimulus properly at the beginning of the sequence so that they know what to look for. The *step size* is the change in stimulus intensity from one testing level to another. Too large a step size gives inaccurate threshold values. Too small a step size results in long, time consuming sequences of correct or incorrect responses between reversals. According to Cornsweet (1962) the right step size is such that no more than four like responses should take place before a reversal of the testing value. Logarithmic steps can be used in the staircases (Cornsweet, 1962). Sometimes it is reasonable to *modify the step size* using a larger step size when far above the threshold in order to reach it more rapidly. Once close to threshold, the step size can be reduced in order to gain a more accurate estimate of the final threshold value. Decision *when to end the sequence* depends on the accuracy required. The sequence can be ended after a fixed number of trials but in that case it

is not known whether an adequate number of reversals has occurred for a successful threshold estimation. Thus, ending after a certain number of reversals yields more reliable results. Since the early reversals may be biased by the choice of starting point it is useful to eliminate their effect by *ignoring the first few reversals* and determining the final threshold on the basis of, for example, the last eight reversals.

When using a conventional staircase the final threshold value can be manipulated by the observer knowing the way the staircase is going. Cornsweet (1962) suggested that two staircases could be interleaved, making the prediction of the next presentation more difficult. In this thesis an interleaved procedure was used in all tasks except flicker and face discrimination tasks.

4.4: Two-alternative forced-choice staircase

It is possible to combine the quick and efficient staircase method with the criterion independent two-alternative forced-choice procedure. However, the traditional staircase method estimates the 50% point on the psychometric function. As is seen from *Figure 4.02* the psychometric function for a two-alternative forced-choice procedure begins at the 50% point since a 50% correct response can be obtained by guessing. Thus, when combining these two methods it is necessary to estimate a different threshold point on the psychometric function. Wetherill and Levitt (1965) modified the staircase so that more than one correct response was needed in succession to decrease the testing value (the Up-Down Transformed Rule, UDTR). Any single incorrect response causes an increase in the testing value. In *Table 4.01* different response sequences are listed with the resulting points on the psychometric function.

Table 4.01: Some threshold points on the psychometric function

Successive correct responses (test value is decreased)	Successive incorrect responses (test value is increased)	Estimated point (%) on psychometric function
1	1	50.0
2	1	70.7
3	1	79.4
4	1	84.1
5	1	87.0
1	2	29.3
1	3	20.6

For example, to estimate the 79% point three consecutive correct responses are needed before the testing value is decreased. The chance for such a sequence at the 50% level is third root of 0.5 = 0.79 or approximately 79% and the sequence will converge to this point on the psychometric function.

4.5: Modification of the two-alternative forced-choice staircase by PEST

The trials close to actual threshold give the most information about the threshold, so to concentrate the testing level around this value Taylor and Creelman (1967) developed "The Parameter Estimation by Sequential Testing" or PEST. As with the previous method, PEST is a set of rules for changing the testing level of the embedded psychophysical procedure. As with the Up-Down Transformed Rule the testing level is varied according to the number of correct or incorrect responses. Before the sequence initiation the initial stimulus level and the initial step size are chosen.

The *change in testing level* is determined as follows. Let us assume that we aim for the 75% correct point on the psychometric function (represented by 0.75 in the formulae below). During the experimental sequence the program counts after each trial the number of correct responses (N_{corr}) and the total number of trials (N_{tot}) since the last change in testing level. The validity of the following two formulae are inspected:

$$N_{corr} \geq (N_{tot} \times 0.75) + W \qquad \text{(formula 1)}$$

and

$$N_{corr} \leq (N_{tot} \times 0.75) - W \qquad \text{(formula 2),}$$

where W is a constant called the deviation limit of the sequential test. The speed and accuracy of the test depends on W. If W is small then the test rapidly converges towards the threshold value but gives a relatively inaccurate final result. If W is large then more trials are needed but the final result is more precise.

Only one of the above formulae can be valid at any one time. When formula 1 is valid, the testing level is lowered, when formula 2 is valid, the testing level is increased. If neither of the formulae is valid the testing level remains unchanged. *Table 4.02* demonstrates the changes in testing level for 75% correct point when W = 1.

Table 4.02: Example of the testing levels for a forced-choice staircase

Trial	N_{tot}	N_{corr}	N_{tot} x 0.75	valid formula	testing level
1. corr	1	1	0.75	none	unchanged
2. corr	2	2	1.5	none	unchanged
3. corr	3	3	2.25	none	unchanged
4. corr	4	4	3	1	down
5. false	1	0	0.75	none	unchanged
6. false	2	0	1.5	2	up
7. corr	1	1	0.75	none	unchanged
8. corr	2	2	1.5	none	unchanged
9. false	3	2	2.25	none	unchanged
10. corr	4	3	3	none	unchanged
11. corr	5	4	3.75	none	unchanged
12. corr	6	5	4.5	none	unchanged
13. corr	7	6	5.25	none	unchanged
14. corr	8	7	6	1	down
15. false	1	0	0.75	none	unchanged
16. corr	2	1	1.5	none	unchanged
17. false	3	1	2.25	2	up etc.

The step size is determined by the responses to previous testing levels. The first step size is usually large and the test starts above threshold. Taylor and Creelman (1967) suggested a set of rules for step sizes, but in this thesis the step sizes in all but the flicker sensitivity and face discrimination tasks were determined simply by the number of reversals (r) so, that step size = $4/2_r$ pixels. Thus, the first step size was 4 pixels, after the first reversal it was 2 pixels, after second reversal 1 and after the third reversal the sequence ended and threshold was taken as the final testing level. The interleaving staircases did not necessarily end simultaneously.

To operate the PEST technique with greater accuracy a modification proposed by Findlay (1978) was applied. The deviation limit of the sequential test (W) was varied through the test. In the early stages of the sequence W was small (resulting in a more rapid convergence toward threshold). When approaching threshold, an increasing value of W was used in order to reach a more accurate final threshold estimate. This modification was achieved by making the deviation limit a function of the number of reversals. W started at 0.5, after the first reversal it was 0.75 and following subsequent reversals a value of 1 was used.

4.6: Observer bias

If the observer is asked to align two targets, there is often a slight difference between the subjective and actual alignment. This offset is called *observer bias*, and has to be taken into consideration when measuring thresholds involving the alignment of targets. If thresholds are defined simply relative to a true vertical, for instance, then the observer bias moves the subjective vertical away from this true vertical and the final estimate will contain a constant error. Staircase routines make it possible to use two interleaved staircases simultaneously. Since each staircase measures the threshold independently from the vertical, it is possible to remove the effect of bias from thresholds, as is shown in *Figure 4.04*. A further advantage in using interleaved staircases is that it becomes more difficult for the observer to manipulate the final threshold value by tracking the staircase.

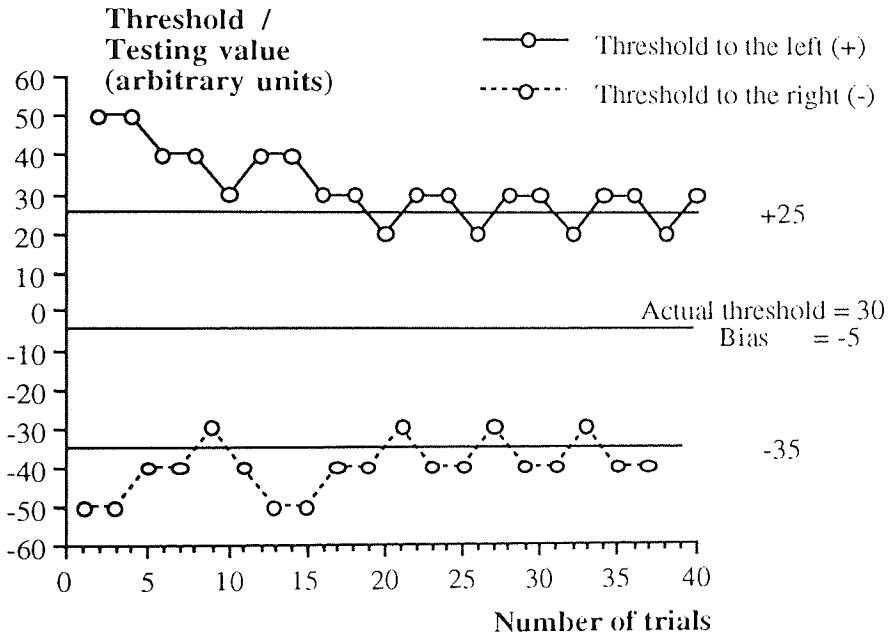

Figure 4.04: An example of two interleaved staircases one for the leftward and one for the rightward responses of the zero physical offset (71% correct). The observers actual threshold is the mean of the absolute values of the thresholds (25 + 35) / 2 = 30 units. Observer bias is the point of subjective alignment and is the mean of the two final threshold values [+25 + (-35)] / 2 = -5 units.

Feedback

In all the experiments in this thesis (the only exception being the flicker detection task) observers were given no feedback. Bias is reduced with feedback, since the subject can respond on the basis of previous feedback. However, the interleaved staircase takes into consideration the effect of bias on thresholds. Further, if the stimulus appears to be tilted right, but the previous feedback indicated that it most likely is tilted left, the observers must

choose between responding on the basis of subjective appearance or on the basis of previous feedback. Since this change of criteria may influence thresholds unpredictably, it is best to be avoided by not giving feedback.

4.7: Apparatus and observers

4.7.1: General

All the experiments were carried out using stimuli generated on a cathode ray tube (CRT) under the control of a microcomputer. In order to avoid the edges of the monitor or any other item within the laboratory acting as a reference, the room lights were extinguished and the edges of the monitor masked with black tape or cardboard. The observer responded to the stimulus either via the keyboard or the mouse. Whenever possible, the sizes of the stimuli were varied simply by altering the working distance to magnify all stimulus features equally. The principal observers of the experiments were myself and DW. In some of the experiments final year optometry students served as subjects as part of their coursework. All the data analysis was done by Macintosh Apple software (Stat View 512+ and Stat Works)

4.7.2: Apparatus

In the majority of experiments the stimuli were presented on a 14 in. high resolution RGB monitor (Eizo Flexscan 8060S) against a dark background and their spatial and temporal parameters were controlled by a Research Machines Nimbus AX microcomputer. Pixel separation was 0.32 mm in the horizontal and 0.7 mm in the vertical direction. Frame rate was 60 Hz. Programs were written in Research Machines Basic language by Dr D. Whitaker. For working distances over 2 m the stimulus was viewed via a mirror, for shorter working distances the monitor was viewed directly. The maximum working distance available was 28 m. The working distance was chosen so that the pixel separation (which determined the smallest step size) was well below the expected threshold.

4.7.3: Apparatus for flicker and face discrimination experiments

The stimuli were generated under computer control (ALR Business Veisa 486/33) on a 16 in. high resolution RGB monitor (Eizo Flexscan 9080i with fast phosphor B22) driven at the frame rate of 60 Hz by a VGA graphics board that generated 640 × 480 pixels. The pixel separation was 0.42 mm × 0.42 mm. The display was used in a white mode. The non-linear luminance response of the display was linearised using the inverse function of the luminance response in stimulus image computations. For the flicker experiment a monochrome signal of 256 intensity levels (8 bits) from a monochrome palette of 4096 (12 bits) was obtained by a

means of a video summation device combining the red, green and blue outputs of the graphics board (Pelli & Zhang, 1991). In the face discrimination experiment a monochrome signal of 1024 intensity levels (10 bits) was obtained from a monochrome palette of 65,536 (16 bits). The luminance waveform of the flicker experiment stimulus was calculated by means of software written in Basic language and translated by Microsoft Professional Basic 7.0 compiler.

The stimuli were created and the experiments were run by means of software developed by Dr R. Näsänen. The software utilized the graphics subroutine library of Professional HALO 2.0 developed by Media Cybernetics. The stimulus was rapidly switched on and off by changing the colour look-up table during the vertical retrace period of the display.

4.8: Spatial scaling procedure

In this section the spatial scaling procedure is explained in detail by using hypothetical data as an example. A set of stimulus sizes was used for threshold measurements at each eccentricity. The size of the stimulus sets increased towards the periphery and these were chosen on the basis of preliminary experiments. All stimuli were magnified or minified versions of one another. At each eccentricity, thresholds were measured as a function of the size parameter of the stimulus, which may be line length, separation of two stimulus components etc...

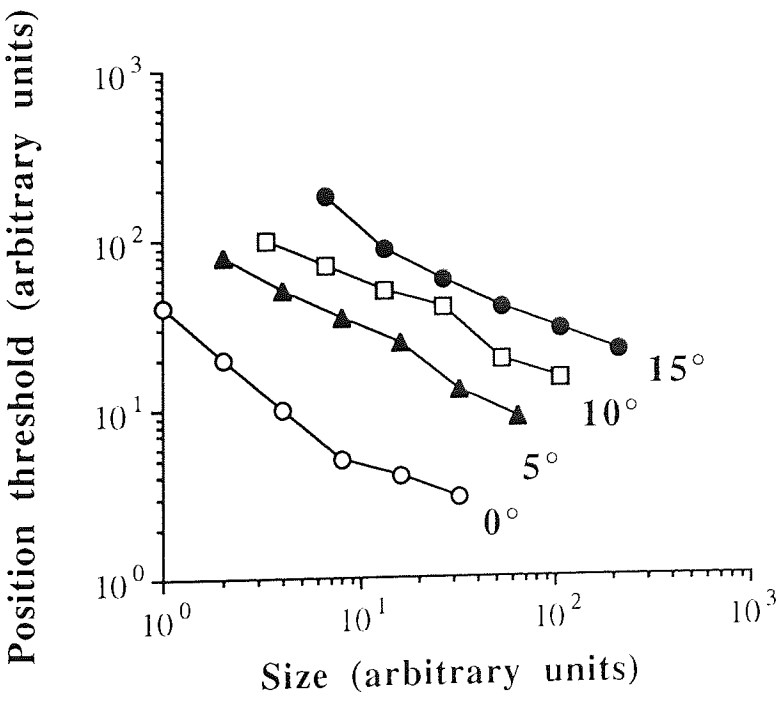

Figure 4.05: Hypothetical position thresholds plotted as a function of size parameter.

Figure 4.05 shows position thresholds for a hypothetical task as a function of stimulus size. The threshold *vs* size curves are displaced relative to one another both along the horizontal and vertical axis. This occurs because the y-axis threshold is a spatial measure. In flicker sensitivity experiments, for instance, where the y-axis represents a non-spatial measure of amplitude modulation, the threshold *vs* size curves are shifted only along the x-axis (Watson, 1987; Johnston, 1987).

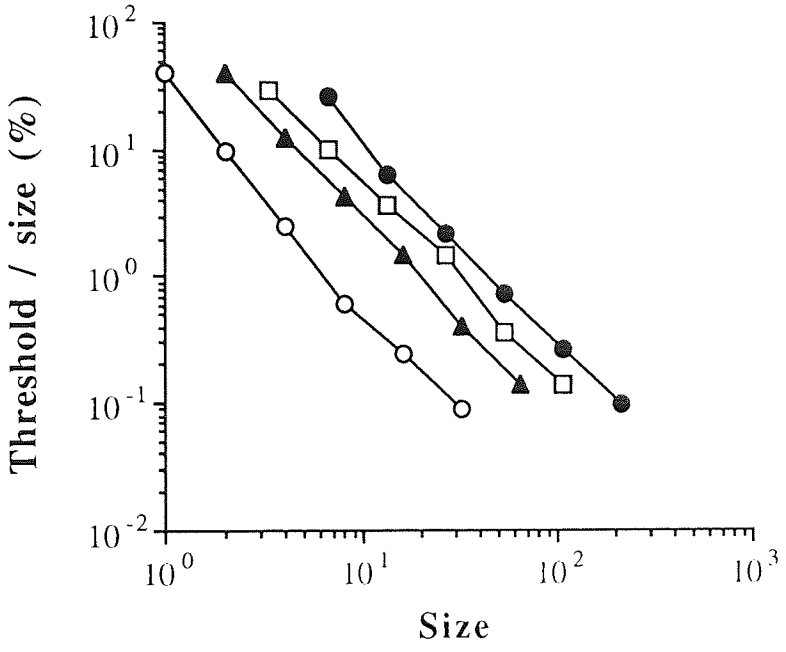

Figure 4.06: Scale invariant thresholds plotted as a function of size.

However, it is possible to replot the data so that threshold offset is not expressed in absolute spatial terms, but relative to the size parameter of the stimulus. Expressing thresholds as a percentage of size plotted against size itself makes the y-axis scale invariant. This is shown in *Figure 4.06.* The curves are now displaced only along the x-axis relative to one another. At this stage a suitable scaling factor applied only along the x-axis makes the threshold *vs* size functions at any eccentricity collapse onto the foveal data.

Scaling the data, E_2

If the concept of spatial scaling holds, functions for successive eccentricities at this stage should be displaced relative to one another only along the size (in this case the x-) axis, as in *Figure 4.06.*

The amount by which successive curves at different eccentricities are displaced relative to the foveal curve is established. The amount of this shift is termed the scaling factor for each

eccentricity. The rate at which the scaling factor increases with eccentricity gives us a direct indication of how fast stimulus size has to be increased towards periphery to maintain performance equivalent to that at the fovea.

To find the value of the scaling factor for a certain eccentricity, the peripheral data was scaled relative to the foveal data. A scaling factor which would equate performance e.g. at 5 deg eccentricity with that at the fovea was determined as follows. The data was examined to find an approximately suitable factor which seemed likely to superimpose the two curves, when the size parameter of each data point at 5 deg eccentricity was divided by the estimated factor. After dividing the sizes with the factor, the sum of the squares of the residual deviations around a best-fitting template (either a linear regression or a second-order polynomial regression curve) was calculated for the data from the two eccentricities now superimposed. This was done to find out how well the estimated factor minimised variance between the foveal and eccentric data. Another estimate of the scaling factor was then made and the the sum of the squares of the residual deviations was calculated again. This process was repeated until a scaling factor was found, which produced a minimum sum of the squares of the residual deviations around the template. Scaling factors for the data in *Figure 4.06* were found in this way for each eccentricity and are shown in *Figure 4.07*. The value of the scaling factor increases with eccentricity, and the data shown is fitted with a linear regression line constrained to pass through a value of unity at 0 deg (fovea) since the scaling factors were obtained relative to the foveal data.

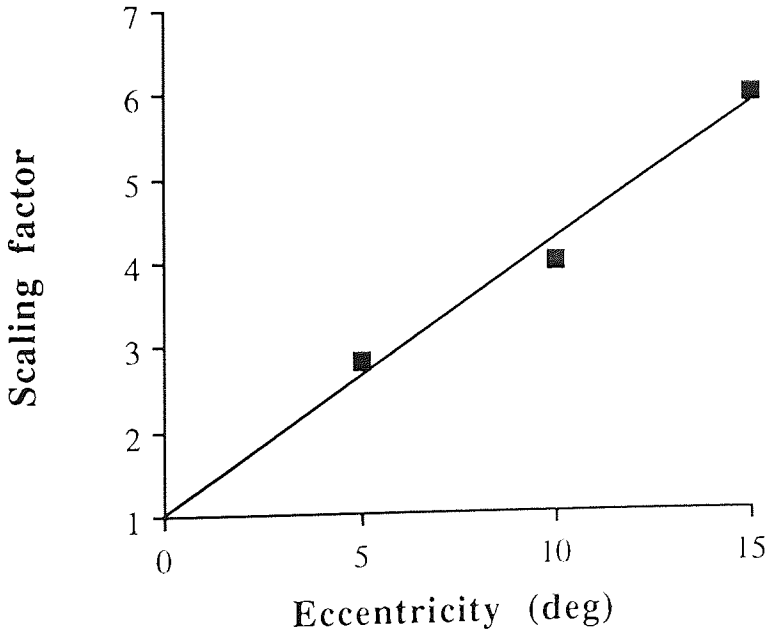

Figure 4.07: The scaling factors plotted against eccentricity.

The scaling factor, F is 1 at E = 0, since the 0 deg data scaled by itself naturally gives the value of 1. If we assume that F increases linearly with eccentricity then F is given by the following basic equation for a line going through points (0,1) and (E,F):

$$F - 1 = S(E - 0) \qquad (4.01)$$

where E is eccentricity and S is the normalised gradient of the linear regression (*Figure 4.08*). Thus,

$$F = 1 + SE \qquad (4.02).$$

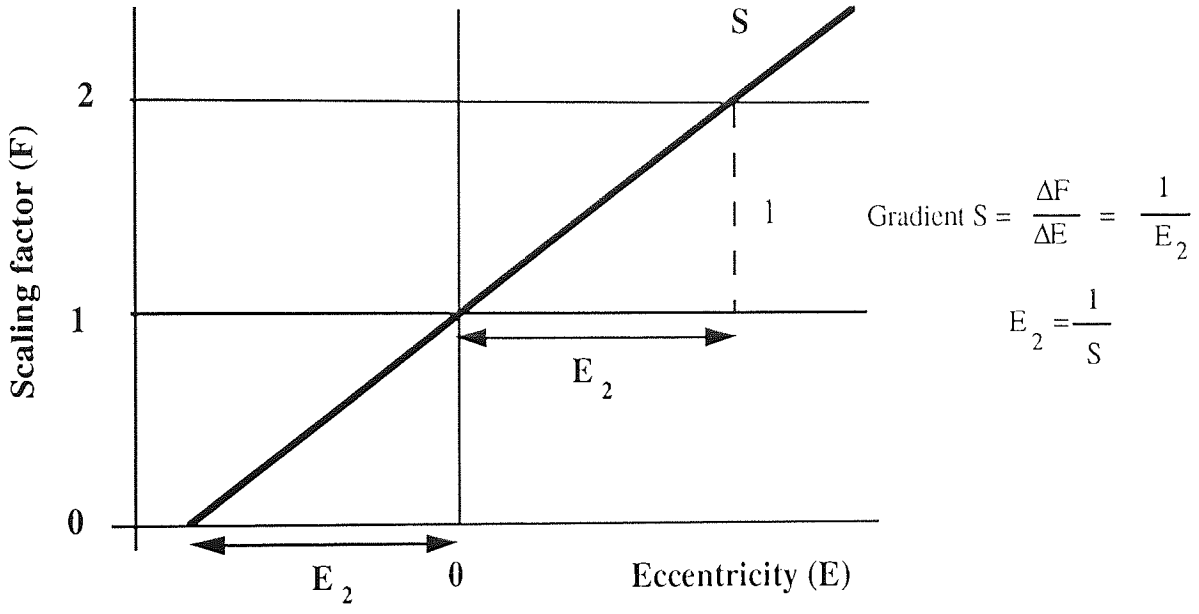

Figure 4.08: A line with a gradient of S goes through (0,1). F = 1 + SE

E_2 is defined as the eccentricity at which the foveal scaling factor F(0) doubles (Levi, Klein & Aitsebaomo, 1985). When E = 0, F(0) = 1. Since E_2 is the eccentricity where F(0) doubles, $F(E_2) = 2$.

Thus, $$2 = 1 + SE_2 \qquad (4.03)$$

therefore, $$E_2 = {}^1/_S \qquad (4.04).$$

The above relationships are shown in geometrical format in *Figure 4.08*.

When peripheral data functions are compared to an eccentricity other than 0 the situation is slightly more complicated. Imagine the foveal data replaced by data of y deg and comparing the peripheral eccentricities relative to that data. The relationship between the scaling factor F and eccentricity E is now given as in equation (4.01) by

$$F - 1 = S(E - y) \quad (4.05)$$

thus,

$$F = 1 + S(E - y) \quad (4.06).$$

In this case, E_2 is found as follows:

$$F(0) = 1 - Sy \quad \text{and since} \quad F(E_2) = 2\,F(0)$$

then

$$F(E_2) = 1 + S(E_2 - y)$$

and

$$2(1 - Sy) = 1 + S(E_2 - y).$$

Thus,

$$1 - Sy = SE_2$$

and

$$E_2 = {}^1/_S - y \quad (4.07).$$

The above relationships are shown in geometrical format in *Figure 4.09.*

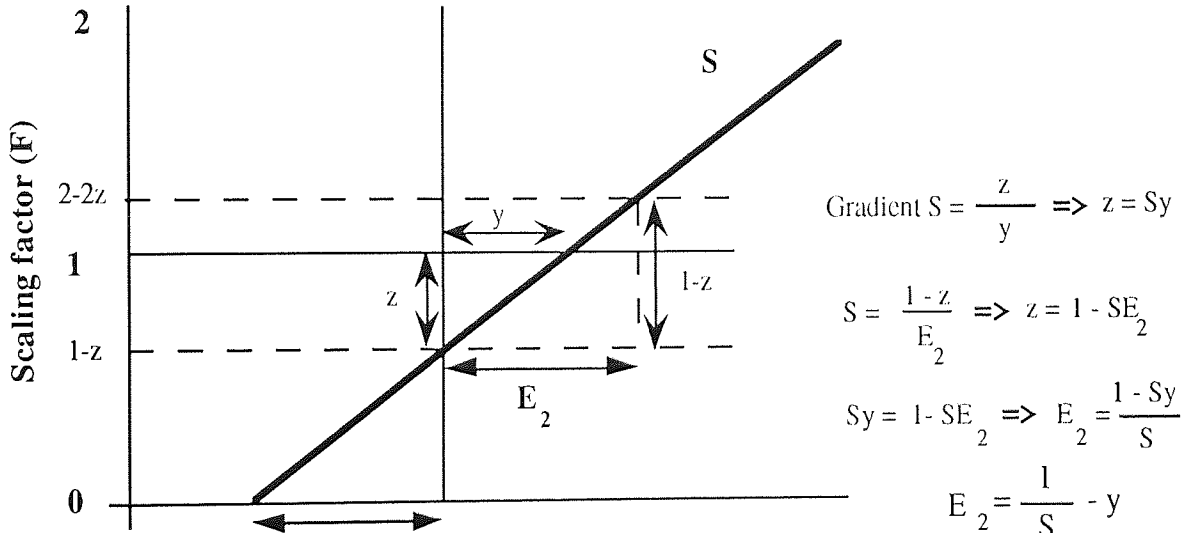

Figure 4.09: A line with a gradient of S goes through (y , 1). $F = 1 + S(E - y)$

Figure 4.10 shows the data from *Figure 4.06* after being scaled, i.e. all stimulus sizes have been divided by an eccentricity-specific factor determined by the linear regression in *Figure 4.07.* The eccentricity-specific factors were found as follows: Since $E_2 = 1/S$ (eq. 4.04)

$$S = \frac{1}{E_2} \quad (4.08),$$

and since $F = 1 + SE$ (eq. 4.02),

$$F = 1 + \frac{E}{E_2} \quad (4.09).$$

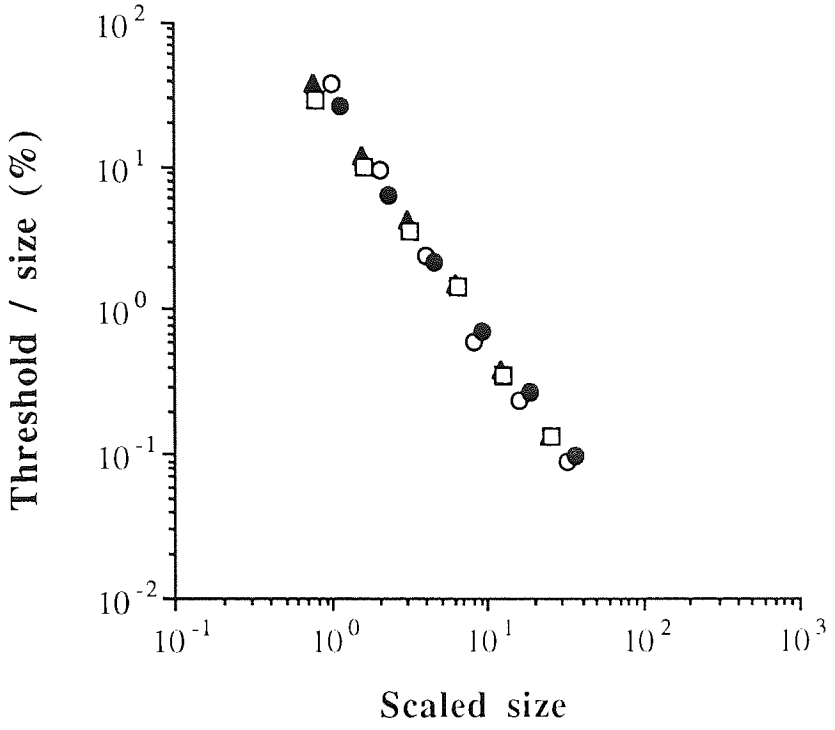

Figure 4.10: Data after scaling the size parameter.

4.9: Unconfounding the effects of separation and eccentricity

The spatial scaling method described above has two important rules. The stimuli should be exact magnified versions of each other and all the features of the stimulus should be presented at the same eccentricity. In certain cases increasing the separation of the stimulus features, e.g. two dots, also increases their actual eccentricity. There is no sense in scaling a task looking for the effect of one variable (eccentricity) if changes in thresholds are also caused by another variable (separation). In particular, the foveal data may reflect a combination of the effects of separation and eccentricity. One way to isolate the factors of separation and eccentricity is to present the stimuli on an isoeccentric arc (Levi, Klein & Yap, 1988; Levi & Klein, 1989; Levi & Klein, 1990a).

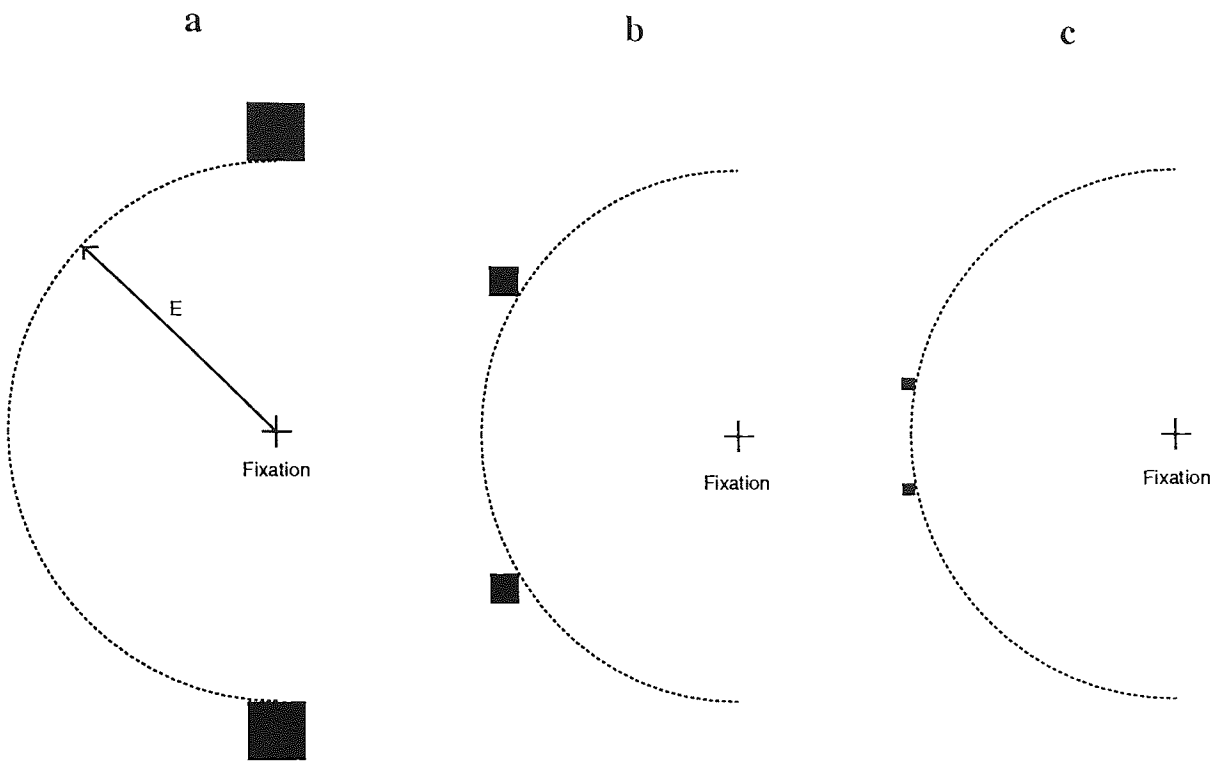

Figure 4.11: The method of dissociating the effects of eccentricity and separation in two-dot vernier task. All stimulus features are presented at the same eccentricity on the circumference of an isoeccentric circle. The eccentricity of the stimulus is defined by the radius of the circle, denoted by E (in arc a). Changes in separation are achieved by moving the features around the circumference of the arc (arcs b and c).

In the experiments in which the stimuli were presented on isoeccentric arcs, e.g. the 2-dot vernier acuity in *Figure 4.11*, the stimulus was on an invisible, imaginary circle whose centre coincided with fixation. The maximum separation for the two dots was always twice the radius of the arc, e.g. at 16 min.arc (0.267 deg) eccentricity the maximum separation available was 32 min.arc. In that situation the outermost dots of the stimulus were symmetrically placed above and below the fovea. At smaller separations the dots were placed closer to each other around the imaginary circle and the fixation point was at its centre. As can be seen from the *Figure 4.11* the stimulus size and separation decrease at the same rate. Thus, all stimuli were simply magnified versions of one another. For greater eccentricities the dots were situated on isoeccentric arcs of corresponding radii.

The arcs have been made circular, thus ignoring any meridional anisotropy which may be present. The justification for this is that in the experiments to be presented, performance only along a single meridian is considered and, in addition, data is collected at relatively small eccentricities.

4.10: Summary

A simple two-alternative forced-choice staircase technique which estimated the 71% correct level as a mean of the last 6 reversals was used to measure thresholds for unreferenced movement detection (Wetherill & Levitt, 1965). Thresholds for vernier offset were measured using a PEST technique (Findlay, 1978) in which the 75% point on the psychometric function was estimated for both rightward and leftward responses using a randomly interleaved procedure. Thresholds for bisection acuity, spatial interval discrimination, referenced displacement tasks, orientation discrimination, and the combination task were also determined using an interleaved two-alternative forced-choice technique with a modified PEST routine (Findlay, 1978), which this time estimated the 80% correct level for both response alternatives.

Flicker sensitivity was measured by a two-alternative forced-choice method with feedback by determining temporal modulation required for 79% correct level (Wetherill & Levitt, 1965). The estimate of threshold contrast was a mean of the last 8 reversals. In the face discrimination task the least distorted image that still could be discriminated from the undistorted image was also determined by a two-alternative forced-choice algorithm with feedback. Two consecutive staircases were used. A random subthreshold starting point was established using the first staircase with one correct - down, one wrong - up -rule. The *second* wrong choice initiated the second staircase, which measured the distortion required for the level of 84 % correct (Wetherill & Levitt, 1965). The estimate of threshold contrast was a mean of the last 8 reversals.

Chapter 5: Spatial scaling of vernier acuity tasks

5.1: Introduction

It has been reported that hyperacuity thresholds rise much faster with with eccentricity than visual acuity and previous estimates of cortical magnification based on ganglion cell density would predict. The discrepancy between vernier and visual acuity was observed as early as 1902 Bourdon, who found that vernier thresholds were about 4 times higher at 1 deg and 40 times higher at 5 deg eccentricity than at the fovea. According to Westheimer (1982) the rate of decline in performance is not quite as drastic, but at 10 deg eccentricity the optimum two-dot vernier thresholds he found are still about ten times higher than at the fovea (see *Figure 5.01*). By comparison, Westheimer determined visual resolution thresholds for gratings, which were only 4 - 5 times higher at 10 deg eccentricity than at the fovea.

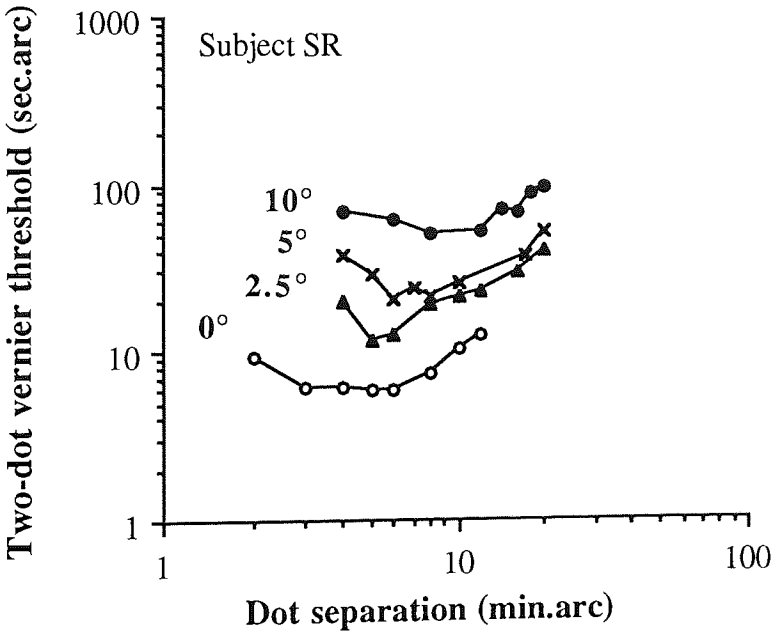

Figure 5.01: The effect of eccentricity and separation on two-dot vernier acuity for subject SR. Thresholds are plotted against the spatial threshold. Dot size was constant, 1 × 1 deg. Redrawn from Westheimer (1982).

Levi, Klein and Aitsebaomo (1985) studied vernier acuity and, according to their results, thresholds for vernier acuity double at about 0.8 deg eccentricity, whereas thresholds for visual acuity thresholds double at about 3 deg eccentricity. This finding led Levi *et al.* to suggest that visual acuity is scaled according to retinal factors whilst the increase in hyperacuity thresholds with eccentricity reflects true cortical magnification. It is worth noting that, inspite the rapid decline towards periphery, vernier acuity remained better than grating

acuity within the central 10 deg eccentricity. The vernier stimulus used by Levi *et al.* (1985) consisted of long, vertical abutting lines but not all studies have found the same dramatic deterioration in vernier acuity with eccentricity which they demonstrate. Levi *et al.* also studied crowding effect in the periphery (see *Chapter 2.4*; Westheimer & Hauske, 1975 study about crowding at the fovea). The interference regions increased in proportion to the unflanked threshold distances towards periphery. The extent of these regions was estimated to be about 60 times the threshold distance.

Virsu, Näsänen and Osmoviita (1987) investigated the ability to detect the vernier offset of two dots (thresholds are plotted in spatial terms in the *Figure 5.02*) in binocular conditions and discovered that their results scaled successfully to a magnification factor predicted by retinal ganglion cell density. Further, the vernier acuity results at various eccentricities plotted in terms of orientation (in deg) resembled the orientation discrimination results obtained by Watt (1984) and Vandebussche, Vogels and Orban (1986), thus supporting the suggestion that orientational acuity underlies the two-dot vernier acuity (Andrews, 1967; Sullivan, Oatley & Sutherland, 1972).

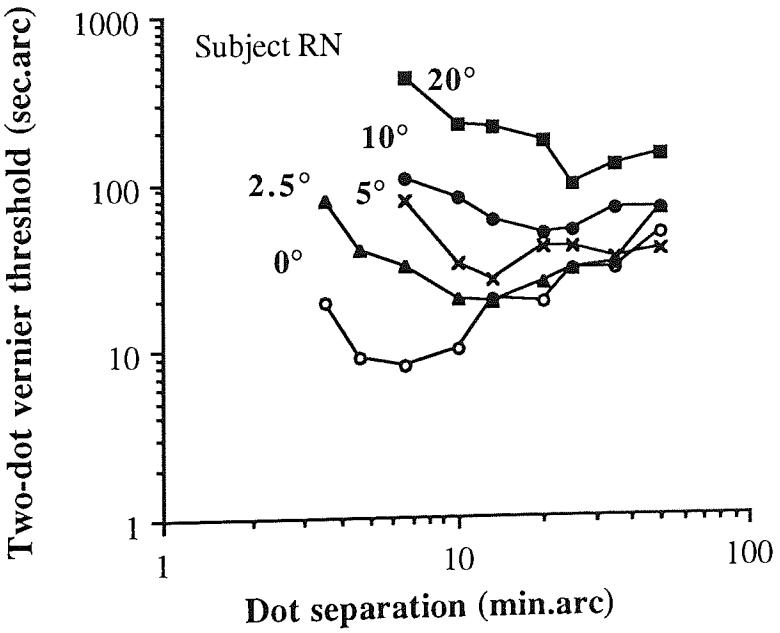

Figure 5.02: The effect of eccentricity and separation on two-dot vernier acuity for subject RN. Thresholds are plotted against the spatial threshold. Dot size was constant 1 × 1 min.arc. Redrawn from Virsu *et al.* (1987).

Beck and Halloran (1985) have suggested that two-dot vernier acuity thresholds are independent of retinal eccentricity, albeit over a small range (2 - 8 deg) in the parafovea. The results from their Experiment 3 (shown in *Figure 5.03*) indicate that with a constant 60

sec.arc dot separation thresholds are unaffected by eccentricity changes, whereas increasing the dot separation by moving the other dot towards periphery elevates thresholds markedly. A constant dot size was used in the study, interdot separations were 1 - 8 deg depending on the condition. Both dots were presented one above the other in the lower visual field. Therefore, the eccentricity of at least one of the dots inevitably changed as separation was altered making it difficult to know in what proportion the eccentricity and dot separation changed the thresholds.

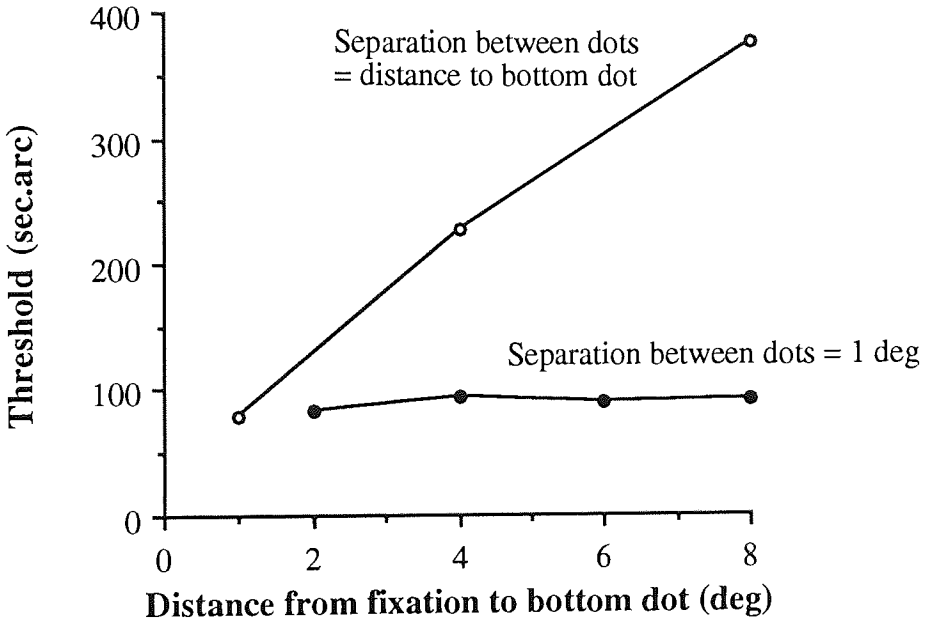

Figure 5.03: The effect of eccentricity and separation on two-dot vernier acuity, average of two subjects. Data from Beck and Halloran (1985).

Although disagreements as to the exact rate at which visual performance decreases with eccentricity are of interest, a potentially more serious problem arises when peripheral thresholds appear quite incompatible with measurements made at the fovea. For example, Westheimer (1982) found, using a two-dot vernier stimulus, that whereas the dot separation which produced optimum thresholds increased only modestly with eccentricity, the threshold itself increased at a much faster rate (*Figure 5.01*). This finding supports the view that several underlying mechanisms may contribute to the final threshold response and that these each scale in different ways with eccentricity (Yap, Levi & Klein, 1989; Hess & Watt, 1990; Levi & Klein, 1990a).

Given the disagreement over the rate at which vernier acuity increases towards the periphery and whether vernier acuity can or cannot be scaled at all, we used the spatial scaling technique described in *Chapter 4* to examine the change in vernier thresholds with increasing

eccentricity for stimulus configurations of both abutting lines and widely separated dots.

5.2: Methods

All stimuli were presented on a CRT as described in *Chapter 4*. Two groups of stimuli were used, one group consisting of abutting lines, the other of vertically separated dots. For the line stimuli, the vertical length of each line at the fovea was either 1, 2, 4, 8 or 16 min.arc and the width was a constant proportion (11%) of the length (see *Figure 5.04*, top). All stimuli were therefore magnified or minified versions of each other. For the dot stimuli, the vertical separation (gap size) of the dots when presented foveally was either 1, 2, 4, 8 or 16 min.arc. The dots were small squares whose width and height was a constant proportion (11%) of the separation (see *Figure 5.04*, bottom). Again, therefore, the stimuli only differed from each other in terms of magnification.

The white vernier targets were presented against a dark background and had a luminance of 34 cd m^{-2}. Room lights were extinguished so that the edges of the screen could not be used as a reference against which vernier offset might be judged. The stimuli appeared for 250 msec following which the observer responded via the keyboard as to whether the top vernier element was offset to the right or to the left of the lower, i.e. a two-alternative forced-choice procedure was used. The next stimulus presentation occurred immediately following the observer's response, which meant that the observers experienced no difficulty due to their level of accommodation returning to its dark-focus position or due to loss of fixation.

Thresholds for vernier offset were measured using a PEST technique (Findlay, 1978) in which the 75% point on the psychometric function was estimated for both rightward and leftward responses using a randomly interleaved procedure. Half the distance between these positions was taken to represent vernier threshold, the mean of the two positions representing vernier bias. Using this kind of technique removes any possible influence of bias upon threshold estimates and is an important factor since bias may neither remain constant with eccentricity nor vary at the same rate as threshold. No feedback was given to the observers during an experimental run. Feedback would be expected to force vernier bias towards zero but have little effect upon vernier acuity. In order to avoid fatigue, data was collected in a large number of short sessions, each lasting approximately 20 minutes. Four threshold estimates, each resulting from approximately 60 trials, were made for randomly chosen combinations of line length / gap size and eccentricity. Final threshold was accepted as a mean of these four estimates.

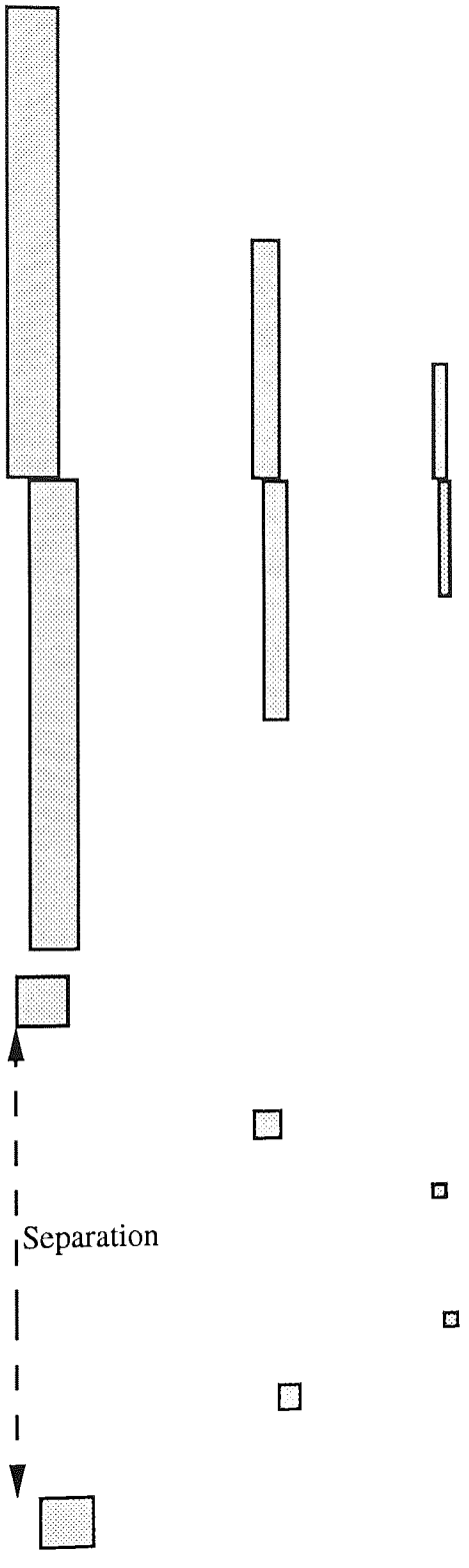

Figure 5.04: Top: Vernier *line stimulus* at three different sizes. Bottom: Vernier *non-isoeccentric two-dot stimulus* at three different sizes. Separation is shown for the largest dot pair.

For peripheral viewing, the stimuli were presented at eccentricities of 5, 10 and 15 deg. Presentation was in the nasal visual field and a central fixation spot was provided. To reduce the possibility of the fixation spot being used as a positional reference, the horizontal location of the stimulus was jittered with a standard deviation equivalent to 0.5% of the eccentricity for subjects DW and DM, and 3% for other subjects. In the periphery stimuli were larger but had the same magnification relative to each other. This was achieved by reducing viewing distance with increasing eccentricity. Foveal viewing distance was 10 m and this was reduced to 2.5 m at 5 deg, 1.5 m at 10 deg and 1 m at 15 deg eccentricity.

Irrespective of eccentricity all stimuli were simply magnified versions of each other. Changing viewing distance is a simple way of changing magnification and avoids problems associated with the resolution of the CRT screen. The choice of suitable eccentric viewing distances was made during extensive pilot experiments. According to the concept of local spatial scale, a stimulus of a certain size at any eccentricity should have its foveal counterpart which differs only in magnification. This procedure of changing viewing distance does not imply an initial choice of scaling factor but simply magnifies the eccentric stimuli so that they are more likely to be roughly equivalent in cortical terms to the foveal stimuli. The experiment could have been carried out with the same stimulus sizes at each eccentricity (i.e. without changing viewing distance at all) but this would have required a far more extensive range of stimulus sizes and resulted in much of the data being superfluous after scaling since many of the stimuli at one eccentricity would be devoid of an equivalent stimulus at another.

The results of two experienced observers (PM and DW) are shown. In addition, a trained observer (DM in all stimulus conditions) and two naïve observers (MD in the line vernier and KL in the isoeccentric two-dot vernier task) participated in the experiment. All were fully corrected moderate myopes with no ocular abnormality and viewing was monocular using the dominant eye.

5.3: Results

Line stimulus

Figure 5.05a shows vernier thresholds as a function of line length for the stimulus consisting of abutting lines. The data for two subjects, PM (above) and DW (below), are shown. For the foveal data, thresholds as low as 6 sec.arc are found for DW. Thresholds increase for both observers as line length is reduced below 4 - 8 min.arc, although this is not as pronounced for observer PM. The results are therefore consistent with those of Sullivan, Oatley and Sutherland (1972) and Westheimer and McKee (1977b). Further, the optimum thresholds at 10 deg eccentricity (about 50 sec.arc) are equal to Westheimer's (1982) findings (*Figure 5.01*).

With increasing eccentricity, thresholds for all line lengths increase markedly but the trend towards reduced sensitivity for smaller line lengths remains. The range of line lengths shifts towards higher values as eccentricity increases, this being a direct consequence of the use of shorter viewing distances.

The threshold *vs* line length curves at each eccentricity are not only displaced relative to one another along the horizontal axis, but are also displaced vertically. This is because vernier offset is itself a spatial measure. This is not true in the experiments where the y-axis represents, for example, a measure of angular orientation discrimination threshold (as in *Chapter 9*) or contrast modulation (as in *Chapter 11*) and is a non-spatial measure. This is why, in the experiments of Watson (1987) and Johnston (1987), the threshold *vs* size curves were shifted only along the x-axis. There is, however, a simple way to present our data, and that is to express vernier offset not in absolute spatial terms, but relative to the size of the stimulus as a whole. *Figure 5.05b* therefore shows vernier threshold as a percentage of line length. Note how this transformation produces a series of curves which are apparently displaced only along the x-axis relative to one another. If the concept of local spatial scale holds, then the threshold *vs* line length functions at any eccentricity should collapse onto the foveal data by the application of a suitable scaling factor only along the x-axis.

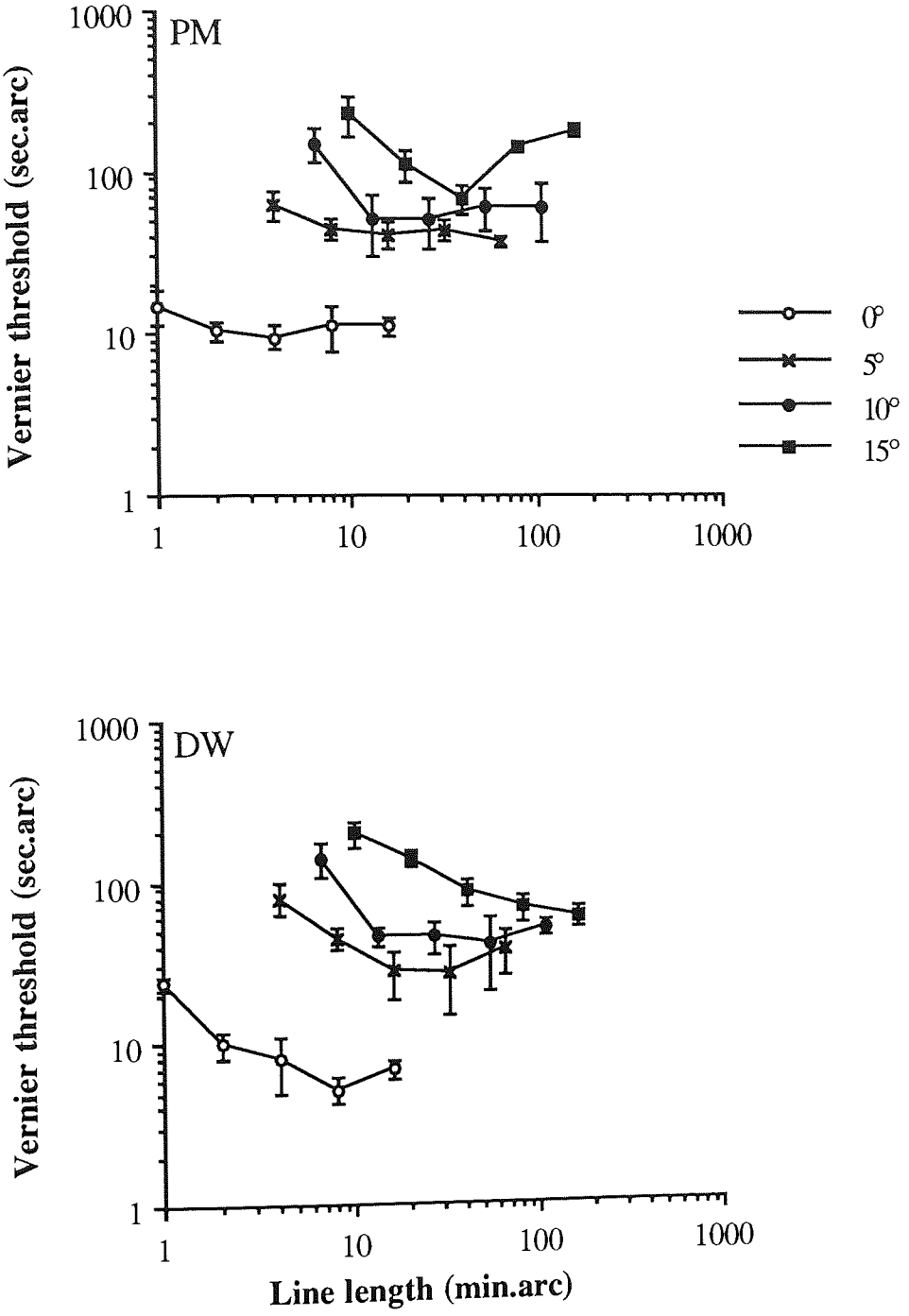

Figure 5.05a: Two-line vernier stimulus. Vernier threshold of two subjects plotted against line length at four retinal eccentricities. Standard errors are shown for each data point.

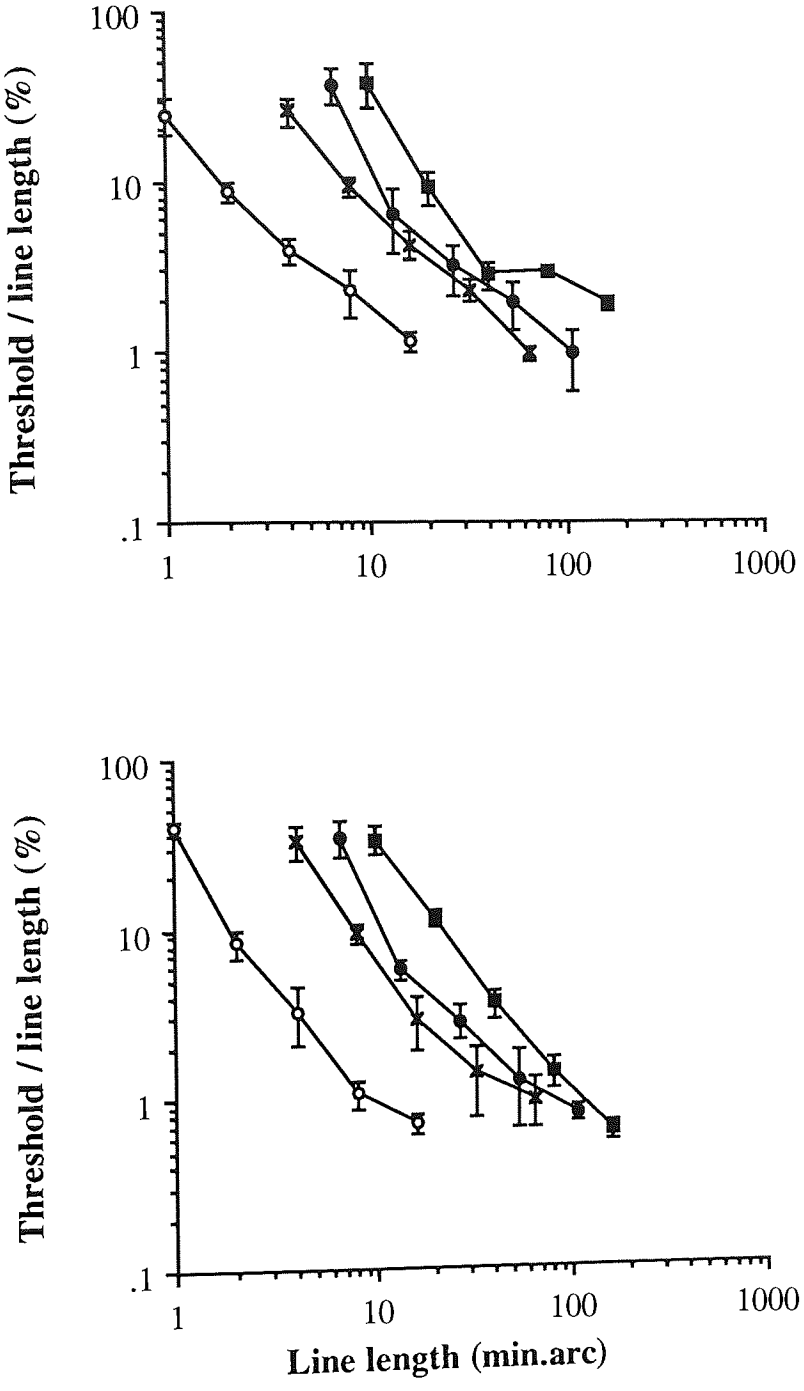

Figure 5.05b: Vernier thresholds expressed as a fraction of line length and plotted against line length. Symbols and subjects as in *Figure 5.05a.*

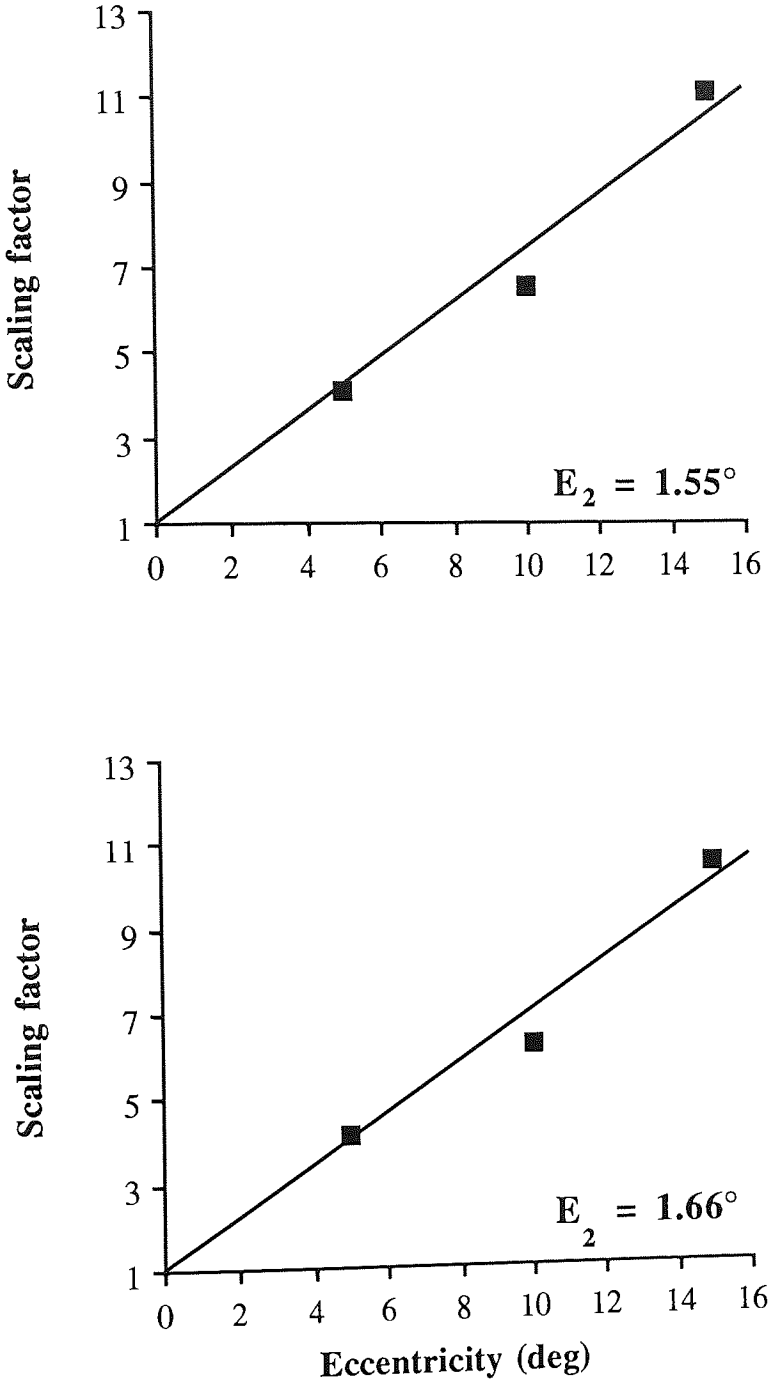

Figure 5.05c: Scaling factors, representing the values by which line lengths for each peripheral stimulus in *Figure 5.05b* must be divided in order to collapse onto the foveal data, plotted against eccentricity. The linear fit has been constrained to pass through a value of unity at 0 deg eccentricity.

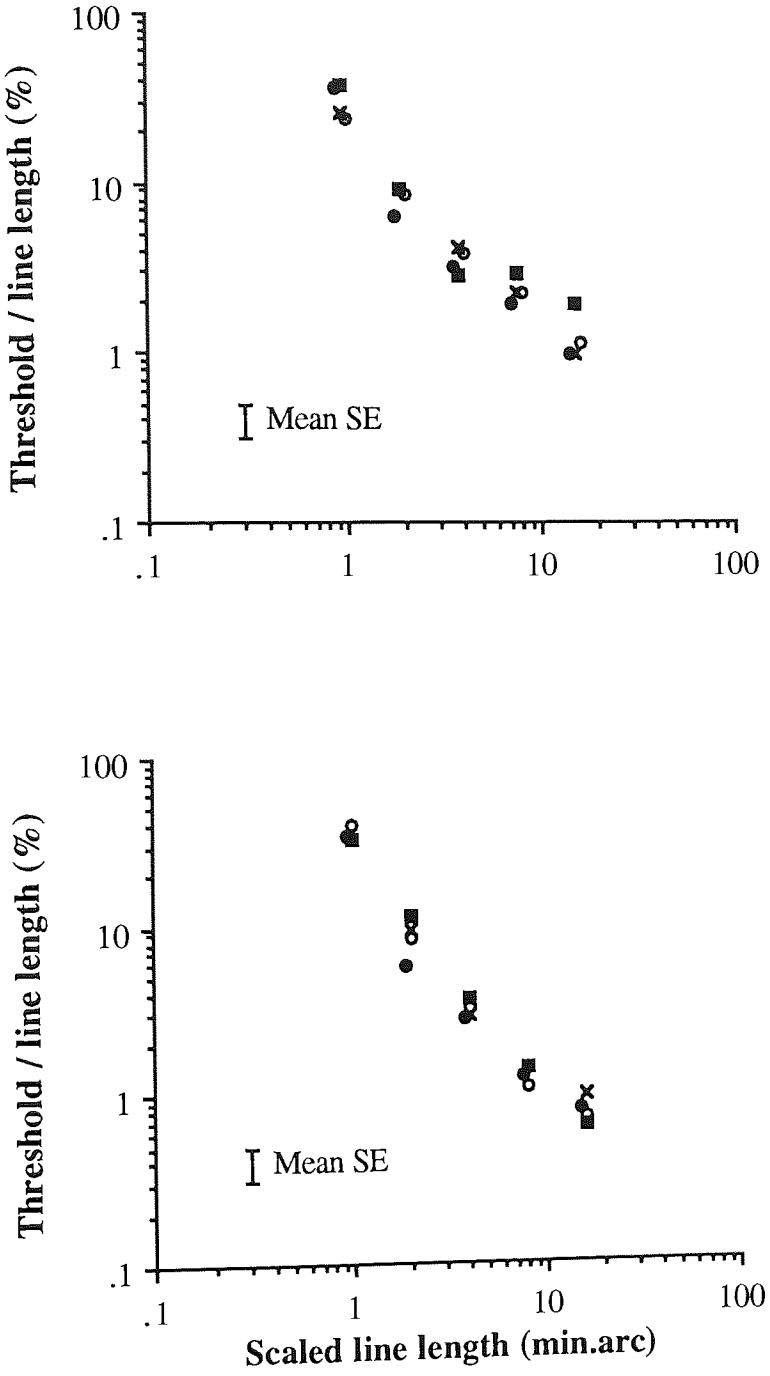

Figure 5.05d: *Figure 5.05b* replotted with the data at each eccentricity scaled according to scaling factor values derived from the linear relationship shown in *Figure 5.05c*. Note how this procedure removes systematic variation between data points at each eccentricity. Mean standard error is shown. Symbols and subjects as in *Figure 5.05a*.

To find the value of this scaling factor at each eccentricity an approximation of the factor was obtained simply by examining the data, and the eccentric line lengths were divided by this estimate. In order to determine how successful this factor was in minimising variance between the foveal and eccentric data, a template was needed in relation to which a sum of squares of residual deviations can be calculated. Since the relationship, when plotted on logarithmic coordinates, is not quite linear (*Figure 5.05b*), a second-order polynomial was used although the choice of template is not crucial. The foveal and the scaled eccentric data were therefore fitted with a second-order polynomial regression curve and the sum of squares of residual deviations around this curve were calculated. Another estimate of the scaling factor was then chosen and the process repeated until a scaling factor was found which minimised the sum of squares of residual deviations around the regression curve and this was then accepted as the final scaling factor for the eccentricity in question.

Note that the scaling process must be performed using logarithmic data, since this ensures that each data point has approximately the same variance irrespective of eccentricity or threshold (Virsu *et al.*, 1987). The same process could be used on the data of *Figure 5.05a*, but in this case the scaling factor must be applied along both axes. Identical results are obtained from both methods, but a shift along just one axis is easier to envisage.

Scaling factors were obtained for the data at 5, 10 and 15 deg eccentricity and are shown plotted against eccentricity in *Figure 5.05c*. The linear regression fit to the data has been constrained to go through a value of unity at 0 degrees eccentricity, since the scaling factors at each eccentricity have been determined relative to the foveal data. The linear relationship describes the data well indicating that, over the range of eccentricities studied, the relationship between the scaling factor, F, and eccentricity, E, may be given by the equation *(4.02)*

$$F = 1 + SE$$

where S is the normalised gradient. The reciprocal of S represents the eccentricity, E_2, at which F doubles, providing a simple indicator of the rate of increase of F (Levi, Klein & Aitsebaomo, 1985). Values of E_2 were found to be 1.55 (± 0.13) deg for PM and 1.66 (± 0.14) deg for DW. For other observers (not shown) E_2 values were 1.78 (± 0.13) deg for DM and 1.23 (± 0.01) deg for MD, an untrained observer.

Figure 5.05d shows the data from *Figure 5.05b* after being scaled according to the above equation. Note how the inter-eccentricity variance has been minimised, with no evidence of systematic variation as a function of eccentricity.

Non-isoeccentric, "traditional" dot stimulus

In *Figure 5.04*, bottom, the non-isoeccentric two-dot stimulus is shown in three different sizes. *Figure 5.06a* shows unscaled vernier thresholds for subject DW plotted against gap size for the stimuli consisting of vertically separated dots. The foveal data demonstrate a U-shaped function with a minimum around the gap size of 4 min.arc, typical of this type of task (Westheimer & McKee, 1977b; Westheimer, 1982; Virsu, Näsänen & Osmoviita, 1987). As before, peripheral thresholds increase with eccentricity but fail to show the foveal-type increase in thresholds at small gap sizes. This difference in shape of the foveal and peripheral curves immediately suggests that scaling of the data is unlikely to be as successful as for the line stimuli. Further, consistent with the findings of Westheimer (1982), optimum gap size appears to increase at a slower rate with eccentricity than do vernier thresholds themselves. Foveal optimum gap size in *Figure 5.06a* is about 4 min.arc, whereas at 15 deg this has risen to about 20 min.arc, a fivefold increase. Over the same eccentricity range, vernier thresholds have increased from 5 sec.arc to around 90 sec.arc, an eighteenfold increase.

Figure 5.06b shows the same data but with threshold expressed as a fraction of gap size. Again, the foveal data appear somewhat dissimilar to the eccentric data, being steeper at small gap sizes but flattening out at larger gap sizes. Note that a slope of zero on the graph indicates proportionality between threshold and gap size, consistent with Weber's law. Scaling factors at each eccentricity were found as described for the line stimulus, and the data fitted by linear regression (*Figure 5.06c*). E_2 values for DW were found to be 1.70 (± 0.08) deg and for DM 1.51 (± 0.18) deg (not shown). *Figure 5.06d* shows the data after scaling, and it is clear that there remains a systematic difference between thresholds at the fovea and at other eccentricities. Specifically, foveal performance is worse when the gap between the dots is small, but thresholds become smaller than in the periphery for large gaps.

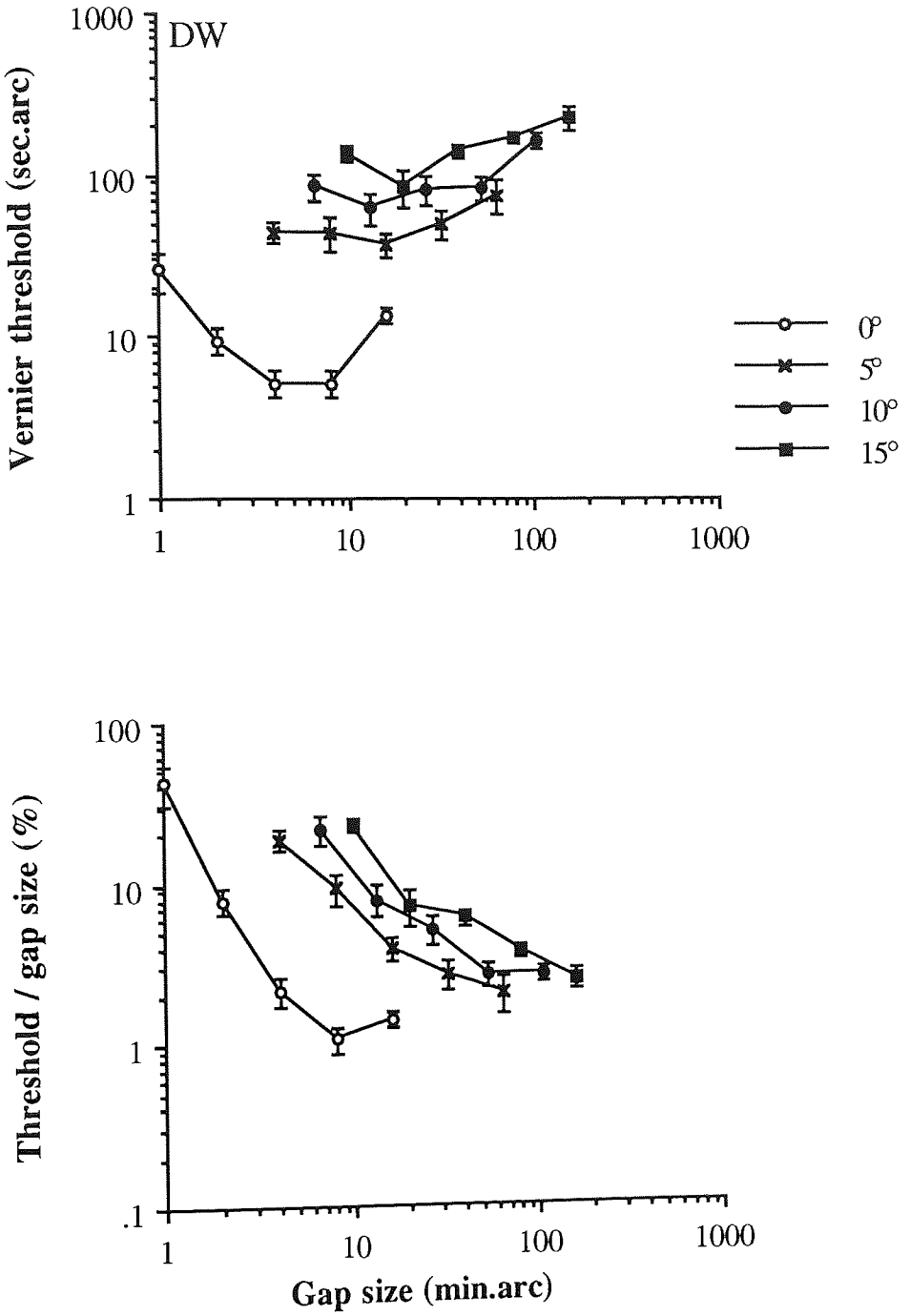

Figure 5.06a and b: Traditional two-dot stimulus. Subject DW. (a) Vernier thresholds plotted against gap size at four retinal eccentricities.
(b) Vernier threshold expressed as a fraction of gap size and plotted against gap size. In both graphs there is a difference between the foveal and peripheral results. Standard errors are shown for each data point.

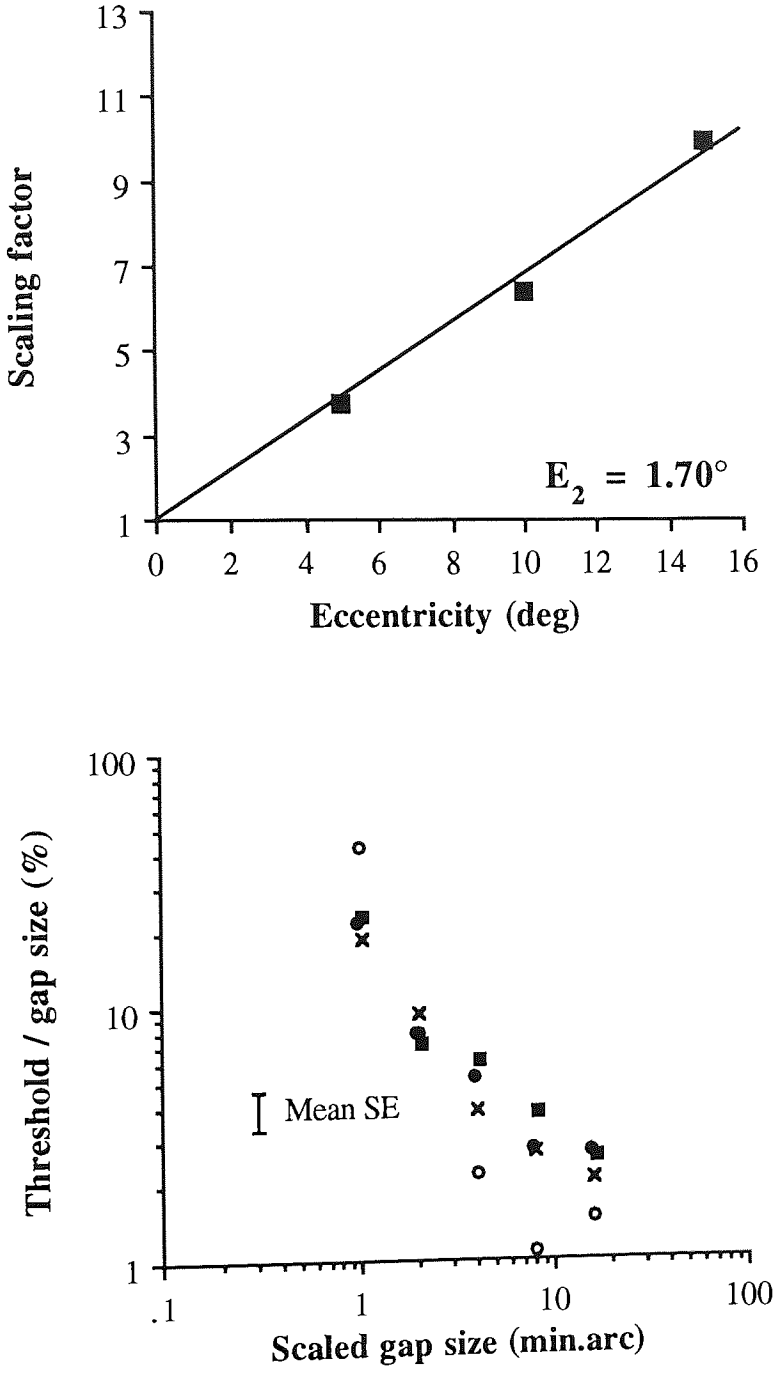

Figure 5.06 c and d: (c) Scaling factors, representing the values by which gap sizes for each peripheral stimulus in *Figure 5.06b* must be divided in order to collapse onto the foveal data, plotted against eccentricity. The linear fit has been constrained to pass through a value of unity at 0 deg eccentricity.
(d) *Figure 5.06b* replotted with the data at each eccentricity scaled according to the scaling factor values derived from the linear relationship shown in (c). Note how some eccentricity-dependent variation in the data remains, with foveal thresholds clearly behaving differently to data at the other eccentricities.

Dissociating the effects of separation and eccentricity

Why is it that scaling appears to be successful for the abutting line stimulus but fails at the fovea for the dot stimulus? Optical factors may have a role to play since the retinal images of stimuli in close proximity overlap considerably. For the two-dot vernier target at small gap sizes this leads to the subjective appearance of the two dots merging together to form a single, brighter target. This would clearly be expected to reduce the ability to detect a horizontal offset of the two dots leading to the bandpass threshold *vs* gap function for foveal viewing as opposed to the more lowpass shape of the peripheral data where physical gap size is greater (see *Figure 5.06a*). This is emphasised by the observation that further, artificial degradation of the retinal image adversely affects two-dot vernier acuity at small, but not large, gap sizes (Williams, Enoch & Essock, 1984).

However, a potentially more serious problem arises in that, as the separation of the two dots is increased, so the actual eccentricity of the dots also increases (imagine the two-dot stimuli in *Figure 5.04* foveally presented). Hence, the foveal data may not be representative of performance at a single eccentricity but may instead reflect a combination of the effects of separation and eccentricity. At eccentricities of 5 - 15 deg, since the eccentricity is large relative to the separation, the changes in eccentricity as separation is increased are far less marked. This may be the reason why foveal and peripheral two-dot vernier acuity could not be adequately scaled. The roles of separation and eccentricity in determining positional thresholds has been the subject of much recent investigation (Levi, Klein & Yap, 1988; Morgan & Watt, 1989; Levi & Klein, 1989; Levi & Klein, 1990a).

One way to isolate the effect of separation without any contaminating influence of eccentricity is to present the stimuli on an isoeccentric arc. Using this method it is impossible to scale peripheral data relative to an eccentricity of zero since it is meaningless to position stimuli on an isoeccentric arc of 0 deg radius. Thus, the smallest two-dot vernier stimulus was presented on an imaginary circle whose radius was 16 min.arc (0.267 deg) and whose centre coincided with fixation. This enabled separations of up to 32 min.arc to be achieved. In the latter case, the dots would be symmetrically placed above and below the fovea. For successively smaller separations, the dots are placed further around the imaginary circle (in the nasal visual field) whilst fixation is maintained at its centre. For other eccentricities, the dots are again maintained on isoeccentric arcs, this time with radii of 5, 10 and 15 deg. *Figure 4.11* shows the stimulus features positioned on the circumference of the arcs.

Results for the isoeccentric two-dot stimulus for subjects PM and DW are shown in *Figure 5.07a*. The shape of the 5, 10 and 15 deg curves are similar to the previous findings (*Figure 5.06a*). This is not too surprising since, at these large eccentricities, separation changes had

little influence over eccentricity. For the two-dot stimulus presented on the isoeccentric arc with 16 min.arc radius, however, the thresholds are quite different from the previous "foveal" data. The curve is flatter and resembles much more the data at larger eccentricities. As before, thresholds were expressed as a function of gap size and scaling factors calculated relative to the 16 min.arc data (*Figure 5.07b*).

The increase in scaling factor with eccentricity is shown in *Figure 5.07c*. The linear fit has been constrained to pass through a value of unity at an eccentricity of 16 min.arc since each peripheral data set was scaled relative to threshold values at this eccentricity. Obviously scaling the 16 min.arc data relative to itself would produce a scaling factor of unity. The relationship between the scaling factor and eccentricity is then given according to the equation *(4.06)*. This equation is discussed in *Chapter 4*, General methods.

$$F = 1 + S(E - 0.267)$$

where S is the gradient of the linear relationship shown in *Figure 5.07c*.

The eccentricity, E_2, at which the foveal scaling factor doubles is then given by the equation *(4.07)*

$$E_2 = {}^{1}/_{S} - 0.267$$

E_2 values were found to be 1.96 (± 0.18) deg for PM and 1.66 (± 0.13) deg for DW. The E_2 values for the other observers (not shown) were 1.88 (± 0.22) deg for DM and 1.06 (± 0.09) deg for KL, an untrained observer. The data after scaling are shown in *Figure 5.07d*. The scaling procedure appears to remove majority of eccentricity dependent variance. However, there remains a slight difference between foveal and peripheral data at large sizes for PM.

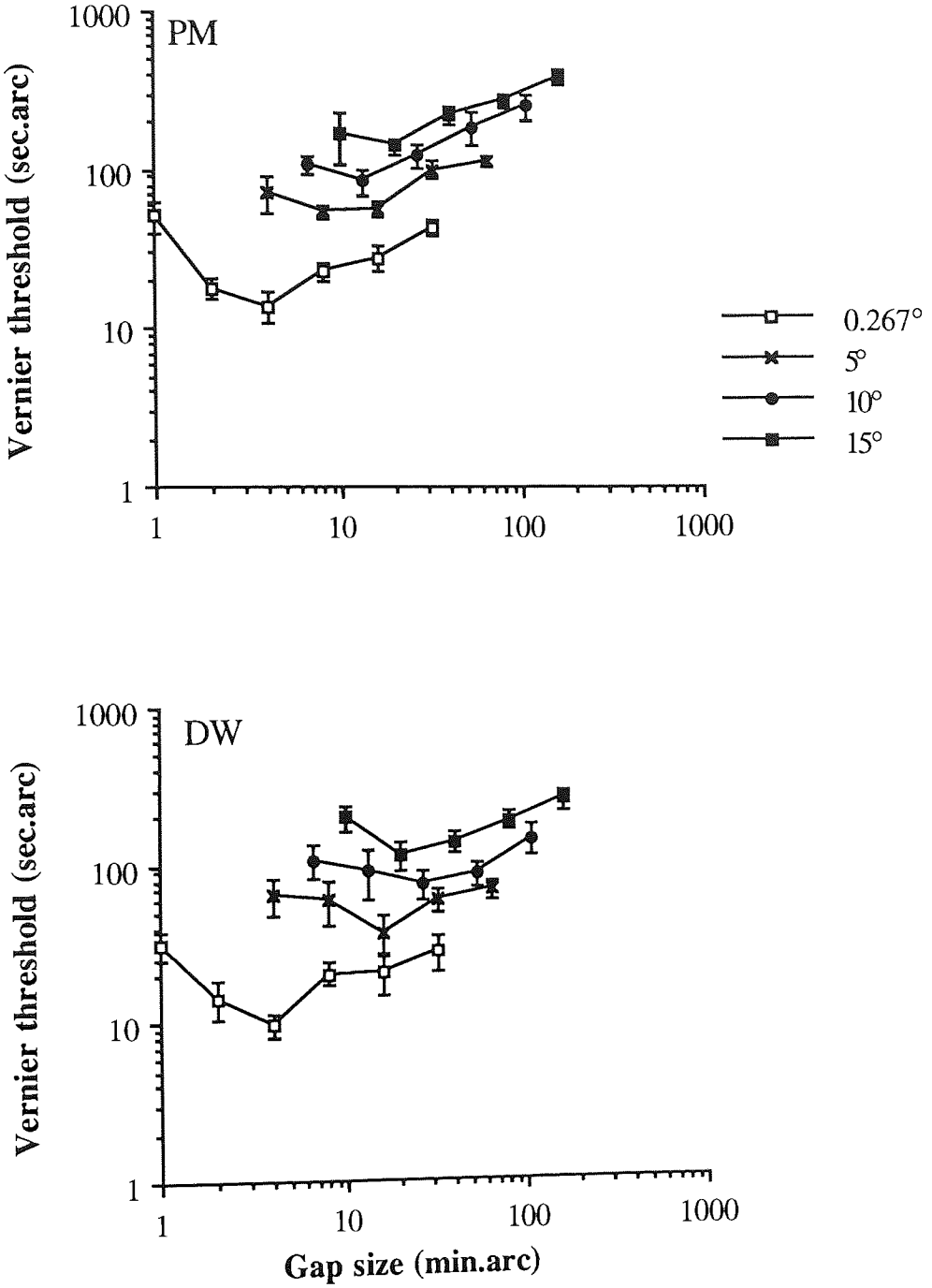

Figure 5.07a: Isoeccentric two-dot stimulus. Vernier thresholds plotted against gap size for a two-dot stimulus presented on an isoeccentric arc as described in the text. The radii of the isoeccentric arcs are shown. Subjects PM and DW.

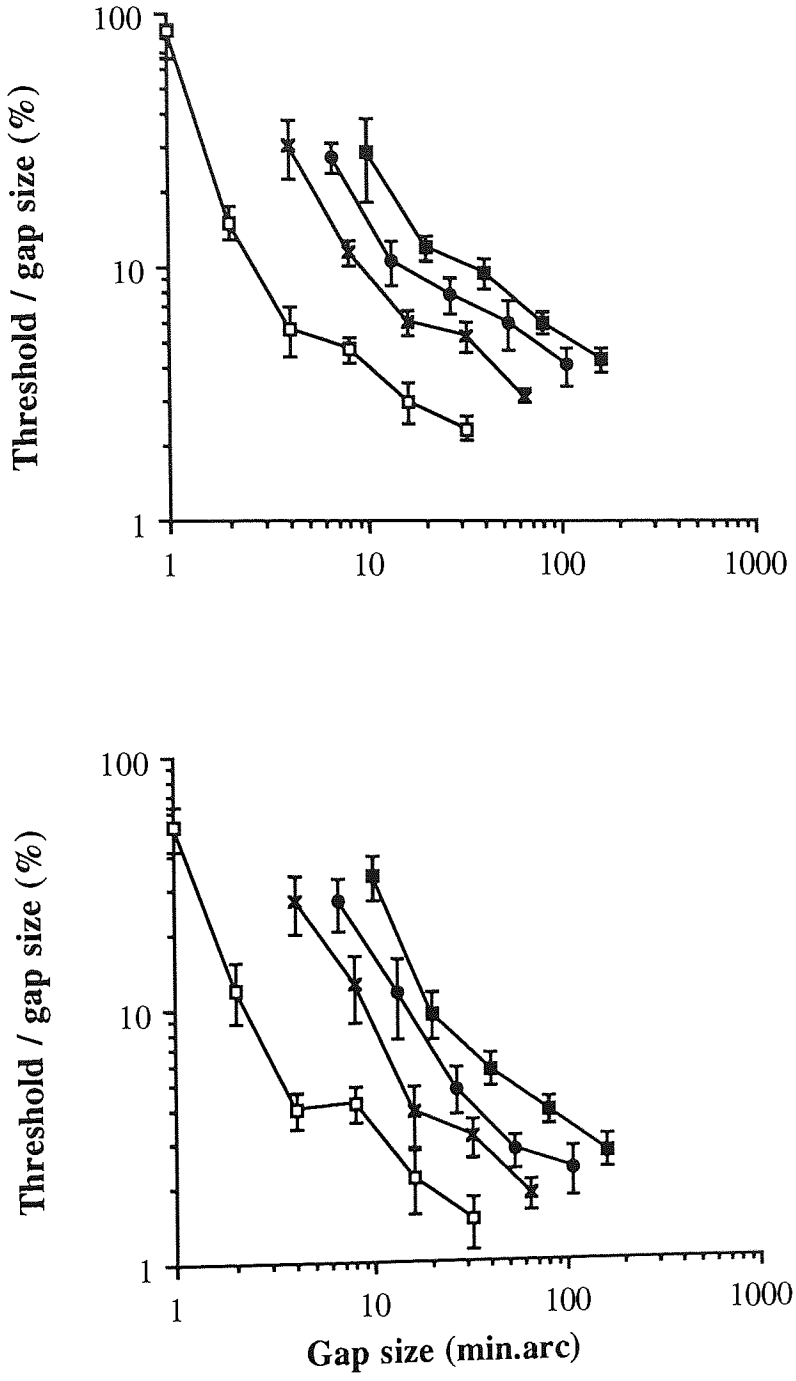

Figure 5.07b: Vernier thresholds expressed as a fraction of gap size and plotted against gap size. Symbols and subjects as in *Figure 5.07a.*

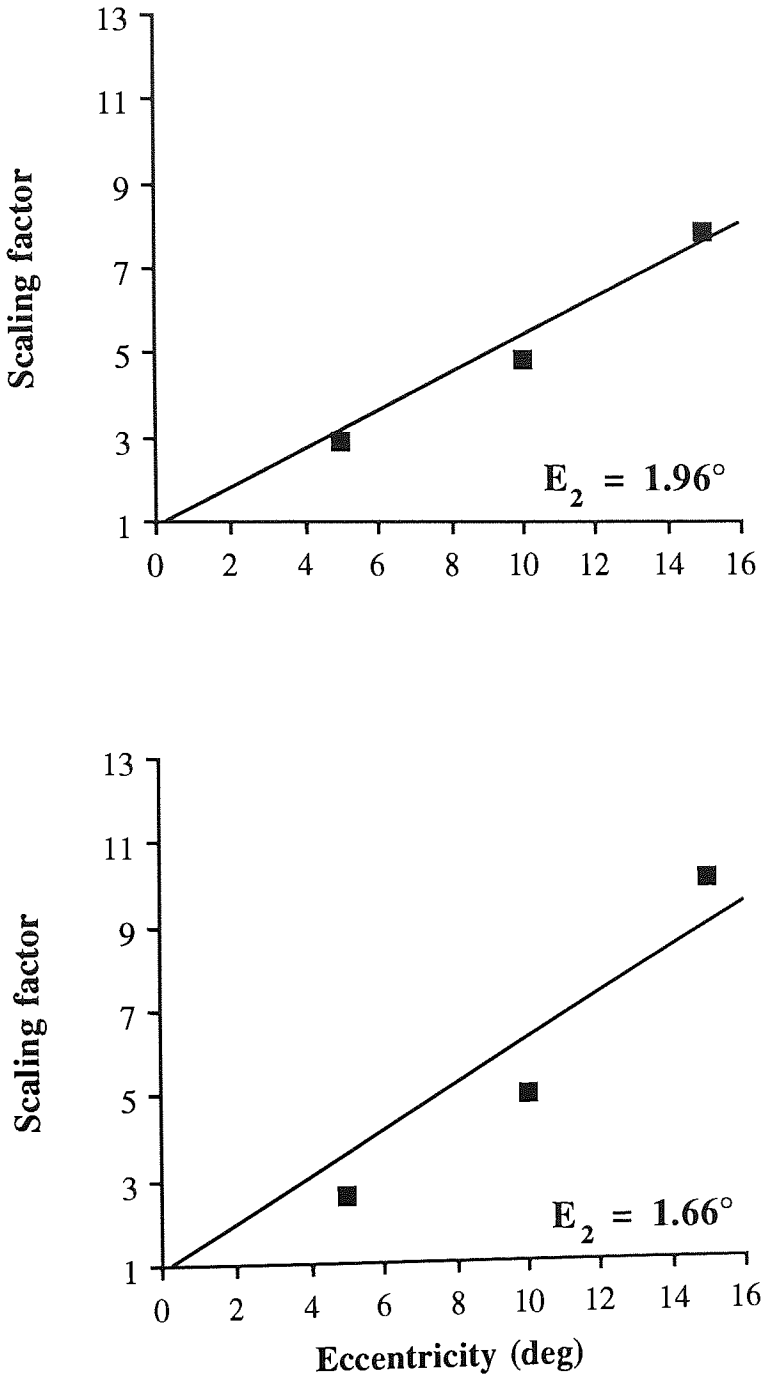

Figure 5.07c: Scaling factors, representing the values by which gap sizes for each peripheral stimulus in *Figure 5.07b* must be divided in order to collapse onto the data at 0.267 deg, plotted against eccentricity. The linear fit has been constrained to pass through a value of unity at 0.267 deg eccentricity refelecting the fact that the "foveal" data was actually obtained at this eccentricity.

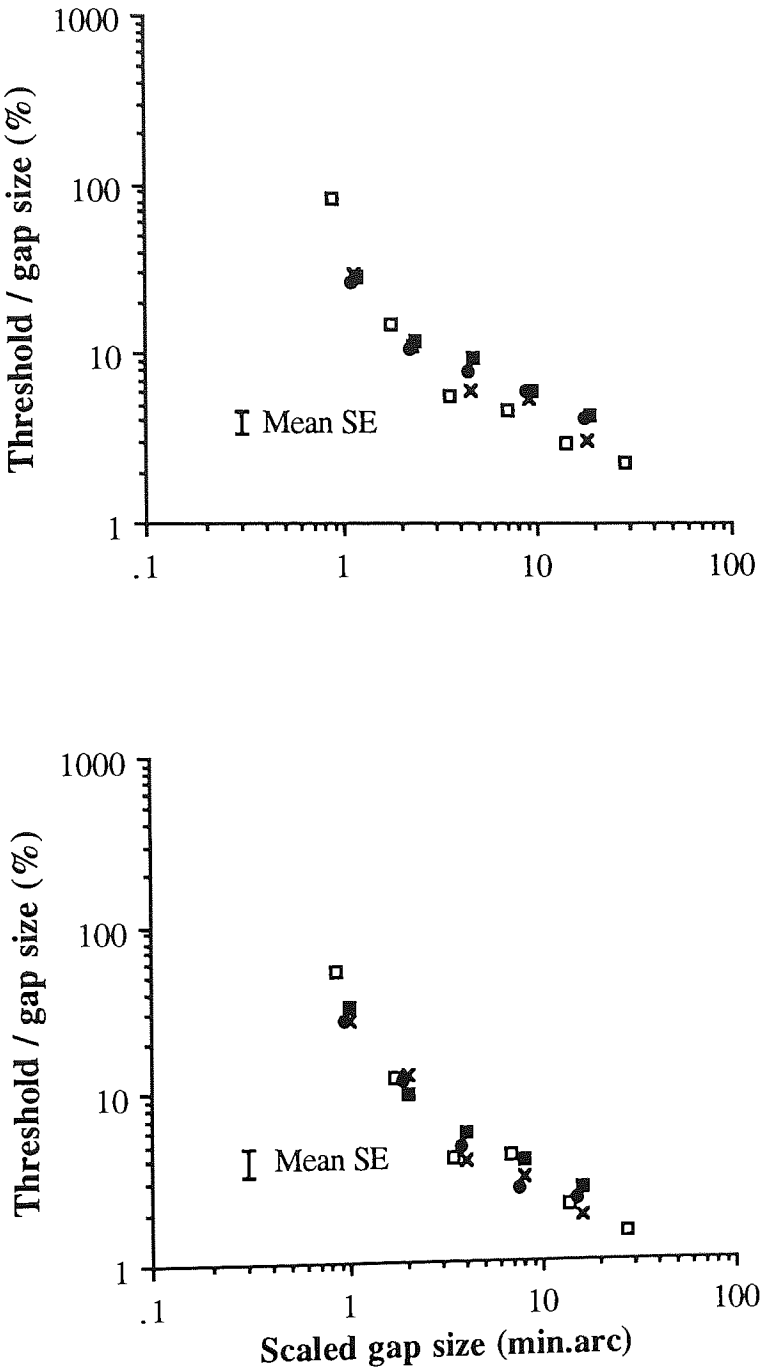

Figure 5.07d: *Figure 5.07b* replotted with the data at each eccentricity scaled according to scaling factor values derived from the linear relationship shown in *Figure 5.07c*. Mean standard error is shown.

Thresholds for the untrained observers followed the same trend as for the trained observers, but, not surprisingly, were somewhat higher. This was especially true for the peripheral observations, and resulted in smaller E_2 values for untrained observers (MD, line stimulus, 1.23 deg and KL, isoeccentric dot stimulus, 1.06 deg). The results suggest that the improvement in foveal vernier acuity observed with practice (McKee & Westheimer, 1978) is accentuated in the periphery.

5.4: Discussion

The results presented here are consistent with what has come to be known as the cortical magnification theory (Virsu, Näsänen & Osmoviita, 1987). In essence, the detectability of any foveal stimulus can be rendered the same in peripheral vision by magnifying the stimulus in every dimension to produce cortical representations of identical size. The value of E_2 provides a simple way of expressing this situation because it represents the eccentricity at which stimulus size must double in order to retain detectability.

In comparing the present data to previous studies concerning the effect of eccentricity on vernier acuity, it is important to note that none of them have used the assumption-free spatial scaling technique described here. In fact, those investigating two-dot vernier acuity chose not to increase the size of their stimuli at all on moving into the periphery. Since their dots had an angular subtense of 1 min.arc or less, it is difficult to avoid the conclusion that undersampling in the periphery had some influence on their findings.

The suggestion of Beck and Halloran (1985) that vernier acuity is independent of eccentricity may be dismissed on the following grounds. In their experiment which seems to best convey this eccentricity-independence (*Figure 5.03*), the separation of the two dots was held at a constant value of 60 min.arc whilst eccentricity varied between 2 and 8 deg. This method fails to account for the fact that optimum separation is itself a function of eccentricity. Thus, for the small eccentricities, the 60 min.arc separation clearly exceeds the optimum separation of 5 - 20 sec.arc (*Figures 5.01 and 5.02*) whereas it may be much closer to the optimum gap size at their largest eccentricity. Hence, the anticipated finding of reduced performance with increasing eccentricity is masked by the use of a constant, large separation.

For abutting line stimuli, Levi, Klein and Aitsebaomo (1985) found that vernier thresholds could be adequately scaled according to an E_2 value somewhere between 0.6 and 0.8 deg. At an eccentricity of 8 deg this would predict a performance 11 - 14 times worse than at the fovea. Wilson (1991) presents two-line vernier data showing that performance falls by a factor of 9 over the same eccentricity. Based upon the present E_2 values for the line stimulus, performance is between 5.5 and 7.5 times poorer at 8 deg eccentricity than at the fovea. The

present data therefore show a less dramatic deterioration as a function of eccentricity than other studies using line stimuli.

Levi *et al.* (1985) used an E_2 value of 0.77 deg with which to magnify their peripheral stimuli consisting of two repetitive gratings one above the other. Such a stimulus tends to reduce the sense of the overall target orientation which is a strong subjective cue in solving vernier tasks, especially in the periphery. However, Levi *et al.* also present data for a more conventional two-dot stimulus which shows the same rapid increase in thresholds away from the fovea. In addition, the length of the lines forming the grating stimulus was sufficiently long at all eccentricities to reach optimum performance. Other differences between Levi *et al.*'s study and the present one include the use of the lower rather than the nasal visual field and radially rather than tangentially oriented stimuli. It would be conceivable that performance in vernier acuity task falls more rapidly along the vertical than the horizontal meridian with increasing eccentricity, as has been found for instance with visual acuity (see *Figure 2.04*, Wertheim, 1891), grating resolution (Rovamo, Virsu, Laurinen & Hyvärinen, 1982), and contrast sensitivity (Harvey & Pöppel, 1972). This would decrease the resulting E_2 value. The ultimate reason for the different rates of decline, however, remains unclear. The present E_2 values represent a compromise between the studies which have found a rapid deterioration in vernier performance (Levi *et al.*, 1985; Wilson, 1991) and those which have found performance to fall at approximately the same rate as, for example, visual acuity and contrast sensitivity (Virsu *et al.*, 1987).

The two-dot vernier studies of Westheimer (1982) and Virsu *et al.* (1987) were very similar to each other with respect to stimulus parameters such as dot size, exposure duration and contrast. Neither scaled stimulus size as a function of eccentricity or considered the fact that changes in separation at the fovea also lead to changes in eccentricity. Despite these similarities, the two studies reached quite different conclusions. Virsu *et al.* (1987) concluded that two-dot vernier acuity could be successfully scaled according to an E_2 value of about 3.1 deg. Westheimer (1982), on the other hand, suggests that a single scaling factor cannot account for changes in two-dot vernier acuity with eccentricity since threshold and optimum separation vary at different rates. The results presented here seem to resolve the issue: provided that stimulus size is scaled appropriately and eccentricity is not allowed to co-vary with separation, a single scaling factor seems to predict the variation in two-dot vernier thresholds with increasing eccentricity (*Figure 5.07a*).

The significance of the rate of decline in performance in any one psychophysical task is difficult to estimate. The problem is highlighted by the fact that for some tasks the decline in sensitivity with eccentricity is much more rapid than the deterioration in vernier acuity described here. Bisection acuity, for instance, seems to belong to this category (Virsu *et al.*,

1987; Klein & Levi, 1987; Yap, Levi & Klein, 1987a). Such a rapid loss of sensitivity is found for certain tasks even when a method of strict spatial scaling is used (Saarinen, Rovamo & Virsu, 1989). The latter study involved an experiment in which observers had to distinguish between patterns which were either identical or mirror symmetric (*Figure 3.30*). Performance fell sharply with increasing eccentricity.

E_2 values do not only vary between tasks, but also within the same task, when the experimental conditions are changed appropriately. When the task is changed so that *three* dots are presented aligned and a slight misalignment of the middle dot is to be detected, E_2 value as small as 0.19 deg has been found in two separate studies. Klein and Levi (1987) aligned their stimulus (consisting of three bright tiny horizontal lines) along the horizontal meridian. Binocular fixation was aimed at the middle component and the eccentricity was changed by decreasing the viewing distance thereby also increasing the dot separation. Toet, Snippe and Koenderink (1988a) presented their stimulus (consisting of three spatially and temporally Gaussian modulated spots at contrast threshold) along the vertical meridian. Monocular fixation was at the middle component in foveal measurements and for peripheral viewing the stimulus was shifted in horizontal direction to vary the eccentricity of the stimulus. Thresholds were measured as a function of stimulus blur. E_2 mentioned above was determined from the data within the central 20 deg eccentricity. Considering the differences in the overall configurations it is actually surprising that these two studies arrived at quite the same E_2 value, Klein and Levi as an average of three and Toet *et al.* as an average of two observers, even though the basic task was the same in both studies. It seems that meridional variations, blur, and contrast have a small effect on three-dot vernier acuity within the central 20 deg eccentricity.

In order for scaling factors from different psychophysical tasks to be adequately compared, a common method should be established for use in all cases. Since it is clear that a scaling factor found in one psychophysical task or calculated on the basis of anatomical data cannot be relied upon to predict performance in any other task, the assumption-free spatial scaling experiment described here and proposed by Watson (1987), Johnston (1987) and Saarinen *et al.* (1989) seems to be the obvious choice.

Certain problems do, however, remain even with the spatial scaling technique, and precautions should be taken in its use. For spatially extended stimuli, different parts of the stimulus will lie at different eccentricities during any presentation. This seems to be the reason why Watson (1987) found that spatial scaling was successful in matching contrast sensitivity for small, high spatial frequency grating patches but not for large, low frequency ones. Similarly, when performance is measured as a function of the separation of stimulus components such as in the two-dot vernier experiment, care must be taken to ensure that

eccentricity effects are not confused with those of separation.

Variables external to the neural processing system may influence thresholds, and their variation with eccentricity may distort final scaling estimates. Eye movements, for example, would preferentially affect foveal vision and high spatial frequencies (Virsu *et al.*, 1987; Drasdo, 1991). Since the degree of optical degradation changes only slowly with eccentricity (Charman, 1983) this would also be expected to produce an apparent reduction in the rate at which performance declines in the periphery. In relation to retinal sampling density, the optical transfer function becomes better with increasing eccentricity and therefore undersampling of the retinal image becomes likely.

A factor which is likely to increase the rate of decline is the procedure of performing a linear regression to the variation in scaling factor with eccentricity. In the present data (*Figures 5.05c, 5.06c, 5.07c*) the residual deviation of the 15 deg data point from the linear regression is consistently in a positive direction. This tends to increase the the gradient of the linear regression, hence reducing the value of E_2. This trend is not, however, consistent amongst observers, since the two naïve, untrained observers demonstrated no such tendency. It is worth noting though, that the eccentricity range over which the estimate of E_2 is made *may* have an effect on the E_2 value, which must be taken into consideration when evaluating the results.

In conclusion, the spatial scaling method used by Watson (1987), Johnston (1987) and Saarinen *et al.* (1989) in which performance is measured as a function of eccentricity for stimuli which are all simply magnified versions of each other has been successfully applied to vernier acuity performance for various stimulus configurations. The technique provides an independent measure of the rate of decline of vernier performance with eccentricity. Previously such measures had only been obtained by making prior assumptions concerning the value of the scaling factor on the basis of physiological data, or by using stimuli in which no account was made for the effects of cortical magnification. The simplicity and effectiveness of this technique made it appealing to examine several other hyperacuity tasks to see if the method would be as successful in matching foveal and peripheral performance for these as it was for the vernier acuity tasks. Therefore, in the following chapters a selection of hyperacuity tasks, as well as movement tasks are studied using the method of spatial scaling.

Chapter 6: Spatial interval discrimination

6.1: Introduction

Performance in different tasks falls at different rates with increasing eccentricity (Weymouth, 1958; Rovamo & Virsu, 1979; Levi, Klein & Aitsebaomo, 1984, 1985). This raises important questions regarding the physiological basis for such differences. Are the differences simply due to the variation of the sampling density across the visual field, and if so, which types of structures are the ones that set the upper limits for performance? Or is there perhaps a qualitative difference in processing different types of tasks?

Estimating of peripheral performance and the rate of decline of that performance towards periphery becomes more complicated when threshold varies both as a function of eccentricity and with the spatial configuration of the stimulus. For example, in a spatial interval discrimination experiment the observer is presented with a pair of dots or lines with a certain separation. The task is to identify whether this gap is larger or smaller than a sequentially presented comparison stimulus or an internally learnt standard. The separation which produces optimum thresholds and the optimum threshold itself both increase with eccentricity but the threshold value increases at a much faster rate (Yap, Levi & Klein, 1989; Levi & Klein, 1990b). The same situation has been found (*Chapter 5*) for two-dot vernier acuity as a function of separation (Westheimer, 1982). These findings run contrary to the concept of spatial scaling which suggests that performance in any task should become equal throughout the visual field simply by equating the differences in sampling density by changing the size of the stimulus appropriately. The spatial scaling approach would predict exact agreement between threshold and the spatial parameters which give rise to it.

The studies of Yap, Levi and Klein (1989) and Levi and Klein (1990b) both compared the E_2 values of optimum separation and resolution with spatial interval discrimination. Yap *et al.* (1989) studied spatial interval discrimination for dots positioned side by side in the lower visual field. Thresholds were determined at eccentricities up to 10 deg and eccentricity was measured along the vertical meridian between the dots, i.e. the method was not strictly an isoeccentric one. E_2 for two observers was found to be 0.6 - 0.8 deg for the task, whereas E_2 in similar conditions for optimum separation was 2.0 deg and for resolution 1.7 - 2.0 deg. *Figure 6.01* shows the templates describing the threshold functions in the spatial interval discrimination task at four different eccentricities. Whereas the optimum threshold elevation is about 14× (from 7 to 100 sec.arc), the increase in the optimum separation is only about 6× (from 0.9 to 5 min.arc) when eccentricity varies from 0 to 10 deg. Thresholds elevate with increasing separation after the minimum thresholds at all eccentricities, as is typical for non-isoeccentric data. Note that separations are clearly smaller than in the present study.

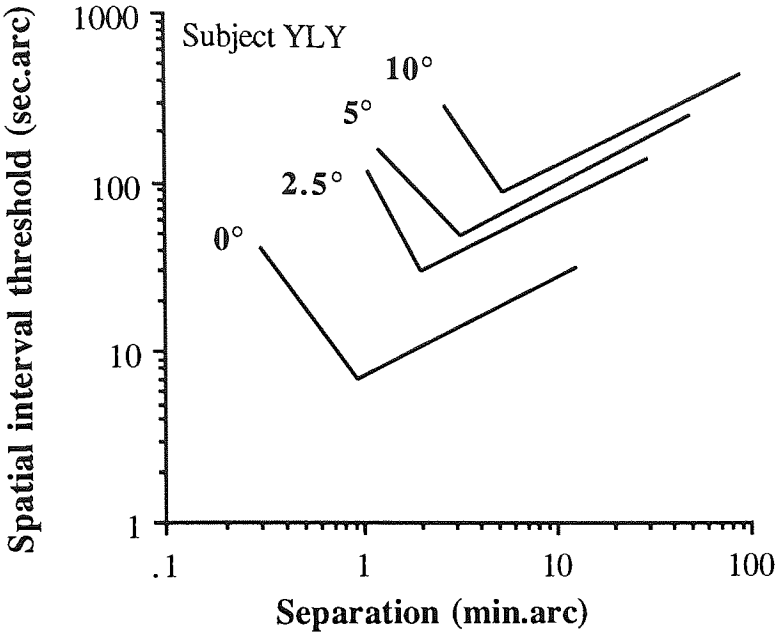

Figure 6.01: Templates for spatial interval thresholds plotted against separation. The stimulus configuration was non-isoeccentric, and the separations used were smaller than in the present study. Redrawn from Yap, Levi and Klein (1989), Figure 1a.

Levi and Klein (1990b) used a stimulus consisting of two thin black horizontal lines one above another in the lower visual field. For three observers E_2 was found to be 0.68 - 0.83 deg for optimal thresholds, 1.9 - 2.4 deg for optimum separation and 2.1 - 2.5 deg for resolution. In this, as well as in the Yap *et al.* (1989) study, the peripheral stimuli were increased according to E_2 of 2.5 deg by changing the viewing distance. Comparison of the E_2 values in these two studies show a similar slow increase of optimum separation relative to optimum thresholds at each eccentricity in the spatial interval discrimination task.

McKee, Welch, Taylor and Bowne (1990) found that thresholds in a spatial interval task for eccentricities ranging 0.15 - 2.4 deg (i.e. separations ranging 18 - 288 min.arc) increased linearly from about 0.7 min.arc to 9 min.arc in agreement with Weber's law. The two vertical lines forming the stimulus were positioned on the horizontal axis and fixation was in the middle of the lines. Changes in separation therefore changes in eccentricity i.e. the stimulus was non-isoeccentric. Line lengths were increased with increasing eccentricity according to an E_2 of 0.8 deg. The data for three observers is shown in *Figure 6.02.* The averaged thresholds increase by a factor of 12.8 between an eccentricity of 0.15 and 2.4 deg. According to equation *4.06* (i.e. substituting 0.15 deg for our smallest eccentricity of 0.267 deg) this represents a gradient, S, of 5.2. Substituting this into equation *4.07* gives an E_2 of 0.04 deg.

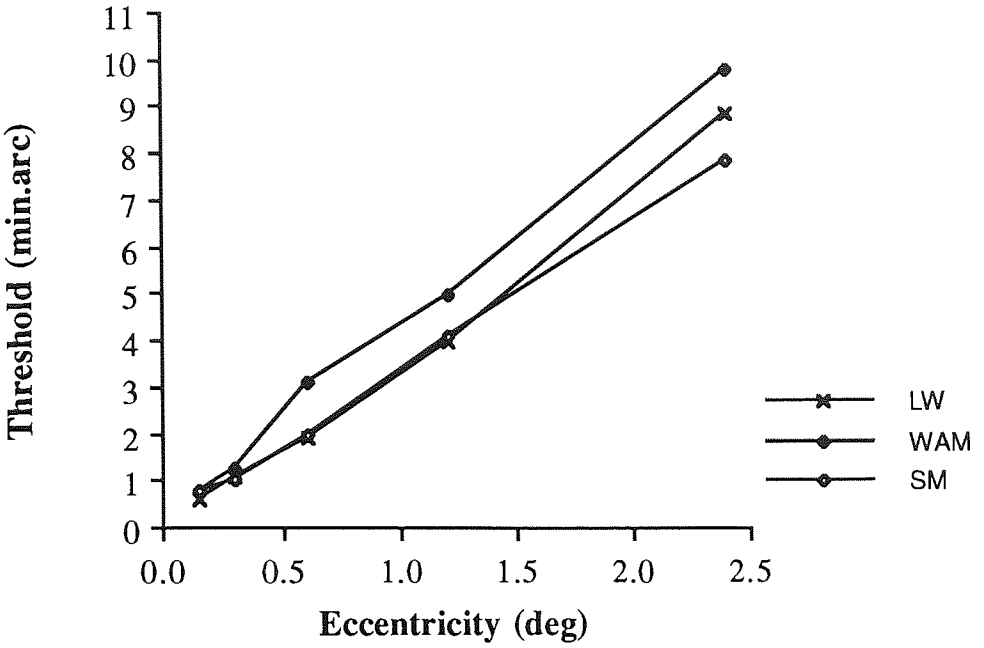

Figure 6.02: Spatial interval thresholds for three subjects plotted against eccentricity. Redrawn from McKee, Welch, Taylor and Bowne (1990), Figure 3.

Failure of Weber's law at large separations

A scaling factor is unique to a single point in visual space. An extensive stimulus cannot possibly be presented so that all parts of the stimulus lie at the same eccentricity. In the case of the spatial interval discrimination experiment, fixation in the foveal presentation would logically lie mid-way between the two dots which comprise the stimulus (as has been the case in most previous studies). Neither dot is therefore actually at an eccentricity of zero, but is instead at some eccentricity determined by the separation of the dots. Therefore, if thresholds are measured as a function of dot separation, then the shape of the function observed reflects not only the effect of separation, but the effect of changing eccentricity as well. There is no sense scaling a task looking for the effect of one variable if the changes in performance are mainly caused by another variable. Specifically, at the fovea, the data is likely to reflect a combination of the effects of separation and eccentricity. At eccentricities of 5 - 15 deg, where the eccentricity is large relative to the separation, changes in eccentricity when separation increases are far less significant.

Thresholds for positional tasks usually increase in proportion to the separation of their features once the separation has exceeded an optimum value (Westheimer & McKee, 1977b; Westheimer, 1979). Whether this phenomenon (an example of Weber's law, which states that the just-noticeable difference in stimulus magnitude is a constant fraction of the stimulus, Weber, 1834) arises due to the increase in separation itself or whether it is a consequence of

increasing the eccentricity of the features has been the subject of several recent studies, including spatial interval discrimination (Levi, Klein & Yap, 1988; Morgan & Watt, 1989; Levi & Klein, 1989; Levi & Klein, 1990a; McKee, Welch, Taylor and Bowne, 1990).

The study paving the way for the truly isoeccentric method was performed by Levi, Klein and Yap (1988), who noted that in previous experiments as separation was increased, portions of the stimulus fell gradually further in the periphery. It is known that position discrimination becomes progressively worse in the periphery (due to increasing receptive field size and spatial uncertainty) thus, perhaps this could account for Weber's law at large separations. To test this hypothesis, they positioned the outmost lines of a three-line bisection stimulus on an isoeccentric arc (the arc has been described in *Chapter 4, Figure 4.11*).

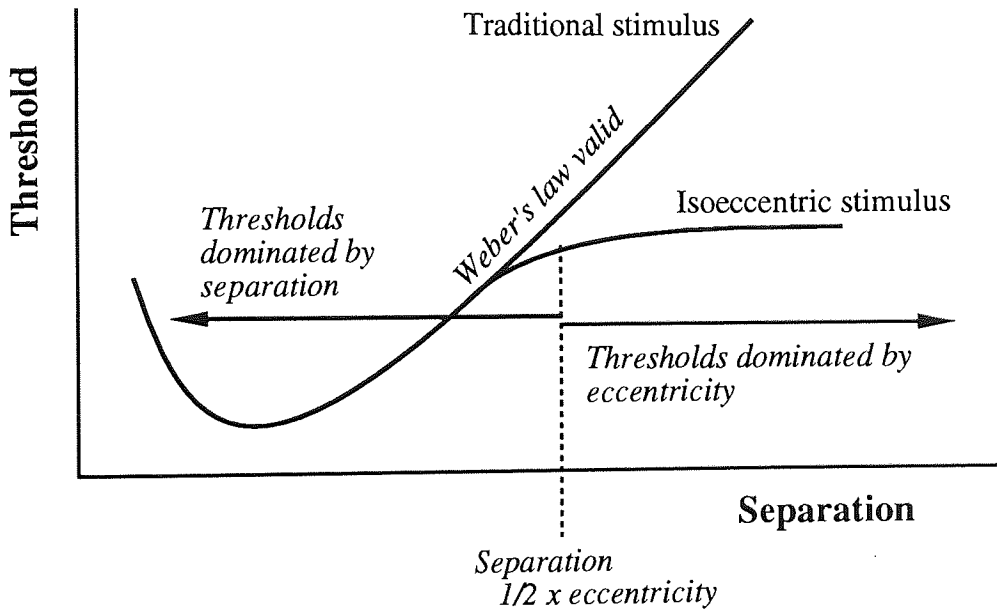

Figure 6.03: A schematic drawing describing Klein and Levi's (1987) theory according to which thresholds at small separations are dominated by target separation, and at large separations (above ≈ 0.5 × eccentricity in question) by eccentricity. At the smallest separations optical blur is eventually the limiting factor for performance. When the isoeccentric method is used, Weber's law fails at large separations and the level at which thresholds saturate is determined by the eccentricity. According to the theory at each separation / eccentricity an observer uses the mechanism which is more sensitive for a given stimulus configuration.

The stimulus was presented at a constant 10 deg eccentricity, so that the centre line was between the outmost lines, i.e. *not* on the arc. The centre line was relatively closer to one of the outer lines and the direction of the offset was to be determined. As the resulting thresholds were practically independent of separation between 2 and 10 deg, showing clear deviation from Weber's law, it was suggested that large separations (larger than about 20 min.arc) are discriminated by estimating the distance across the cortex between the patterns of

excitation produced by the individual lines. The results were confirmed with a spatial interval task for which the stimulus was identical to the bisection stimulus, but the other of the outer dots was excluded. These results were in agreement with a theory originally proposed by Klein and Levi (1987) according to which thresholds would be dominated by target separation at small separations, whereas at large separations the thresholds were dominated by eccentricity (see *Figure 6.03*). However, Weber's law is so pervasive in sensory physiology that the failure of the law surprised even the authors. Thus, more thorough studies were called for.

Morgan and Watt (1989) criticized Levi *et al.*'s (1988) study in that i) only one eccentricity was used, ii) the bisecting point was not on the arc but at a different eccentricity from the points that define the eccentricity thus perhaps cancelling out the effects of separation, iii) for the smallest separation the increase in threshold might have been caused partly by resolution failure in the periphery. To support their criticism, Morgan and Watt presented results obtained with arcs of circles as stimuli. The subject had to compare the length of two arcs presented sequentially along the circle, whilst fixation was maintained at the centre of the circle. Thresholds increased with increasing arc length and depended little on the eccentricity. This result was not altered by expressing thresholds as a function of chord length or by varying the curvatures of the arcs.

In their reply to Morgan and Watt, Levi and Klein (1989) pointed out that i) additional data acquired at several eccentricities and presented in Levi and Klein (1990a, see an example of the data in *Figure 6.04*) scaled simply with eccentricity as would be expected if target eccentricity is the limiting factor for position judgments, ii) the results in a two-line spatial discrimination experiment with no middle line did indeed exhibit lower thresholds at the smallest separation, which had already been suggested by Levi *et al.* (1988) and, iii) resolution thresholds at 10 deg eccentricity were 40 times smaller than the separation and thus not the reason for elevated thresholds at small separations. Further, Levi and Klein (1989) argued that an arc length task used by Morgan and Watt is increasingly difficult when the the arc becomes longer, and this was the basic reason for elevated thresholds for longer arcs.

Levi and Klein (1990a) present data to support the suggestion of two separate mechanisms for position judgments. The spatial interval discrimination experiments were performed in the lower visual field, the two vertical bright lines were positioned on an isoeccentric arc, and presentation time was 200 msec. In *Figure 6.04* thresholds are plotted against separation. According to the authors at separations smaller than 0.5 × eccentricity thresholds appear to be proportional to feature separation, showing little dependence on eccentricity. At large separations thresholds no more behave according to Weber's law but are dependent on eccentricity and essentially independent of separation (*Figure 6.04*). The data for subject DL

shows the failure of Weber's law at large separations and was chosen to be presented here also because it allows comparison with the present data.

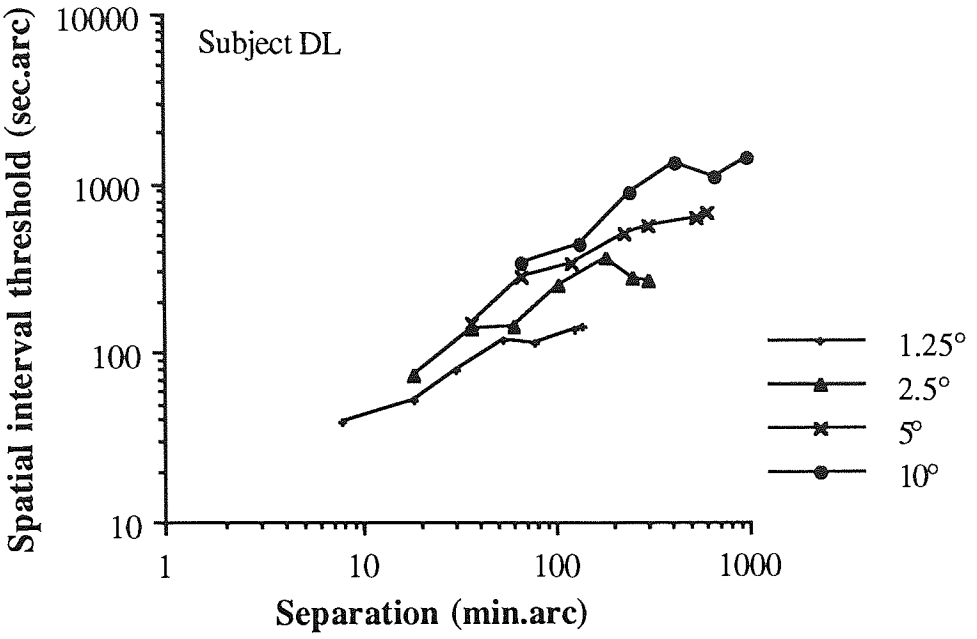

Figure 6.04: Isoeccentric spatial interval discrimination thresholds are plotted against separation. Redrawn from Levi and Klein (1990a), Figure 8.

E_2 value derived from the above data is likely to be inaccurate because the smallest eccentricity measured is large (1.25 deg). The reason for this is almost certainly due to the large uncertainty involved in predicting E_2 values when data from eccentricities close to the fovea is not available. If analysed using the method described in this thesis and substituting 1.25 instead 0.267 deg in equation *4.07* the E_2 value becomes -0.3 deg.

Burbeck and Yap (1990b) present essentially similar results to those of Levi and Klein (1990a) obtained in the temporal visual field for a stimulus consisting of two 4 × 32 min.arc rectangles. Only the eccentricities of 2.5, 5, and 10 deg were studied thus, E_2 values are not determined here. Overall, the shape of the threshold functions were similar to Levi and Klein's (1990a) and seem to support the theory of two mechanisms, one very sensitive to separation and only somewhat sensitive to eccentricity and the other very sensitive to eccentricity and only somewhat sensitive to separation.

To study the relationship between separation and eccentricity McKee, Welch, Taylor and Bowne (1990) presented two line *pairs* so that fixation was in the middle of the pairs and the task was to discriminate which pair had wider separation. Between the pairs the separation was 72 min.arc, each pair was thus at 36 min.arc eccentricity. When the separation within the pairs was changed without altering the nominal eccentricity, thresholds remained unchanged.

Thus again in this stimulus configuration eccentricity, not separation, was the limiting factor for the threshold lending support to Klein and Levi's theory of two localization mechanisms.

In this chapter the eccentricity-related decline in performance is studied for spatial interval discrimination to examine whether the simple concept of spatial scaling holds and if the thresholds can be scaled simply with eccentricity, as has been suggested by Yap *et al.* (1989) and Levi and Klein (1990a,b). In the spatial interval discrimination task performed for this thesis the different parts of the stimulus were presented on an arc surrounding fixation so that all parts of the stimulus lay at the same eccentricity (Levi, Klein & Yap, 1988; Levi & Klein, 1989; Levi & Klein, 1990a).

6.2: Methods

The stimuli were presented on a CRT as described in General methods. The stimulus luminance was 40 cd m^{-2}. In order to remove the reference clues apart from the stimulus itself, the room lights were extinguished. Further, the horizontal location of the stimuli was jittered from trial to trial. Fixation stimuli were presented briefly before each trial in order to maintain accommodation and ensure that the stimuli appeared at the appropriate eccentricity.

The two experienced observers were PM and DW. Viewing was monocular with the dominant eye. Thresholds were determined using a two-alternative forced-choice technique with a modified PEST routine (Findlay, 1978) which estimated the 80% correct level for both response alternatives to exclude that any potential effect of bias on thresholds. No feedback was given. For each combination of eccentricity and the spatial parameters of the task, four threshold measurements were taken in random order. Final threshold was a mean of these four measurements.

A variation of the usual, "traditional" spatial interval task was used. The features which demarcate the interval (small squares) are maintained at the same eccentricity by placing them on the circumference of an imaginary arc whose centre coincides with fixation (*Figure 6.05*). This has been termed an isoeccentric arc and was introduced at the end of the *Chapter 4* and used for the isoeccentric presentation of the two-dot vernier acuity task in *Chapter 5*. Separation is defined as the horizontal distance between the two squares, and is varied simply by moving the two squares around the arc as shown in *Figure 6.05*. In addition, to satisfy the requirement that all stimuli should simply be magnified versions of each other, the size of each square is constrained to be a constant fraction (in this case 11%) of the separation.

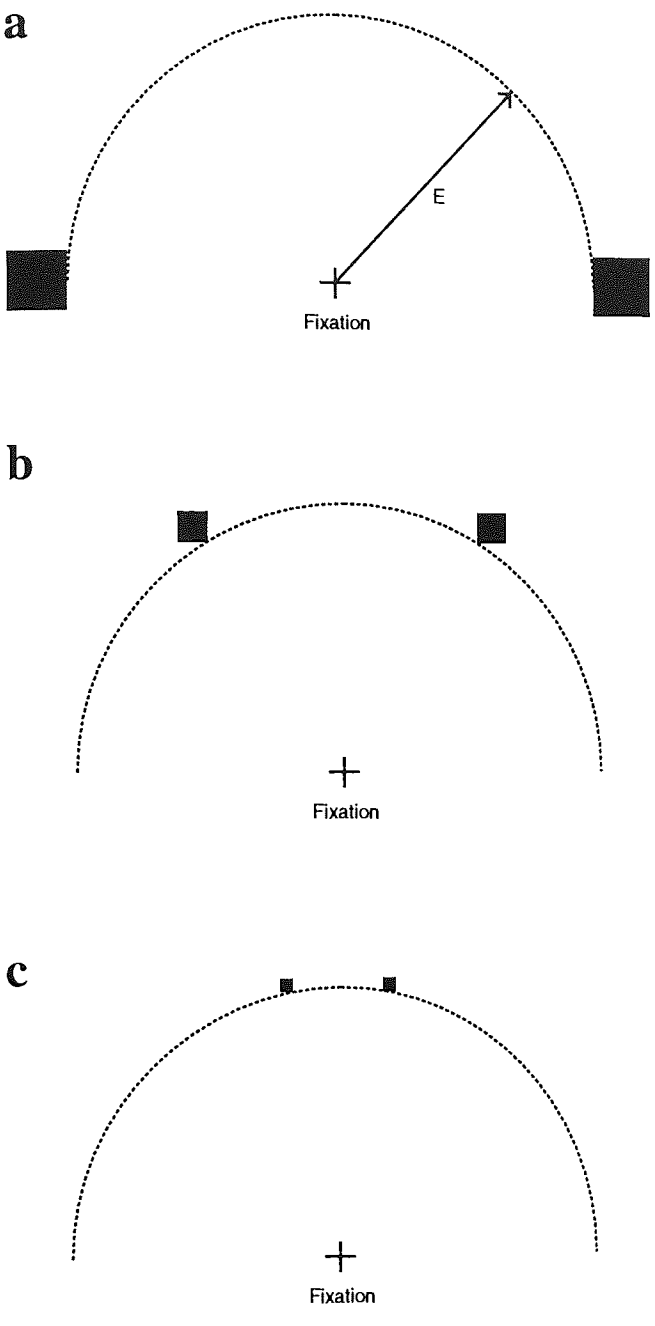

Figure 6.05: The method of dissociating the effects of eccentricity and separation for spatial interval discrimination task. The circle itself is invisible to the observer, who maintains fixation at its centre with the aid of a fixation line which is present up to the onset of the stimulus, but not during the stimulus presentation itself. The eccentricity of the stimulus is defined by the radius of the arc, denoted by E. Changes in the spatial parameter of the task, i.e. separation, are achieved by moving the features around the circumference of the arc.

The size of the individual features (squares) is a constant fraction of the separation. Hence, all stimuli are simply magnified versions of one another. The maximum separation of the stimulus features is clearly equal to the diameter of the arc, in which case the features appear on either side of fixation (a).

Examples of large, medium and small separations are shown in *Figure 6.05*. Eccentricity is defined by the angular radius of the arc and changes in this parameter may be visualised by simply moving the page closer (increasing eccentricity) or further away (reducing eccentricity). In all conditions, the task of the observer was to determine whether a subsequently-presented test interval was wider or narrower than the standard interval. The size of the squares in both presentations remained the same. Thresholds can be measured for several different standard intervals and eccentricities in this way.

The procedure has the disadvantage that performance cannot be established at an eccentricity of zero degrees. Hence, it is necessary to choose an eccentricity near zero and use this against

which performance at more peripheral locations can be compared. The smallest eccentricity used was 0.267 deg (16 min.arc). Note that the diameter of the arc represents the upper limit on the range of separations which can be obtained. In practice, different eccentricities were obtained by a combination of varying viewing distance and modifying the physical size and separation of the stimuli on the CRT. Viewing distance varied between 20 and 0.6 metres. Eccentricities between 0.267 and 7.5 deg in the upper visual field were investigated. At each eccentricity, spatial interval discrimination thresholds were measured as a function of the standard separation of the two squares.

Since the stimuli were presented in darkness, a red fixation line was presented for 750 msec prior to the appearance of the two squares of the spatial interval task. The luminance of the fixation line was sufficiently low that no after-images were noticed by the observers. The mid-point of the line represented the centre of the isoeccentric circle on whose circumference the squares were to be presented. The observer was required to maintain fixation at this point throughout the stimulus trial. The fixation line disappeared and the standard stimulus was immediately presented for a duration of 500 msec. There then followed an inter-stimulus interval during which the screen was blank. Next the test stimulus appeared for a duration of 500 msec, and the observer responded via the keyboard as to whether the spatial interval in the test stimulus was larger or smaller than the standard. Immediately following this response, the fixation line appeared again and the sequence continued until the end of the psychophysical routine (usually around 50 - 70 trials). Data was gathered for two different inter-stimulus intervals, 50 and 500 msec. Note that no fixation point or line was present simultaneously with the stimuli since this could have been used as a clue for solving the task.

6.3: Results

Figure 6.06a shows spatial interval thresholds for two observers plotted against separation at each of the five eccentricities studied. Inter-stimulus interval was 50 msec. At all eccentricities, thresholds increase steadily with increasing separation. *Figure 6.06b* shows thresholds expressed as a percentage of separation replotted against separation itself (i.e. as a Weber fraction). Note that at no eccentricity does the Weber fraction remain constant but decreases to around 5% as separation is increased. The reason why each function was not continued to larger values of separation in order to determine whether a distinct plateau occurred in the Weber fraction is that, as a consequence of using isoeccentric stimuli, there is an upper limit to the separations for which we can obtain data. By expressing thresholds as a fraction of separation, the y-axis of *Figure 6.06b* has been made scale invariant.

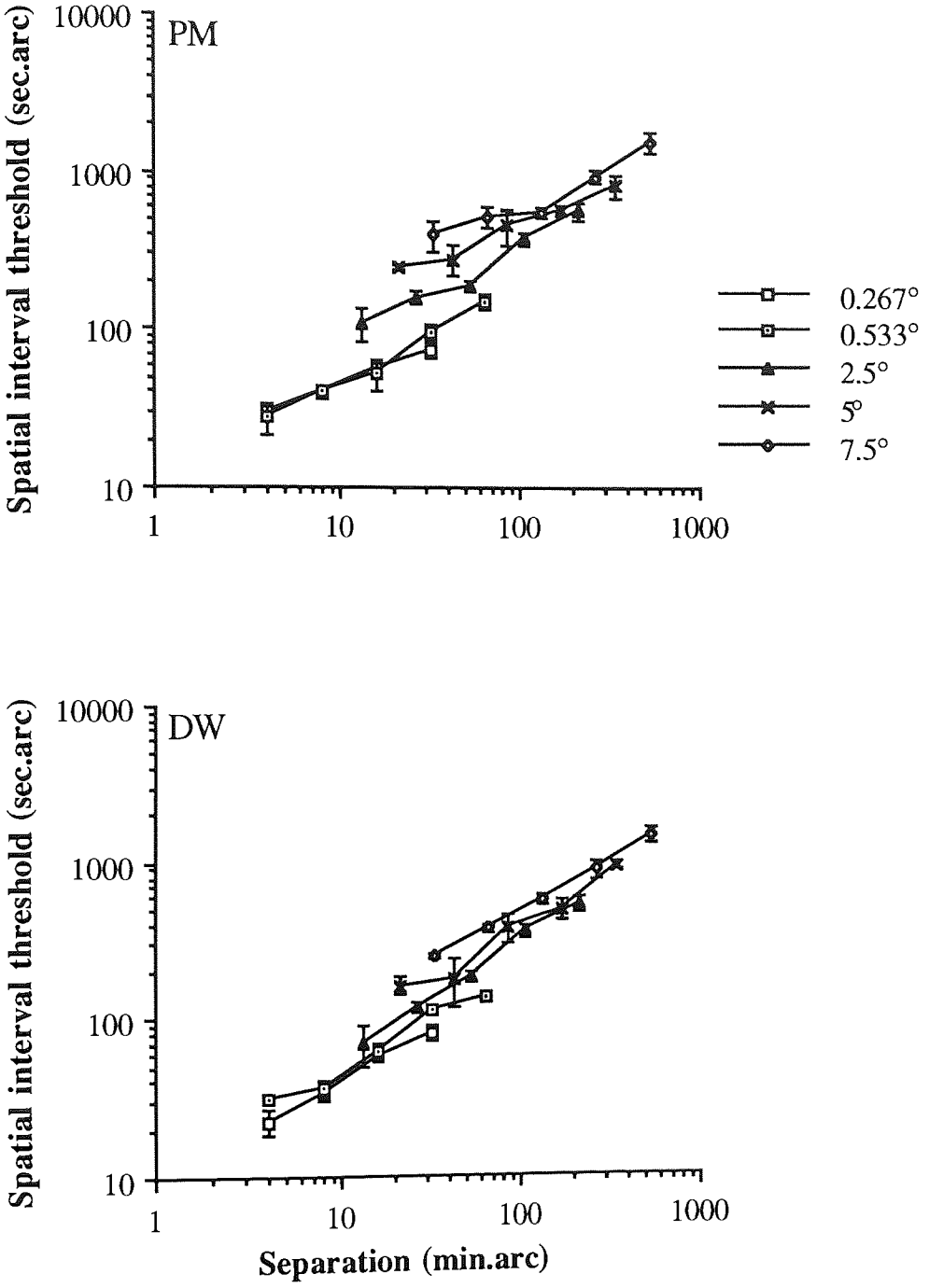

Figure 6.06a: Spatial interval thresholds for PM and DW plotted against separation. Inter-stimulus interval was 50 msec. Different symbols represent different eccentricities, achieved by varying the radius of the isoeccentric arc and are shown, as well as the standard errors.

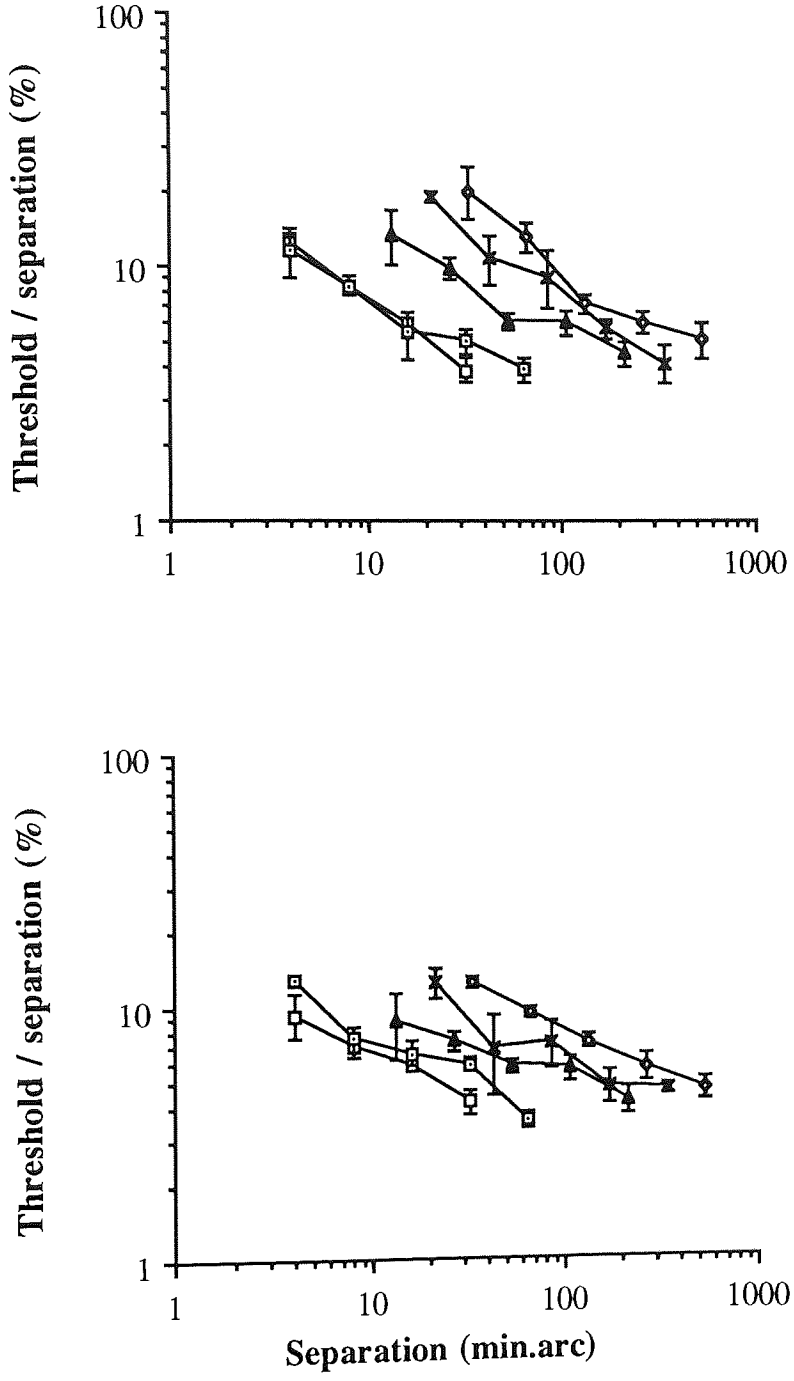

Figure 6.06b: The data replotted with threshold expressed as a percentage of separation (i.e. as a Weber fraction). Symbols and subjects as in (a).

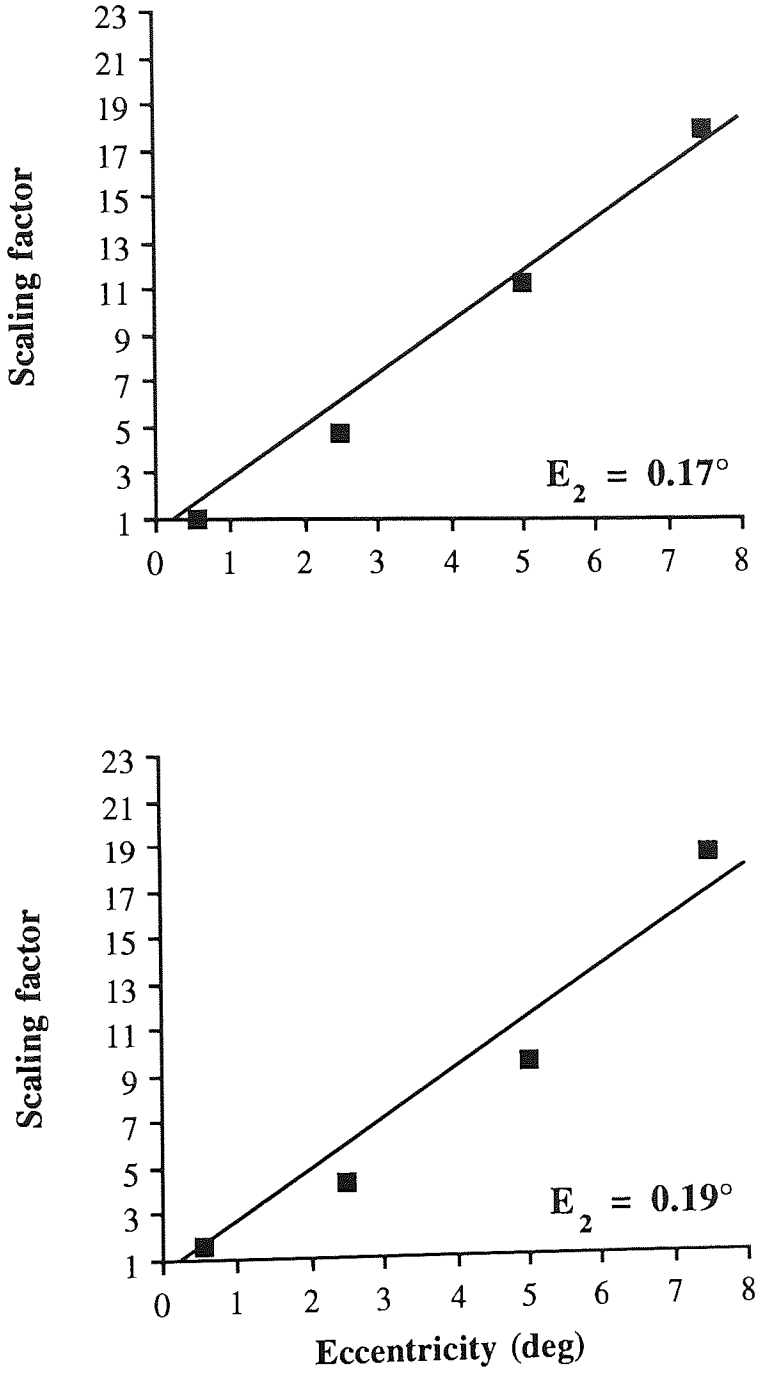

Figure 6.06c: Scaling factors obtained at each eccentricity relative to the smallest eccentricity of 0.267 deg. The line of least squares is constrained to pass through the point (0.267, 1).

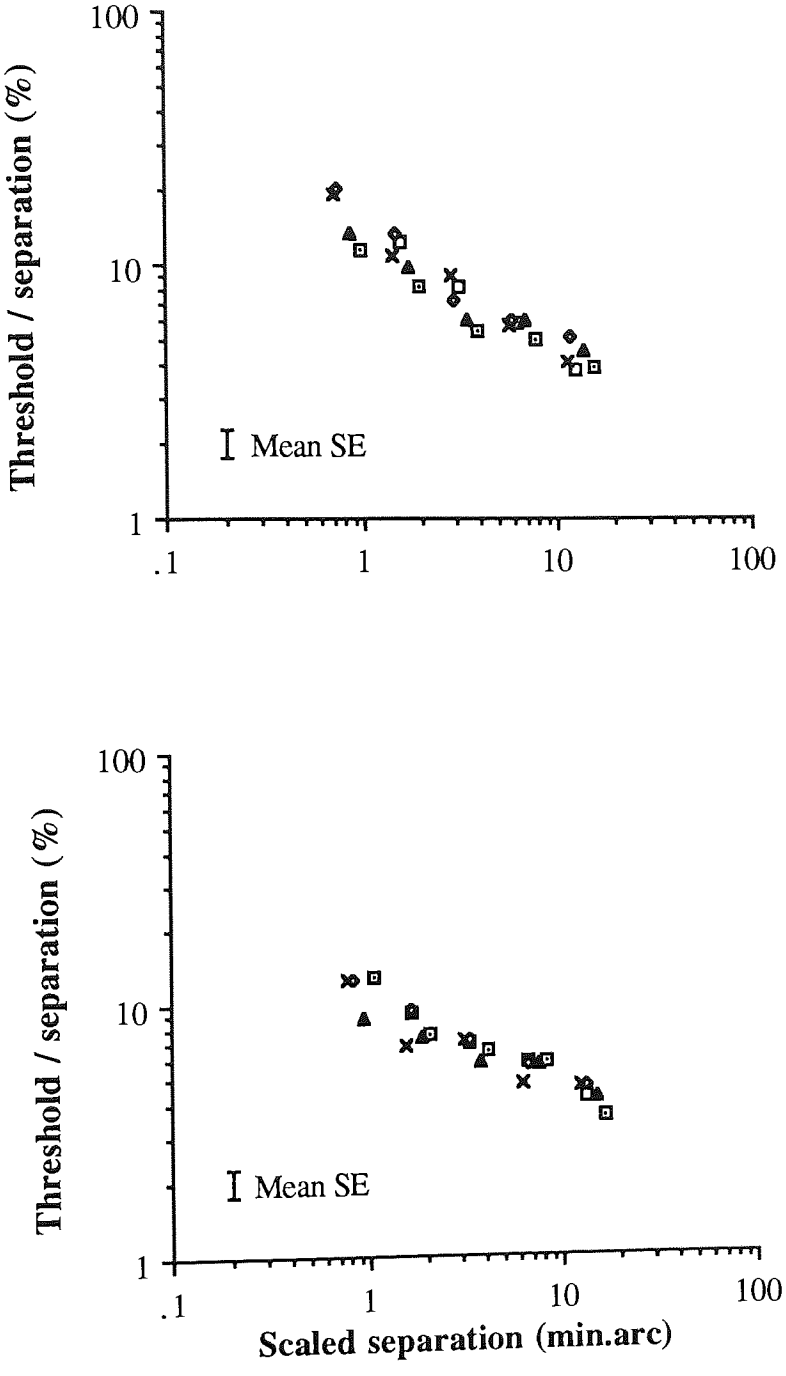

Figure 6.06d: The data of *Figure 6.06b* with the separation values at each eccentricity having been scaled along the size (x-) axis. Note how the eccentricity dependent variance of the data is removed in this way.

If the concept of spatial scaling holds, one would expect functions for successive eccentricities to be displaced relative to one another only along the size (in this case the x-) axis and this is exactly what is found. Scaling factors were found for each eccentricity using the method described in the General methods and are shown in *Figure 6.06c*. The value of the scaling factor increases with eccentricity, and the data shown is fitted with a linear regression line constrained to pass through a value of unity at the eccentricity of 0.267 deg since the scaling factors were obtained relative to the data at this eccentricity.

Sinc an isoeccentric paradigm was used, there was no direct estimate of the scaling factor for an eccentricity of zero. However, the linear regression can be extrapolated to an eccentricity of zero in order to find the foveal scaling factor. E_2 can be determined according to equation *4.07* as

$$E_2 = (^1 / _S) - 0.267.$$

The gradients of the regression lines in *Figure 6.06c* are 2.29 (± 0.16) for PM and 2.19 (± 0.24) for DW. Hence E_2 values for this spatial interval discrimination task are 0.17 (± 0.03) deg (PM) and 0.19 (± 0.05) deg (DW).

Using an isoeccentric paradigm, it is impossible to obtain data at zero degrees eccentricity. Thus, data from other eccentricities is scaled relative to 0 deg according to the equation *4.09*. *Figure 6.06d* shows the data from all eccentricities shown in *Figure 6.06b* after having been scaled. No eccentricity dependence remains, indicating that spatial scaling has been successful for this task and that performance at different eccentricities can be related simply by a change of scale.

Since it is debatable whether fixation can be successfully maintained at an eccentricity as small as 0.267 deg, a control experiment was performed. The red fixation line was removed and observers were allowed to foveate mid-way between the two dots, as is the traditional procedure in a spatial interval task. The data of PM and DW from 0.267 deg eccentricity and the corresponding data acquired without the fixation line are compared in *Figure 6.07a* and *b*. The difference between the two data sets suggest that the method using fixation was successful. At large separations there is little difference between thresholds measured by both techniques. This is to be expected, because the eccentricity of the dots is similar for the isoeccentric and non-isoeccentric stimulus. However, as the separation decreases, the eccentricity of the dots is steadily reduced in the non-isoeccentric condition. This results in significantly lower thresholds than those obtained for the isoeccentric stimulus.

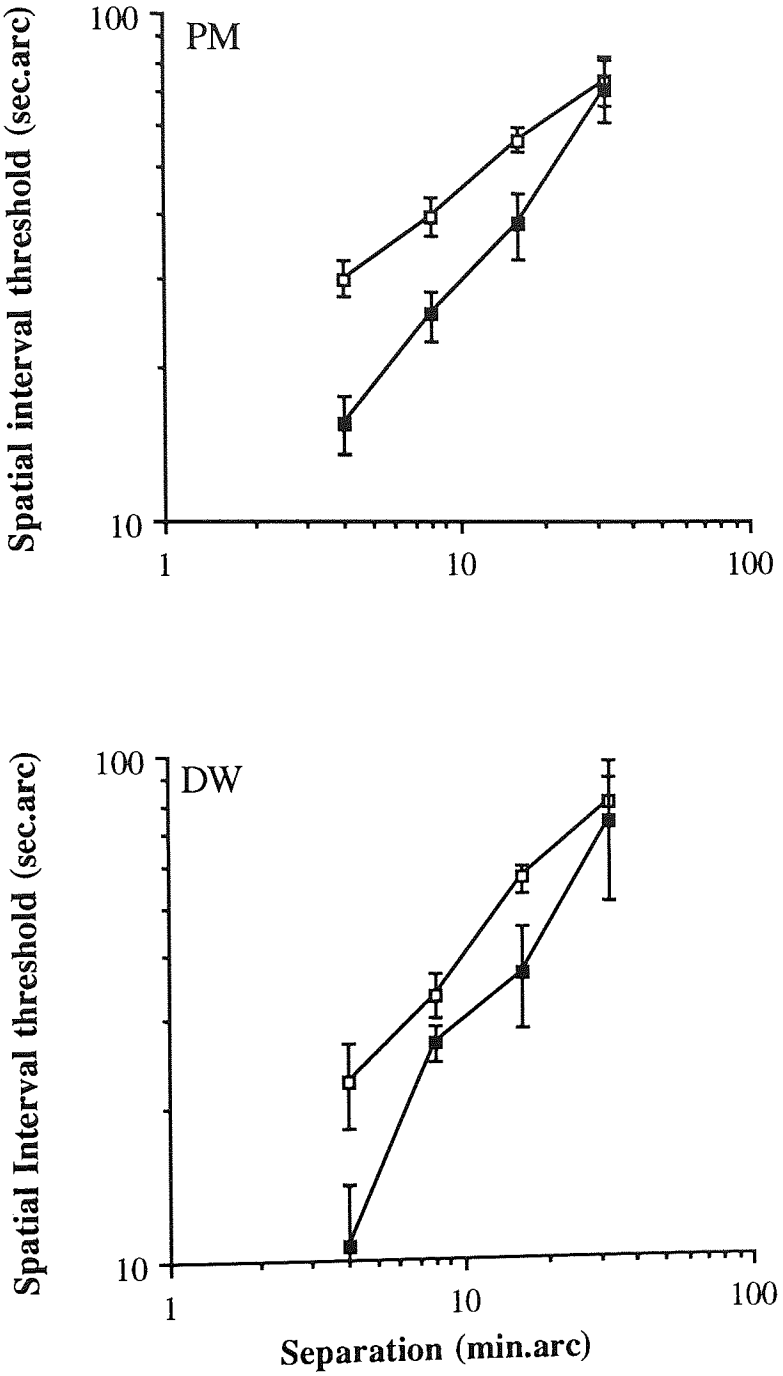

Figure 6.07a,b: Spatial interval discrimination thresholds plotted against separation for two different stimuli. Open squares: Isoeccentric data at 0.267 deg eccentricity. Filled squares: Data acquired conventionally, by foveating at the centre of the stimulus. Note the increased gradient of the functions for the conventional method. Standard errors are shown.

The data in *Figure 6.07* demonstrate the contributions of separation and eccentricity to spatial interval discrimination thresholds. The slope of increase in the isoeccentric threshold data (0.45 and 0.63 for PM and DW, respectively) reflect the effect of separation. The steeper gradients of the non-isoeccentric data (0.73 and 0.88, respectively) represent a combination of the effects of separation and eccentricity.

Data for an inter-stimulus interval of 500 msec is shown in *Figure 6.08a-d.* Increasing the inter-stimulus interval from 50 to 500 msec has little effect on thresholds. Again, spatial interval thresholds increase as a function of separation, and when plotted as a Weber fraction show a gradual improvement to around 5% at larger separations. Scaling factors again increase in an approximately linear fashion with eccentricity. E_2 values were 0.22 (± 0.01) deg for PM but somewhat lower, 0.07 (± 0.01) deg for DW. As with the 50 msec data, scaling the data from each eccentricity according to these E_2 values removed the eccentricity dependence (*Figure 6.08d*).

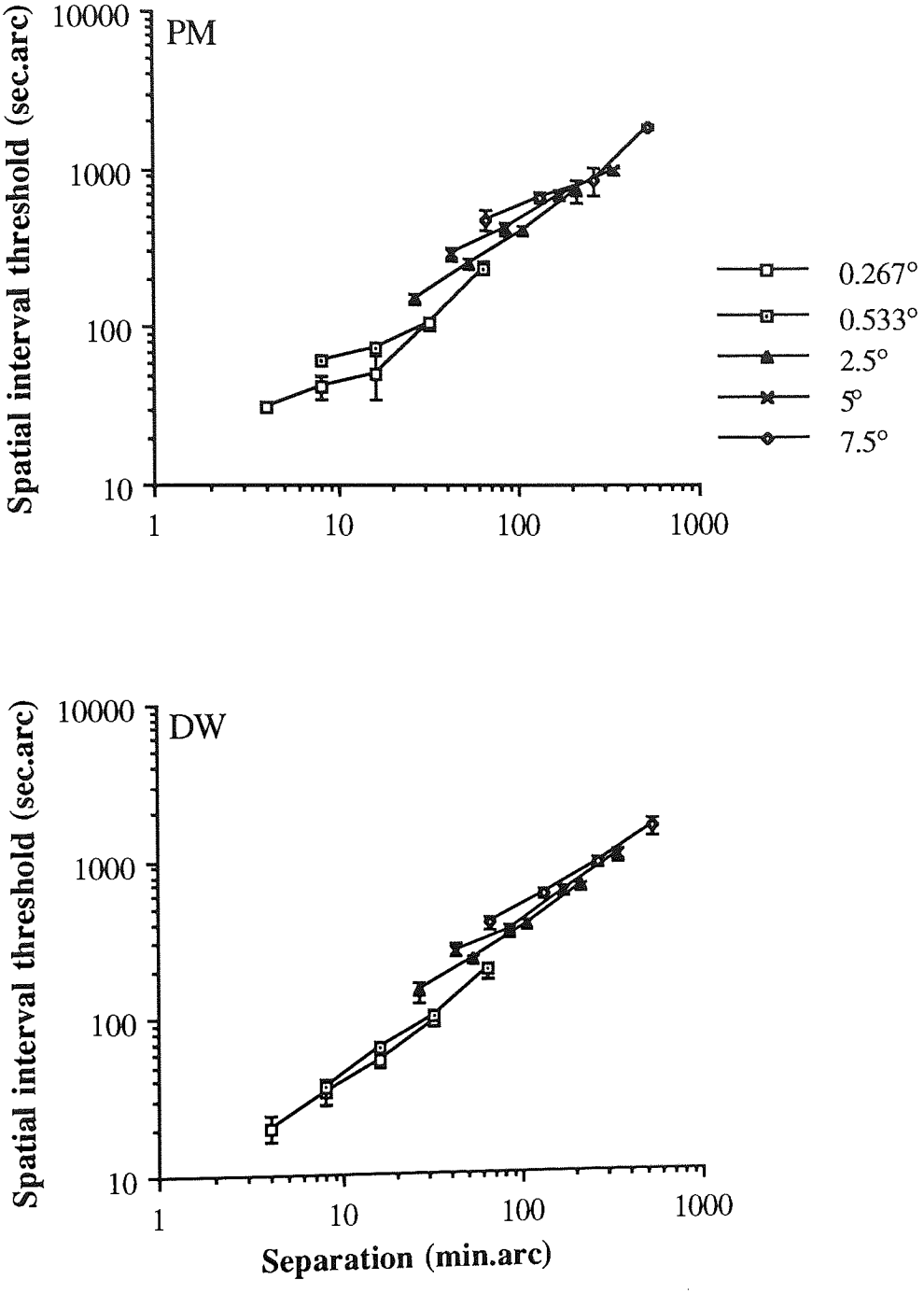

Figure 6.08a: Spatial interval thresholds for PM and DW for an inter-stimulus interval of 500 msec. Other details as in *Figure 6.06a.*

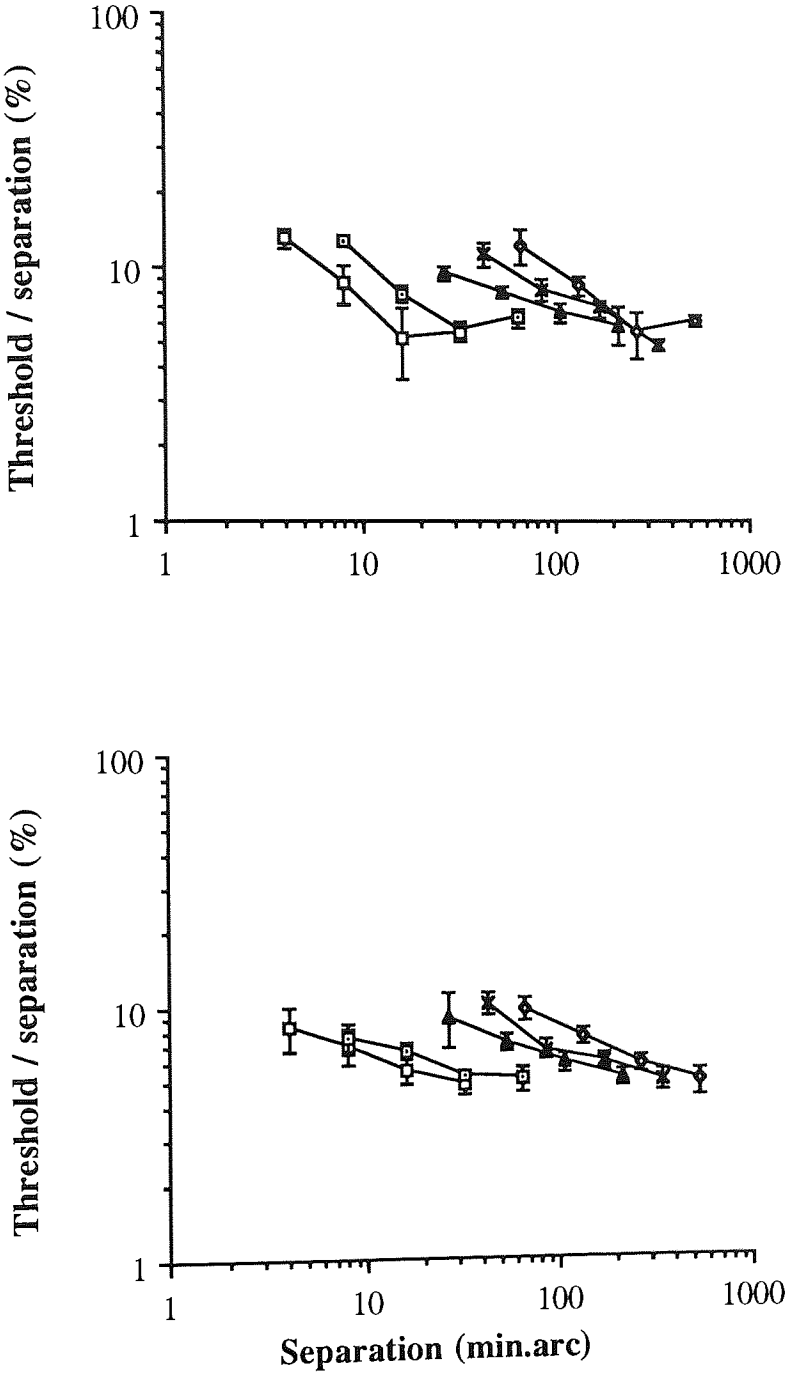

Figure 6.08b: The data of *Figure 6.08a* replotted with threshold expressed as a percentage of separation.

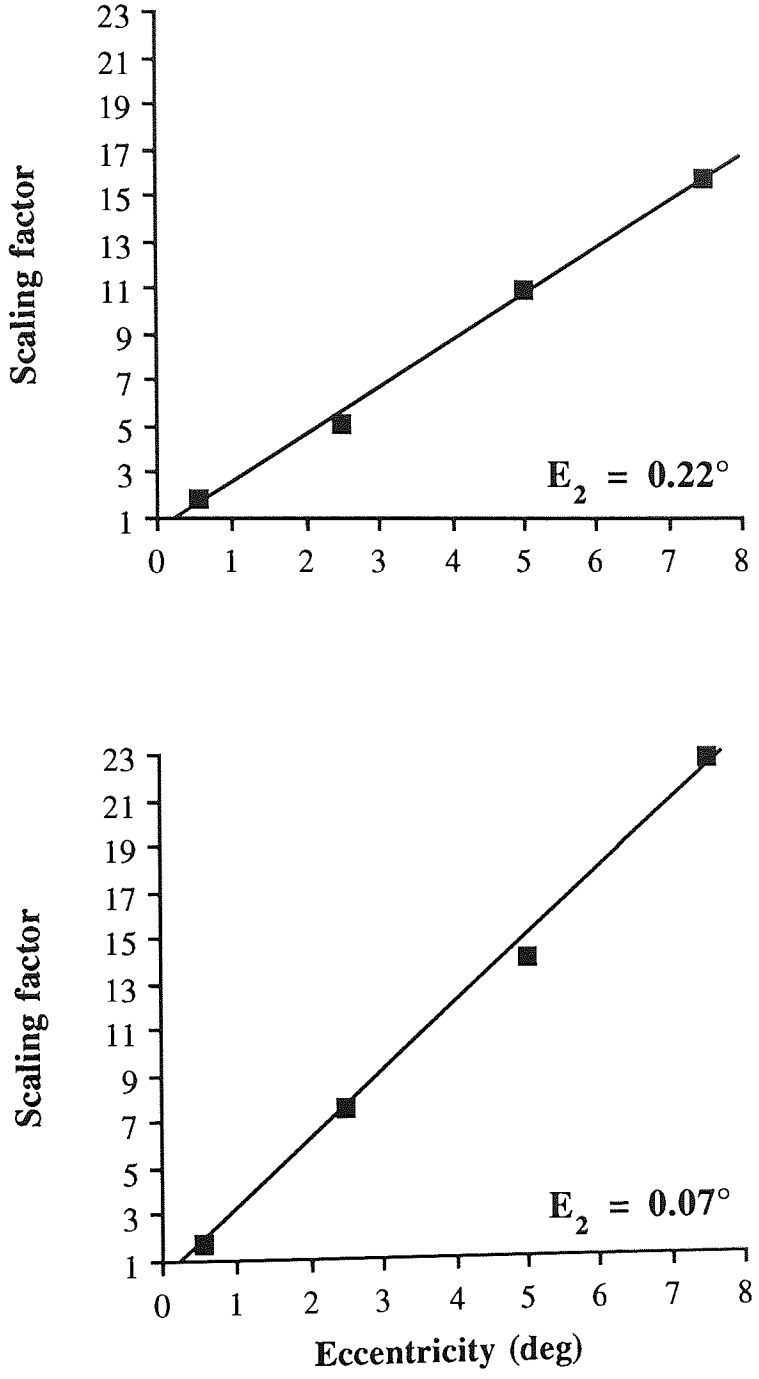

Figure 6.08c: Scaling factors obtained at each eccentricity relative to 0.267 deg.

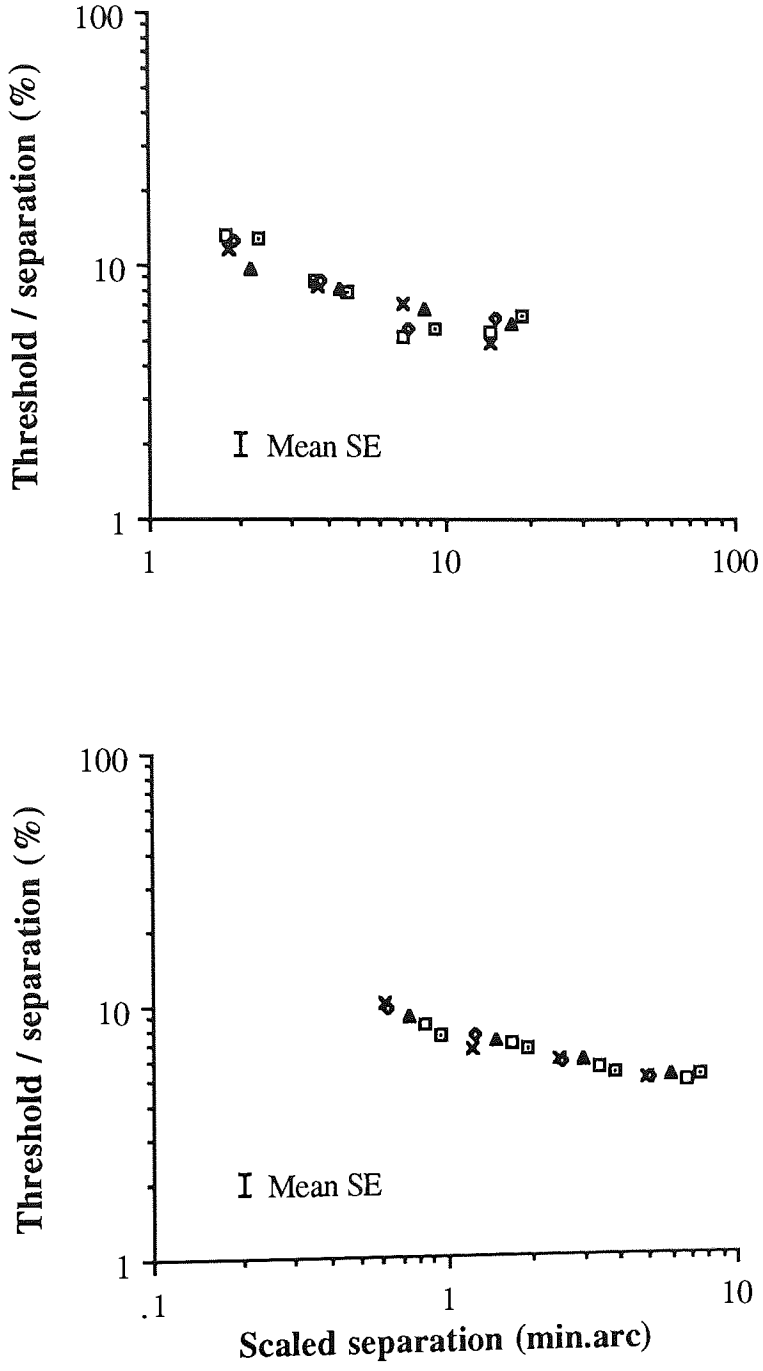

Figure 6.08d: The data of *Figure 6.08b* with the separation values at each eccentricity having been scaled along the size (x-) axis.

6.4: Discussion

The present E_2 values for spatial interval discrimination of 0.07 - 0.22 deg are smaller than some previous estimates of 0.6 - 0.83 deg (Yap, Levi & Klein, 1989; Levi & Klein, 1990b). The present values are, however larger than for the isoeccentric spatial interval data of Levi and Klein (1990a) for which the E_2 is about -0.3 deg when determined by the present method of analysis, see the text in connection with *Figure 6.04*. In addition, the present E_2 values are larger than found for the decline of width discrimination by McKee, Welch, Taylor and Bowne (1990) whose results indicate an E_2 of approximately 0.04 deg.

Unfortunately the use of widely differing methods of comparing central and eccentric visual performance means that comparison of E_2 values is often tenuous, if not meaningless. In the case of spatial interval discrimination the previous studies examining in the periphery have either scaled stimulus size according to a pre-chosen value (Yap, Levi & Klein, 1989; Levi & Klein, 1990a) or have allowed eccentricity and separation to co-vary (Levi & Klein, 1990b), which naturally may affect thresholds. As for the data presented in *Figures 6.01* and *6.04* (Yap *et al.*, 1989 and Levi & Klein, 1990a, respectively) the individual eccentricity functions can be compared, although in *Figure 6.01* the stimulus separations used were far smaller than in the present experiments. However, the few overlapping largest separations in *Figure 6.01* are very similar to present data.

In *Figure 6.09a,b* the 2.5 and 5 deg eccentricity data of Levi and Klein (1990a) are compared with the two corresponding eccentricities of present data acquired at 50 msec inter-stimulus interval. Levi and Klein stated their threshold level to be equivalent to 75% correct thus, the thresholds have been rendered comparable with the present (80% correct) data by multiplying them by 1.25 (Elliot, 1964). The data are remarkably similar both in shape and in magnitude. However, the present data at 50 (as well as 500) msec inter-stimulus interval does not seem to level off at the largest separations as does the data of Levi and Klein (1990a). It is naturally possible that the saturation could have occurred for the present data at larger separations.

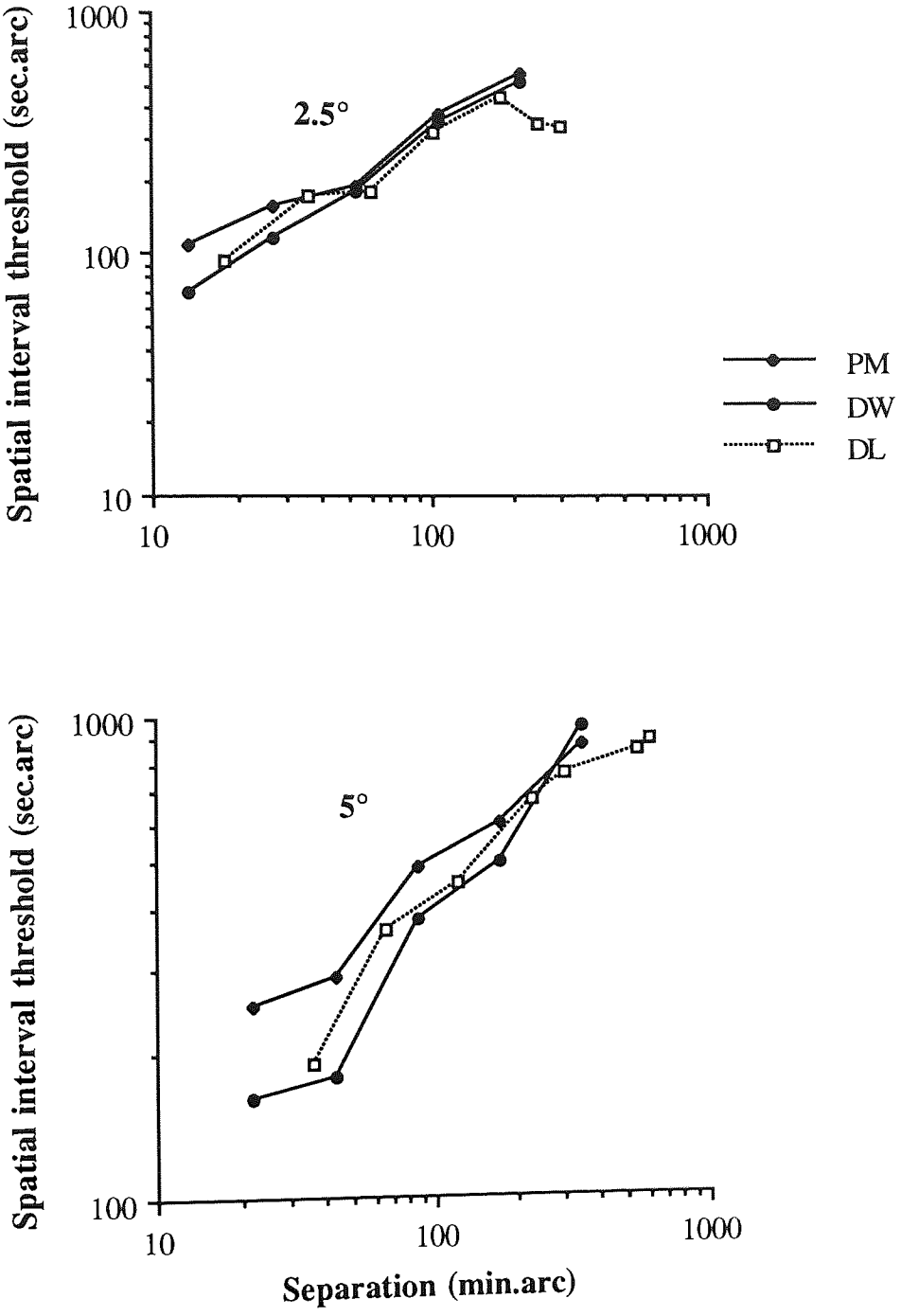

Figure 6.09a,b: The 2.5 and 5 deg eccentricity data of Levi and Klein (1990a) compared with the corresponding present data acquired at 50 msec inter-stimulus interval.

For spatial interval discrimination, Yap, Levi and Klein (1989) and Levi and Klein (1990b) found E_2 values of 0.6 - 0.83 deg for optimal thresholds but E_2 values of 1.9 - 2.4 deg for optimal separation. Note that the use of the non-isoeccentric method means that the "foveal" data does not actually represent performance at 0 deg eccentricity, but at an eccentricity which

varies depending upon separation. Since E_2 values reflect the eccentricity at which "foveal" performance doubles, it is critically important to quantify foveal performance correctly. This seems to be the most likely explanation as to why optimum separation and threshold increased at different rates in these studies whereas this complex situation is not found in the present study nor in others using isoeccentric stimuli (e.g. Levi & Klein, 1990a).

The present experiments are complementary to the studies which have kept stimulus size the same but varied separation at each eccentricity (Levi, Klein & Yap, 1988; Levi & Klein, 1990a). Whilst such experiments directly test for the effect of separation, drawing conclusions about the variation of performance with eccentricity may be considered inappropriate since performance at different eccentricities is not being compared using stimuli which are magnified versions of one another. The stimuli used in the present experiments have been developed to study the effect of eccentricity *per se*. The data presented here therefore fill an important gap in the literature regarding visual performance and eccentricity. However, the present results do not clarify the issue of the relative contributions of separation and eccentricity to Weber's law. The reason is that at any given eccentricity, our stimuli varied in size (which represented a constant fraction of separation), and so any trend found at a constant eccentricity may be due to a combination of varying separation and changing stimulus size. However, tasks such as spatial interval discrimination depend on the spatial interval rather than on the features which demarcate it, unless separation is very small (Westheimer & McKee, 1977b; Levi & Westheimer 1987). The following experiment was designed to test this allegation for the present stimulus configuration.

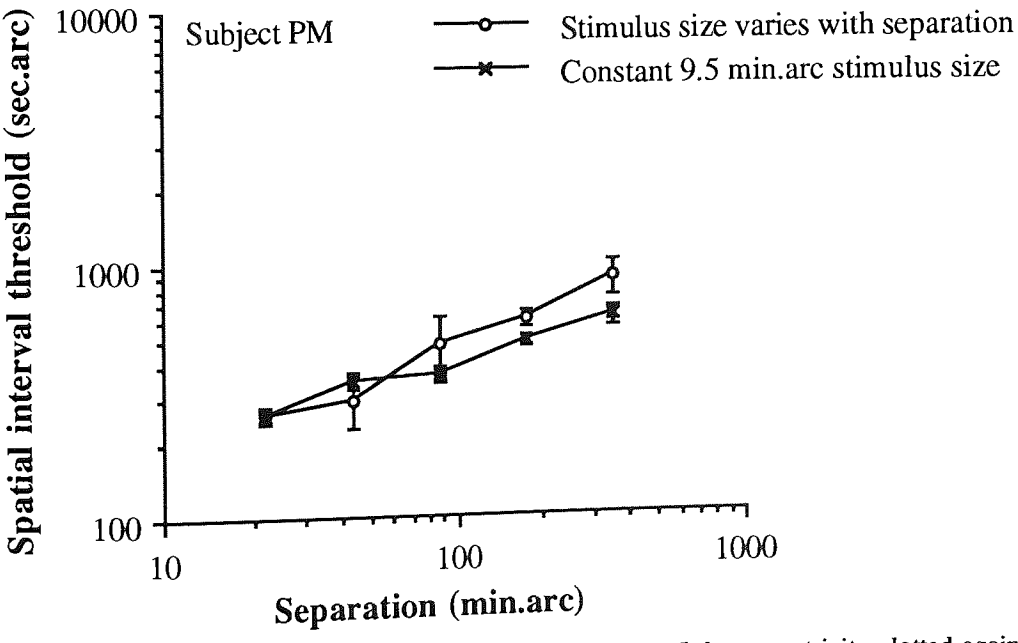

Figure 6.10: Spatial interval discrimination thresholds at 5 deg eccentricity plotted against separation for two different stimuli. Standard errors are shown.

The 5 deg eccentricity data set of 50 msec inter-stimulus interval was repeated with a constant square size (the side of the square was 9.5 min.arc), and the results were compared with the corresponding previous data where the stimulus size had been varied as a function of separation. Below 86 min.arc separation the varying sizes were smaller than 9.5 min.arc, above 86 min.arc separation the varying sizes were larger than 9.5 min.arc. Although all differences were small, an additional analysis was performed using the Wilcoxon signed-rank test. The test showed that the two threshold functions could not be considered significantly different ($p = 0.225$).

The departure from Weber's law suggested by Levi *et al.* (1987) was not found for the present spatial interval discrimination data at 50 and 500 msec inter-stimulus intervals. The results do not, however, necessarily disqualify the theory. The present stimuli were designed to quantify eccentricity dependence, not to investigate changes in performance at a fixed eccentricity. Since the stimuli in the present experiments increased in size as a function of separation, the squares comprising the stimulus at the largest separations may have been larger than optimal. This may have caused the thresholds to continue to increase at the largest separations instead of levelling off.

Chapter 7: Bisection acuity

7.1: Introduction

Bisection acuity measures the ability to *bisect* a spatial interval between two points or lines. It is very similar to spatial interval discrimination, and is actually sometimes called a three-line spatial interval discrimination. Typically, three lines or dots are presented side by side and the observer is required to decide whether the centre line is to the right or the left of the middle of the stimulus defined by the position of the outer lines. The centre line is often at fixation, but the whole set of lines/dots may also be presented in the periphery, aligned in either the tangential or the radial direction (Yap, Levi & Klein, 1987a,b).

As with spatial interval thresholds, changes in gap size for a conventional bisection task are necessarily associated with a change in the eccentricity of the outer two stimulus components of the task. Some foveal studies with fixation in the middle of the stimulus have already been presented in the *Chapter 2.4.3* (Andrews & Miller, 1978; Westheimer & McKee, 1979; Klein & Levi, 1985). The following studies have extended the experiments to the peripheral visual field having kept the fixation traditionally in the middle of the stimulus (Klein & Levi, 1987) or placing the stimulus components in the periphery side by side (Yap, Levi & Klein, 1987a,b), and in addition, keeping the outer stimulus components on isoeccentric arcs determining the eccentricity of the stimulus (Levi, Klein & Yap, 1988; Levi & Klein, 1990a). None of the previous studies, however, have combined the spatial scaling method with the isoeccentric presentation. When stimulus size has been increased towards periphery, a pre-chosen factor has been used.

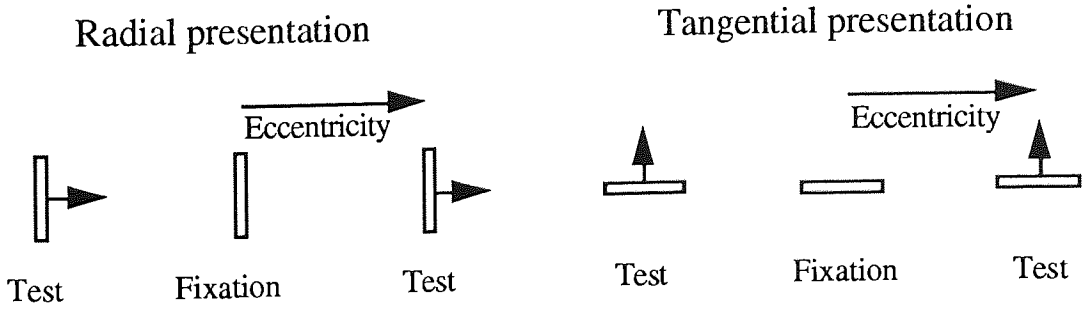

Figure 7.01: The two stimulus configurations used by Klein and Levi (1987).

Klein and Levi (1987) measured position acuity up to 10 deg eccentricity for three-dot bisection and three-dot vernier tasks. Thresholds were determined for a stimulus positioned along the horizontal meridian in i) the radial direction (bisection task, lines vertical, displacement horizontal) and ii) the tangential direction (vernier task, lines horizontal, displacement vertical), the stimulus configurations are shown in *Figure 7.01*. Fixation was in

the middle of the stimulus. The size and separation of the stimulus components was scaled by varying the viewing distance. For eccentricities less than 0.4 deg viewing distance was 10.8 m, and the dot separation was varied on the screen, whereas at 10 deg eccentricity the viewing distance was 0.38 m, i.e the peripheral stimulus dimensions were chosen arbitrarily. Vernier thresholds increased linearly with eccentricity, which led the authors to suggest that three-dot vernier thresholds are set by a single orientation mechanism at all eccentricities. Bisection thresholds, however, increased relatively sharply at small eccentricities (below about 0.5 deg) in comparison with the larger eccentricities. Levi and Klein reported E_2 values of 0.15 - 0.31 deg for three observers for the bisection task. Due to the non-linearity of the data and, specifically, the choice of stimulus configuration, comparison of the E_2 value with the present values is futile. On the basis of these and some previous bisection acuity results (Klein & Levi, 1985), Klein and Levi have developed the model described schematically in *Figure 6.03.* According to the model, thresholds for position acuity are set by two different mechanisms, one dominant at large, the other dominant at small eccentricities.

Yap, Levi and Klein (1987a) used a stimulus configuration where, at the fovea, fixation was at the middle of the stimulus, and the whole stimulus set was shifted down along the inferior vertical field meridian for peripheral viewing (2.5, 5, and 10 deg eccentricities). The presentation was thus non-isoeccentric. The size of the stimulus was scaled by varying the viewing distance according to an E_2 of 0.77 deg. The resulting E_2 values for the bisection task were 0.59 and 0.55 deg (two observers) for briefly (150 msec) flashed, vertically elongated dots. Increasing presentation time clearly improved foveal thresholds but had practically no effect on the 10 deg eccentricity thresholds. Thus, the E_2 value for a longer presentation than 150 msec would have been smaller than the average 0.57 deg suggested in the study.

When separation is small, there is a clear difference between three-dot bisection and two-dot spatial interval discrimination. At small separations thresholds are lower for two-dot spatial interval discrimination (*Figure 6.01*) than for three-dot bisection (*Figure 7.02*). In the periphery, performance in these two tasks for large separations has been found to be similar (Levi, Klein & Yap, 1988; Levi & Klein, 1989), which is also seen when comparing *Figures 6.01* and *7.02*. Typically, neither non-isoeccentric data shows levelling off at large separations.

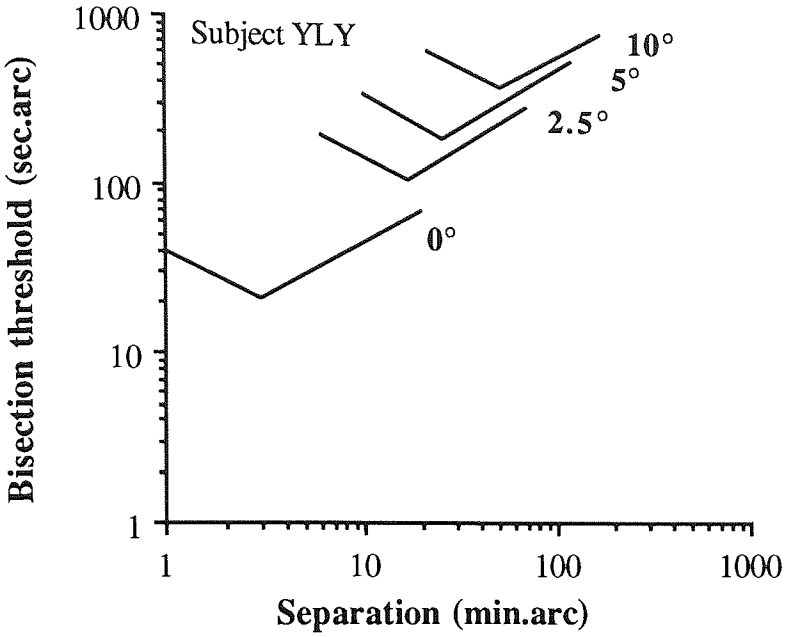

Figure 7.02: Templates for non-isoeccentric bisection thresholds plotted against separation. Note that threshold increase does not saturate at large separations, which is typical for non-isoeccentric data. Redrawn from Yap, Levi and Klein (1987a), Figure 2a.

Yap, Levi & Klein (1987b) investigated bisection acuity as a function of orientation for a variety of feature separations and field meridians at eccentricities of 0 - 10 deg for two observers. The size of the stimulus was scaled by varying the viewing distance according to an E_2 of 0.77 deg. In the fovea, horizontal and vertical bisections were better than oblique bisections. At eccentricities of 5 - 20 deg "isoeccentric bisection" (tangential offset) was better than "radial bisection". The direction of offset was more important than the the orientation of the stimulus, the result was found both for three-dot vernier acuity and bisection acuity. Further, two-dot spatial interval thresholds were also lower for offsets in the tangential than in the radial direction. In the periphery, displacements in the tangential direction are easier to detect than in the radial direction (Klein & Levi, 1987; Yap, Levi, Klein, 1987b). Peripheral resolution shows a similar asymmetry, being better for radial than for tangential gratings (Rovamo, Virsu, Laurinen & Hyvärinen, 1982).

The study by Levi, Klein and Yap (1988) has been described in the previous chapter. In short, to test whether Weber's law still applied at large separations when the effect of changing eccentricity was removed, they positioned the outmost lines of a three-line bisection stimulus on an isoeccentric arc. The stimulus was presented at a constant 10 deg eccentricity so that the centre line was between the outmost lines, comparable to the stimulus configuration in *Figure 7.04b*. The direction of the offset of the centre line from the middle was to be determined. The resulting thresholds were practically independent of separation

between 2 and 10 deg, showing clear deviation from Weber's law.

Levi and Klein (1990a) investigated bisection acuity in the lower visual field, where the two outer short vertical bright lines were positioned on an isoeccentric arc which determined the eccentricity, and the middle line was between the dots as in *Figure 7.04b.* Stimulus exposure duration was 200 msec. The size of the stimulus was scaled by halving stimulus size each time eccentricity was halved. This corresponds to increasing the stimulus size with eccentricity according to an E_2 of 0 deg. (At the fovea the stimulus size would have become infinitely small, zero. Therefore, the eccentricity E_2, at which the stimulus size is 2×0 is still 0 deg). In *Figure 7.03* thresholds are plotted against separation. At moderate separations thresholds appear to be proportional to feature separation. At large separations thresholds fail to obey Weber's law since they are dependent on eccentricity but are practically independent of separation (*Figure 7.03*). The data shows the failure of Weber's law at large separations and allows comparison with the present data. E_2 values reported for bisection acuity by Levi and Klein were 0.47 and 0.44 deg (observers JT and KH, respectively). When the data of JT is analysed with the present method, E_2 becomes 0.31 deg (see data analysis in discussion).

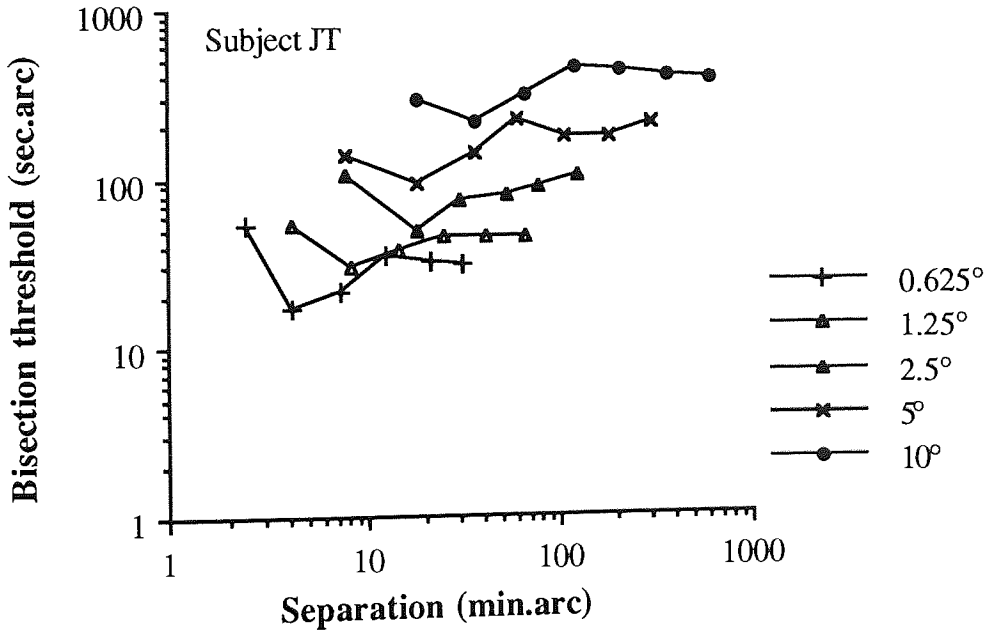

Figure 7.03: An example of isoeccentric bisection thresholds plotted against separation. The stimulus configuration used was relatively similar to that used for the experiments presented in this thesis. Redrawn from Levi and Klein (1990a) Figure 3.

In this chapter the eccentricity-related decline in performance is studied for bisection acuity using the technique of spatial scaling.

7.2: Methods

The stimuli were presented on a CRT as described in General methods. The stimulus luminance was 40 cd m^{-2}. The two experienced observers were PM and DW. Viewing was monocular with the dominant eye. Thresholds for the bisection were determined using a two-alternative forced-choice technique with a modified PEST routine (Findlay, 1978) which estimated the 80% correct level for both response alternatives, thus excluding any potential effect of bias on thresholds. No feedback was given. For each combination of eccentricity and the spatial parameters of the task, four threshold measurements were taken in random order. Final threshold was accepted as a mean of these four measurements.

In order to maintain constant eccentricity independently of gap size, the features of the bisection task were positioned on an isoeccentric arc (*Figure 7.04a*). Gap size is now defined as the distance between either outer feature and a vertical midline passing through fixation (see *Figure 2.15a*) and, as for the spatial interval task, is varied simply by moving the outer two features around the isoeccentric arc. Such stimuli satisfy the requirement that all features should be at the same eccentricity, but the requirement that all stimuli are simply magnified versions of each other breaks down. This is because, on moving the outer features around the arc, the vertical distance between the centre dot and the outer dots changes in a non-linear manner with separation. Hence, changing the magnification of the stimulus along the horizontal meridian does not lead to a corresponding change in magnification along the vertical.

Figure 7.04b shows an alternative arrangement, in which the criterion of making all stimuli simply magnified versions of each other holds true. However, in this sequence of stimuli, we have sacrificed the criterion that all parts of the stimulus should be at the same eccentricity. In fact, there exists no stimulus arrangement which will allow us to measure bisection thresholds whilst satisfying these two requirements of spatial scaling. Despite this, arguments may be made for the use of both sequences of stimuli shown. Since we are interested in relative localization along the horizontal, and the stimuli in *Figure 7.04a* are indeed all magnified versions of each other along this meridian, then their use may be justified. Alternatively, for the stimuli in *Figure 7.04* one may argue that the central feature of the stimulus would simply act as a marker and would not play a crucial role in defining the spatial requirement of the task which is governed entirely by the outer two features, and these are indeed isoeccentric with respect to change in gap size. For these reasons bisection acuity was investigated using both of these stimulus paradigms. In all cases, the size of the squares was maintained at 11% of the gap. The task of the observer was to decide whether the centre square was to the left or to the right of an imaginary vertical mid-way between the outer squares.

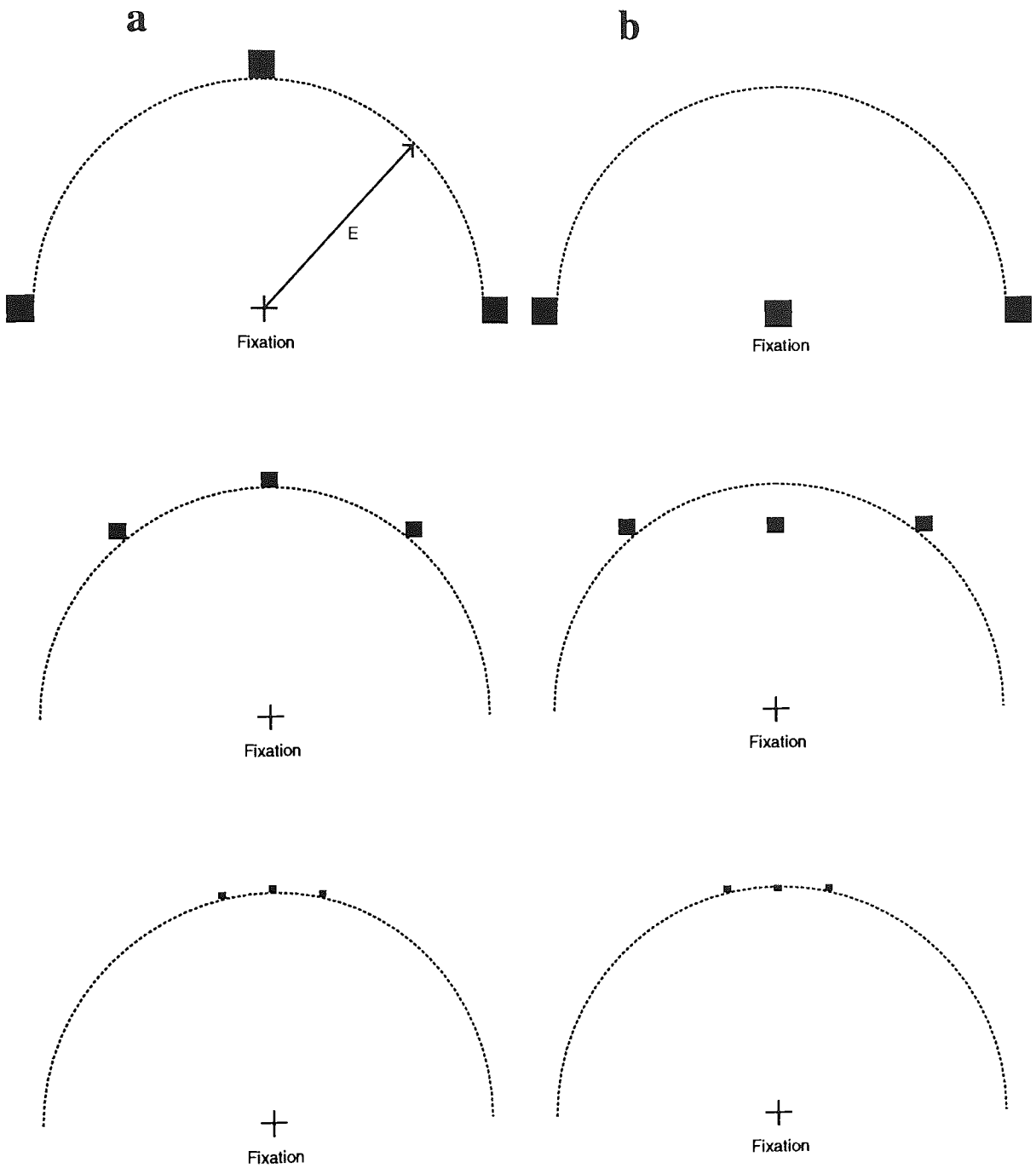

Figure 7.04: Two different stimulus series used for measuring bisection acuity.
(**a**) All stimulus features are positioned around the circumference of an imaginary arc whose radius defines the eccentricity. The spatial parameter, gap size, is defined by the distance between either outer square and a vertical line passing through fixation. Gap size is varied by moving the outer squares around the circumference of the arc. Again, the square size is a constant fraction of the gap size. Thus, in the horizontal direction, all stimuli are simply magnified versions of each other. However, along the vertical this isomagnification arrangement no longer holds.
(**b**) The outer squares are positioned around the circumference of the arc, and the middle square is positioned mid-way between them. This has the advantage that all stimuli are perfect replicas of each other in both the horizontal and vertical directions, differing only in magnification. However, all the stimulus features are not at the same eccentricity, since the eccentricity of the centre square varies as a function of gap size.

As in the spatial interval task, the smallest isoeccentric arc had a radius of 0.267 deg (16 min. arc). Different eccentricities were obtained by a combination of varying viewing distance and modifying the physical size and separation of the stimuli on the CRT. Viewing distance varied between 17.5 and 0.5 m. Eccentricities between 0.267 and 7.5 deg in the upper visual field were investigated and, at each eccentricity, bisection thresholds were measured as a function of gap size.

Since stimuli were presented in darkness, a red fixation line appeared for 750 msec prior to the appearance of the three squares of the bisection task. The mid-point of this line represented the centre of the isoeccentric circle on which the squares were to be presented. The observer was required to maintain fixation at this point throughout the stimulus trial. The fixation line then disappeared and the bisection stimulus was immediately presented for a duration of 500 msec. The observer then responded via the keyboard as to whether the middle square appeared to be situated to the left or right of the midline determined by the outer squares. Immediately following this response, the fixation line appeared again and the sequence continued until the end of the psychophysical routine. The horizontal location of the stimuli was jittered from trial to trial.

7.3: Results

Bisection thresholds are plotted against gap size in *Figure 7.05a* for either five (PM) or six (DW) different eccentricities. Data was obtained using the stimulus sequence shown in *Figure 7.04a.* The functions are generally flatter than for spatial interval discrimination, and tend to follow a shallow u-shaped pattern. The increase in threshold at small gap sizes has been repeatedly demonstrated for bisection acuity and is thought to be due to crowding (Yap, Levi & Klein, 1987a, 1989; Levi & Klein, 1990a). This seems quite likely because at these small separations the three features of the bisection task are almost side by side.

Figure 7.05b shows the data plotted as Weber fractions. Note that the Weber fraction decreases steadily as a function of gap size at each eccentricity, to reach a value of 1 - 2% at the largest gaps. This represents a marked departure from Weber's law (which predicts a constant Weber fraction) and has been noted before for isoeccentric bisection acuity (Levi & Klein, 1990a). Functions for different eccentricities are displaced relative to one another along the size axis.

Scaling factors for each eccentricity were determined relative to the data at the smallest eccentricity (0.267 deg) and are shown in *Figure 7.05c.* The linear regression has been constrained to pass through a value of unity at 0.267 deg eccentricity, and the gradients are 2.95 (± 0.25) for PM and 2.86 (± 0.34) for DW. These correspond to E_2 values of 0.07 (± 0.03) and 0.08 (± 0.04) deg.

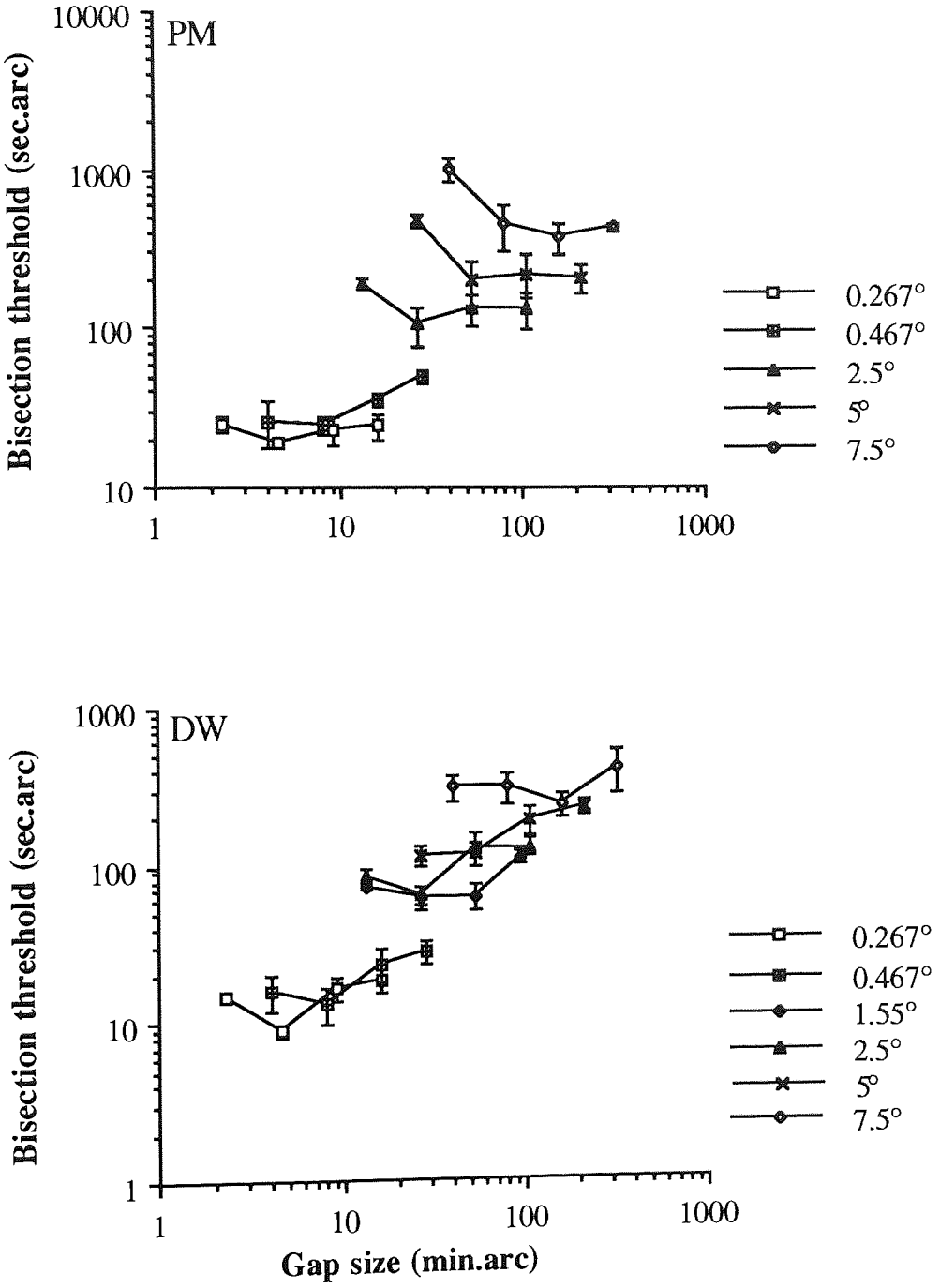

Figure 7.05a: Bisection thresholds for the stimulus configuration shown in *Figure 7.04a* plotted as a function of gap size. Different eccentricities were achieved by varying the radius of the isoeccentric arc and are shown, as well as the standard errors. Note the difference in ordinate scale between the subjects.

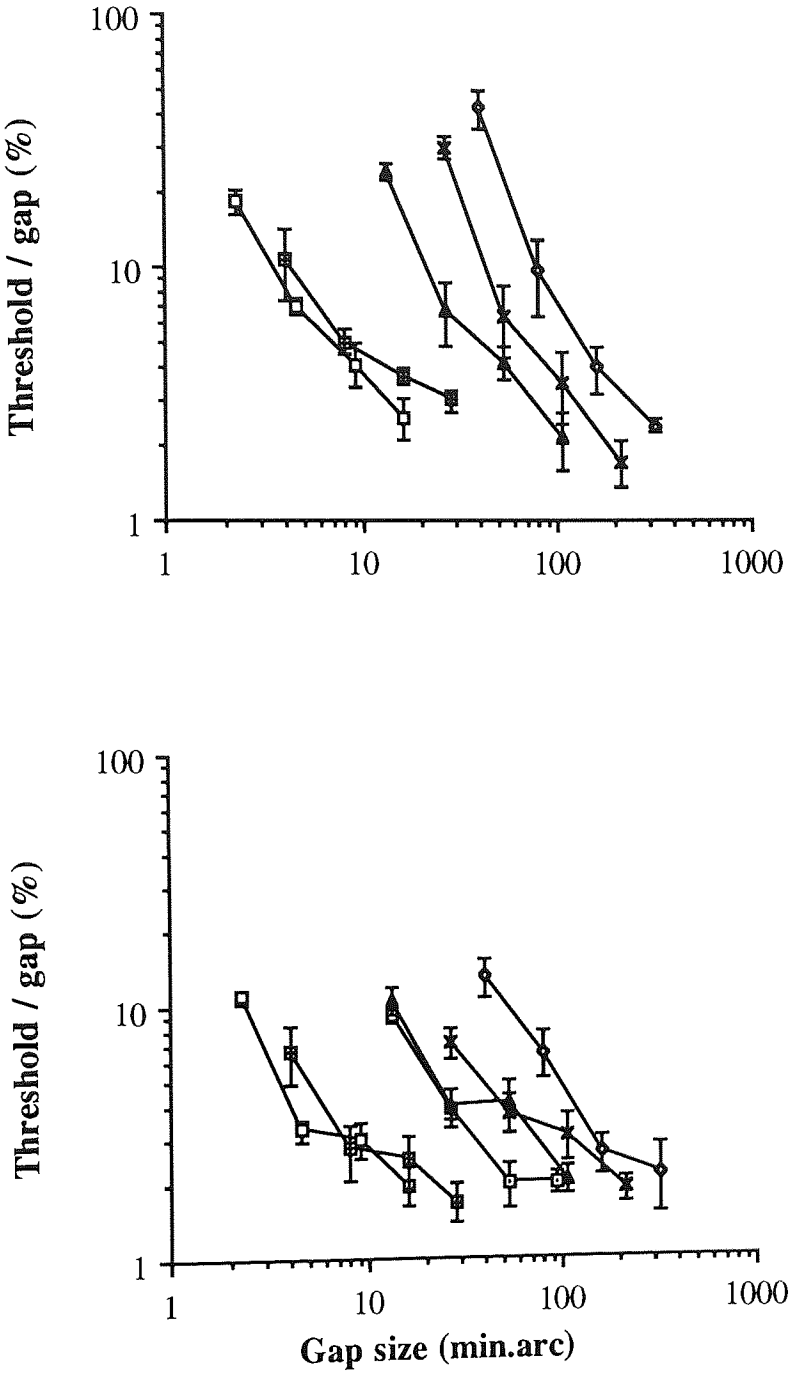

Figure 7.05b: Data replotted with threshold expressed as a percentage of gap size. Symbols and subjects as in (a).

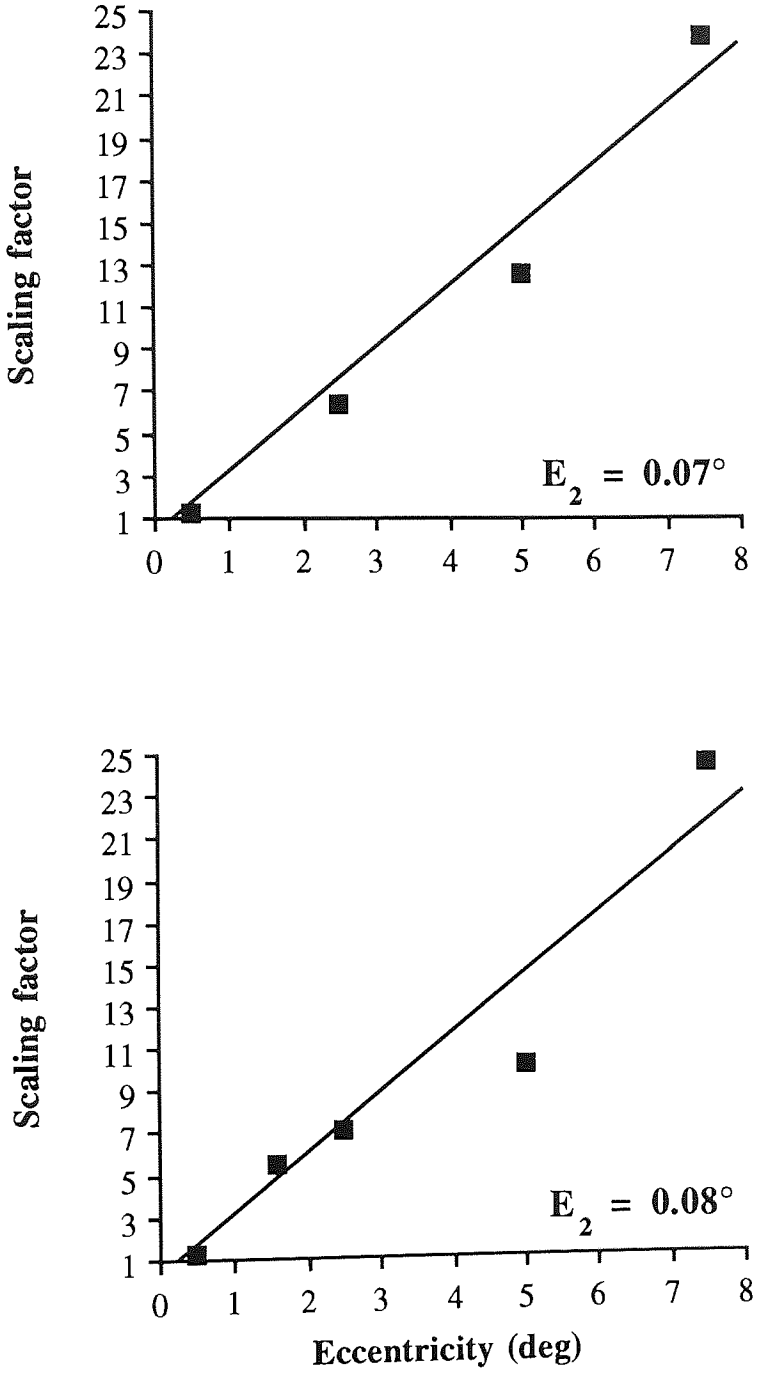

Figure 7.05c: Scaling factors obtained at each eccentricity relative to the smallest eccentricity of 0.267 deg. Note that the line of least squares is constrained to pass through the point (0.267, 1).

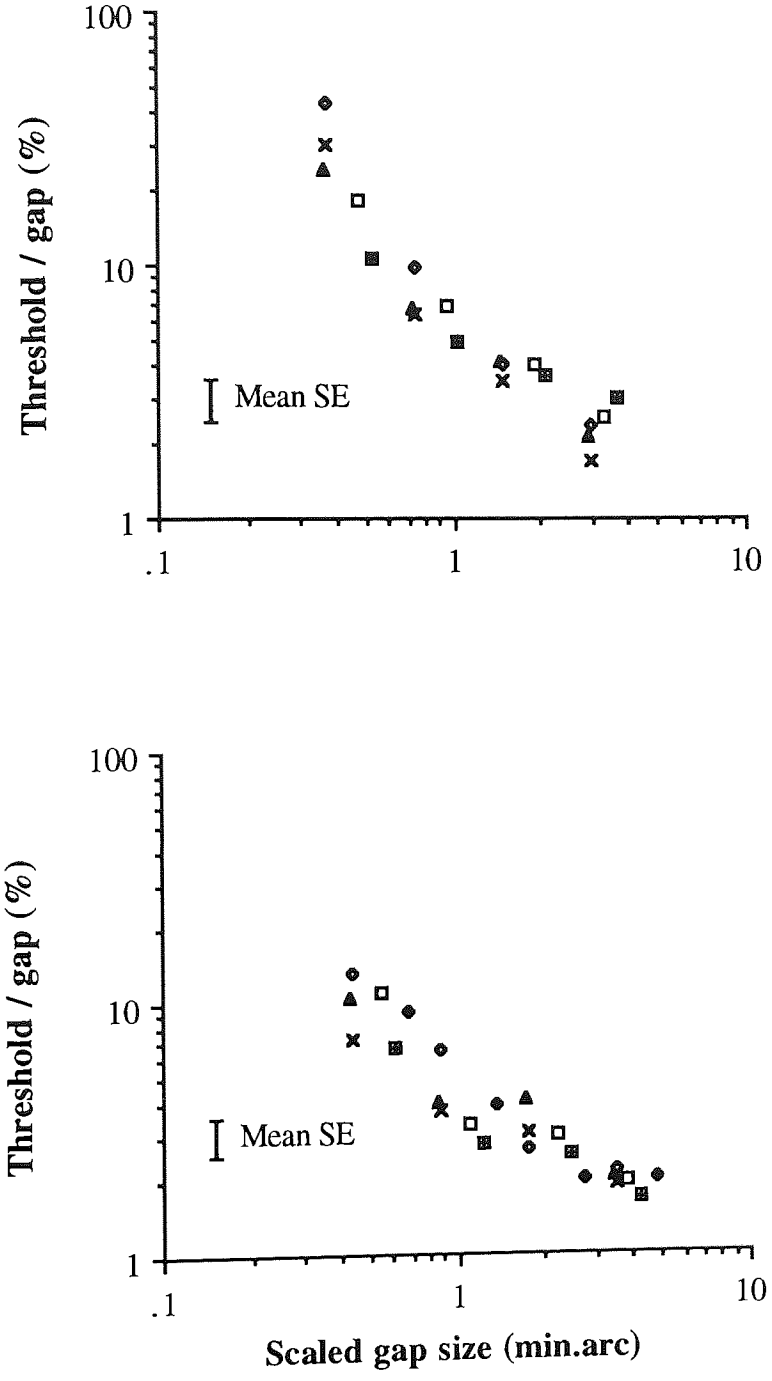

Figure 7.05d: The data of *Figure 7.05b* with the gap sizes at each eccentricity having been scaled along the size (x-) axis according to equation *4.09*. Note how the eccentricity dependent variance of the data is removed in this way.

Since an isoeccentric paradigm was used, there was no direct estimate of the scaling factor for an eccentricity of zero. However, the data from other eccentricities can be scaled relative to 0 deg according to equation *4.09* (see *Chapter 4*) since

$$F = 1 + (^{E} / E_2).$$

In *Figure 7.05d* the data from each eccentricity have been plotted after scaling according to the above equation. No eccentricity dependent variance appears to remain, indicating that for bisection acuity as well as spatial interval discrimination, performance at various eccentricities can be explained simply on the basis of a change of scale.

Bisection thresholds using the second stimulus configuration (*Figure 7.04b*) were more problematic. The function relating bisection thresholds to gap size are shown in *Figure 7.06a*. In comparison to the first stimulus configuration both PM and, to a lesser extent, DW demonstrate an improved performance at smaller eccentricities. This has the effect of making scaling factors larger, especially for PM, than those for the first stimulus configuration. The result of this is that E_2 values turn out to be negative. Gradients for scaling factors as a function of eccentricity were 5.19 (± 0.17) for PM and 4.28 (± 0.29) for DW, leading to negative E_2 values of -0.10 (± 0.01) deg and -0.03 (± 0.02) deg. This clearly makes data scaling by previously used equation *4.09* impossible. However, rather than scaling relative to the foveal factor, the data can still be scaled relative to 0.267 deg according to equation *4.06*:

$$F = 1 + S(E - 0.267),$$

the resulting data are shown in *Figure 7.06d.*

There are two reasons why the situation resulting in negative E_2 values may have arisen. It may be due to the fact that the stimulus features were not maintained at a constant eccentricity (*Figure 7.04b*). Alternatively, it may be due to the method of extrapolating the linear function of the scaling factor to the fovea. The assumption of linearity may break down at very small eccentricities. Hence, a more appropriate method may have been to concentrate on data collection at small eccentricities. The use of an isoeccentric arc smaller than 0.267 deg would assist in this procedure.

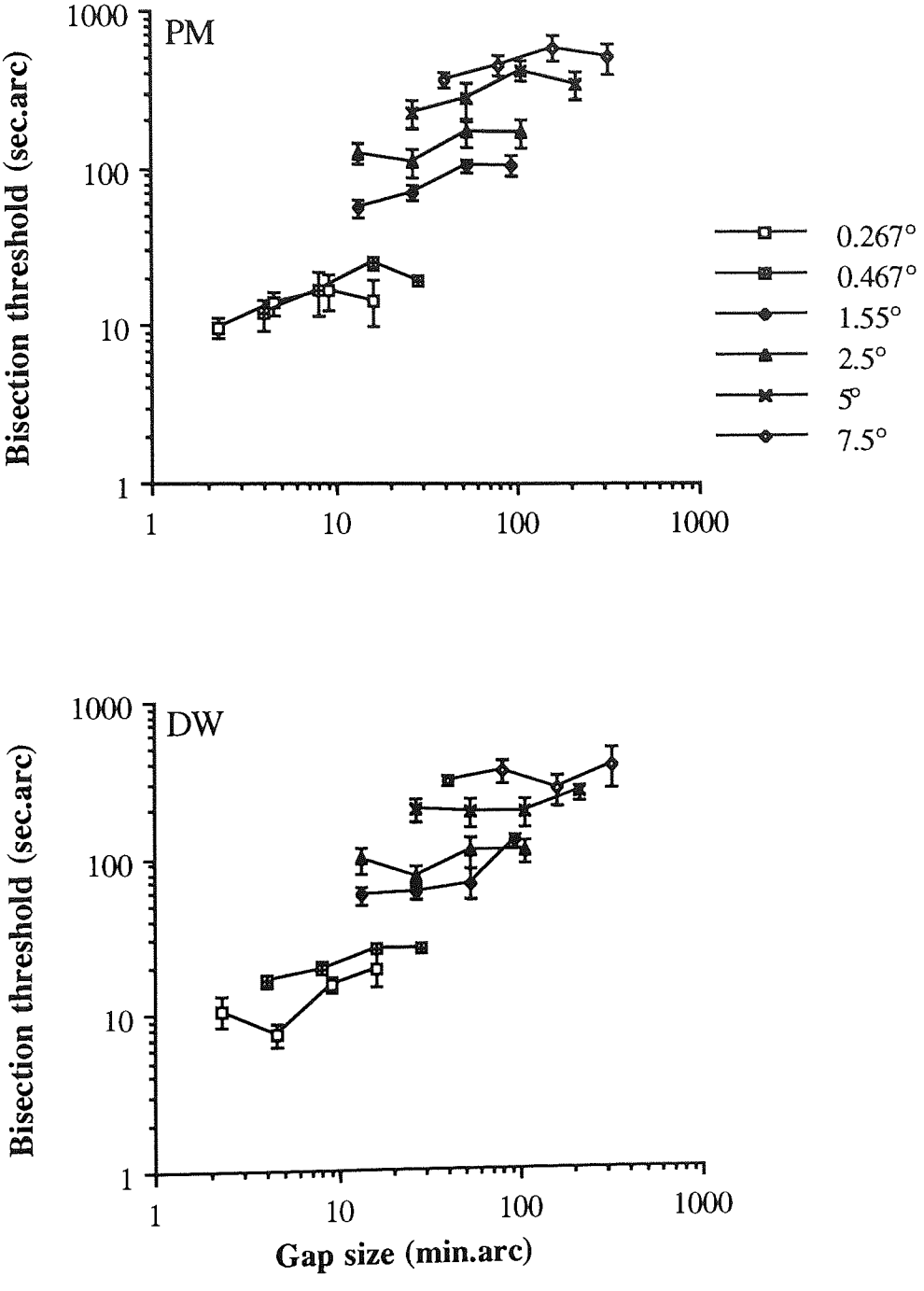

Figure 7.06a: Bisection thresholds for the stimulus configuration shown in *Figure 7.04b* plotted as a function of gap size.

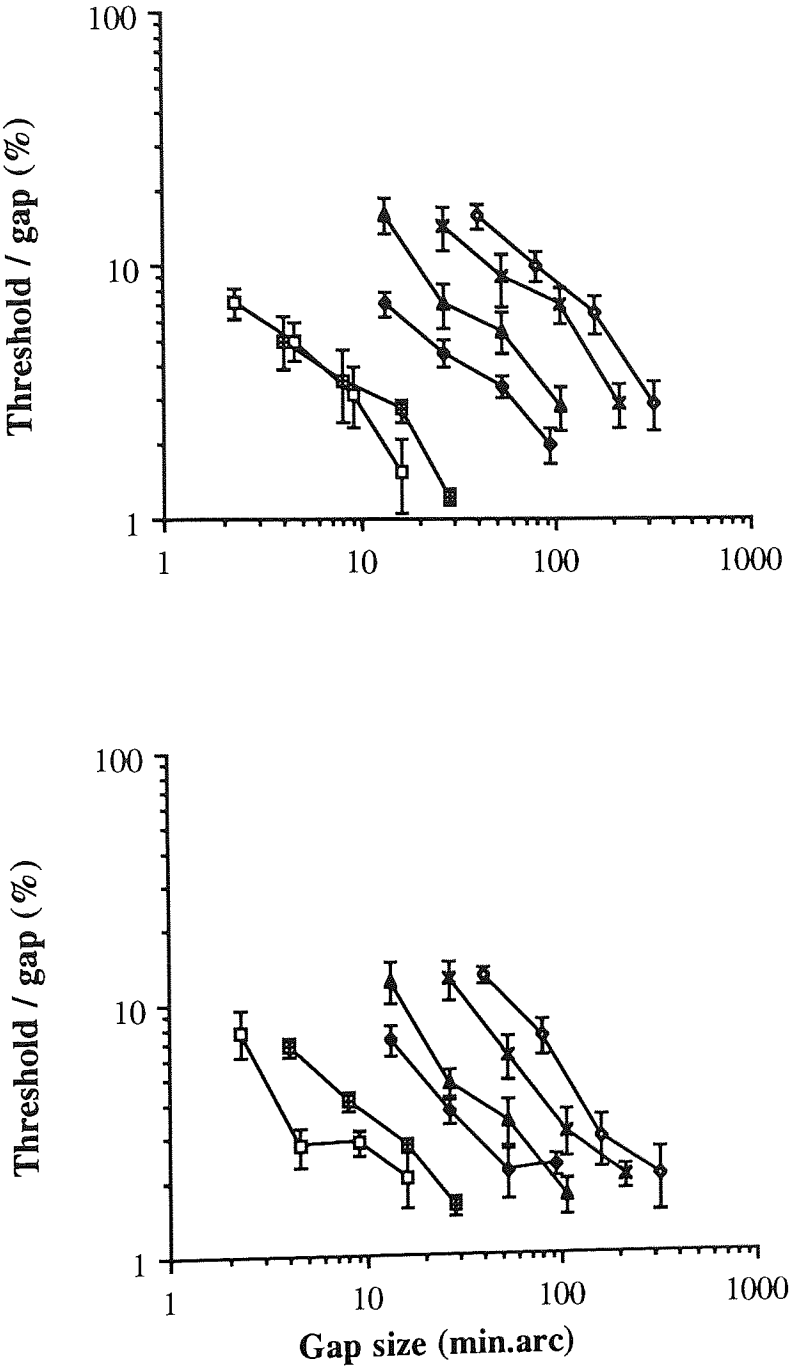

Figure 7.06b: Data replotted with threshold expressed as a percentage of gap size.

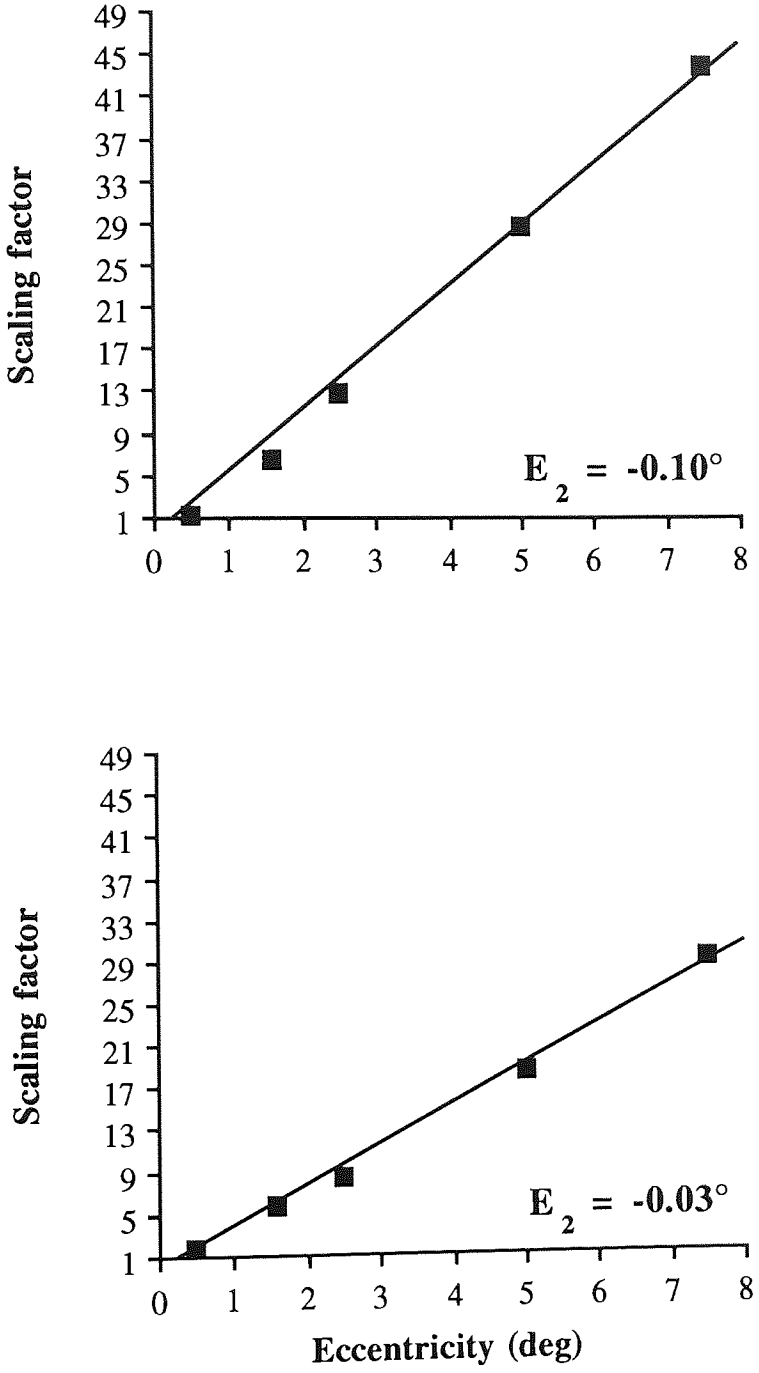

Figure 7.06c: Scaling factors obtained at each eccentricity relative to the smallest eccentricity of 0.267 deg. The line of least squares is constrained to pass through the point (0.267, 1).

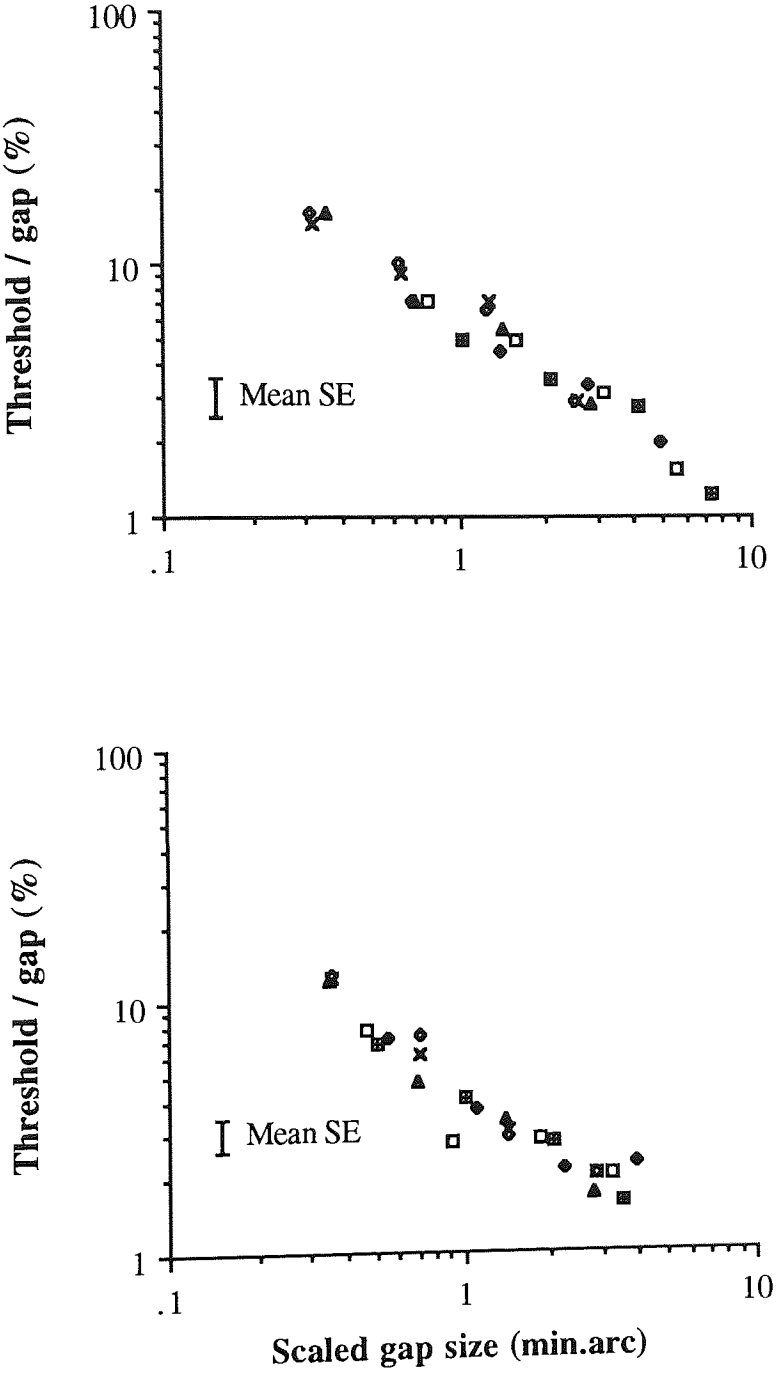

Figure 7.06d: The data of *Figure 7.06b* with the gap sizes at each eccentricity having been scaled along the size (x-) axis relative to 0.267 deg according to equation *4.06*.

6.4: Discussion

Comparing the present results with other studies is again complicated by the fact that in some experiments the stimulus size has not been scaled (Levi, Klein & Yap, 1988; Levi & Klein,1990a), it has been scaled according to a pre-chosen value (Yap, Levi & Klein, 1987a,b; Klein & Levi, 1987; Levi *et al.*, 1988; Levi & Klein, 1990a) or eccentricity and separation have co-varied (Klein & Levi, 1987; Yap *et al.*, 1987a,b).

Both optimum separation and optimum threshold have been shown to increase at similar rates for non-isoeccentric three-dot bisection acuity (Yap *et al.*, 1987a, *Figure 7.01*) with an E_2 value of approximately 0.6 deg. Since eccentricity was measured with reference to the centre dot, changes in separation affected the eccentricity of the two outer dots. Our present E_2 estimate (0.07 - 0.08 deg) is smaller, but resembles the low E_2 values (0.15 - 0.31 deg) reported by Klein and Levi (1987) who took into consideration the confounding effects of separation and eccentricity by defining eccentricity as the angular distance of the outer dots from the central fixation dot.

The isoeccentric bisection acuity functions of Levi and Klein (1990a) at 1.25, 2.5 and 5 deg eccentricity are compared with the present results at the eccentricities of 1.55, 2.5 and 5 deg in *Figure 7.07*. At 2.5 deg eccentricity the functions are shown separately in the top panel for clarity. Thresholds in the Levi and Klein study were measured at the 75% correct level, but have now been made comparable with the present thresholds (determined at the 80% correct level) by multiplying them by 1.25 (Elliot, 1964). The general shape of the threshold functions of Levi and Klein (1990a) in *Figure 7.03* appears to be well in agreement with the shape and level of the present threshold functions. Levi and Klein investigated a wide range of separations, being interested in the effect of separation on thresholds at each eccentricity, whereas that was not necessary for the present study, which was designed solely to determine the eccentricity dependence in bisection acuity performance. The thresholds of JT are naturally somewhat lower at 1.25 deg eccentricity than thresholds of DW at 1.55 deg, but otherwise JT and DW show fairly similar thresholds. The thresholds of PM are consistently slightly higher than those of JT and DW independent of eccentricity.

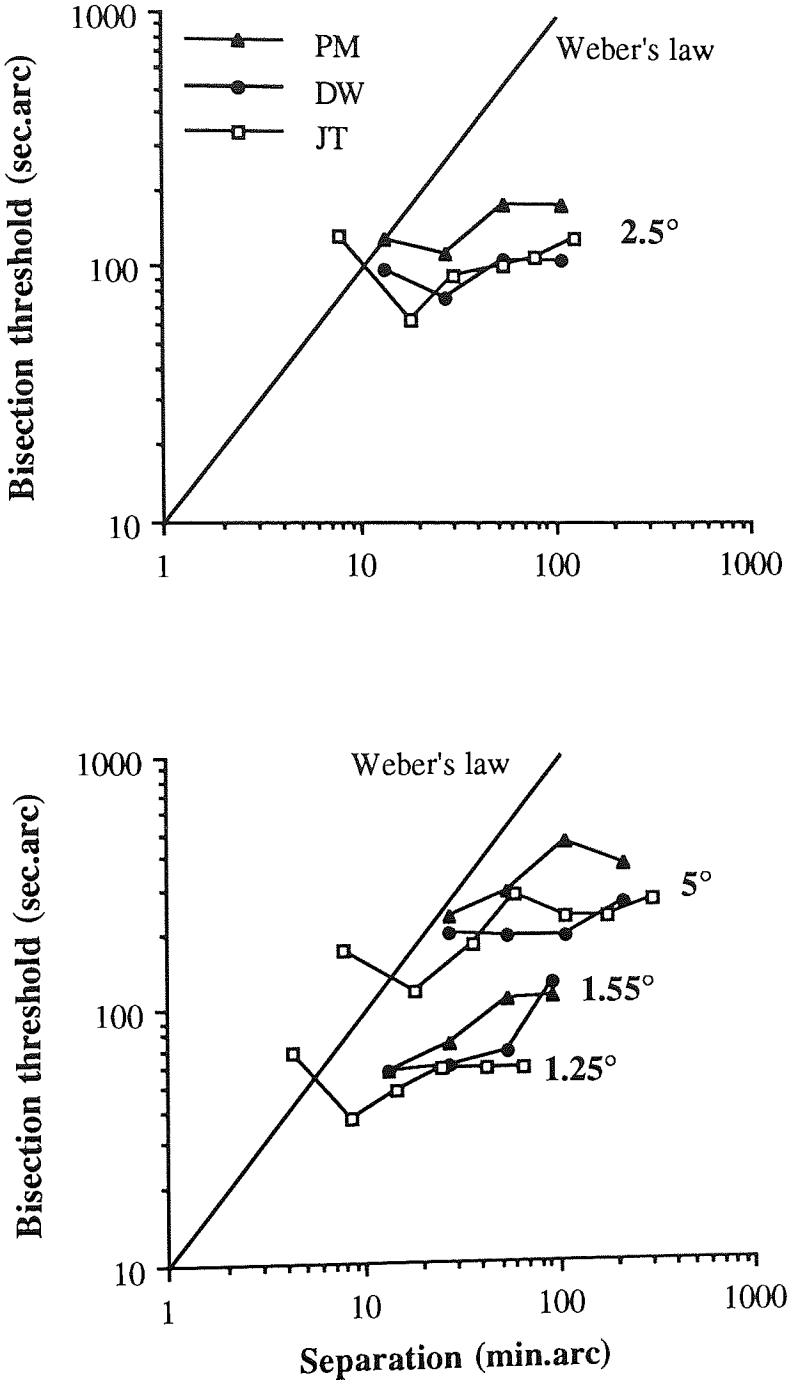

Figure 7.07: A comparison of the threshold functions of the Levi and Klein (1990a) -study (subject JT) and the present experiment (PM and DW). Stimulus configuration *7.04b*, eccentricities 1.55 (1.25 for JT), 2.5, and 5 deg. Triangles - PM; Circles - DW; Squares - JT.

The isoeccentric bisection acuity data of Levi and Klein (1990a) was shown in *Figure 7.03* for subject JT. When the data was analysed using the present method, thresholds were first divided by separation, the percentage thresholds are shown plotted against separation in

Figure 7.08.

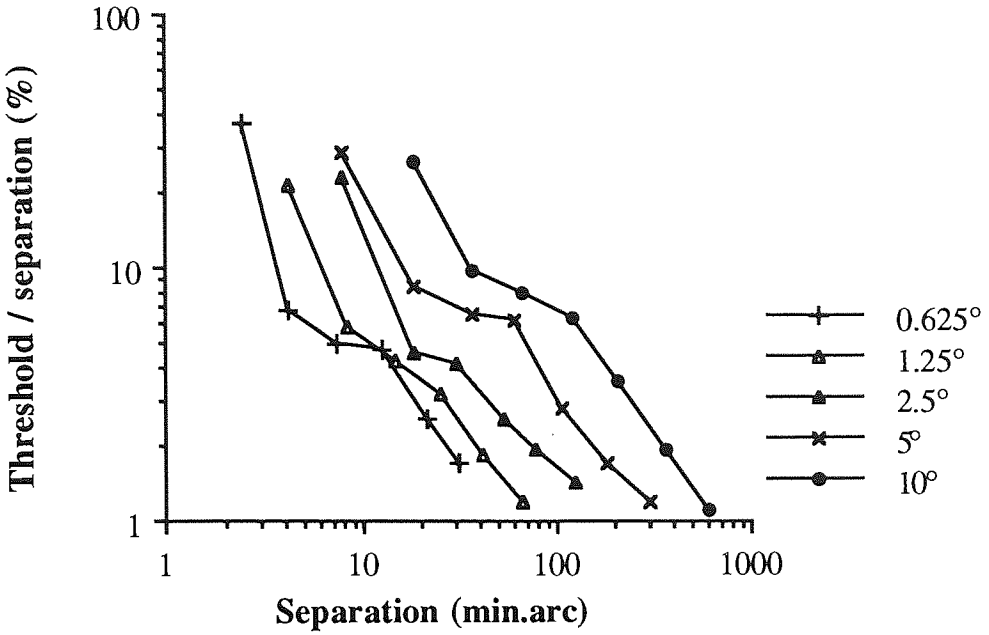

Figure 7.08: Percentage thresholds plotted against separation (Levi & Klein,1990a). Stimulus configuration as in *Figure 7.04b.*

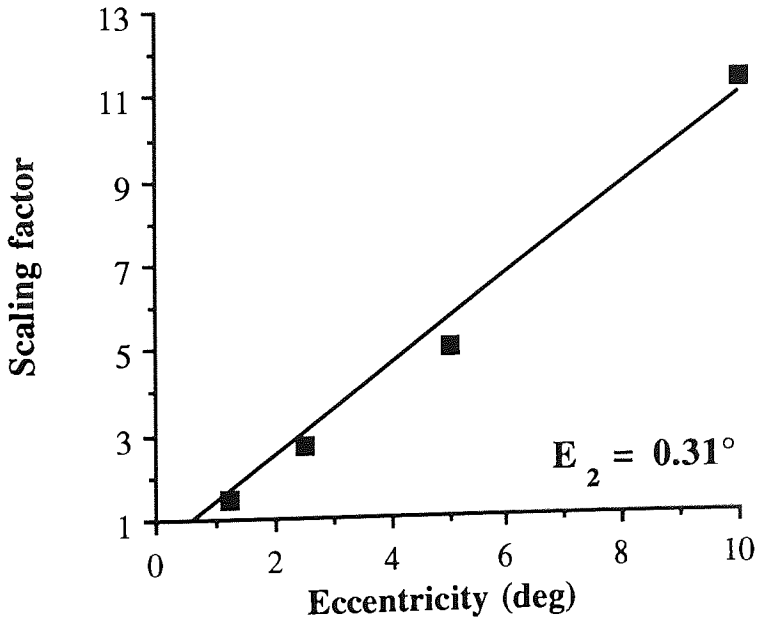

Figure 7.09: Scaling factors (based on *Figure 7.08*) obtained at each eccentricity relative to the smallest eccentricity 0.625 deg. The line of least squares is constrained to go through the point (0.625, 1).

Scaling factors were obtained on the basis of the horizontal shifts between the 0.625 deg eccentricity function and each eccentric function. The resulting scaling factors are shown in

Figure 7.09. An E_2 of 0.31 deg was found, but scaling the data relative to the fovea was not possible with that value. When the smallest eccentricity studied is as large as 0.625 deg and E_2 value is very small, scaling the data with factors obtained by equation *4.09* ($F = 1 + {}^{E}/_{E_2}$) distorts the results by misaligning the percentage threshold function at 0.625 deg from the functions of the other eccentricities. However, *as was the case with the present data acquired using this same stimulus configuration* shown in *Figure 7.04b*, it was possible to scale the data in *Figure 7.08* relative to the 0.625 deg eccentricity using the equation *4.06*; according to which $F = 1 + S(E - 0.625)$. The resulting percentage threshold *vs* scaled separation functions are shown in *Figure 7.10.* This scaling procedure clearly removes the eccentricity dependence of the data of Levi and Klein.

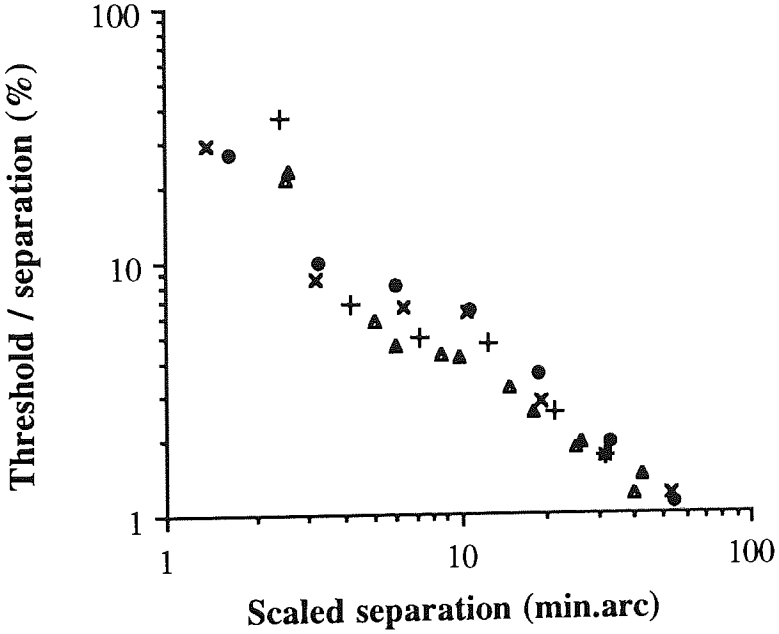

Figure 7.10: Data from *Figure 7.08* replotted against the scaled separation. Scaling was done relative to the smallest (0.625 deg) eccentricity. Symbols as in *Figure 7.08.*

The present bisection acuity data shows a marked departure from Weber's law (see *Figures 7.05b, 7.06b,* and *7.07*) and are thus consistent with other recent isoeccentric bisection studies, such as Levi *et al.* (1988), who investigated a constant 10 deg eccentricity, and Levi and Klein (1990a), who extended their study to cover an eccentricity range of 0.625 - 10 deg. This departure supports the view that stimulus eccentricity plays a major role in producing the Weber's law relationship found in conventional (non-isoeccentric) bisection acuity tasks (Klein & Levi, 1987; Yap, Levi & Klein, 1987a).

Chapter 8: Displacement thresholds

8.1: Displacement detection

8.1.1: Introduction

Performance in the bisection task just described presumably reflects the ability to discriminate between the two spatial intervals formed by the central feature and each of the outer features. The spatial interval discrimination task, on the other hand, required two intervals to be distinguished when presented sequentially rather than simultaneously. It is possible, however, to present the spatial interval task without any inter-stimulus interval. In this *displacement* task, two features having a certain separation appear for a short period following which one of the features suddenly changes position, either making the spatial interval wider or narrower. The two features then remain at this new separation for a short period before disappearing (see the left side of *Figure 8.01*).

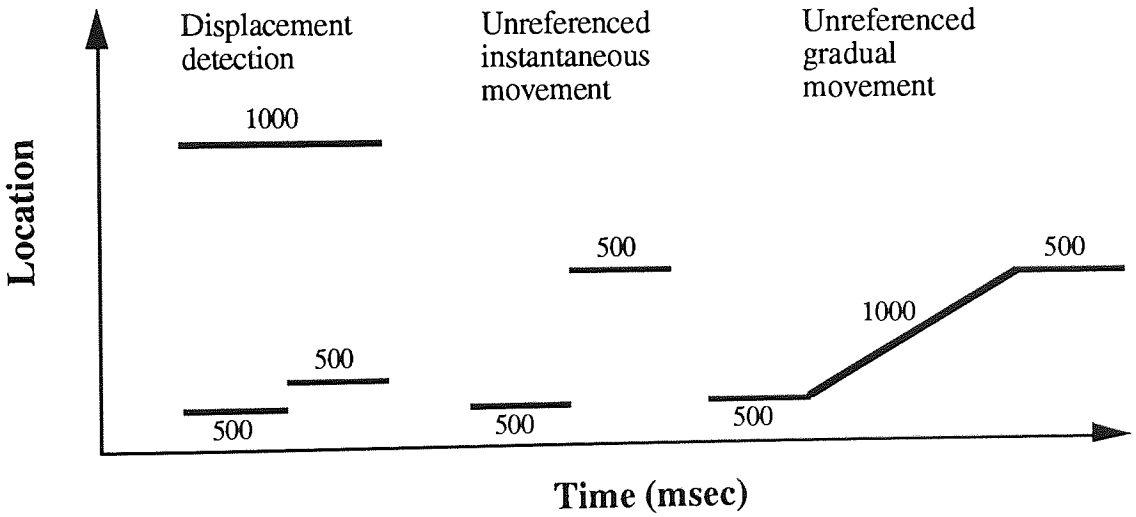

Figure 8.01: A visualisation of the parameters in the three tasks presented in this chapter. Left, *displacement detection*, where two dots were shown simultaneously for 500 msec, after which one of the dots abruptly changed position and remained in this new position for 500 msec. In the middle, *unreferenced instantaneous movement* which actually was a replica of the displacement detection task, but now without a reference reference dot. On the right, *unreferenced gradual movement* , where a dot was presented without any reference for 500 msec, it then moved with constant velocity to a new location, remained there for a further 500 msec and disappeared.

Displacement detection involves detecting the sudden displacement of one feature relative to another stationary one. Threshold values lie in the same range as other hyperacuities. Displacement detection thresholds show a very weak dependence on the separation of the two features, representing a complete deviation from Weber's law (Westheimer, 1979, data shown in *Figure 2.14* as "step change in spatial interval"; Legge & Campbell, 1981).

However, this is only true if the displacement is instantaneous (Whitaker & MacVeigh, 1990). In the next experiment, displacement detection is investigated as a function of eccentricity using an isoeccentric paradigm.

8.1.2: Methods

The stimulus consisted of two small squares presented around the circumference of an imaginary arc in the upper visual field as in *Figure 6.05*. Prior to the appearance of the squares a horizontal red fixation line appeared for 750 msec, and the subject was required to fixate the mid-point of this line which represented the centre of the isoeccentric circle. The fixation line then disappeared and the two squares were presented with a certain separation. After 500 msec, one of the two squares underwent a sudden displacement either to the left or to the right. This made the interval between the squares either wider or narrower. The two squares remained visible for another 500 msec after which they disappeared. The subject's task was not to decide which one of the squares moved (this is an extremely difficult decision in the absence of any other stationary information), but whether the movement made the separation of the squares wider or narrower. Immediately after a response, the fixation line reappeared and the sequence continued in this way until threshold was established. As in the other experiments, the isoeccentric arcs were placed at various eccentricities by a combination of changing viewing distance and varying the position and size of the features on the CRT. The radii of the isoeccentric arcs varied between 0.533 and 10 deg and viewing distance varied between 10 and 0.9 m. All stimuli were simply magnified versions of each other, since square size was maintained at a constant fraction (11%) of the separation.

8.1.3: Results

Displacement thresholds are plotted against separation in *Figure 8.02a*. Rather than an increase as a function of separation, there appears to be, if anything, a gradual improvement in sensitivity as the separation of the features grows. It is possible that the slight increase in sensitivity observed is a product of the increase in stimulus size at larger separations since the size of the squares was proportional to their separation. However, since the present experiment and stimuli are designed to examine the *inter-eccentricity variance*, not threshold variation at a single visual field location, this aspect will not be dealt with more thoroughly.

The Weber fraction for this task falls rapidly with increasing separation (*Figure 8.02b*) and reaches values of around 0.3%. Similar values have been found for non-isoeccentric displacement thresholds (Legge & Campbell, 1981; Whitaker & MacVeigh, 1990). Functions for successive eccentricities are displaced relative to one another along the size axis.

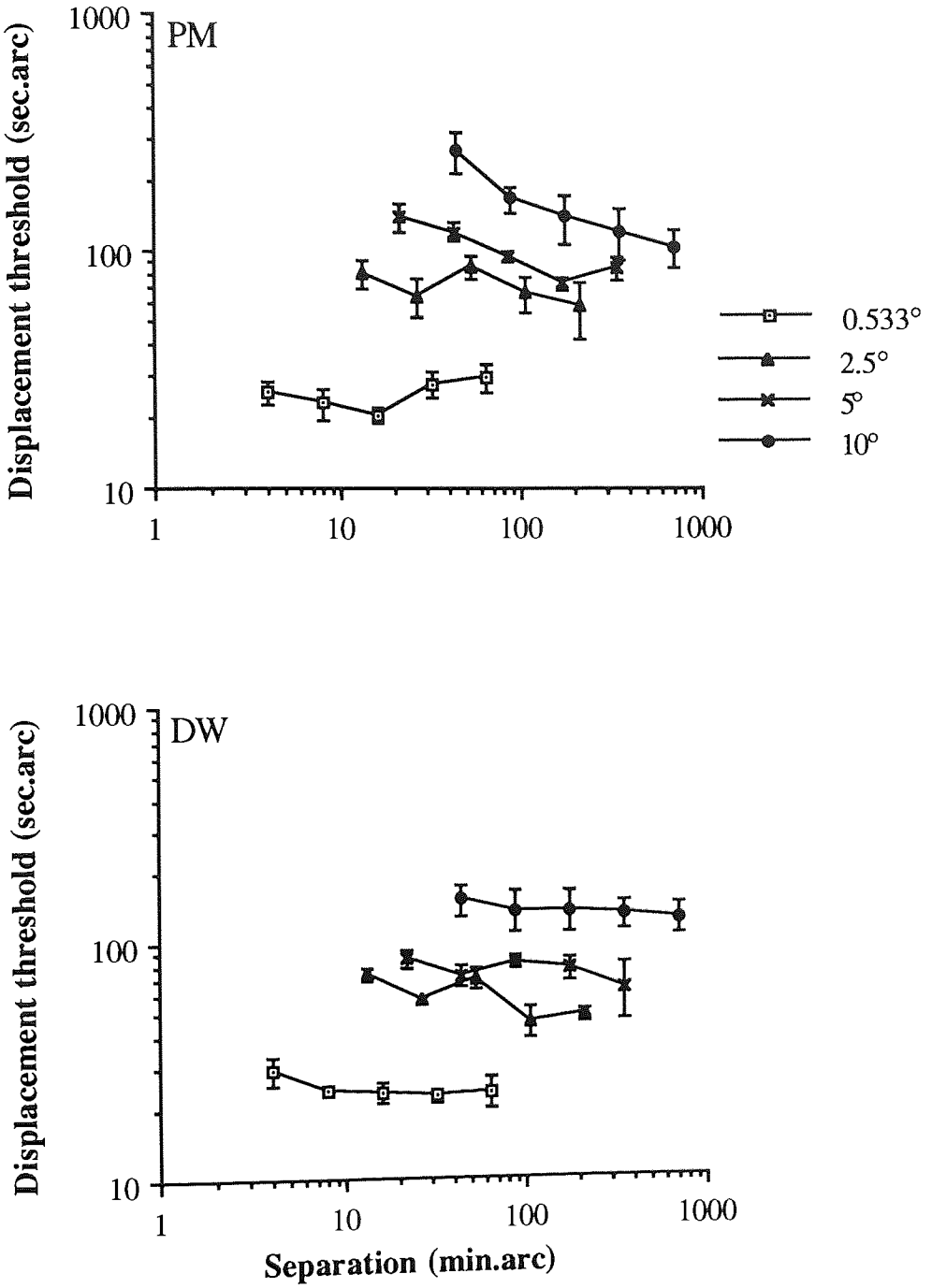

Figure 8.02a: Displacement thresholds for instantaneous referenced displacement plotted against separation.

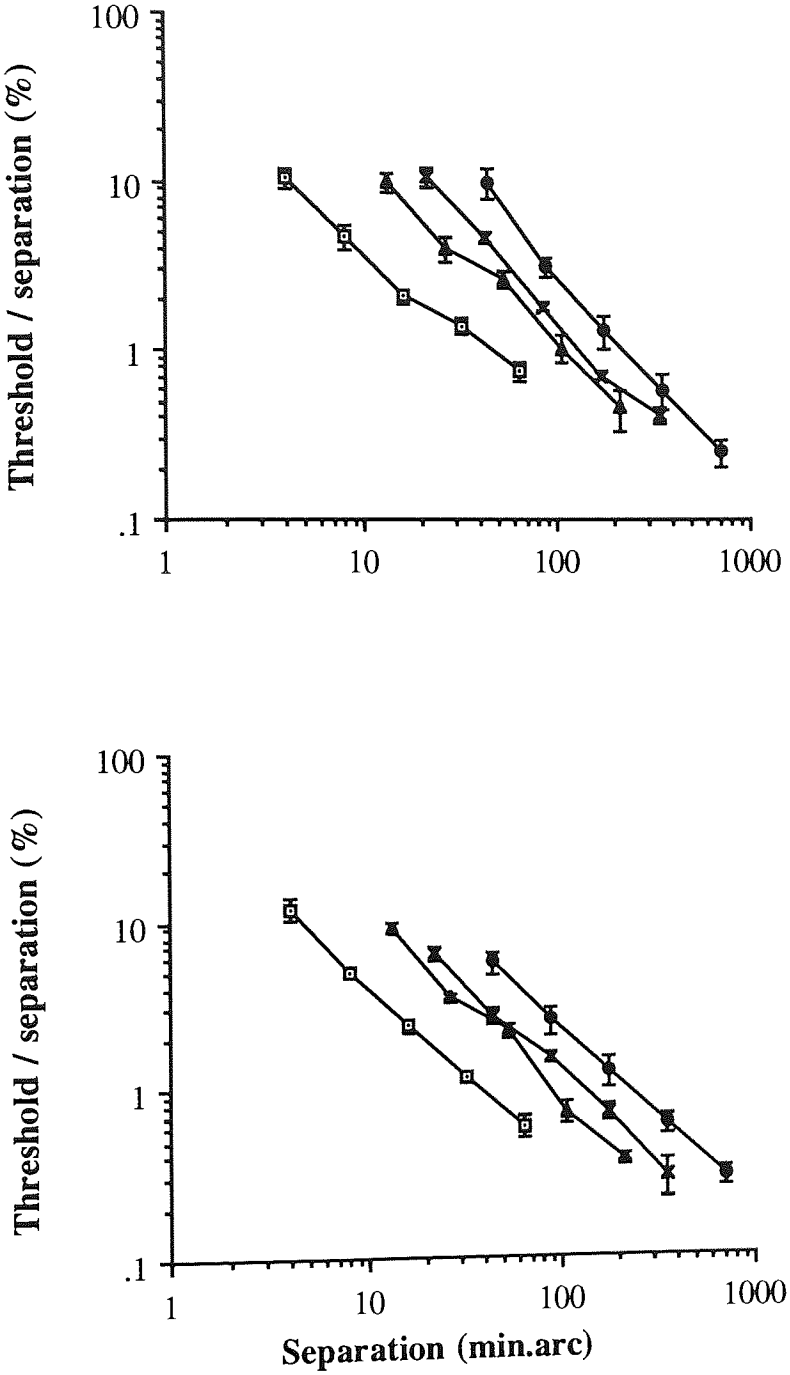

Figure 8.02b: The data replotted with threshold expressed as a percentage of separation.

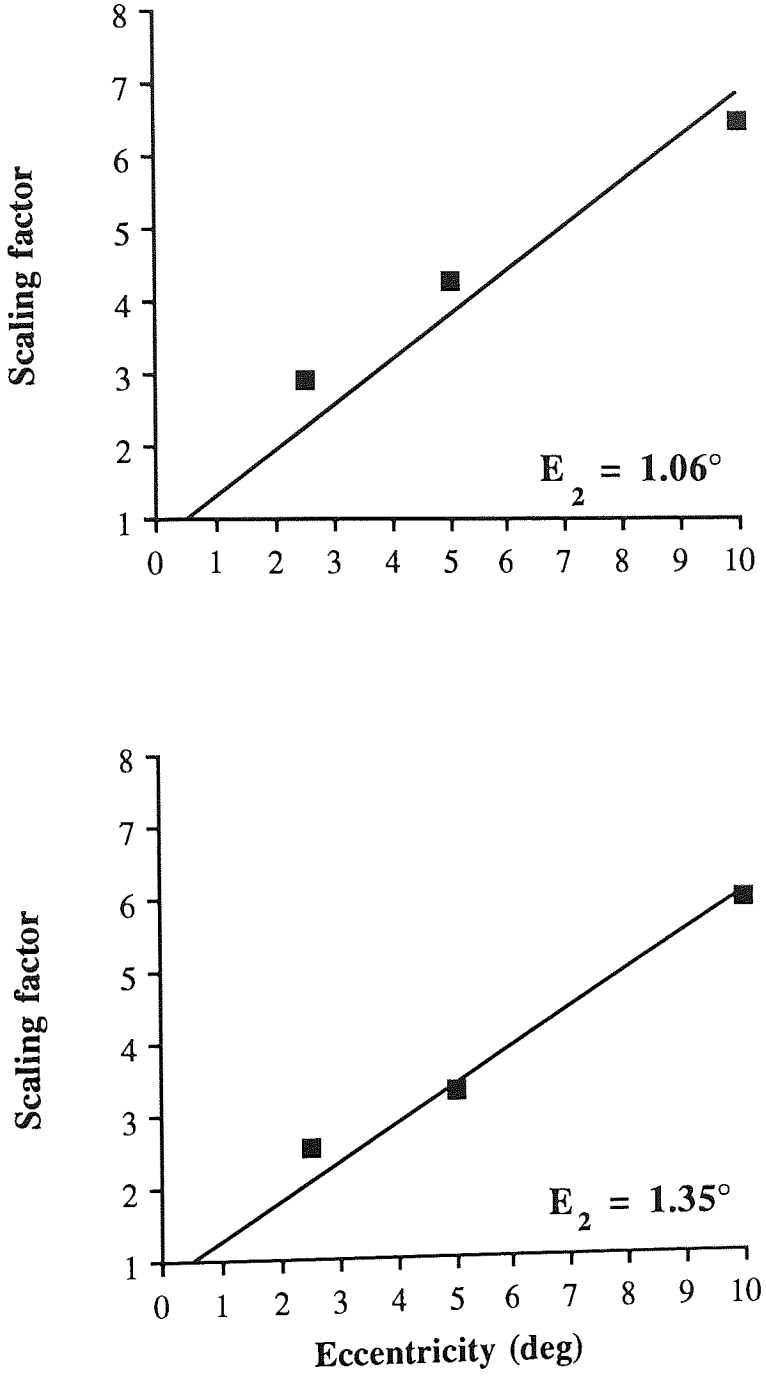

Figure 8.02c: Scaling factors obtained at each eccentricity relative to the smallest eccentricity of 0.533 deg. Note that the line of least squares is constrained to pass through the point (0.533, 1).

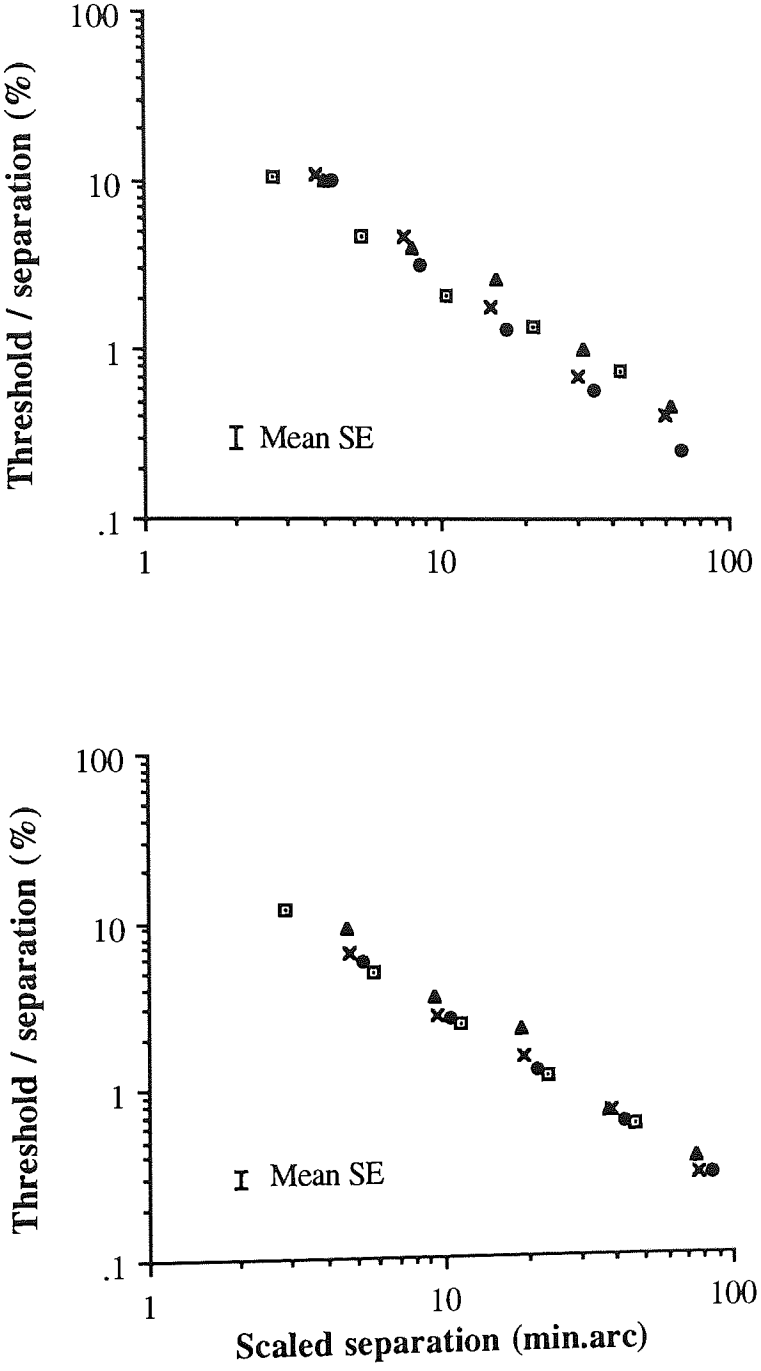

Figure 8.02d: The data of *Figure 8.02b* with the separations at each eccentricity having been scaled along the size (x-) axis according to equation *4.09*. Note how the eccentricity dependent variance of the data is removed in this way.

As before, scaling factors were determined for each eccentricity relative to the most central data (in this case at 0.533 deg eccentricity) and are plotted in *Figure 8.02c*. The linear regression has been constrained to pass through a value of 1 at 0.533 deg eccentricity. The gradients of the regression lines are 0.63 (± 0.09) for PM and 0.53 (± 0.05) for DW, and the E_2 values given by

$$E_2 = (1 / S) - 0.533$$

turn out to be 1.06 (± 0.23) and 1.35 (± 0.18) deg.

Figure 8.02d shows the data of *Figure 8.02b* after scaling according to equation *4.09*. Data from all eccentricities collapse together to form a single function.

8.2: Unreferenced displacement detection

8.2.1: Introduction

It has long been established that, for central vision, the detection of object displacement becomes more difficult in the absence of other stationary objects (Aubert, 1886). If this absence of references were to affect displacement thresholds for central, but not peripheral vision, then one would expect that referenced and unreferenced displacement detection would fall off at different rates with eccentricity. This is indeed the case. Leibowitz, Johnson & Isabelle (1972) present data for unreferenced motion thresholds which within the central 20 deg and without large refractive errors decline at a rate corresponding to an E_2 of about 12 deg. Levi, Klein and Aitsebaomo (1984) used a grating as a stimulus for unreferenced instantaneous displacement discrimination. The peripheral gratings were scaled by changing the viewing distance according an E_2 of 2.5 deg. According to their results unreferenced displacement discrimination falls off slower than the same observer's grating acuity. The unreferenced displacement thresholds decline at a rate corresponding to an E_2 of 5.6 - 13.9 deg, whereas the presence of a reference renders the E_2 1.3 deg.

In the following pages the rate at which unreferenced displacement thresholds decline with eccentricity is investigated using a method of spatial scaling. In addition, since the enhancing effect of references upon displacement thresholds is highly dependent upon the temporal characteristics of the displacement (Leibowitz, 1955; Johnson & Scobey, 1982; Whitaker & MacVeigh, 1990) data for both instantaneous and gradual displacement is presented. The parameters for these tasks were shown in *Figure 8.01*.

8.2.2: Methods

The stimulus consisted of a single square presented on the CRT and viewed in complete darkness so that all other stationary references were removed. In order to guide fixation so that the square was presented at the appropriate eccentricity, a red fixation line appeared for 750 msec beforehand and the subject was required to maintain fixation at the mid-point of this line throughout the stimulus trial. The fixation line disappeared just before the onset of the stimulus so that it could not act as a reference relative to which movement could be judged. The stimulus then immediately appeared, remained stationary for 500 msec and then underwent one of two types of displacement. The first was an instantaneous displacement, as in the previous experiment, whereas the second was a gradual displacement of 1000 msec duration. Subsequent to the displacement the stimulus remained stationary for a further 500 msec before its disappearance. Both types of movement are therefore examples of what is known as stop-go-stop movement (see *Figure 2.18*). The subject was then required to respond as to whether the direction of displacement had been leftward or rightward. After response the fixation line reappeared and the sequence continued. The presence of a stationary reference such as the fixation target prior to, but not during, stimulus presentation has been shown to have virtually no effect on performance in this type of task (Whitaker & MacVeigh, 1990).

Displacement thresholds were measured for both types of displacement using a series of stimulus sizes (all magnified versions of each other) at eccentricities between 0 and 10 deg in the upper visual field, as was previously done for the referenced displacement.

8.2.3: Results

Unreferenced displacement thresholds for the instantaneous displacement are shown as a function of stimulus size in *Figure 8.03a.* Foveal thresholds decrease steadily from around 100 sec.arc to 50 sec.arc as the stimulus size increases. These values are comparable to unreferenced displacement thresholds found in other studies (Legge & Campbell, 1981; Levi, Klein and Aitsebaomo, 1984; Whitaker & MacVeigh, 1990). The improvement in sensitivity is presumably due to the increased number of receptors involved as stimulus size increases. Functions for successive eccentricities follow a similar pattern, but are simply shifted up and to the right relative to the central data. In *Figure 8.03b* threshold is plotted as a fraction of square size in order to make the y-axis scale invariant. Functions at different eccentricities are now simply displaced along the x-axis relative to one another.

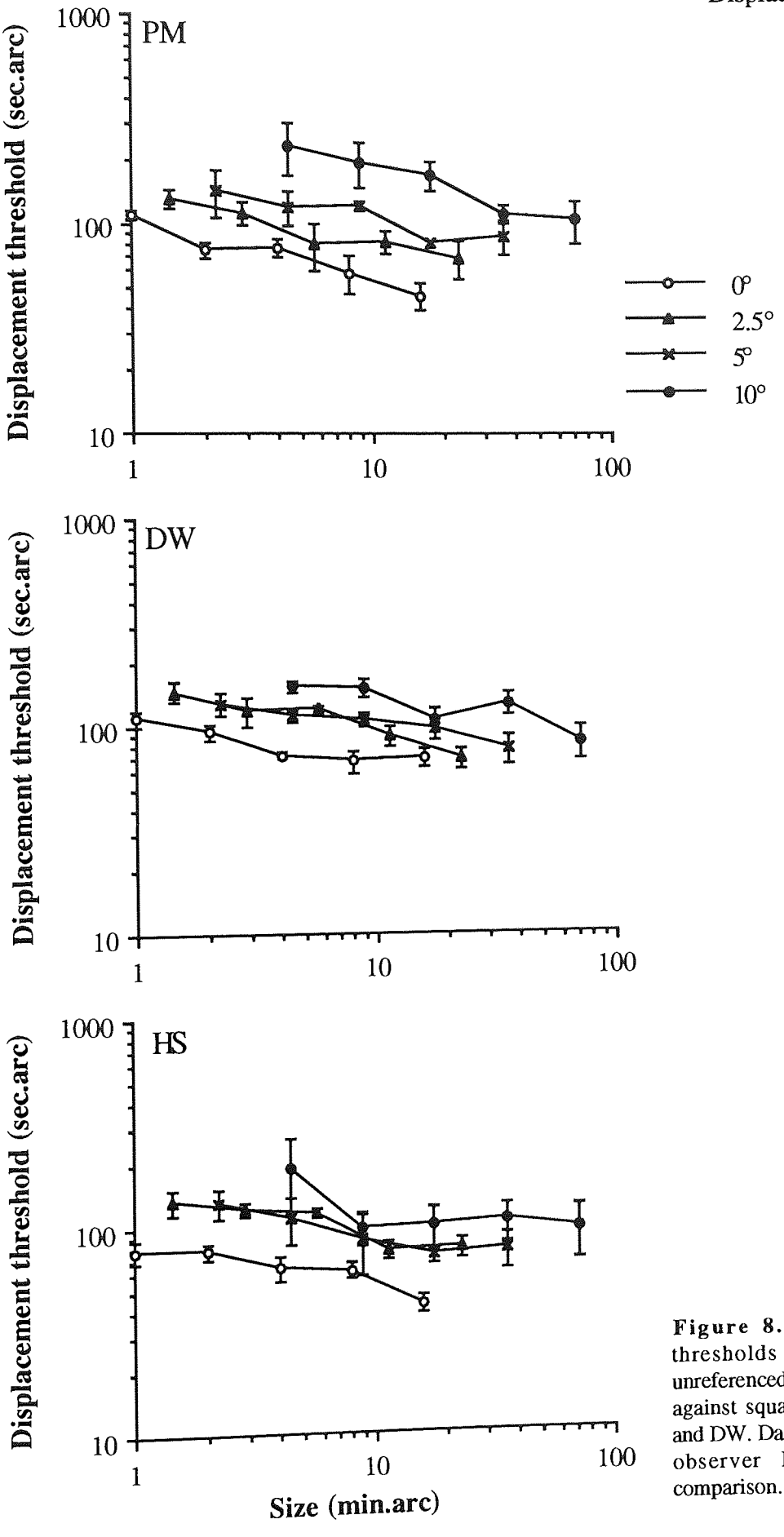

Figure 8.03a: Displacement thresholds for instantaneous unreferenced displacement plotted against square size. Subjects PM and DW. Data for an inexperienced observer HS is shown for comparison.

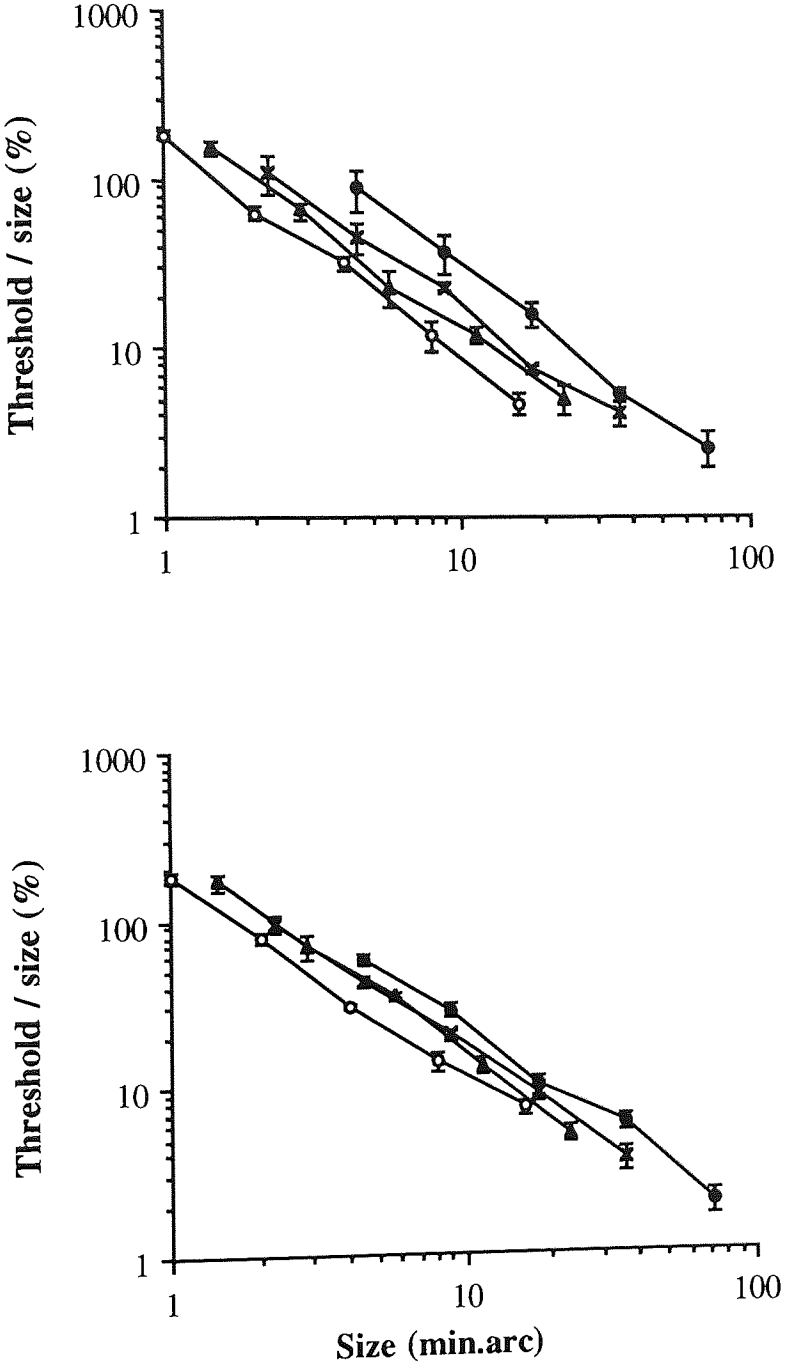

Figure 8.03b: Data replotted with threshold expressed as a percentage of size.

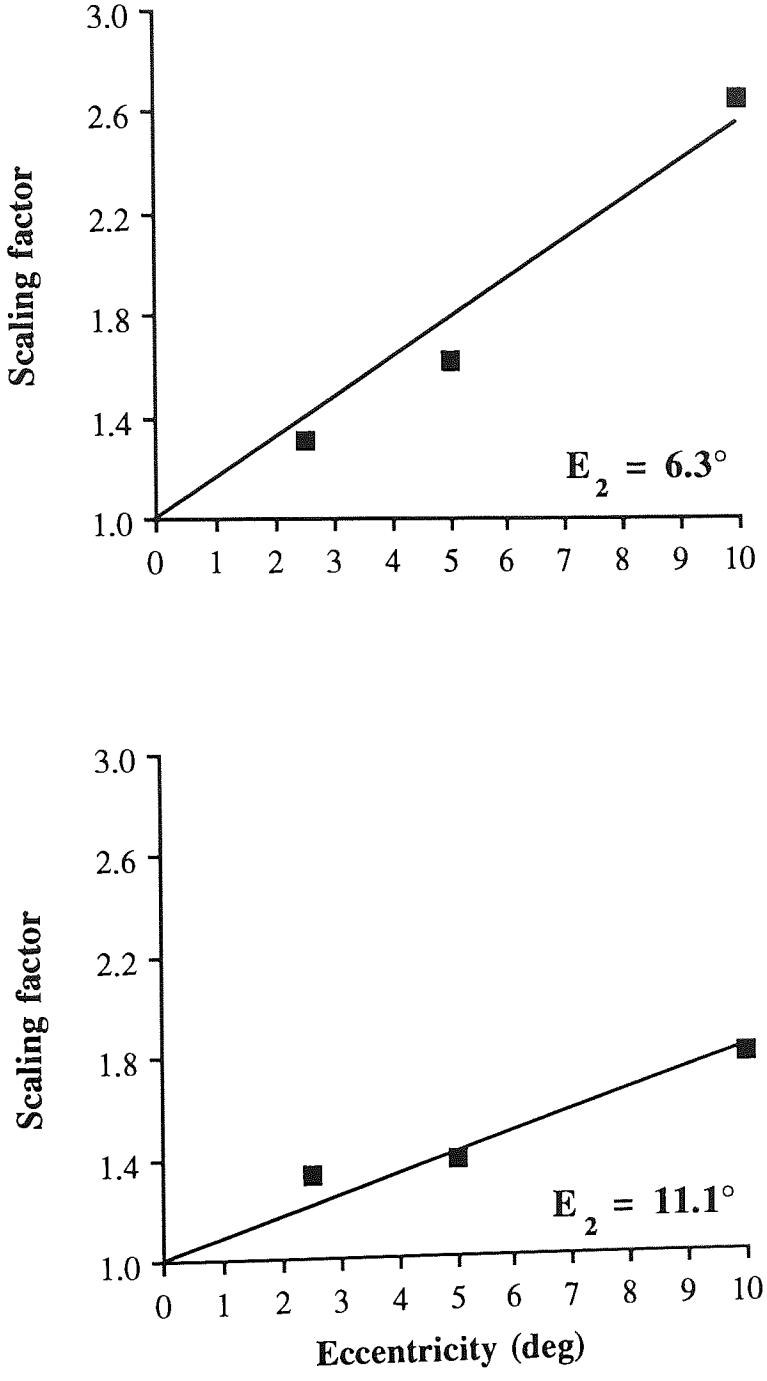

Figure 8.03c: Scaling factors obtained at each eccentricity relative to the smallest eccentricity of 0 deg. Note that the line of least squares is constrained to pass through the point (0, 1).

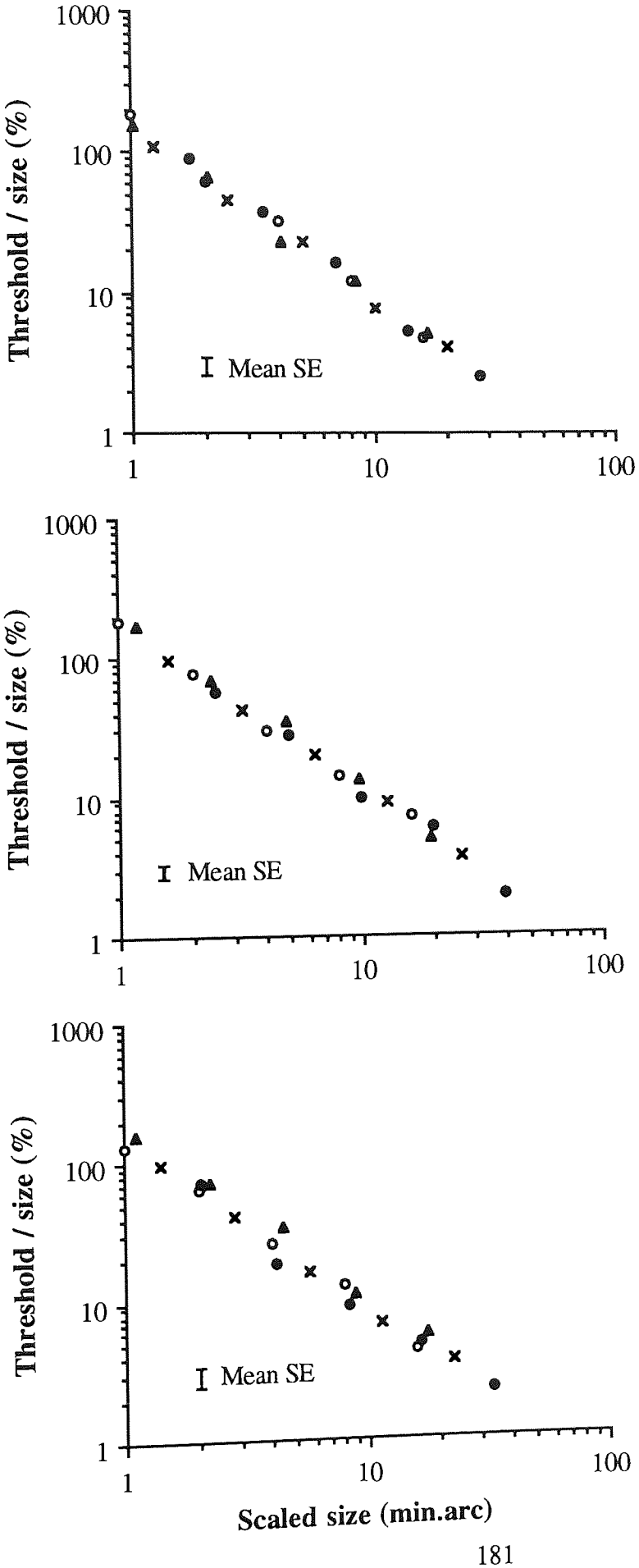

Figure 8.03d: The data of PM and DW from *Figure 8.03b* with the separations at each eccentricity having been scaled along the size (x-) axis. The eccentricity dependent variance of the data is successfully removed in this way. Data for an inexperienced observer HS is shown for comparison.

The scaling factors necessary to make the foveal and eccentric functions collapse together are shown in *Figure 8.03c*. Scaling factors increase approximately linearly with eccentricity, and the linear regression lines (constrained to pass through a value of 1 at 0 deg eccentricity) have gradients of 0.158 (± 0.018) for PM and 0.090 (± 0.011) for DW. These correspond to E_2 values of 6.3 (± 0.7) and 11.1 (± 1.4) deg respectively.

Figure 8.03d shows the data for each observer scaled by substituting their relevant E_2 values into equation *4.09*. This appears highly successful in removing eccentricity dependence. Given the slight discrepancy between the E_2 values for the two highly trained observers, the experiment was repeated using two naïve observers who underwent minimal training before data collection began, the data for the other naïve observer is shown for comparison in *Figures 8.03a* and *8.03d*. Despite the lack of training, their threshold level and the trend of the data was very similar to the other observers. The E_2 values were 8.6 (± 2.0) for HS and 7.9 (± 1.5) deg for SS (not shown).

Figure 8.04a-d shows similar data for the gradual displacement of duration 1000 msec. The first thing to note about the thresholds is that they are much greater than for the instantaneous displacement. This reduction in sensitivity for unreferenced movement at longer durations is consistent with other reports (Johnson & Scobey, 1980, 1982; Whitaker & MacVeigh, 1990). Again the data were transformed by dividing by size (*Figure 8.04b*), so that shifting the resultant functions horizontally is equivalent to scaling the original data in both horizontal and vertical dimensions. Scaling of the data (*Figure 8.04c*) revealed gradients of 0.054 (± 0.008) for PM and 0.074 (± 0.006) for DW, corresponding to E_2 values of 18.5 (± 2.7) and 13.5 (± 1.1) deg respectively. Scaling by these individual E_2 values removed eccentricity dependence.

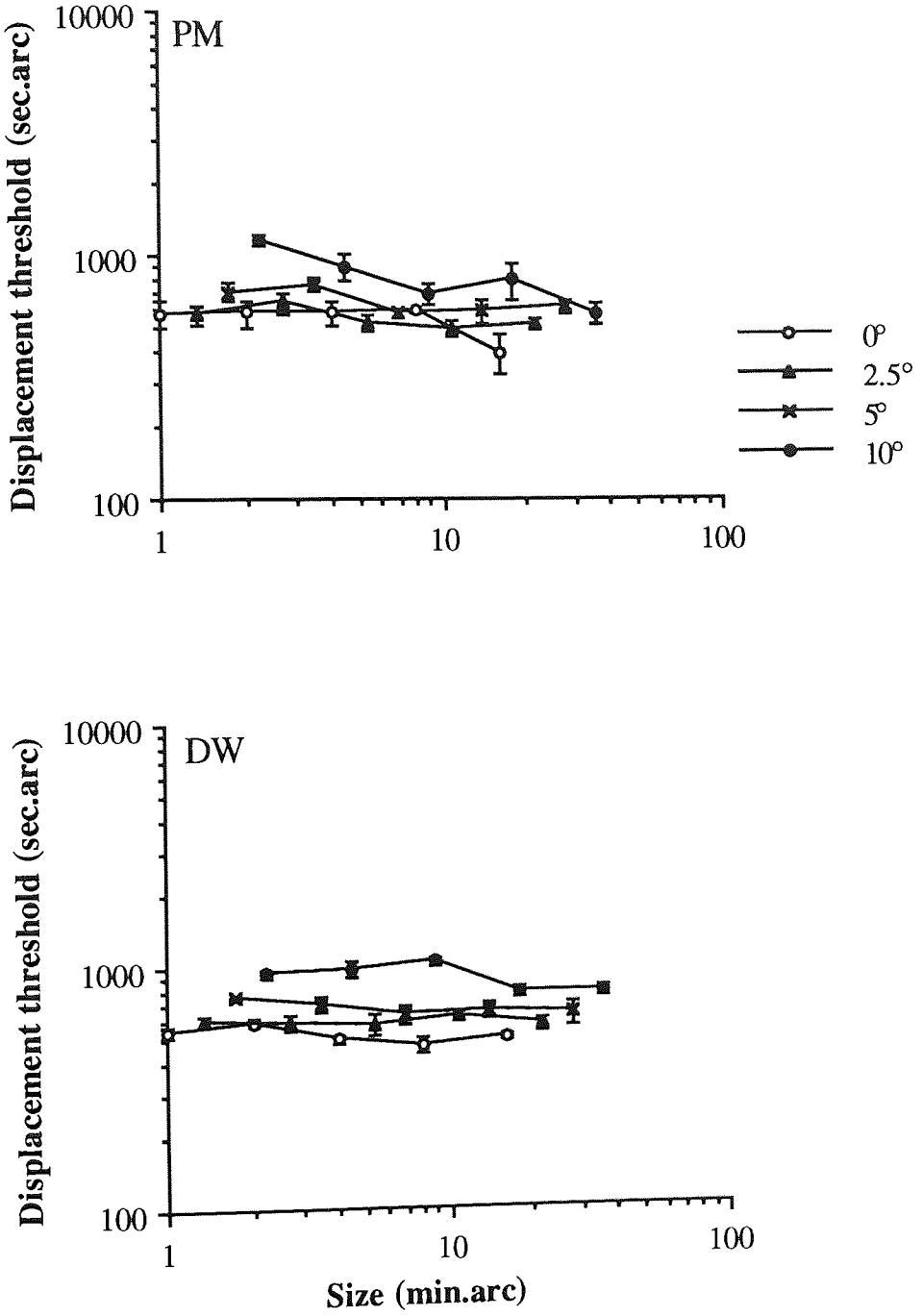

Figure 8.04a: Displacement thresholds for gradual unreferenced displacement plotted against square size.

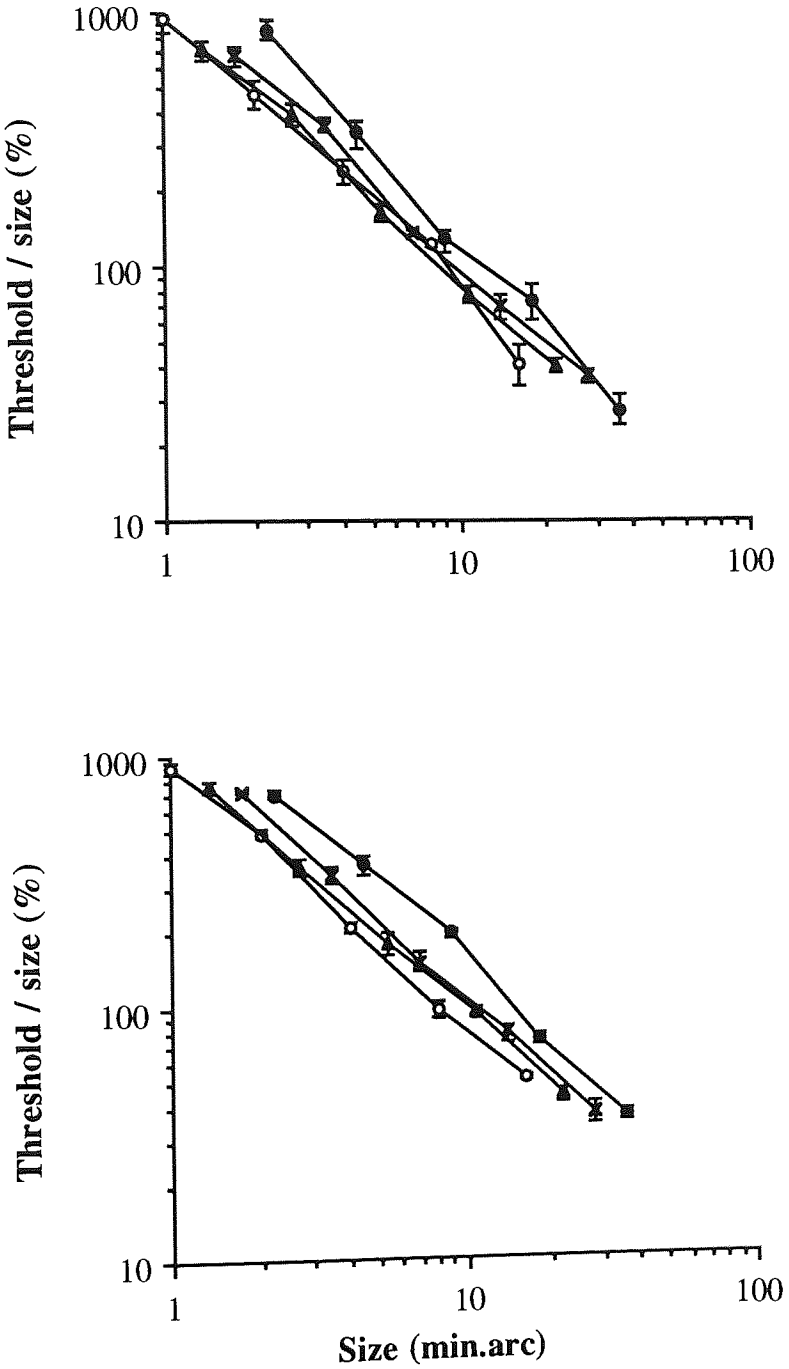

Figure 8.04b: Data replotted with threshold expressed as a percentage of size.

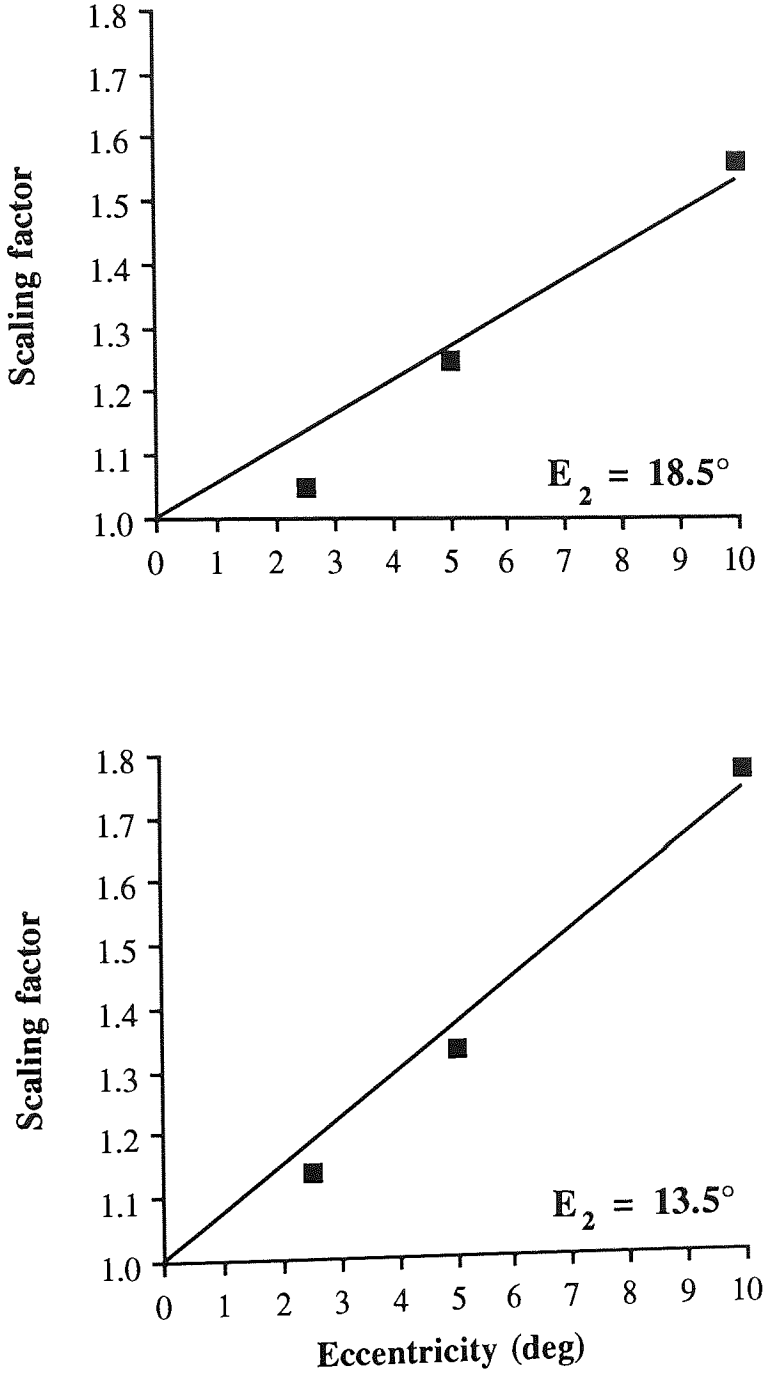

Figure 8.04c: Scaling factors obtained at each eccentricity relative to the smallest eccentricity of 0 deg. The line of least squares is constrained to pass through the point (0, 1).

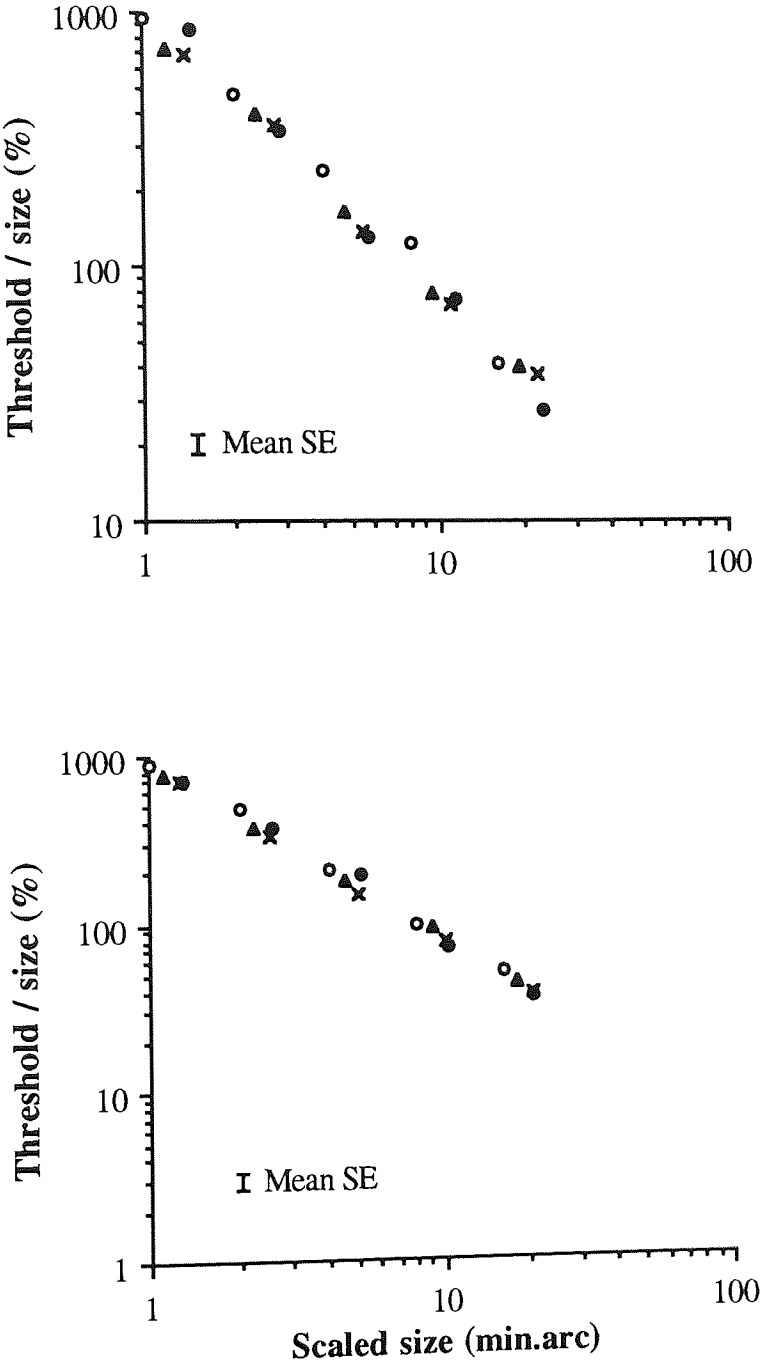

Figure 8.04d: The data of *Figure 8.04b* with the separations at each eccentricity having been scaled along the size (x-) axis. The eccentricity dependent variance of the data is removed in this way.

8.3: Discussion

With regard to movement and displacement detection, there is plenty of information comparing foveal and peripheral performance in various tasks, but quantitative comparison of the data is sometimes difficult due to the large variety of spatial and temporal configurations examined. Leibowitz, Johnson and Isabelle (1972) investigated the effect of refractive error on peripheral motion thresholds within 0 and 80 deg eccentricities and a 1 sec motion duration. Unreferenced displacement thresholds increased at a rate corresponding to an E_2 of about 12 deg (based on thresholds at 0, 10, and 20 deg eccentricities), when refractive errors were corrected or small.

Tyler and Torres (1972) studied peripheral (0 - 20 deg) referenced and unreferenced motion sensitivity as a function of oscillation frequency using a sinusoidally moving line as a stimulus. With increasing eccentricity, referenced motion declined much more slowly than visual acuity relative to the fovea. Further, at frequencies below 10 Hz, removal of reference line decreased foveal movement sensitivity markedly, whereas this effect was much smaller at 20 deg eccentricity.

Johnson and Leibowitz (1976), Johnson and Scobey (1980) and Post and Leibowitz (1981) investigated motion thresholds as a function of movement duration. Johnson and Leibowitz (1976) and Post and Leibowitz (1981) used an unreferenced, moving dot as a stimulus at the fovea, at 30, and at 60 deg eccentricity. They found that between about 100 and 1000 msec duration thresholds were independent of duration both at the fovea and in the periphery. On the basis of the results of Johnson and Leibowitz (1976) within 30 deg eccentricity, thresholds were 4 times the foveal thresholds, which results in an E_2 of 10 deg. In a similar way, an E_2 of 13 deg is found for the data of Post and Leibowitz (1981).

Johnson and Scobey (1980) studied the movement of a bright line at the fovea and 18 deg eccentricity. References were not available in the vicinity of the stimulus and line length was a constant 40 min.arc. At a duration of 1000 msec, displacement thresholds at 18 deg eccentricity were 2.46 times the foveal thresholds, which results in an E_2 of 12 deg. These values correspond relatively well with the present 13.5 - 18.5 deg E_2 values for gradual movement. In the same study foveal and peripheral performance were independent of duration below about 50 msec. For these *short* durations of movement, thresholds at 18 deg eccentricity were 3 times the foveal thresholds, which results in an E_2 of 9 deg.

Post, Scobey and Johnson (1984) investigated motion sensitivity for unidirectional and oscillatory displacements within 2.5 and 80 msec duration. Stimulus configuration was as in Johnson and Scobey (1980), apart from the line stimulus being longer (2.9 deg). Thresholds

for unidirectional displacement were independent of duration, depending only on eccentricity. The rate at which the thresholds increased up to 17 deg eccentricity corresponds to an E_2 of about 12 deg. The E_2 values above compare well with the present unreferenced instantaneous displacement E_2 values of 6.3 - 11.1 deg.

Wright and Johnston (1985) measured threshold displacement amplitude for detecting square-wave oscillatory motion of a sinusoidal grating. Towards the periphery (upper visual field) the grating size was increased according to an E_2 of 2.4 deg (the value suggested by Rovamo & Virsu, 1979). Threshold displacement amplitude was found to increase with eccentricity approximately according to the rate set by cortical magnification values. An E_2 based on the data becomes 2 deg. Position cues were eliminated only close to the stimulus grating so that the displacement can not be considered completely unreferenced. Wright (1987) used scaled-size sinusoidal moving gratings to determine displacement sensitivity at different eccentricities as a function of temporal frequency. Peripheral stimulus sizes were increased (according to the preliminary data) by an amount that equated sensitivity at each eccentricity with that at the fovea. According to the results, a spatial scaling factor of 4.4 was needed at 16 deg eccentricity to equate foveal and peripheral performance, this corresponds to an E_2 of 4.7 deg. E_2 values obtained with gratings seem to fall between the present values of unreferenced displacements (above 6.3 deg) and referenced displacement (below 1.35 deg).

In the periphery, movement thresholds become progressively larger, as all the above mentioned studies have shown. Whereas Leibowitz *et al.* (1972), for instance, argue that unreferenced displacement sensitivity for 1 sec movement duration declines faster than visual acuity, Westheimer (1979) presents data for the detection of instantaneous displacement suggesting that performance declines with eccentricity at approximately the same rate as visual acuity. Although it was not actually mentioned whether any references were present or not the present E_2 values would suggest that this was the case. McKee and Nakayama (1984) found that relative motion detection (for a movement duration of 52 msec) falls off somewhat more rapidly than visual acuity measured with sinewave gratings at the eccentricity range of 0 - 40 deg. According to their data, E_2 for relative motion detection is about 1.7 deg, whereas E_2 for grating acuity is about 2.7 deg.

The results of Levi, Klein and Aitsebaomo (1984) allow a direct comparison of referenced and unreferenced displacement discrimination as a function of eccentricity. Unreferenced displacements at the fovea were found to be equally accurate as the observer's grating acuity. Foveal thresholds for referenced displacement discrimination were about 18 sec.arc (present minimum thresholds were 21 sec.arc), whereas thresholds for unreferenced displacement discrimination were 40 - 60 sec.arc (present minimum thresholds were 45 - 68 sec.arc). An E_2 of 1.3 deg was found for referenced displacement discrimination (compared with the

present estimates of 1.06 and 1.35 deg). For unreferenced instantaneous displacement Levi *et al.* (1984) find E_2 values of between 5.6 and 13.9 deg, again comparable to the present estimates (6.3 - 11.1 deg).

The present results tend to suggest that E_2 becomes even greater as the duration of the movement phase of the displacement increases, i.e. velocity decreases. One factor affecting this tendency may be that it is more difficult to keep fixation steady when the slowly moving target is close to the fovea. Further, oculomotor noise in cortical terms is larger relative to the foveal than peripheral thresholds. Therefore, oculomotor noise preferentially degrades foveal thresholds, and this has the effect of increasing the E_2 value. The difficulty in holding fixation steady was especially pronounced for subject PM (with the largest E_2 for gradual unreferenced movement discrimination, 18.5 deg), who found that the stimulus appeared to arbitrarily change direction, at times even twice, during the 1000 msec presentation.

The implication of the large difference in E_2 values for referenced and unreferenced displacement is that, although the presence of stationary references improves displacement detection considerably at the fovea, their effect becomes much less pronounced at greater eccentricities, as suggested by Tyler and Torres (1972).

Chapter 9: Orientation discrimination

9.1: Introduction

At the fovea a short line suffers from optical and neural blurring and its orientation is difficult to determine. Increasing line length improves performance (measured in terms of angle of orientation) (*Figure 2.20*) until, for sufficiently long lines, performance becomes independent of line length. It is widely accepted that the line length needed for best performance increases with eccentricity, as would be expected if the periphery were related to the fovea by a simple change of scale (Scobey, 1982; Vandenbussche, Vogels & Orban, 1986). However, there is some evidence which suggests that the situation is not so simple.

Figure 9.01: Angular orientation thresholds from Vandenbussche, Vogels and Orban (1986). Thresholds have been converted to 80% correct level, the scale is the same as in the present figures to allow comparison (see discussion).

Vandenbussche *et al.* (1986) present angular orientation threshold *vs* line length functions at the fovea and in the periphery. The data is redrawn in *Figure 9.01*. If the periphery differed from the fovea simply by a change of scale, such functions would be expected to be of the same shape but displaced horizontally along the size axis relative to one another, without any vertical shift. However, according to their measurements and as can be seen in *Figure 9.01*, the gradients of the functions are steeper in the periphery. The results are pooled from three standard stimulus orientations (horizontal, vertical and right oblique) and of two subjects at eccentricities 0, 15, and 30 deg. The data appears to suggest that peripheral orientation

discrimination thresholds remain slightly poorer than their foveal counterparts even at very long line lengths. In addition, Spinelli, Bazzeo and Vicario (1984) performed an orientation matching experiment using experimentally acquired optimal size for sinusoidal gratings at each eccentricity (10, 20 and 30 deg) and found that peripheral performance could not be equated with that at the fovea despite appropriate magnification.

The above findings are in conflict with the concept that peripheral performance can be equated to that at the fovea simply by an appropriate change of scale, a concept which has been shown to hold true for many other tasks in the previous chapters. The aim in the present study is to use the spatial scaling method in order to compare orientation discrimination in the fovea and periphery to discover whether qualitative as well as quantitative differences are present for this task. Using this data a model for orientation discrimination is then developed.

9.2: Methods

The white line stimulus was presented against a dark background on a CRT as described in General methods. The stimulus luminance was 40 cd m^{-2}. All the lights in the room were turned off so that the observer could not use the screen edges or any other clue within the laboratory as a reference. As a further precaution, the horizontal stimulus location was jittered by 5% of the screen size from trial to trial.

Orientation discrimination thresholds were measured at the fovea and at 2.5, 5, 10 and 15 deg eccentricities in the nasal visual field. Thresholds were measured for a sequence of magnified versions of the stimulus. Each successor in a series was magnified by a factor of 2. The stimuli were lines whose width was always 11% of their length. In the periphery the stimulus set consisted of larger stimuli still having the same magnification relative to each other. This increment in size was achieved by reducing viewing distance with increasing eccentricity. Foveal viewing distance was 10 m and this was reduced to 4 m at 2.5 deg, 2 m at 5 deg, 1 m at 10 deg and 0.65 m at 15 deg eccentricity. Pilot experiments were used to choose eccentric viewing distances. The precise distances have no bearing on the eventual scaling factors, but need to be established approximately since there is no sense performing experiments with peripheral stimulus sizes which have no foveal counterpart.

A fixation point was presented for 500 msec. It then disappeared but the subject was required to maintain fixation at the location where the fixation point had been. Immediately after the disappearance, the line stimulus was presented for a duration of 500 msec at the required eccentricity. The subject had to decide whether the line was tilted clockwise or counter-clockwise from vertical. After the observer had responded via the keyboard the fixation point reappeared to mark the beginning of the next trial. This gave the observer a chance for a short

pause when needed. Also, to avoid fatigue, data was collected in a large number of sessions lasting about 20 - 30 minutes. Each threshold estimate resulted from about 50 - 80 trials and the final threshold represents a mean of four to eight estimates.

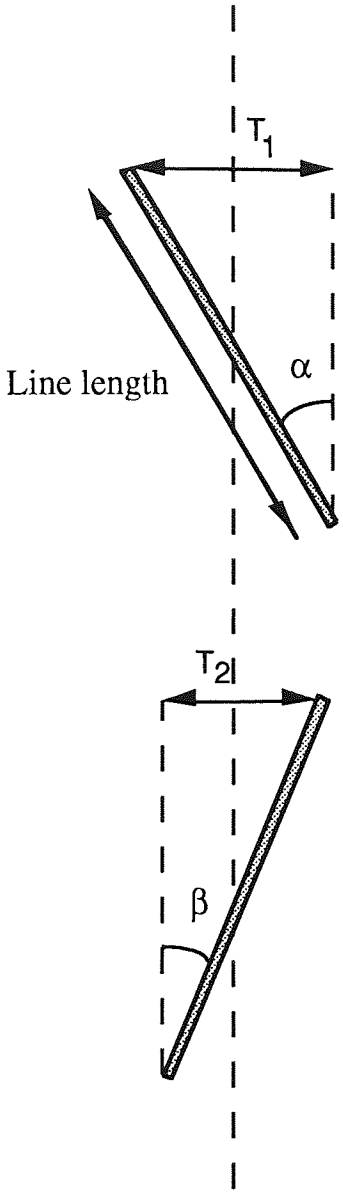

The 80% correct level was found for both clockwise and counter-clockwise responses using a randomly interleaved two-alternative forced choice procedure with a modified PEST routine (Findlay, 1978). This method excluded the possible effect of a subjective orientation bias on thresholds. Thresholds may either be expressed in spatial or in angular terms, as demonstrated in *Figure 9.02.* In the spatial domain, offset thresholds (measured in sec.arc in the visual field) between the top and bottom of the line were determined independently within the interleaved procedure for both clockwise and counter-clockwise responses (T_1 and T_2). The mean of T_1 and T_2 was taken to represent offset threshold. Bias is the absolute difference $|T_1 - T_2|/_2$ between the subjective vertical (midway between clockwise and counter-clockwise threshold positions) and the true vertical. In angular terms (measured in deg of rotation), threshold is the mean of α and β, whilst bias is $|\alpha-\beta|/_2$ The observers were given no feedback.

Figure 9.02: Schematic drawing of the stimulus as viewed by the observer. Threshold estimates are made for both clockwise and counter-clockwise directions of tilt. Orientation thresholds may then be defined in two ways. In spatial terms, threshold = $(T_1+T_2)/_2$ (sec.arc) and bias = $|(T_1-T_2)/_2|$ (sec.arc). In angular terms, threshold = $(\alpha+\beta)/_2$ and bias = $|(\alpha-\beta)/_2|$.

Two observers (DW and PM) were highly trained in making both foveal and peripheral orientation judgements. A third observer (KL) was untrained. The task was performed monocularly with the dominant eye. All observers were moderately myopic (<4.00DS), pre-presbyopic and wore their distance refractive correction.

9.3: Results

In *Figure 9.03a* spatial offset thresholds in sec.arc in the visual field are plotted against line length at each of the five eccentricities. The resulting curves are in general u-shaped, thus demonstrating an optimum at each eccentricity. It is clear that the optimum length increases with increasing eccentricity (Scobey, 1982; Vandenbussche *et al.,* 1986). In addition to the increase in optimum line length, minimum offset threshold increases from approximately 15 sec.arc at the fovea to 100 - 200 sec.arc at 15 deg eccentricity.

Figure 9.03b shows the same data expressed in terms of the threshold angle of orientation. Note that measurements expressed in angular terms are independent of magnification, similar to contrast thresholds but unlike spatial thresholds such as those shown in *Figure 9.03a.* The functions at each eccentricity decline with increasing line length, initially quite rapidly, but then more gradually, suggesting that a plateau is likely to occur at very long line lengths. The minimum threshold seems to be the same for all eccentricities. Note that the shapes of the curves at different eccentricities are similar - they simply appear to be displaced along the horizontal axis relative to one another. The amount of this displacement reveals the rate at which performance deteriorates with increasing eccentricity. Logarithmic axes are used throughout to ensure that each data point has approximately the same variance irrespective of threshold level (Virsu, Näsänen & Osmoviita, 1987).

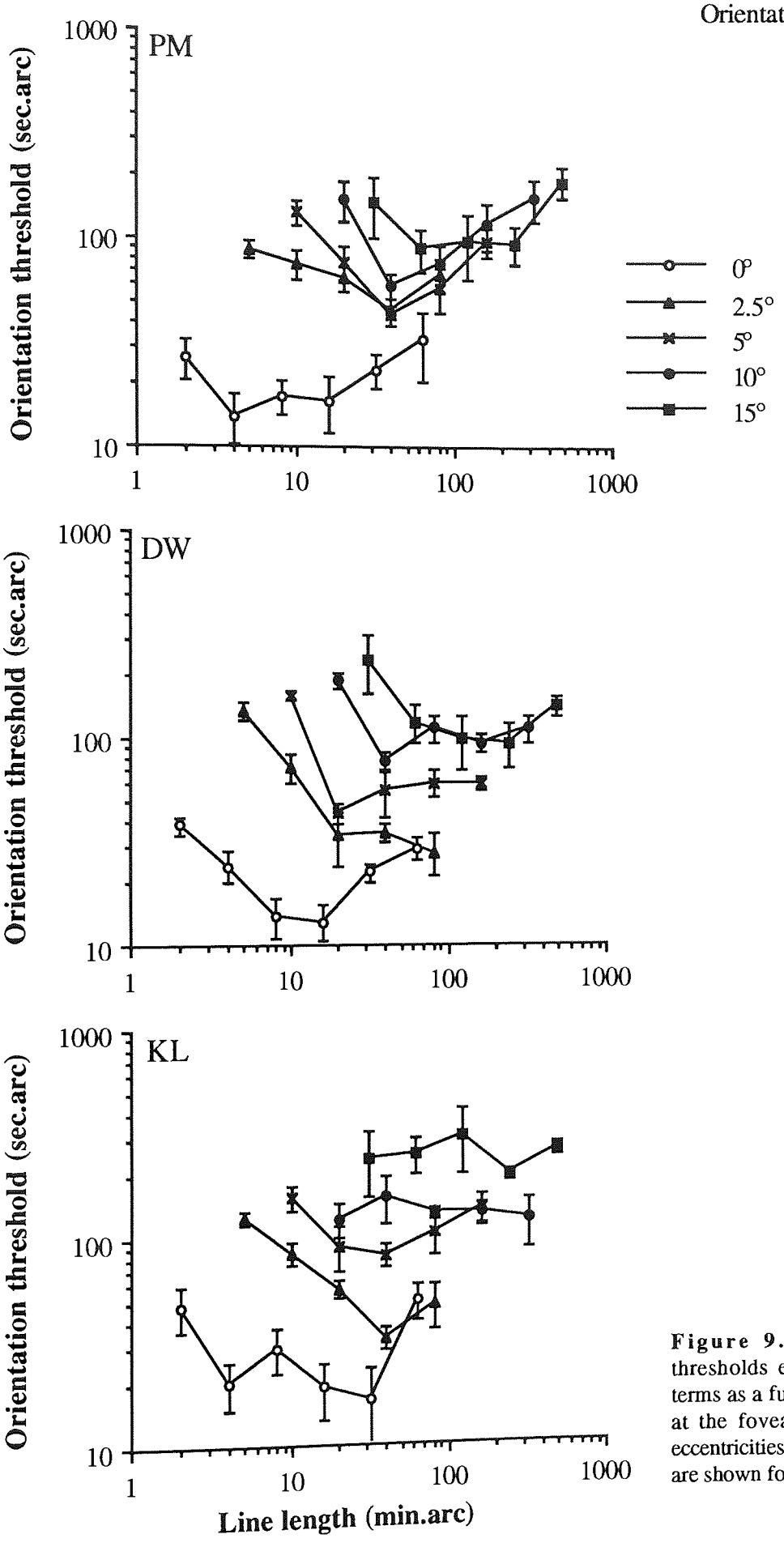

Figure 9.03a: Orientation thresholds expressed in spatial terms as a function of line length at the fovea and at four other eccentricities. The standard errors are shown for each point.

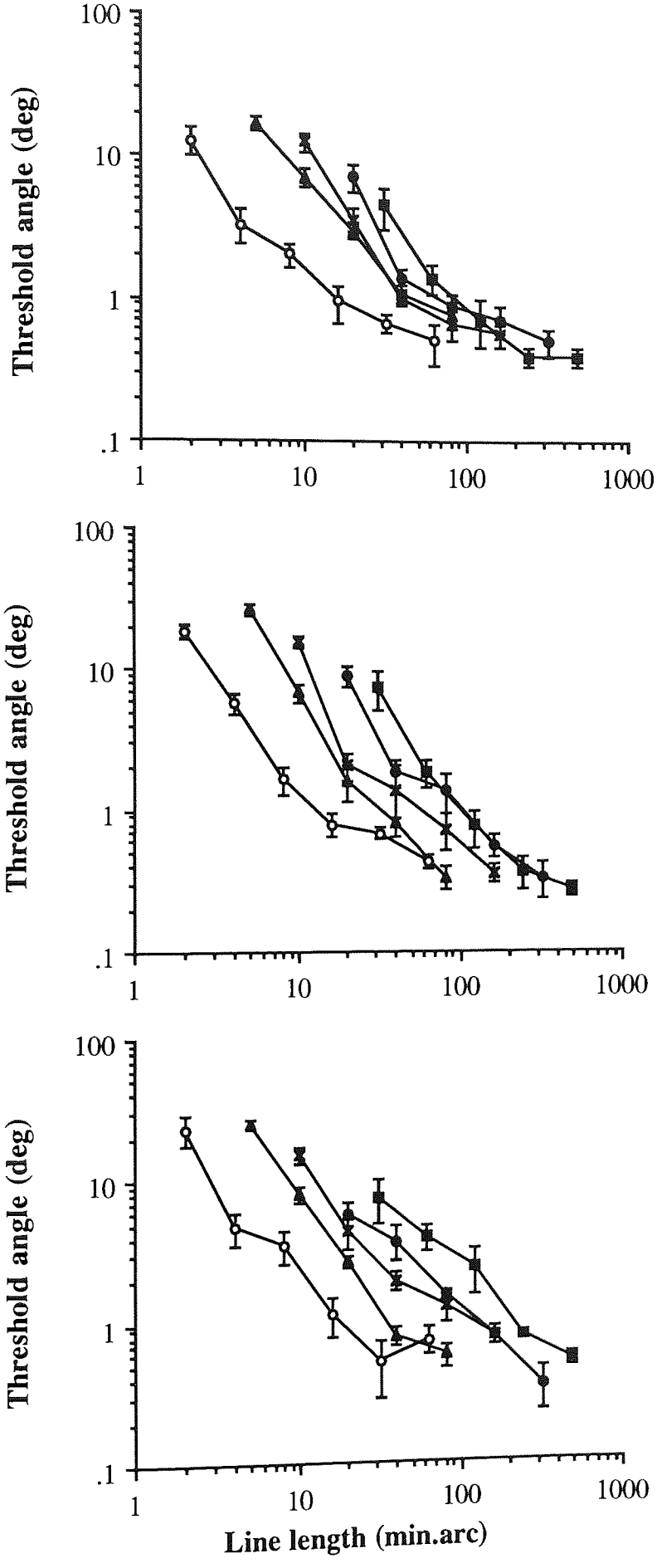

Figure 9.03b: Orientation thresholds from *Figure 9.03a* expressed in angular terms (deg of rotation) and plotted against line length.
Since angular measurements were unaffected by magnification, this procedure renders the y-axis scale invariant.

Scaling factors were next found at each eccentricity which were required to shift the peripheral data leftwards along the x-axis in order to bring the data points into alignment with the foveal data. An approximate factor was estimated from visual inspection of the data and the line length values of the peripheral data points were divided by this estimated factor. To determine how well this factor minimised variance between the foveal and eccentric data points, a second-order polynomial regression curve was fitted to the combination of the two data sets. All the parameters of this curve were allowed to float freely in order to obtain the best possible fit. The sum of squares of residual deviations around this curve was calculated. The process was then repeated with another estimate until a scaling factor was found which minimised the sum of squares of residual deviations. This factor was then accepted as the final scaling factor for the eccentricity in question. Scaling factors for other eccentricities were obtained in a similar way.

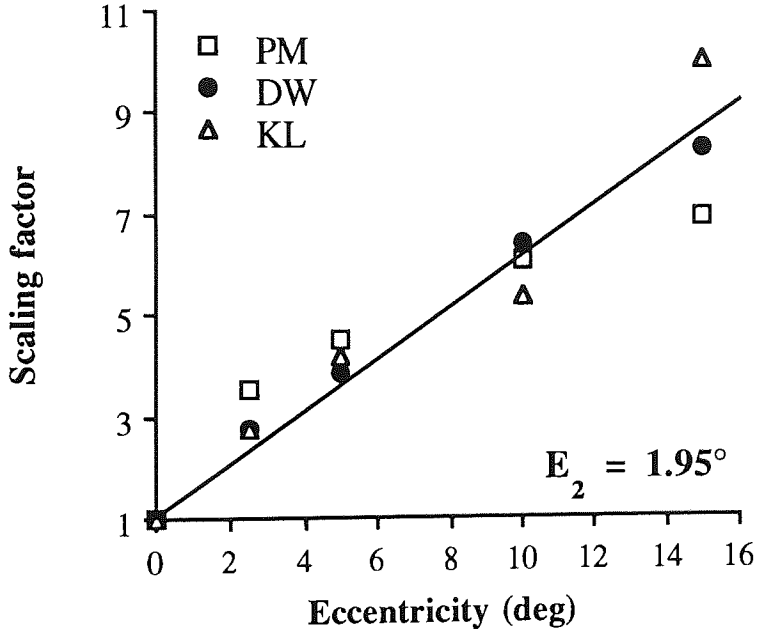

Figure 9.03c: Scaling factors, as derived in the text, are shown plotted as a function of eccentricity. The data has been fitted with a least square line. The line has been constrained to pass through (0,1), since all the scaling factors are established in relation to the data at zero deg eccentricity. The inverse of the gradient of the line indicates E_2.

Figure 9.03c shows the scaling factors obtained at each eccentricity for all three subjects. The factors are plotted against eccentricity and the data has been fitted with a linear regression line since the increase in orientation discrimination appears reasonably linear, as is the case for many other spatial acuities within 15 deg of the fovea (Weymouth, 1958). The foveal scaling factor is constrained to be 1, since the foveal data scaled onto itself gives the value of 1. From the gradient of the linear regression, S, according to equation *4.04*, $E_2 = {}^1/_S$ thus, E_2 was found to be 1.95° (± 0.11) deg and the explained variance (r^2) for the line of least

squares was 0.84. Therefore, according to the equation *4.09*,

$$F = 1 + {}^{E}/_{1.95°}$$

In *Figure 9.03d* the data of each observer from *Figure 9.03b* has been scaled according to the above equation. It is immediately clear that this single parameter E_2 is successful in removing almost all of the eccentricity dependent variance from the data, since all data points collapse together to form a single function. The only exception is perhaps the data of PM which demonstrates a slight overall inferiority (higher thresholds) at 2.5 deg. This can be explained by the relatively large deviation of PM's 2.5 deg scaling factor from the regression line in *Figure 9.03c*.

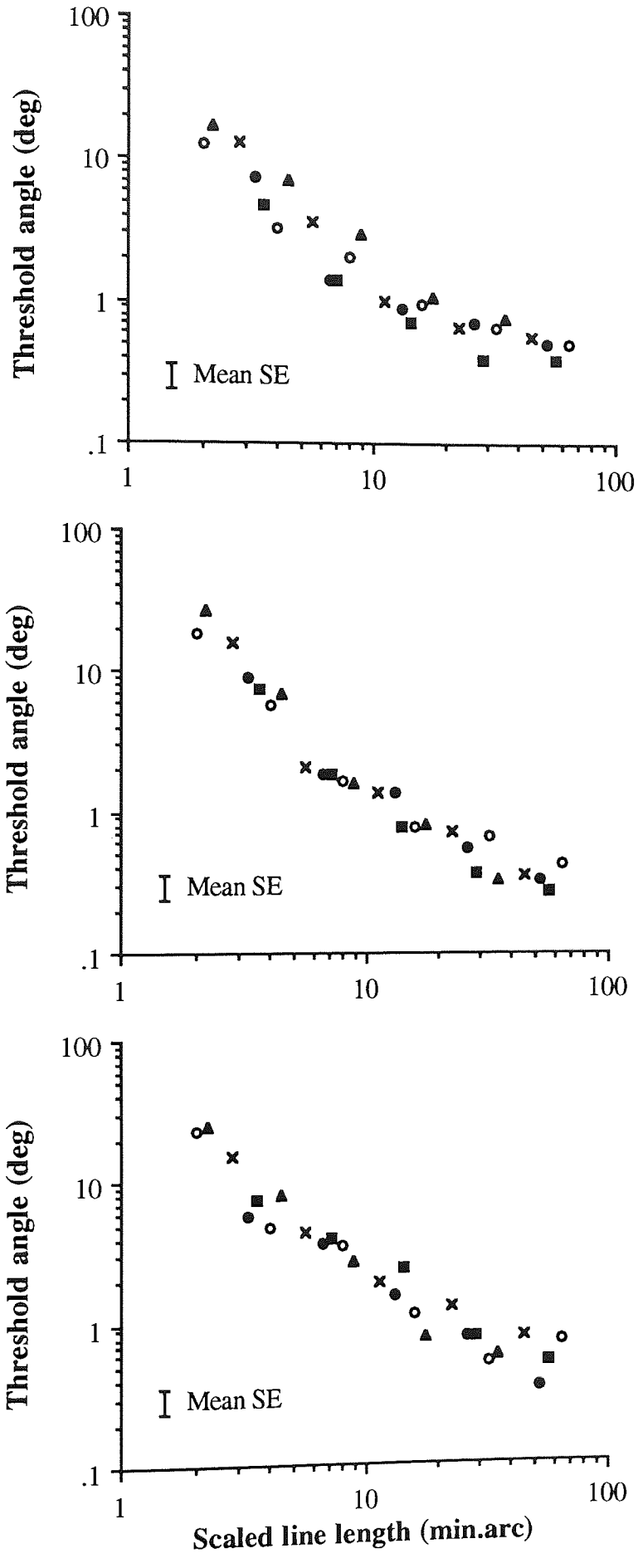

Figure 9.03d: All line lengths for each observer have been scaled according to the least square line shown in *Figure 9.03c*. Angular thresholds are plotted against the scaled line lengths. Mean standard error is shown. This scaling procedure appears to have been successful since little systematic variation between the data points at different eccentricities remains.

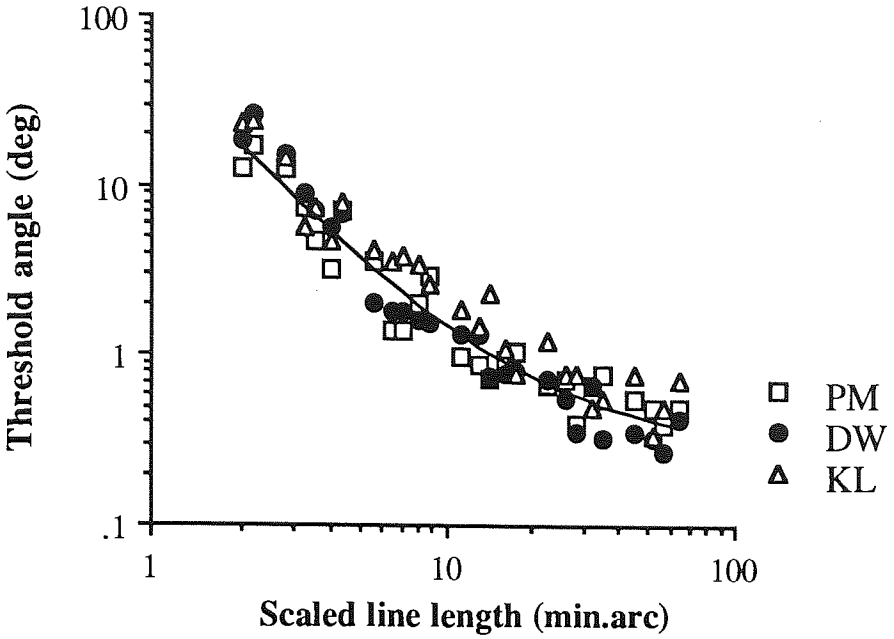

Figure 9.03e: The scaled data of all subjects have been plotted together. The smooth curve is the relative least squares fit of equation $Th = Th_{min} (1 + {}^{Lc}/_{Ls})^{1/p}$ to the data. Th is the orientation threshold in degrees and Ls is the scaled line length in min.arc. The explained variance reached its maximum of 93% when p = 0.5. At this value Th_{min} = 0.267 deg and critical length Lc = 14.5 min.arc.

The scaled data of all subjects have been replotted together in *Figure 9.03e*. Orientation discrimination threshold in angular terms decreases with increasing scaled line length until at very long line lengths performance tends to become independent of line length. To comply with this it is now assumed that threshold raised to an exponent p is linearly related to the inverse of scaled line length:

$$Th^p = k_1 + k_2/L_s \qquad (9.01)$$

where Th is threshold angle, L_s is the scaled line length, and k_1, k_2, and p are parameters of the model. Equation *9.01* means that at long line lengths Th is constant and equal to $Th_{min} = k_1^{1/p}$ but at short line lengths Th decreases in proportion to $L_s^{-1/p}$. Equation *9.01* can be transformed to

$$Th^p = Th_{min}{}^p + k_2/L_s \qquad (9.02).$$

The critical line length marks the transition between the decreasing (at short line lengths) and constant (at long line lengths) parts of equation *9.02*. Respectively, these are $Th^p = k_2/L_s$ and $Th^p = Th_{min}{}^p$. At their crossing point $Th_{min}{}^p = k_2/L_s$. Therefore, the critical scaled length is $L_c = k_2\, Th_{min}{}^{-p}$, which means that $k_2 = L_c\, Th_{min}{}^p$. Equation *9.02* then becomes

$$Th = Th_{min} (1 + L_c/L_s)^{1/p} \quad (9.03).$$

When $L_s = L_c$, then Th is equal to $2^{1/p}$ times the threshold minimum.

Using different values of p, equation *9.01* was fitted to the data by finding the minimum of

$$G = \sum_{j=n}^{j} \{(Th_j^p - k_1 - k_2/L_{sj}) / Th_j^p\}^2 \quad (9.04).$$

In the following text subscript j is left out for clarity. It is necessary to calculate the relative least squares curve by minimising the percentage error, as in equation *9.04*, because the range of Th is two log units. Otherwise the deviations of the large Th values from the least-squares curve would dominate the fitting procedure. Equation *9.04* is first transformed to

$$G=\Sigma(1 - k_1 Th^{-p} - k_2 Th^{-p} L_s^{-1})^2 \quad (9.05).$$

Equation *9.05* is then transformed to

$$G=\Sigma[1-k_1x_1 - k_2x_2]^2 \quad (9.06),$$

where $x_1 = Th^{-p}$ and $x_2 = Th^{-p} L_s^{-1}$. The task is now to find the values of k_i (i = 1, 2) that minimize G. Therefore, G is derived with respect to each k_i and the equations $\partial G/\partial k_i = 0$ are solved. Thus,

$$\partial G/\partial k_i = \Sigma 2[1 - k_1x_1 - k_2x_2] (-x_i) = 0 \quad (9.07),$$

which gives the following equations

$$k_1\Sigma(x_1^2) + k_2\Sigma(x_2x_1) = \Sigma x_1 \quad (9.08),$$

$$k_1\Sigma(x_1x_2) + k_2\Sigma(x_2^2) = \Sigma x_2 \quad (9.09),$$

which are transformed to a matrix equation of the type Az = b:

$$\begin{pmatrix} \Sigma (x_1^2) & \Sigma (x_2x_1) \\ \Sigma (x_1x_2) & \Sigma (x_2^2) \end{pmatrix} \quad \begin{pmatrix} k_1 \\ k_2 \end{pmatrix} = \begin{pmatrix} \Sigma x_1 \\ \Sigma x_2 \end{pmatrix} \quad (9.10).$$

The matrix equation *9.10* was solved by finding the inverse of matrix A to provide the equation $z = A^{-1}b$, where z gives the values of k_i (i = 1, 2). In practice, equation *9.10* was solved by using the matrix commands of Basic language.

The goodness of the fit to the threshold data was estimated by calculating the variance of the observed data from the predicted data and expressing this as a proportion of total variance. This is usually expressed as the percentage of variance explained by multiplying it by 100. The proportion was calculated using the following equation:

$$r^2 = 1 - \Sigma(\log Th - \log Th_{est})^2 / \Sigma(\log Th - Z)^2 \qquad (9.11),$$

where $Z=n^{-1}\Sigma \log Th$. The values of Th_{est} were calculated by means of equation *9.01*. It is necessary to use logTh rather than Th, because thresholds are plotted on a logarithmic scale.

When the value of p was 0.5, the explained variance (r^2) was at maximum (93%). At this value k_1 and k_2 were 0.5072 and 7.341, respectively. Thus $Th_{min} = k_1^{1/p} = 0.257$ deg and $Lc = k_2/k_1 = 14.5$ min.arc.

According to equation *4.09*, $L_s = L / (1+ E/_{1.95^\circ})$, where L is line length in min.arc, E is eccentricity in deg of visual field. Hence, equation *9.03* becomes

$$Th = 0.257^\circ [1 + 14.5' L^{-1} (1+E/_{1.95^\circ})]^2 \qquad (9.12).$$

As shown by *Figure 9.02e*, equation *9.12* predicts orientation discrimination threshold in angular terms for all subjects, eccentricities (0 - 15 deg), and line lengths.

9.4: Discussion

The results demonstrate that foveal and peripheral orientation discrimination can be made equivalent simply by magnifying peripheral stimuli by an appropriate amount. This is consistent with what has come to be known as the general magnification theory (Virsu, Näsänen & Osmoviita, 1987), the validity of which has been demonstrated for a wide variety of spatiotemporal visual tasks (Rovamo & Virsu, 1979; Johnston & Wright, 1986; Watson, 1987; the previous experimental chapters). By the use of the spatial scaling method angular orientation discrimination thresholds, when plotted as a function of line length, produce functions of the same shape in foveal and peripheral vision, the only difference being a regular magnification increment from one eccentricity to the next.

The rate at which magnification needs to increase in order for orientation discrimination thresholds to remain constant in the periphery is defined by the parameter E_2, which was found to be 1.95 deg. The lower the value of E_2 the faster the rate at which stimulus size must increase in the periphery in order to retain performance equivalent to that at the fovea. In

the chapters thus far, E_2 values have varied enormously between tasks, from as low as 0.1 deg for bisection acuity to over 15 deg for unreferenced movement detection. The present E_2 for detecting the orientation of tilted lines is similar to that for both line and two-dot vernier acuity (*Chapter 5*), which makes it interesting to consider whether these different stimulus configurations are simply measuring the same visual capacity (Sullivan, Oatley & Sutherland, 1972; Westheimer, 1981). There are obviously important differences between these configurations. For example, the sudden step at the intersection of an abutting vernier target renders such a stimulus broad-band in the orientation domain. On rare occasions (for the largest line stimuli), the step itself is resolved at the intersection of the two line components, and the task tends to be performed by this very localized cue. In general, however, the subjective impression is that the vernier judgement is based on the overall orientation of the entire line. Therefore, the overriding connection between them may still be one of orientation analysis.

The scaling of the present data is at odds with the findings of Vandenbussche *et al.* (1986, see *Figure 9.01*) and Spinelli *et al.* (1984) who found that an increase in magnification could not equate orientation performance in the fovea and periphery. However, Vandenbussche *et al.* (1986) used an extremely low stimulus luminance (0.14 cd m^{-2}) combined with a constant 0.25 deg line width at all eccentricities, which could explain why their optimum orientation discrimination thresholds were 1 - 2 deg at the fovea, and even larger in the periphery. Spinelli *et al.* (1984) were performing a somewhat different task to the present one. Instead of measuring orientation discrimination, they used a method of adjustment to investigate the ability to match the orientation of a peripheral grating with that of a foveally presented reference grating. Despite magnification of the peripheral stimuli, performance still became worse with increasing eccentricity. Peripheral contrast sensitivity for Gabor patches (Watson, 1987) and moving sine wave gratings (Koenderink, Bouman, Bueno de Mesquita & Slappendel, 1978c) at *low* spatial frequencies can not be equated with that at the fovea, which would be consistent with the finding of Spinelli *et al.* (1984). Given the importance of this finding, it should be confirmed using a forced-choice spatial scaling technique.

Westheimer (1982) also measured orientation discrimination as a function of eccentricity, although a method of spatial scaling was not used. His thresholds were considerably lower than the present ones both at the fovea and in the periphery probably due to the binocular viewing as opposed to the monocular observations in the present experiment. In *Figure 9.04* thresholds from subject GW, which represent the 75% correct response level, have been converted (Elliot, 1964) to correspond the present data obtained at 80% correct level. When the spatial scaling technique was used (as in *Figures 9.03b-d*) to find E_2 values for his data, the values were entirely consistent with the present ones, E_2 values being 2.28 ($\pm$ 0.38) deg for subject GW and 1.85 ($\pm$ 0.10) deg for subject SR.

1000

Figure 9.04: Orientation thresholds from the present study for subject PM and of Westheimer (1982) study for subject GW compared. Thresholds of GW are consistently lower at each eccentricity, probably due to binocular viewing. Open symbols, PM - filled symbols, GW.

Figure 9.05: Orientation thresholds from the Paradiso and Carney (1988) study and for comparison, 10 deg eccentricity function for subject PM, present study. Note that the present thresholds are clearly lower.

Paradiso and Carney (1988) also present orientation discrimination data as a function of line length at the fovea and at several different eccentricities up to 50 deg, threshold functions up to 20 deg eccentricity, combined from two observers, are presented in *Figure 9.05*, threshold level of 75% has been converted to 80%. Thresholds are higher than in the present study, which is easily seen from the 10 deg eccentricity threshold function of PM (included for comparison only). Viewing was monocular, without references, the task was to indicate which of the two sequentially presented lines was not vertical. It is possible that this type of comparison increased thresholds since, according to Heeley and Buchanan-Smith (1990) orientation acuity decreases about 50% when the observers are made to base their judgements on the orientation differences between the two stimuli on every trial, rather than using a recognition process that is calibrated against an internal standard. In agreement with the present findings, sufficient magnification of peripheral stimuli resulted in performance similar to that at the fovea and, in addition, a similar inverse dependency of threshold against line length was found. In order to scale their data Paradiso and Carney (1988) used an E_2 of 0.77 deg, as suggested for vernier acuity by Levi, Klein and Aitsebaomo (1985). However, an examination of their data suggests that scaling with our mean E_2 estimate (1.95 deg) would have provided a better fit, and scaling the data with the present method (only the eccentricities shown in *Figure 9.05* included) actually results in an E_2 of 2.4 deg. The inadequate foveal function at short line lengths inevitably introduces some uncertainty into this estimate.

Several important findings emerge from equation *9.12*. Firstly, Th = 0.257 deg for very long lines, in agreement with the low angular thresholds found at the fovea by Andrews (1967), Andrews, Butcher and Buckley (1973) for long lines and Watt (1987) for referenced thin lines. Other studies have found slightly higher minimum thresholds, from 0.3 - 0.6 deg (Westheimer, Shimamura & McKee, 1976; Burbeck & Regan, 1983; Beck & Halloran, 1985; Morgan, 1986; Paradiso & Carney, 1988; Regan, 1989; Heeley & Buchanan-Smith 1990; Skottun, Bradley & Freeman, 1986; Spinelli *et al.*, 1984) up to 1-2 deg (Vandenbussche *et al.*, 1986), as mentioned in *Chapter 2.4.5*.

Equation *9.12* also predicts that Th = 1.03 deg at the critical line length (14.5 min.arc at the fovea). Note that these two threshold values are independent of eccentricity, whereas the critical line length itself increases from 14.5 min.arc at E = 0 deg to 126 min.arc at E = 15 deg.

Another prediction of the equation regards the lower limit of orientation discrimination. This occurs when the angular threshold reaches 45 deg, since it implies that a line tilted 45 deg clockwise from vertical can just be discriminated from a line tilted 45 deg anti-clockwise. Hence, the angle between the two is 90 deg, which is the maximum possible difference in orientation between two crossed lines. At the fovea, this angular threshold corresponds to a

line length of 1.19 min.arc according to the equation *9.12*. This represents the shortest theoretical line length for which orientation discrimination should be possible. An experiment was performed to obtain a direct measure of the minimum line length at which two perpendicular lines could be discriminated at the 80% correct level. This produced values of 1.45, 1.43 and 1.59 min.arc for DW, PM and KL respectively. This difference between observed and predicted minimum line length demonstrates a failure of the model at very short line lengths which is probably due to the detrimental effect caused by optical blur.

Andrews (1967) derived an ideal detector model to explain his foveal orientation discrimination data. According to his model the logarithm of the angular threshold should decrease with a slope of -1.5 as a function of logarithmic line length. This prediction fits the observed data well at short line lengths, but at longer line lengths the slope of decrease in thresholds in his study is -0.5. Our model is different from that of Andrews (1967) in that the slope of decrease varies from -2 at very short line lengths to 0 at very long line lengths. This explains why Andrews managed to fit his experimental data reasonably well using two intersecting lines with slopes -1.5 and - 0.5.

E_2 values vary enormously from one task to another as the experimental chapters thus far have shown. However, it is likely that tasks which rely upon similar neural mechanisms display similar E_2 values. Conversely, it could be argued (Toet & Levi, 1992) that tasks which display similar E_2 values are mediated by the same neural structures, thereby providing some hints as to the properties of the neural processor used. For example, tasks such as vernier acuity (E_2 = 1 - 2 deg) and curvature detection (E_2 = about 2 deg, Whitaker, Latham, Mäkelä & Rovamo, 1993) may be based upon a simple process of orientation discrimination and thereby should demonstrate similar peripheral gradients to those found in the present chapter.

In summary, orientation discrimination thresholds were measured at the fovea and in the periphery using a method of spatial scaling. Foveal and peripheral functions relating orientation thresholds to line length differed simply by a change of scale or magnification. The data predict that the eccentricity at which stimulus size must double to produce a level of orientation discrimination equal to that at the fovea is 1.95 deg. By combining data from all observers, an equation was developed which allows to predict orientation discrimination thresholds for an average observer over a range of different eccentricities and line lengths. For any given eccentricity, the equation makes important predictions regarding the minimum threshold for orientation discrimination and the shortest line length at which orientation discrimination is possible.

Chapter 10: The effect of eccentricity on simultaneous performance in two separate tasks

10.1: Introduction

Experiments in this thesis so far have been involved in quantifying the spatial scale of the visual system for various individual tasks. The findings can be summarized by stating that the rate at which peripheral stimuli need to be increased in size to maintain foveal performance levels varies enormously between tasks. The experiment in this chapter is designed to test one possible reason for this phenomenon.

It is quite surprising that such diverse peripheral gradients exist in a visual system which is commonly thought of as comprising several sequential, fixed stages of neural processing (retina, primary visual cortex, and beyond). It is much easier to imagine a system which consists of just a single magnification factor corresponding to the expansion of the neural site at which visual performance is limited. This was no doubt one of the attractive features of the "cortical magnification factor", which assumed that all tasks could be equated across the visual field by applying a single rate of scale change corresponding to the rate of change of neural processing machinery at the level of the primary visual cortex. It has been suggested that the diverse peripheral gradients are due to differences in the visual field coverage of many individual neural sites, each of which is the limiting stage of processing for a given task. Thus, the eccentricity dependence of the task in question reflects the weighting assigned to different parts of the visual field at the corresponding neural site involved. On the basis of the results presented so far in this thesis, a large number of such sites would be necessary. This suggestion is rather difficult to test in psychophysical experiments.

An alternative possibility is that there exists a plasticity within the neural machinery of the cortex by which the eccentricity dependent allocation of neural resources is actually varied depending on the task involved as has been suggested by Van Essen and Anderson (1990). This dynamic allocation of resources would have to be low-level since we are usually quite unaware of any conscious decision to change our attentional resources across the visual field based upon the task with which we are faced. However, this suggestion is supported by the finding that a task-dependent allocation of neural resources has actually been demonstrated by means of single cell recording in the primate visual system (Richmond, Wurtz & Sato, 1983). Further, there is considerable evidence for improvement in peripheral visual performance when attention is shifted toward the location of stimulus presentation (Beck & Ambler, 1973; Treisman & Gelade, 1980; Tsal, 1983; Kröse & Julesz, 1989; Saarinen, 1993a,b). This indicates that some dynamic allocation of neural resources must be possible in human vision, albeit in the conscious rather than the subconscious domain. However, the

studies mentioned above concentrated on shifts of attention from one visual field location to another. What the present experiments are aiming to discover is whether the distribution of attention across the visual field can change depending on the task. For example, for tasks where early detection or discrimination is vital, such as the presence of movement, attention may be distributed rather evenly across the entire field. For others, the "aperture" of attention may be concentrated close to the fovea, enabling such tasks to be performed optimally only by central fixation.

The present experiment tests i) what happens to the E_2 values of two individual tasks when they are presented simultaneously in a same location, ii) whether a shift in the allocation of neural resources can explain the diverse peripheral gradients for different visual tasks. If two tasks are chosen which demonstrate quite different peripheral gradients individually, then forcing observers to perform the two tasks simultaneously should result in the gradients becoming identical, since different distributions of neural allocation are not likely to occur for stimuli presented at the same time.

10.2: Methods

The stimuli were presented on a CRT as described in General methods. The stimuli consisted of two white square dots (luminance 40 cd m^{-2}) presented against a dark background. They were viewed in complete darkness to avoid any visible references around the stimuli. Black cardboard was used as a mask in front of the screen to hide reflections from the edges of the display. The dots were presented side by side in the upper visual field and were positioned around an imaginary, invisible isoeccentric arc in order to dissociate the effects of eccentricity and separation (see *Figure 10.01*). The size of the dots was always 11% of their separation, so that all stimuli were simply magnified versions of one another. Four separations were investigated at each of four eccentricities. Eccentricity and separation were varied by changing both viewing distance and the dimensions of the stimuli on the monitor. For the smallest eccentricity (0.267 deg) viewing distance was 17.5 m. This was reduced to 2.5 m at 2.5 deg, 1.5 m at 5 deg and 1 m at 7.5 deg eccentricity.

A stimulus sequence would proceed as follows. Firstly, a long, horizontal red fixation line (of sufficiently low luminance to avoid after-images) was presented and the subject was to fixate throughout the trial to the point determined by the middle of this line. The line then disappeared and, immediately, the first stimulus (consisting of the two dots with a given separation) appeared. After the two dots had been present for 500 msec they then disappeared. There was a 50 msec inter-stimulus interval after which the two dots reappeared, but with a different separation and in a different vertical position (see *Figure 10.01*). The subjective impression was of a vertical displacement of the stimuli, either up or

down, and a change in the spatial interval (gap) between the dots.

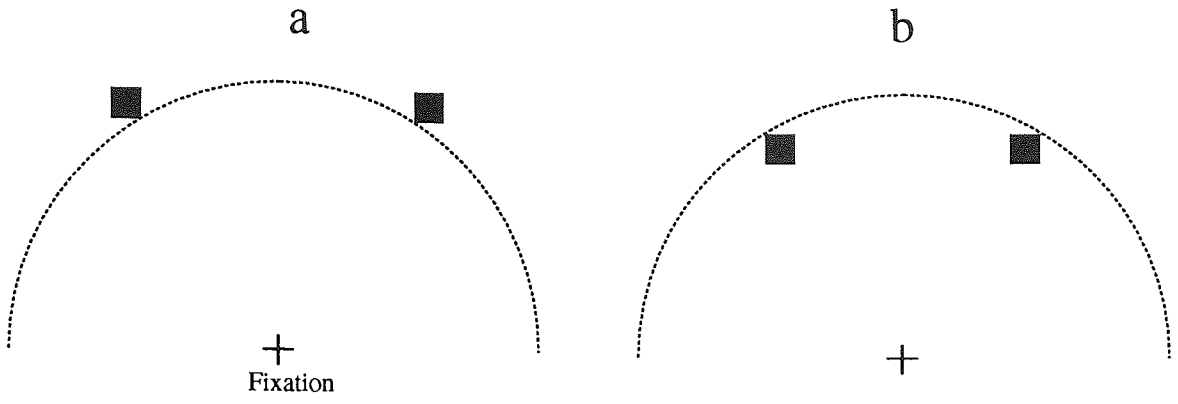

Figure 10.01: An example of the stimulus configuration, (a) first presentation, (b) second presentation. The task was to determine the positional shift of the squares either i) only in horizontal direction (separation increases/decreases), ii) only in vertical direction (dot pair up/down), or iii) judge both dimensions simultaneously.

The task of the observer was to compare the new position of the dots with those of the previous presentation. The task was performed in three ways; i) by judging only the vertical displacement of the dots (i.e. whether they had moved up or down), ii) by judging only the separation of the dots (i.e. whether the separation had become larger or smaller) or, iii) by judging both of these dimensions simultaneously (and giving two responses after each sequence, one regarding the displacement and the other regarding the change in spatial interval). Stimulus presentation was identical in all three cases.

Immediately following the observer response(s) via the keyboard the stimulus sequence began again with the presentation of the red fixation line. This continued, usually for around 60 - 80 trials until the end of the psychometric routine. Thresholds were determined using a two-alternative forced-choice technique with a modified PEST routine (Findlay, 1978) which estimated the 80% correct level for both response alternatives. When the subject was to make decisions about both the spatial interval and the displacement, two separate PEST routines were run concurrently and the whole sequence only ended when both individual routines had finished. Final threshold was accepted as the mean of at least four individual threshold estimates.

One experienced, highly trained observer (PM) and one naïve subject (AB) who underwent substantial training before data collection began, participated in the experiment. The main results were confirmed using a third experienced observer (DW). All subjects were moderately myopic ($\leq$4.50 DS) and wore their distance refractive correction throughout. All were pre-presbyopic and used their dominant eye.

10.3: Results

Figure 10.02a-d shows spatial interval thresholds for both observers for the task in which the subject made decisions only about the change in spatial interval of the stimulus. As expected, the data follow the same trend as was found in *Chapter 6*. Further, the data scale well with eccentricity and PM demonstrates exactly the same E_2 to that found in *Chapter 6* for the 50 msec inter-stimulus interval task. AB shows a slightly larger E_2, although again this accounts well for the eccentricity dependence of the data apart from a single data point representing the smallest foveal stimulus.

Figure 10.03a-d shows the data for the displacement task on its own. E_2 values for this task (which is a type of discrete displacement - see *Chapter 2, Figure 2.18*) have not been described previously in this thesis. The E_2 values of both observers are similar, and account for the eccentricity dependence of the data very well. It is important to note that E_2 values for the displacement task are much larger than corresponding values for the spatial interval task, i.e. these represent two tasks which, individually, possess quite different types of eccentricity dependence.

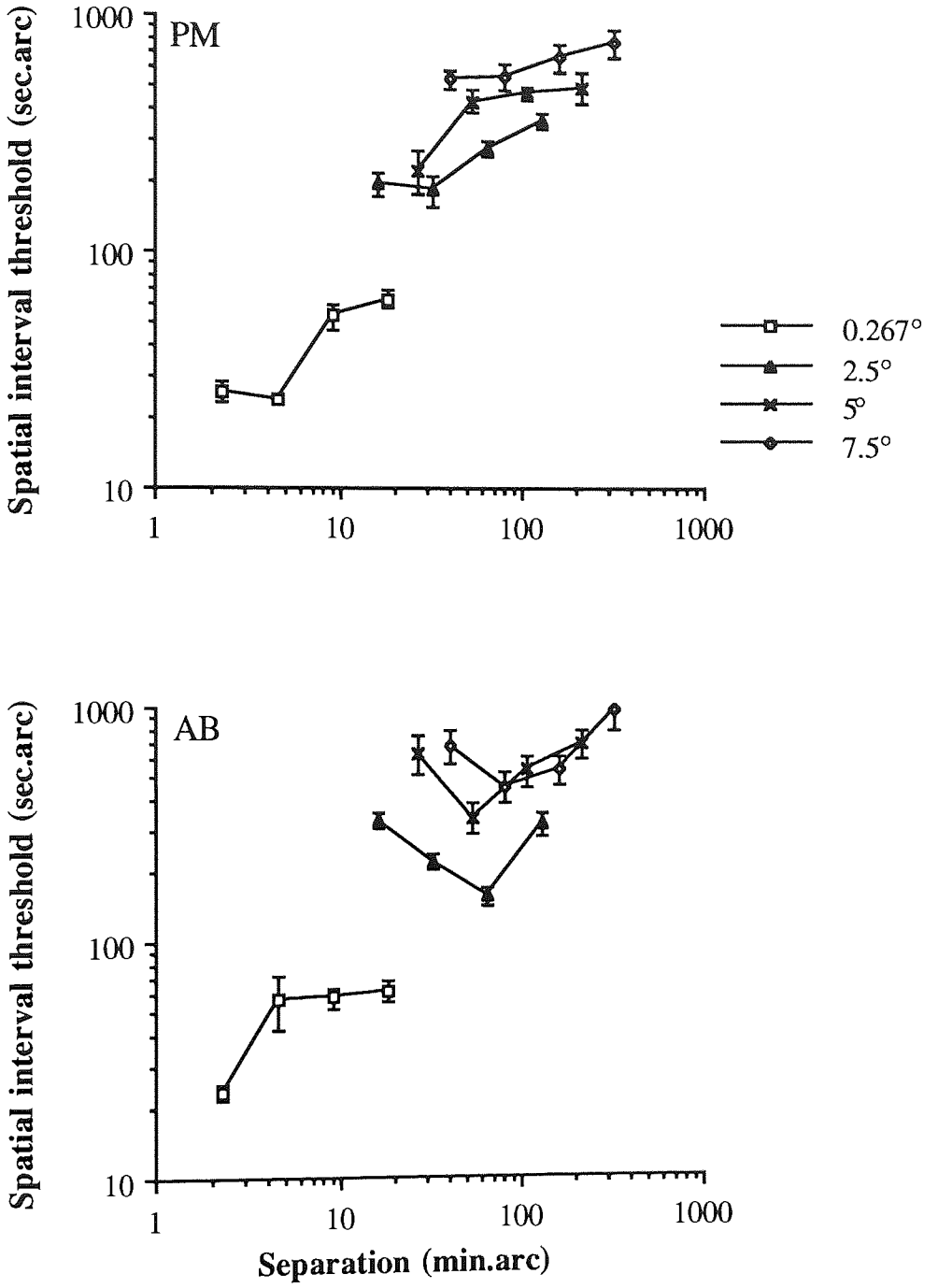

Figure 10.02a: Individual spatial interval thresholds for PM and AB plotted against separation. Different symbols represent different eccentricities, achieved by varying the radius of the isoeccentric arc and are shown, as well as the standard errors.

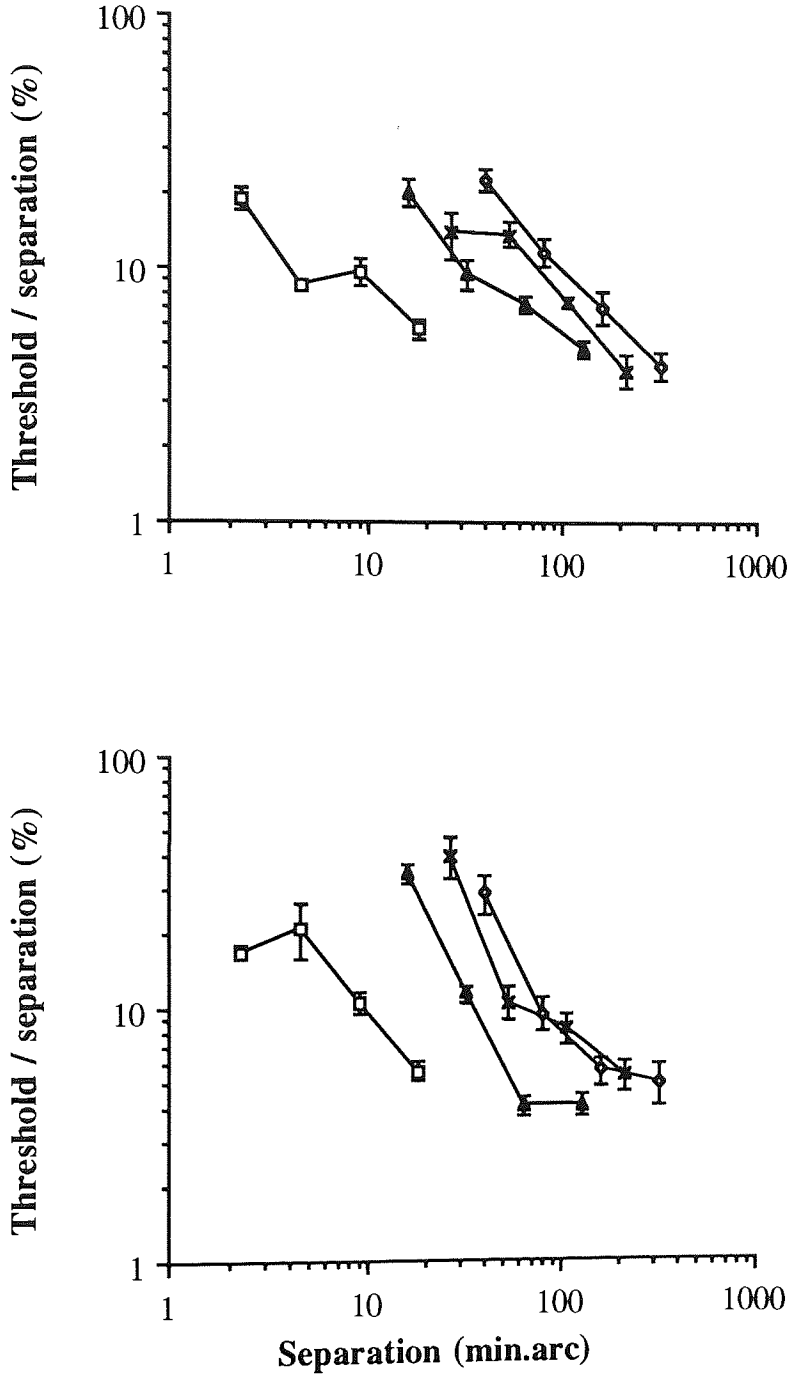

Figure 10.02b: The data replotted with threshold expressed as a percentage of separation. Symbols and subjects as in (a).

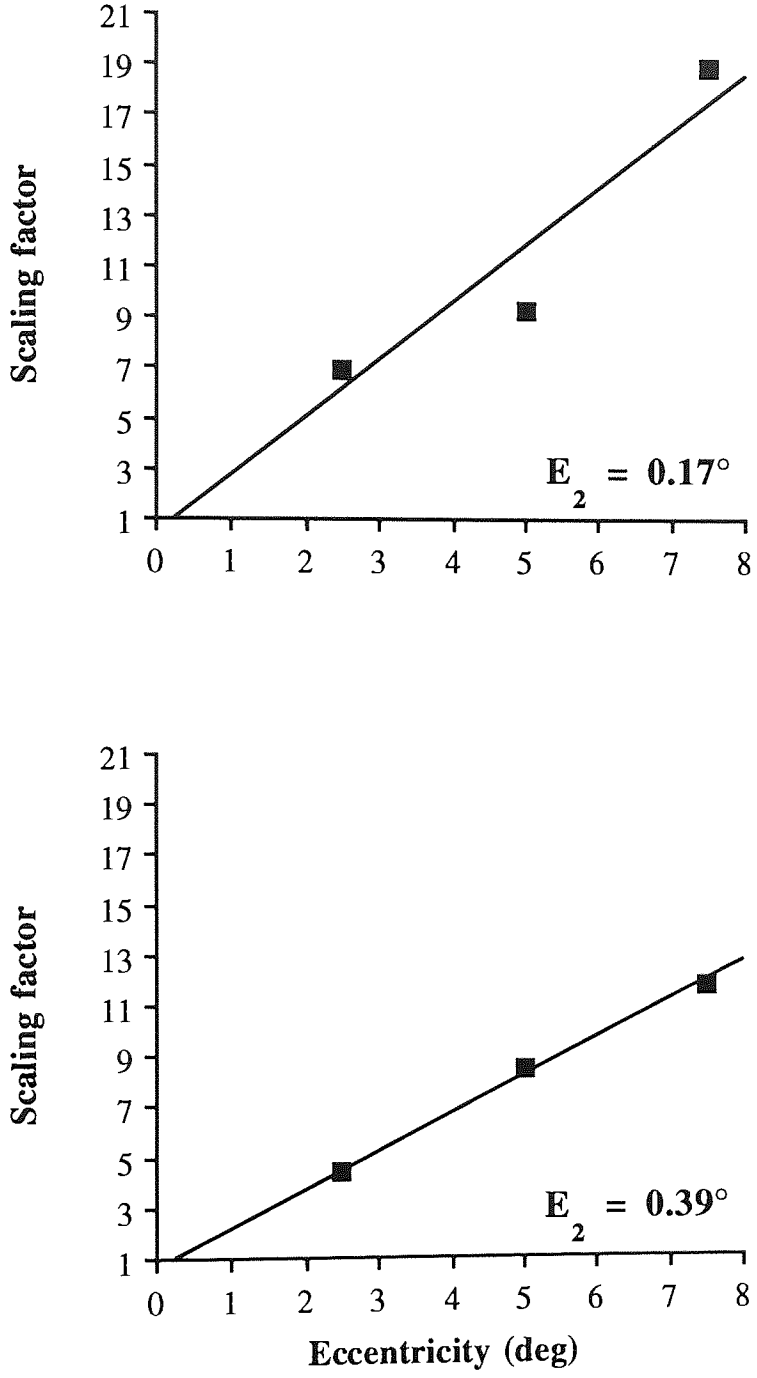

Figure 10.02c: Scaling factors obtained at each eccentricity relative to the smallest eccentricity of 0.267 deg. The line of least squares is constrained to pass through the point (0.267, 1).

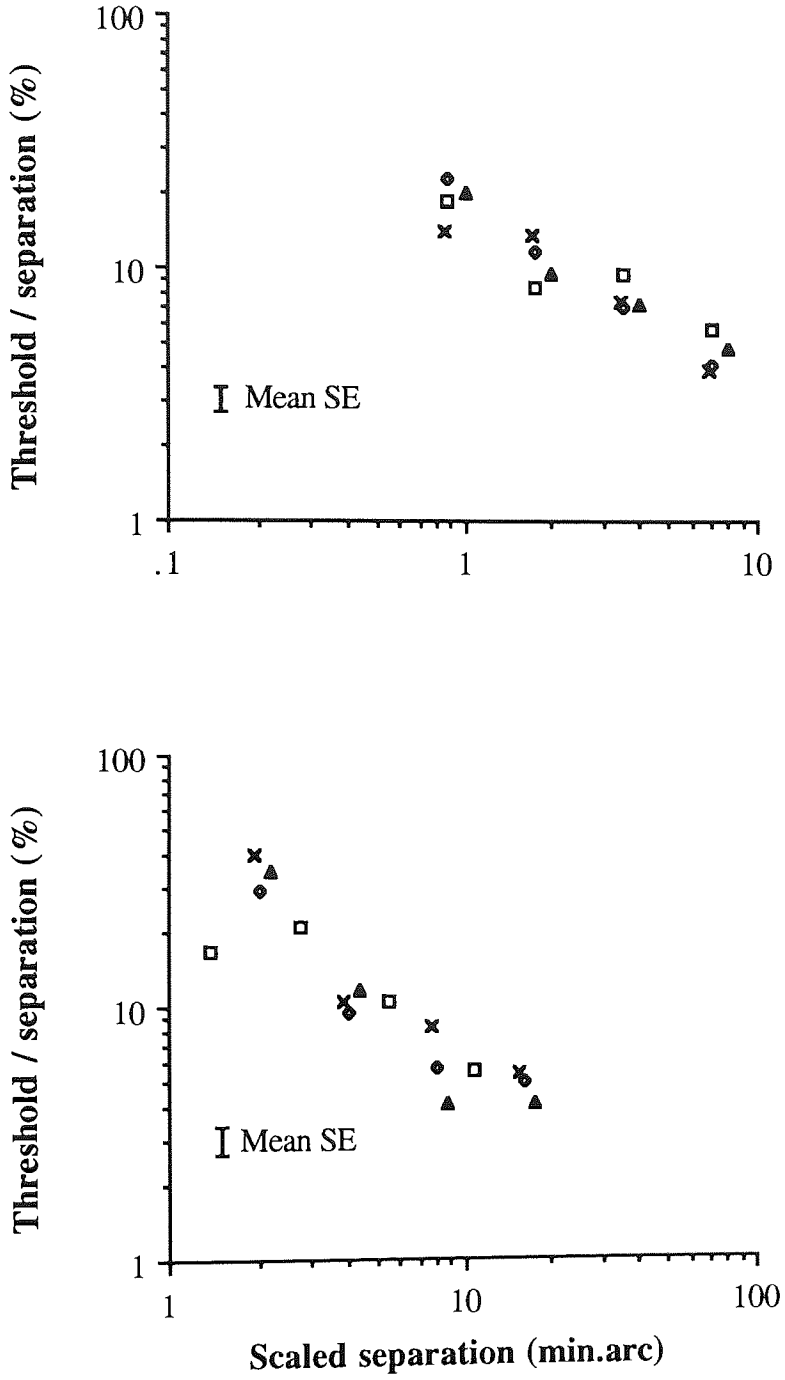

Figure 10.02d: The data of *Figure 10.02b* with the separation values at each eccentricity having been scaled along the size (x-) axis.

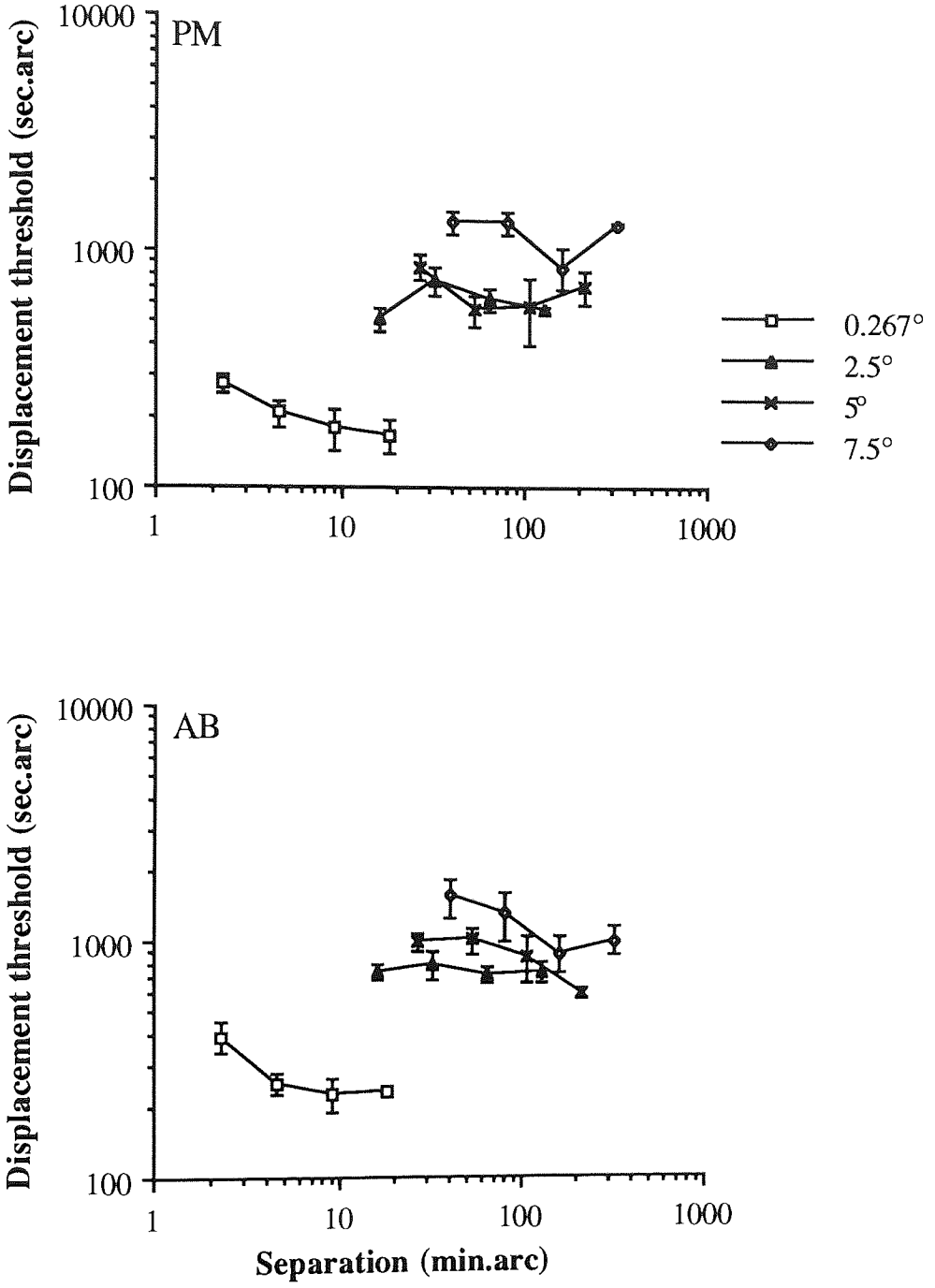

Figure 10.03a: Individual displacement thresholds plotted against separation.

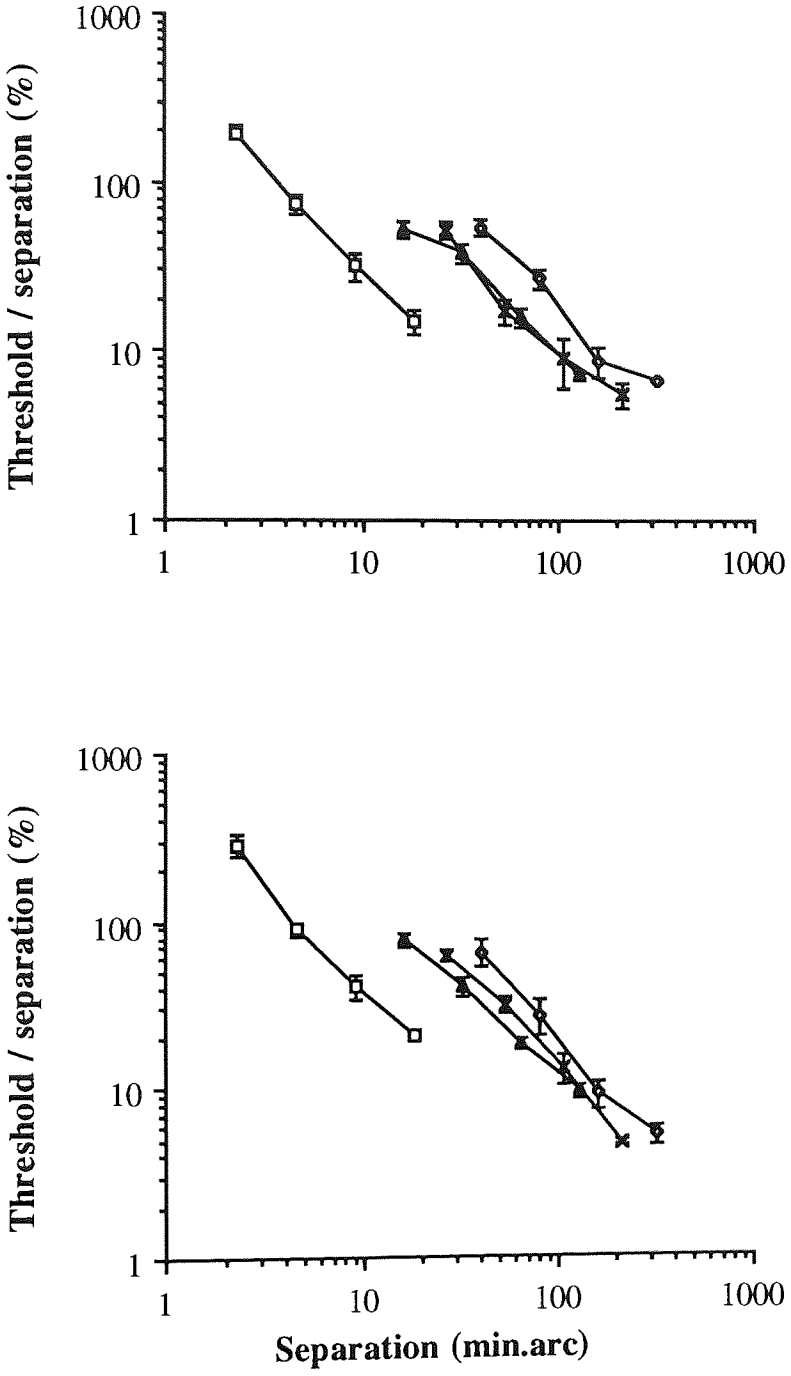

Figure 10.03b: The data replotted with threshold expressed as a percentage of separation.

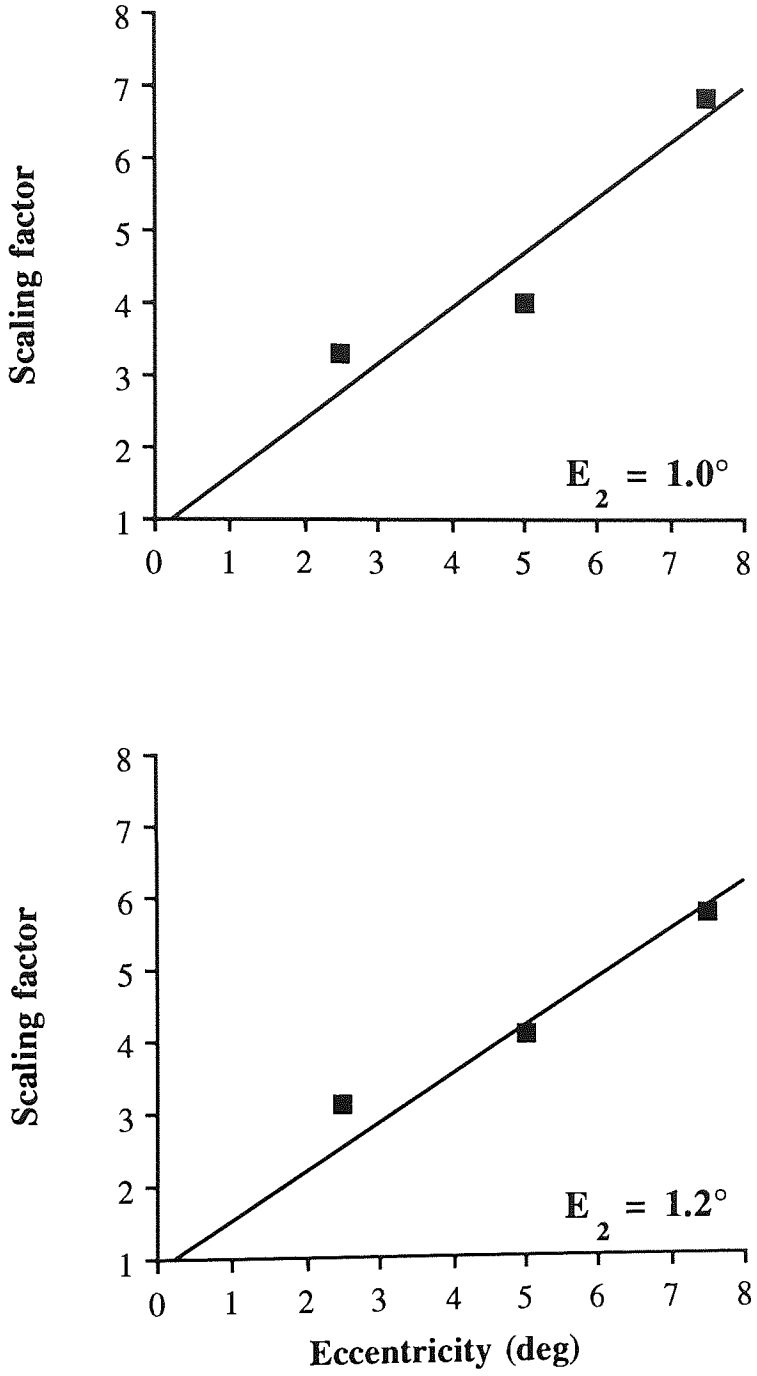

Figure 10.03c: Scaling factors obtained at each eccentricity relative to the smallest eccentricity of 0.267 deg.

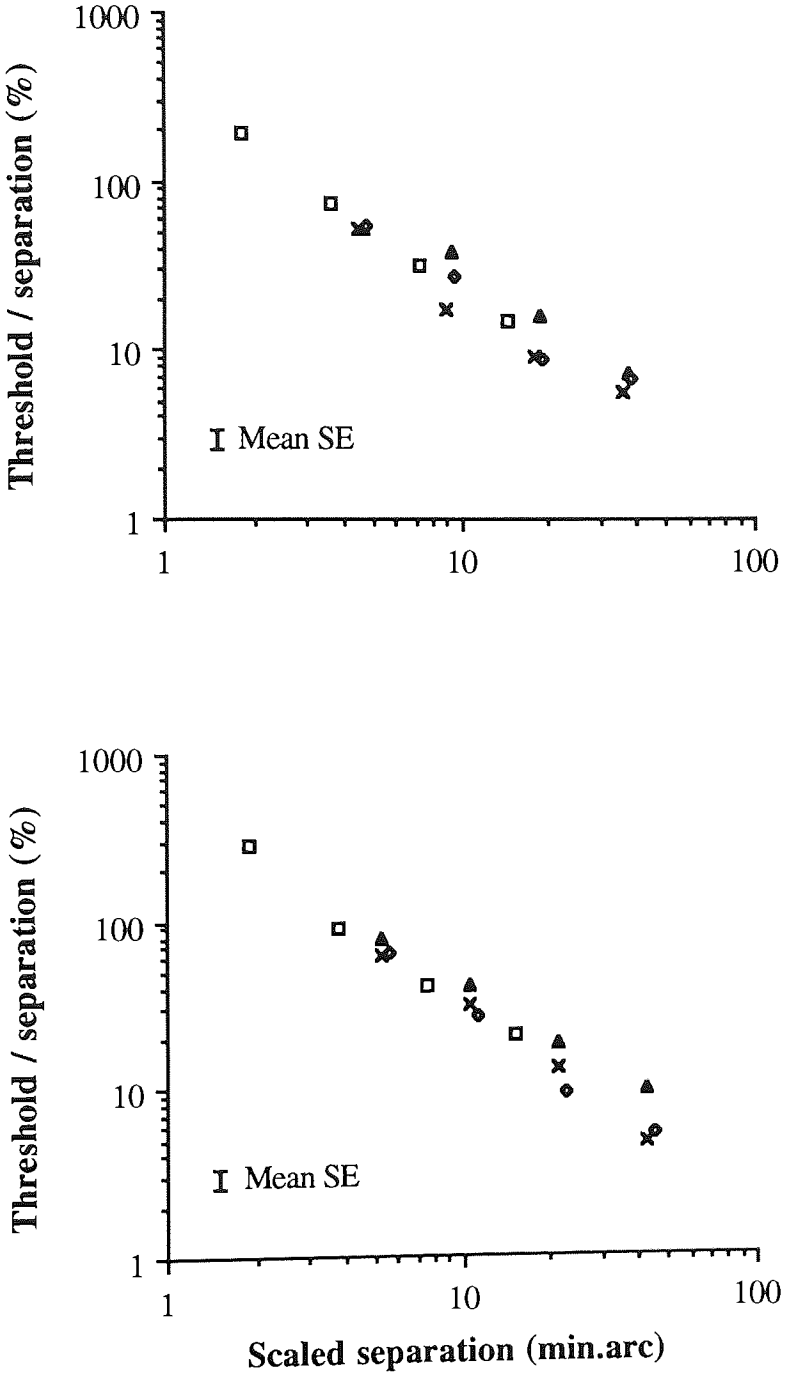

Figure 10.03d: The data of *Figure 10.03b* with the separations at each eccentricity having been scaled along the size (x-) axis.

Figure 10.04a-d shows spatial interval thresholds, but this time for the task in which spatial interval judgements and displacement judgements had to be made simultaneously. The data are remarkably similar in shape to the data of *Figure 10.02* and this is reflected in the almost identical E_2 values in the two conditions. *Figure 10.05a-d* shows the corresponding data for the task in which displacement judgements had to be made at the same time as spatial interval decisions. Again, the data of individual observers is almost identical to their data for making displacement judgements alone (*Figure 10.03*) and the E_2 values are almost exactly the same. For both spatial interval and displacement discrimination, therefore, it appears to make no difference to their eccentricity dependence (or the actual thresholds themselves) whether the tasks are performed alone or in combination with decisions about other stimulus parameters. In both conditions the E_2 values for the two tasks remain entirely different.

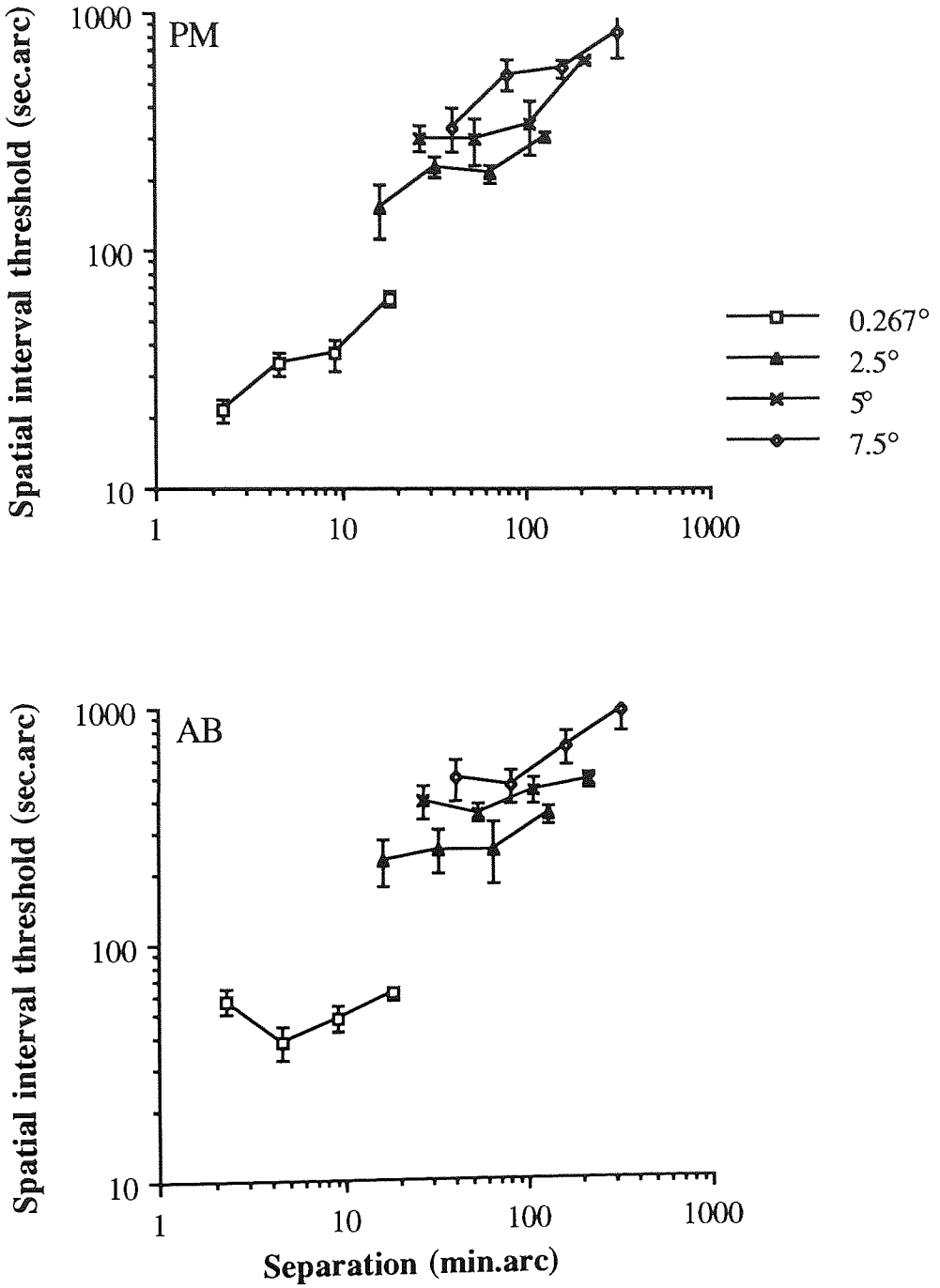

Figure 10.04a: Spatial interval thresholds obtained in combined response condition plotted against separation.

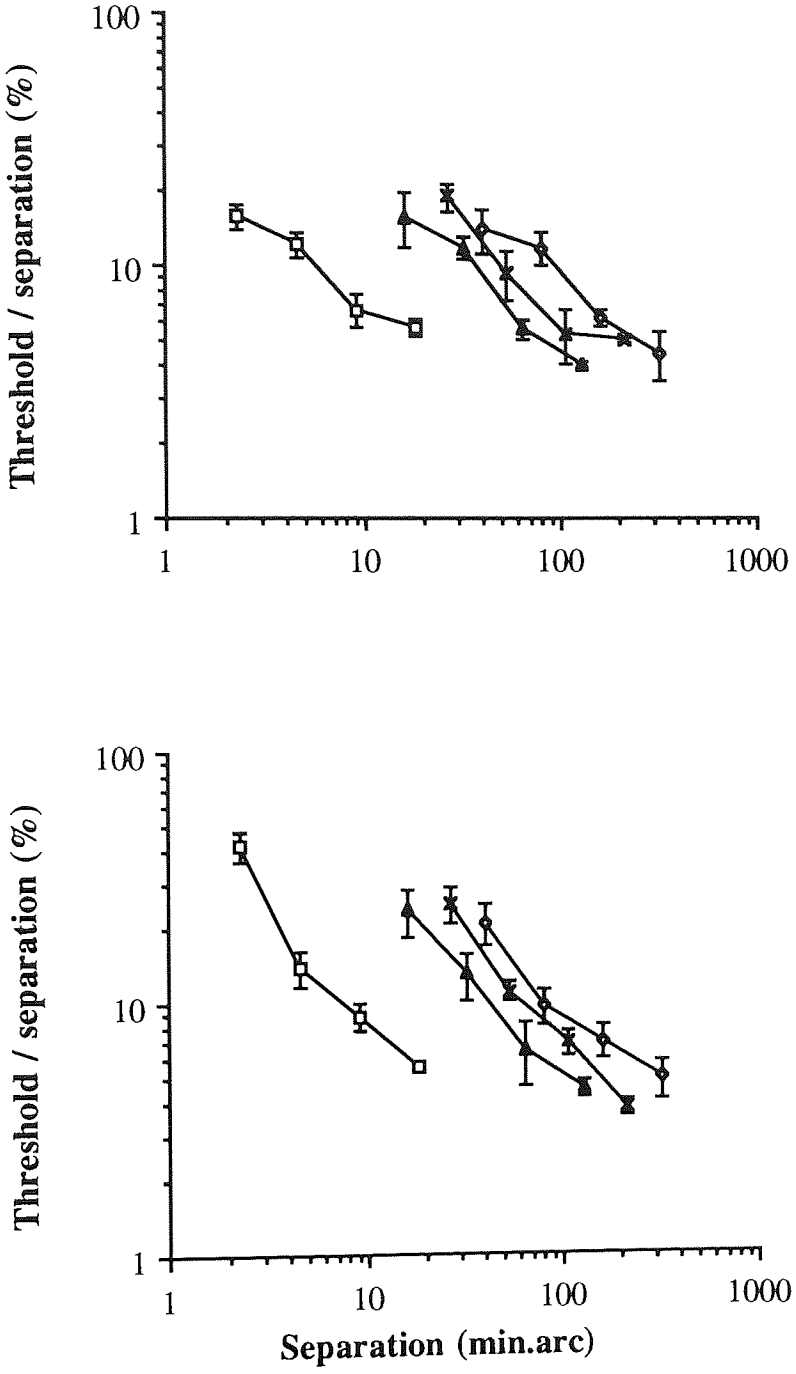

Figure 10.04b: The data replotted with threshold expressed as a percentage of separation.

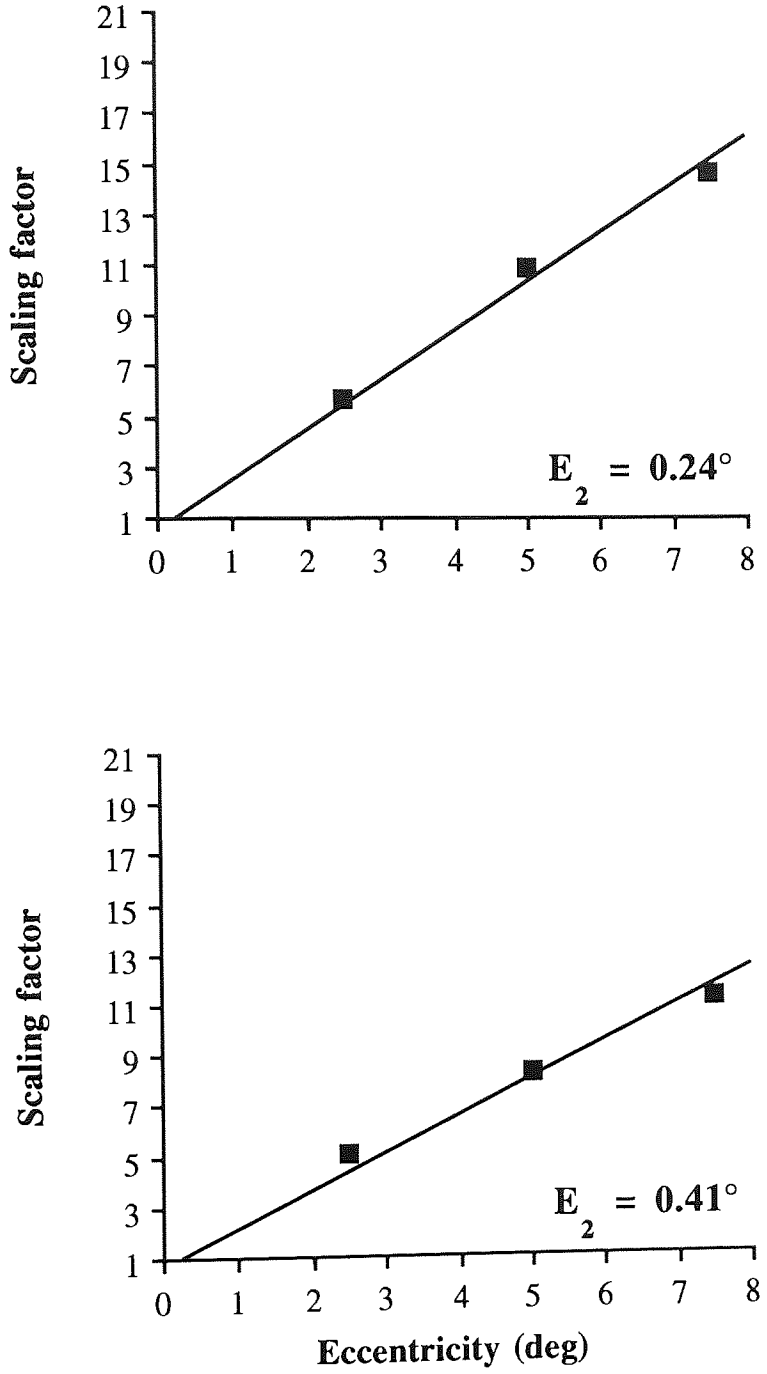

Figure 10.04c: Scaling factors obtained at each eccentricity relative to the smallest eccentricity of 0.267 deg.

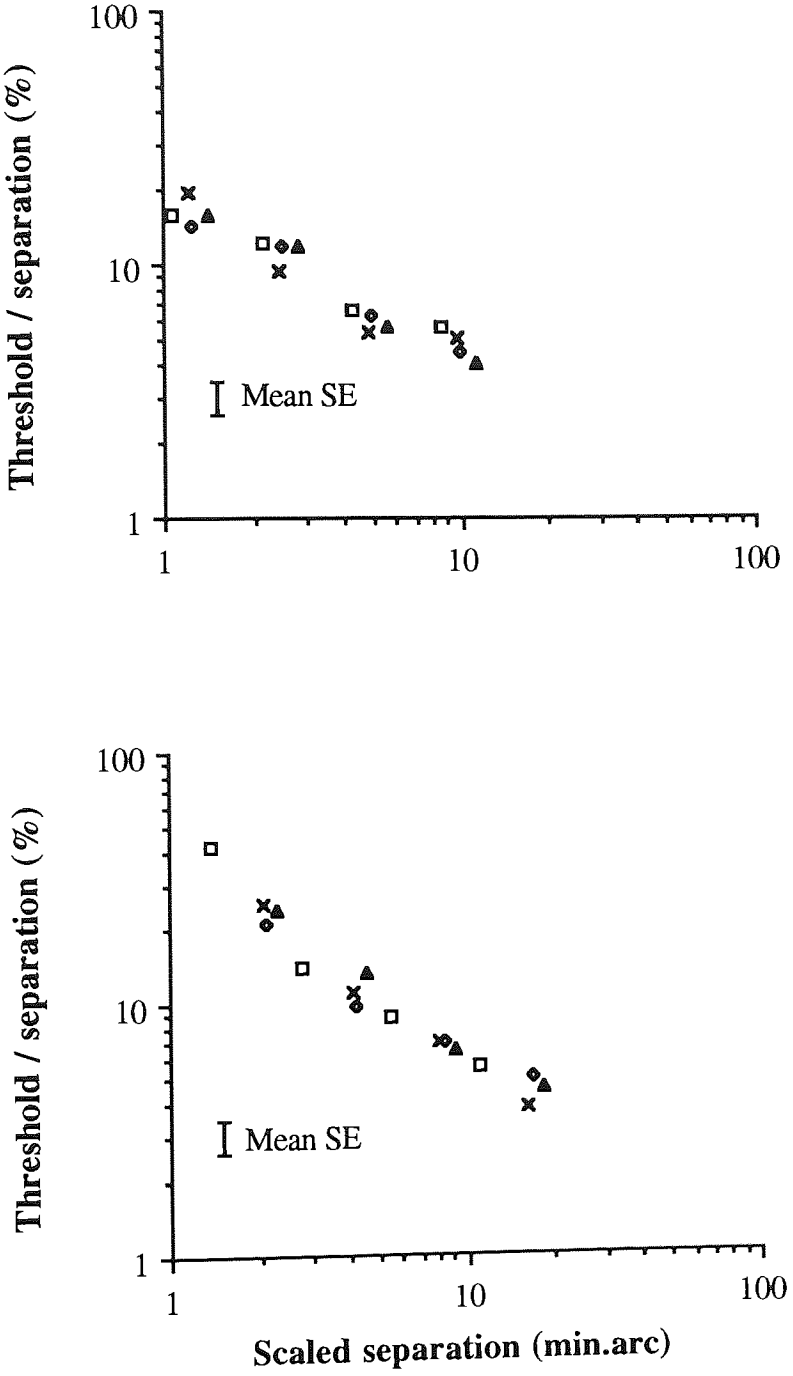

Figure 10.04d: The data of *Figure 10.04b* with the separation values at each eccentricity having been scaled along the size (x-) axis.

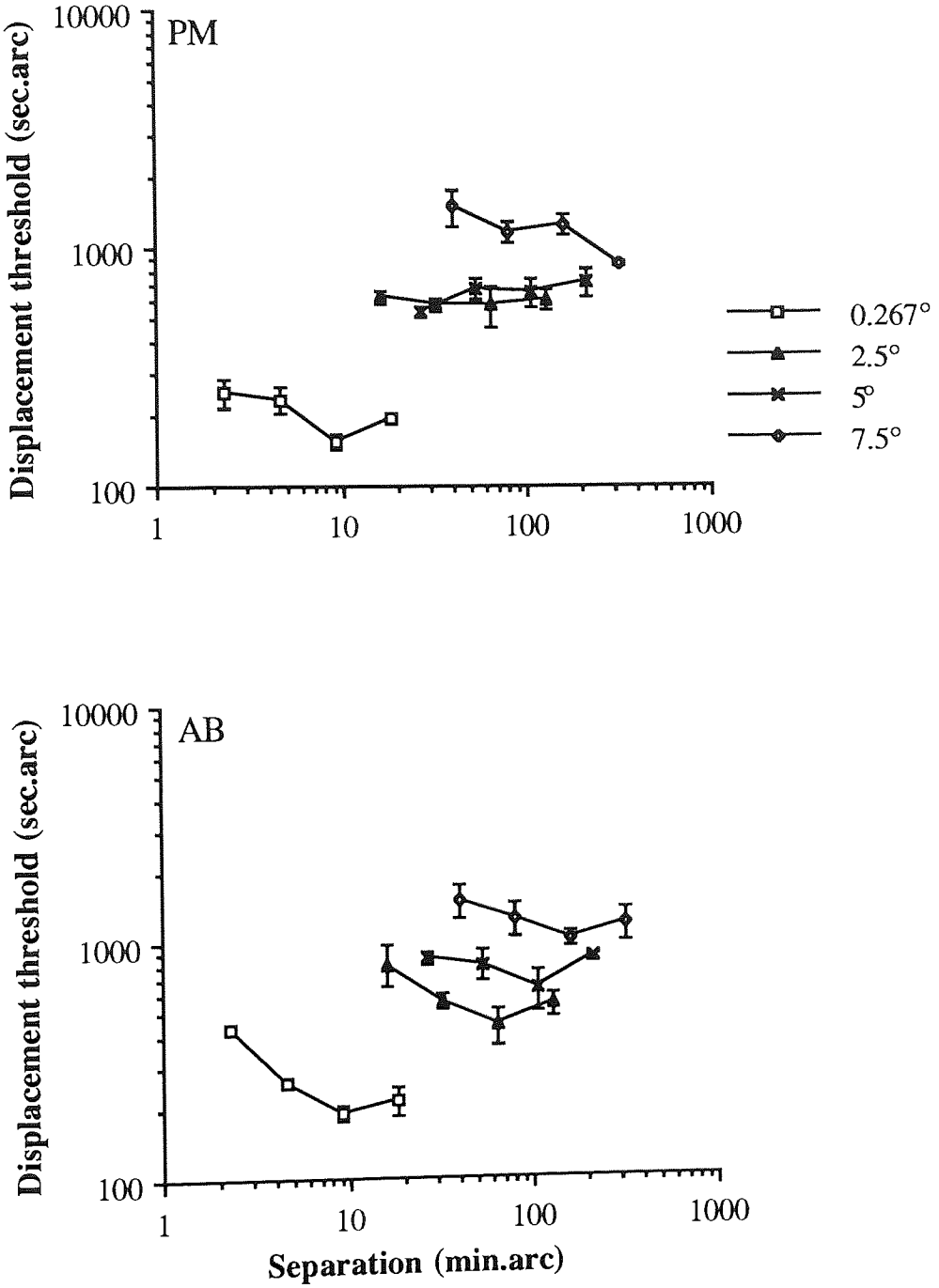

Figure 10.05a: Displacement thresholds obtained in combined response condition plotted against separation.

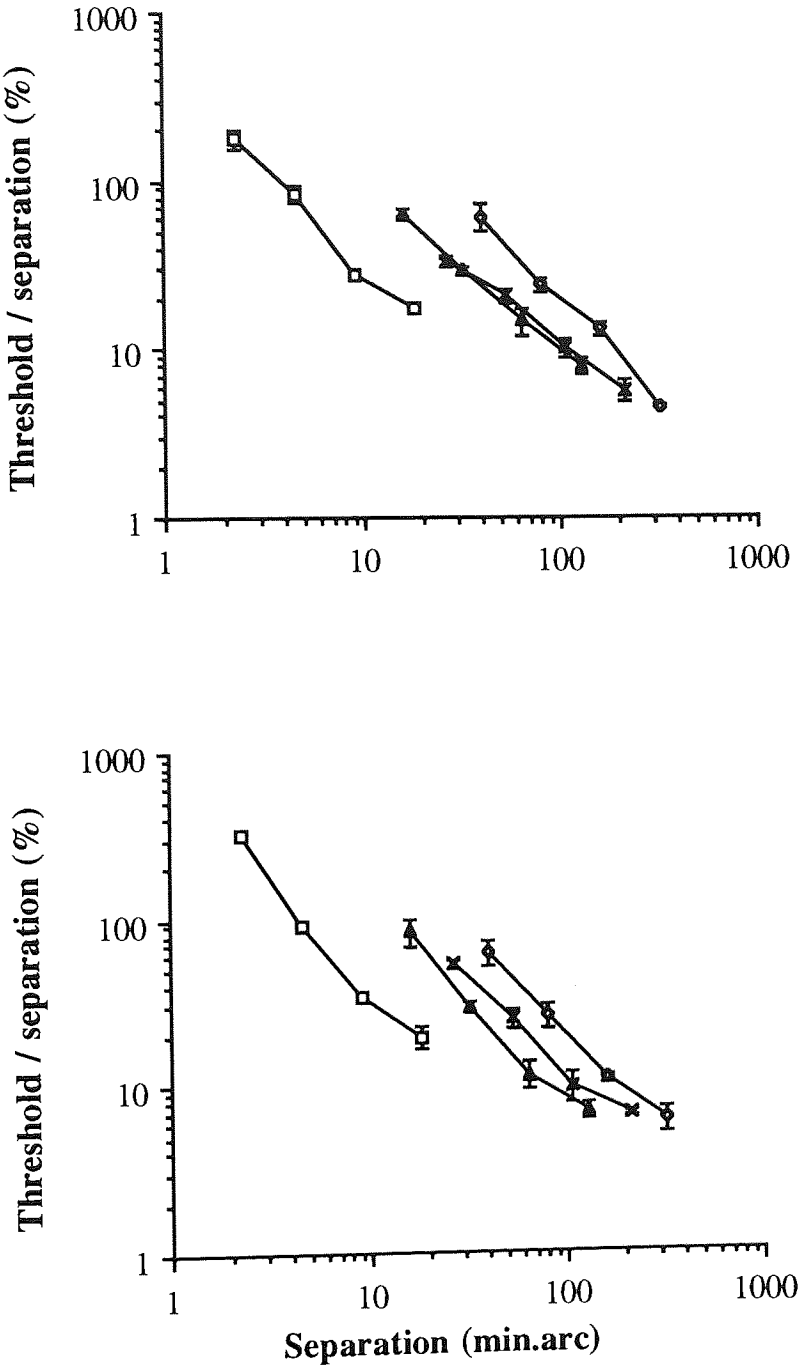

Figure 10.05b: The data replotted with threshold expressed as a percentage of separation.

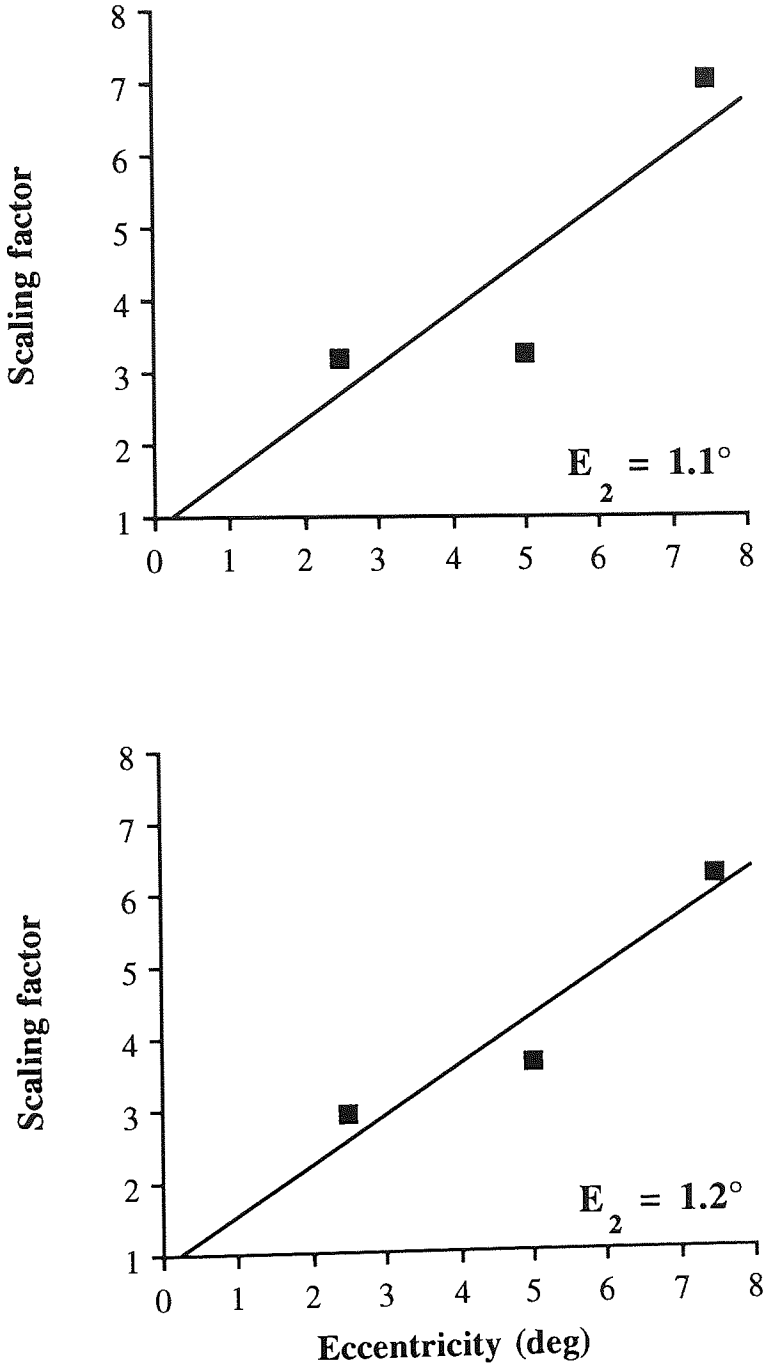

Figure 10.05c: Scaling factors obtained at each eccentricity relative to the smallest eccentricity of 0.267 deg.

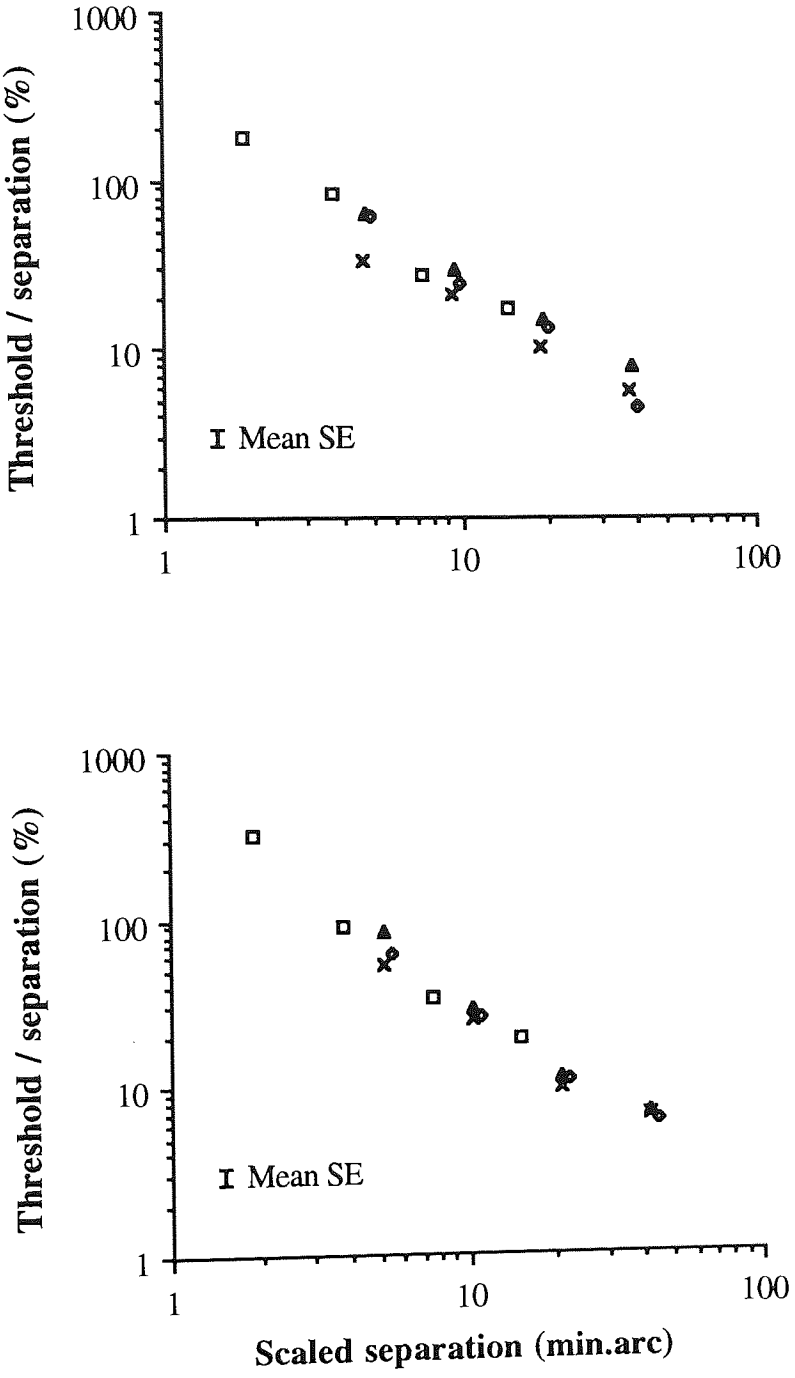

Figure 10.05d: The data of *Figure 10.05b* with the separations at each eccentricity having been scaled along the size (x-) axis.

It may be claimed that the exposure duration of 500 msec was too long, and that it may be possible that a shift of neural allocation occurred during even this short period. In other words, after making a decision regarding the change in one stimulus parameter (either displacement or spatial interval) a shift of neural allocation could occur before the second decision needed to be made. In order to test this possibility, the exposure duration of both comparison and test stimuli was reduced to 50 msec. The inter-stimulus interval remained at 50 msec. In addition, to exclude the possibility that the effective stimulus duration was increased due to the persistence of visible after-images, a post-stimulus mask consisting of a bright homogeneous field (luminance 40 cd m^{-2} i.e. the luminance of the stimulus squares) was flashed for a duration of 1 second immediately after the presentation sequence ended. This control experiment was performed by subject PM.

Figure 10.06a-d shows results with the shortened duration, for the spatial interval judgment made individually, or made in combination with a decision regarding displacement. Threshold levels and eccentricity dependence are the same in both conditions. The same data for the displacement task, either performed alone or in combination with spatial interval judgments is shown in *Figure 10.07a-d*. Again, thresholds and eccentricity dependence do not appear to show any difference depending upon whether a single or a combined decision strategy needs to be adopted. Comparison of the data obtained using the 50 msec presentation time with the corresponding data obtained from the longer exposure duration (*Figures 10.02 - 10.03*) does, however, show that thresholds are slightly higher at all eccentricities for the shorter exposure. This is to be expected given the well documented effect of exposure duration on positional thresholds (Burbeck, 1986; Watt, 1987; Burbeck & Yap, 1990c)

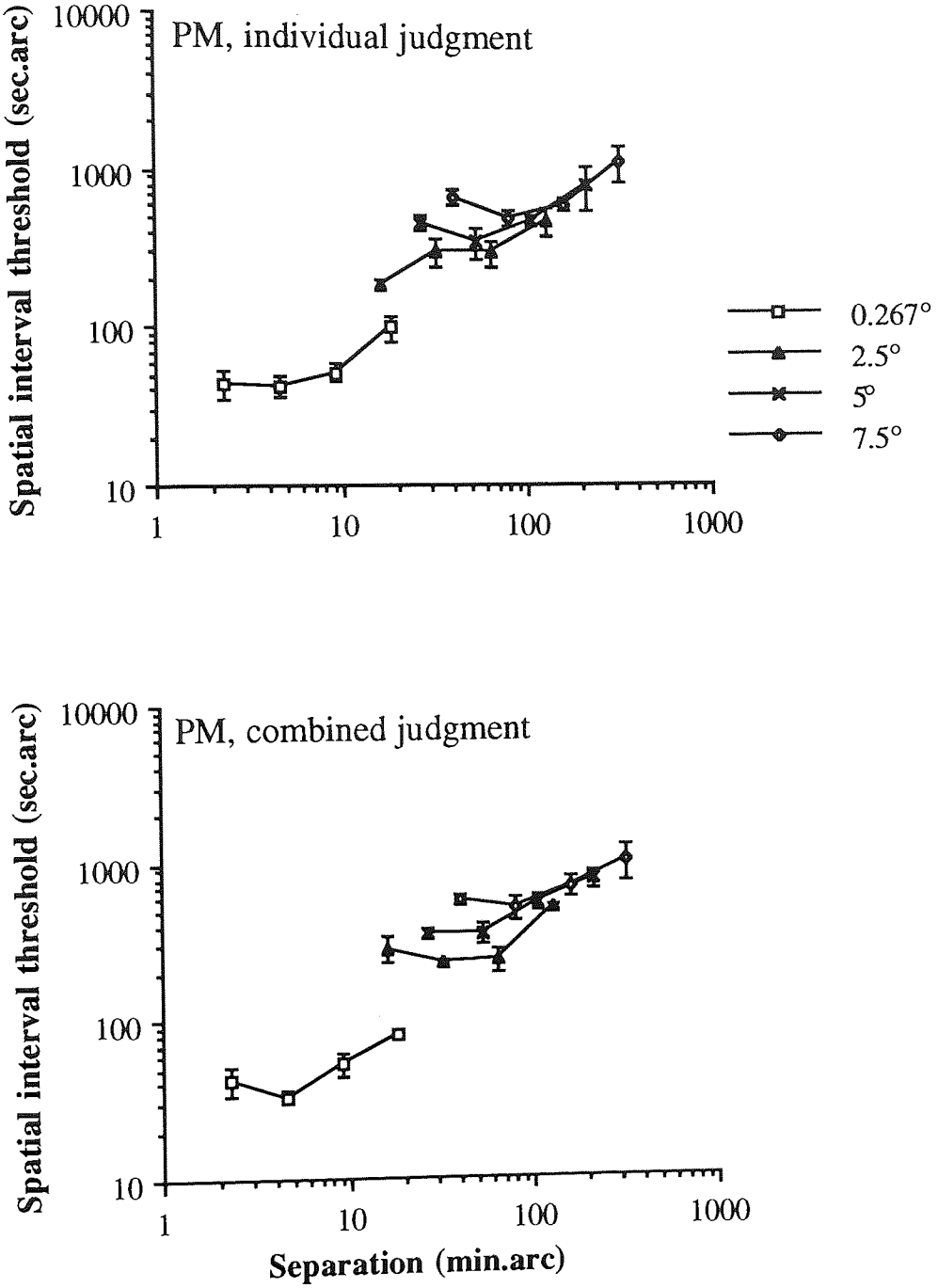

Figure 10.06a: Spatial interval thresholds obtained in individual and combined response condition plotted against separation, stimulus duration 50 msec.

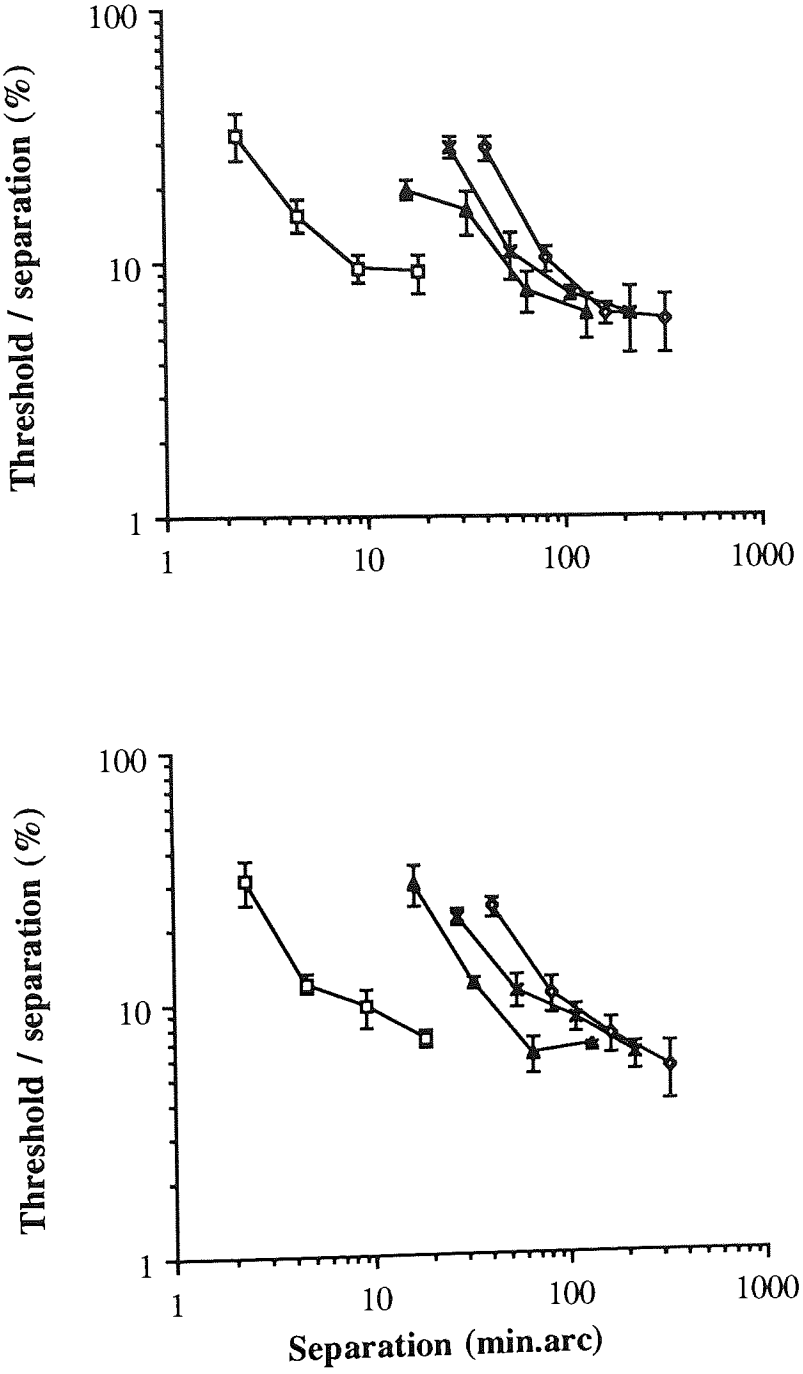

Figure 10.06b: The data replotted with threshold expressed as a percentage of separation.

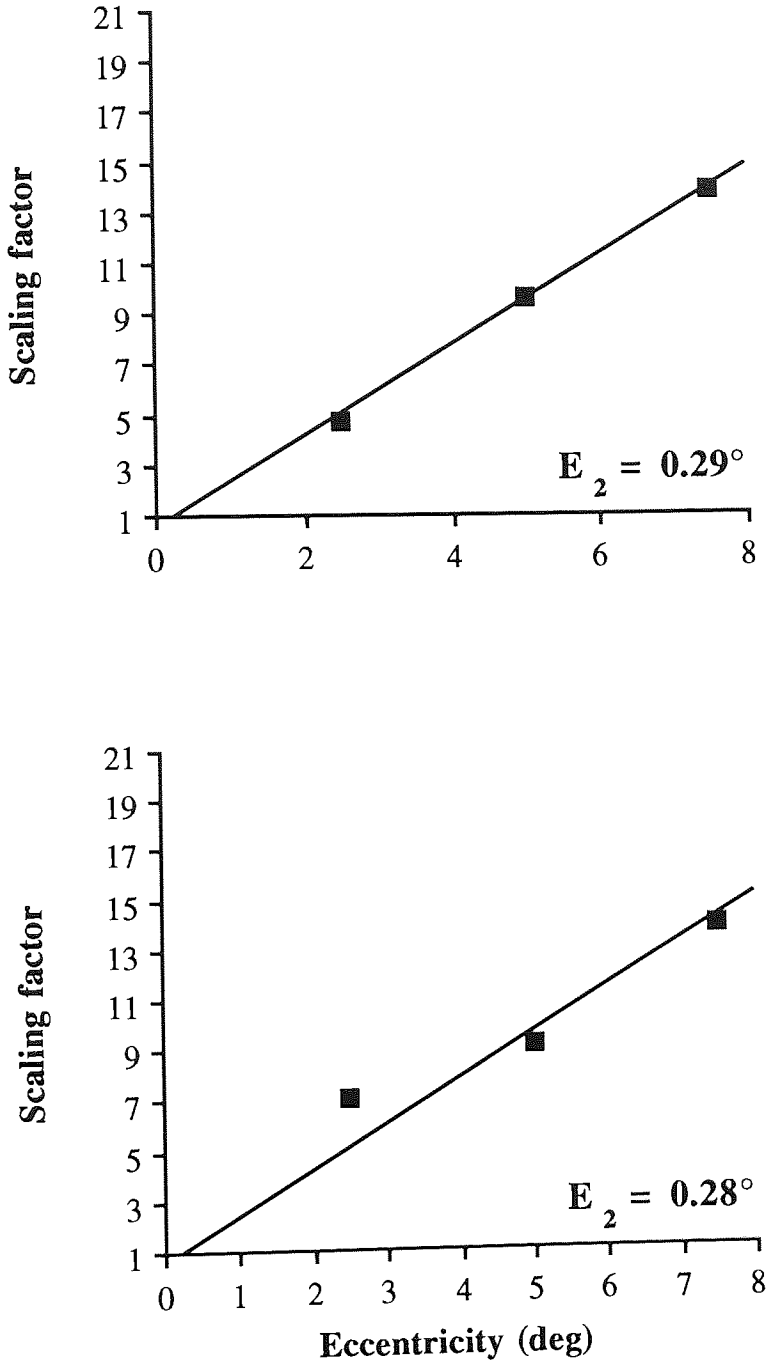

Figure 10.06c: Scaling factors obtained at each eccentricity relative to the smallest eccentricity of 0.267 deg.

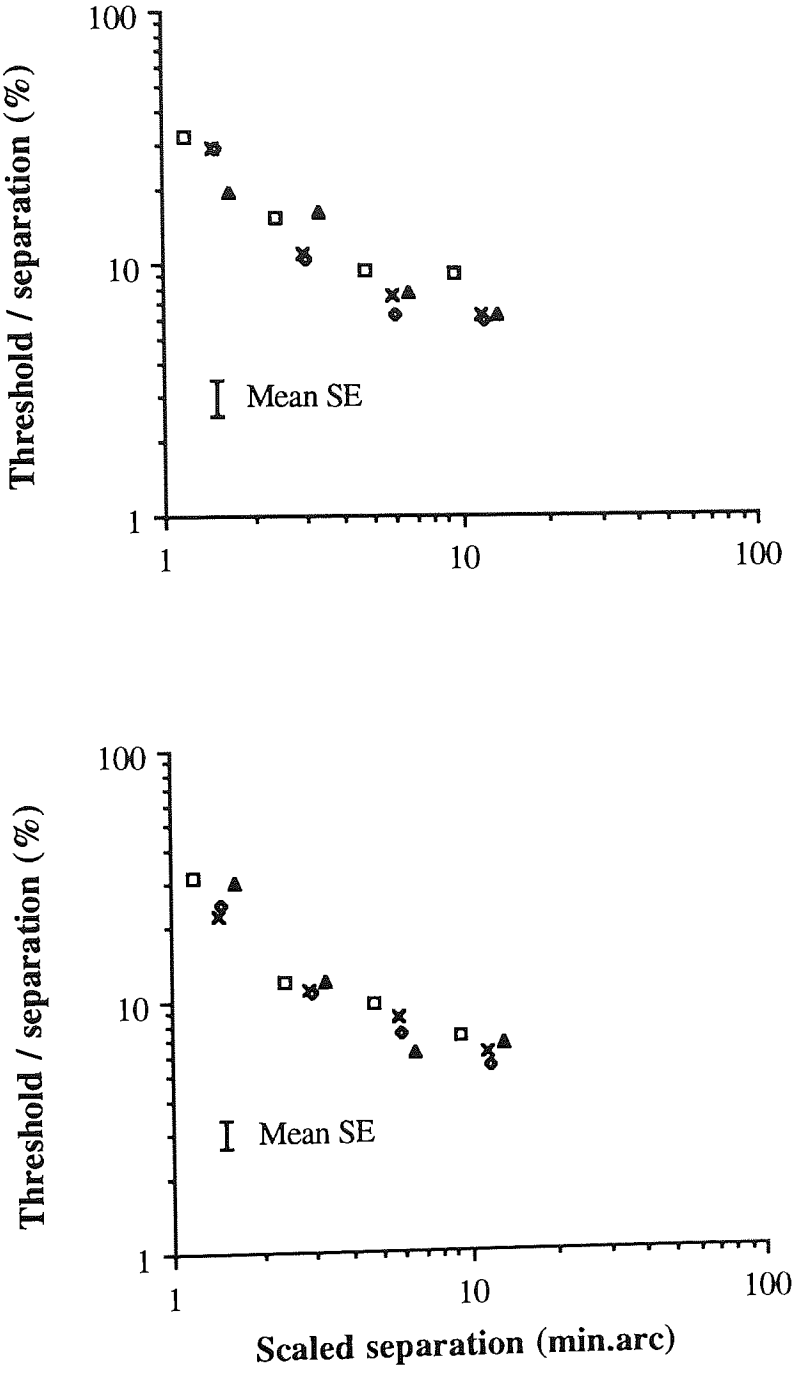

Figure 10.06d: The data of *Figure 10.06b* with the separation values at each eccentricity having been scaled along the size (x-) axis.

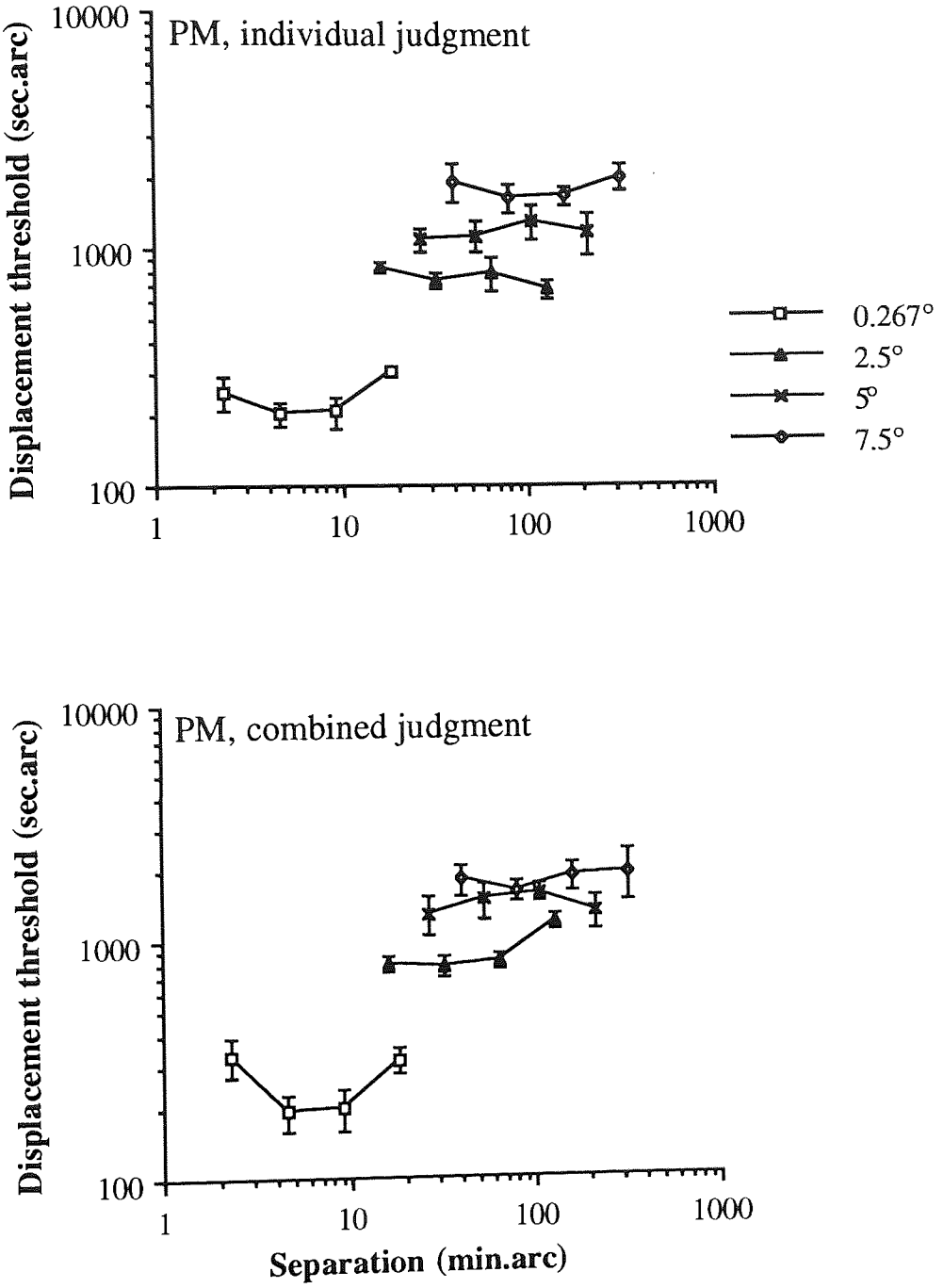

Figure 10.07a: Displacement thresholds obtained in individual and combined response condition plotted against separation.

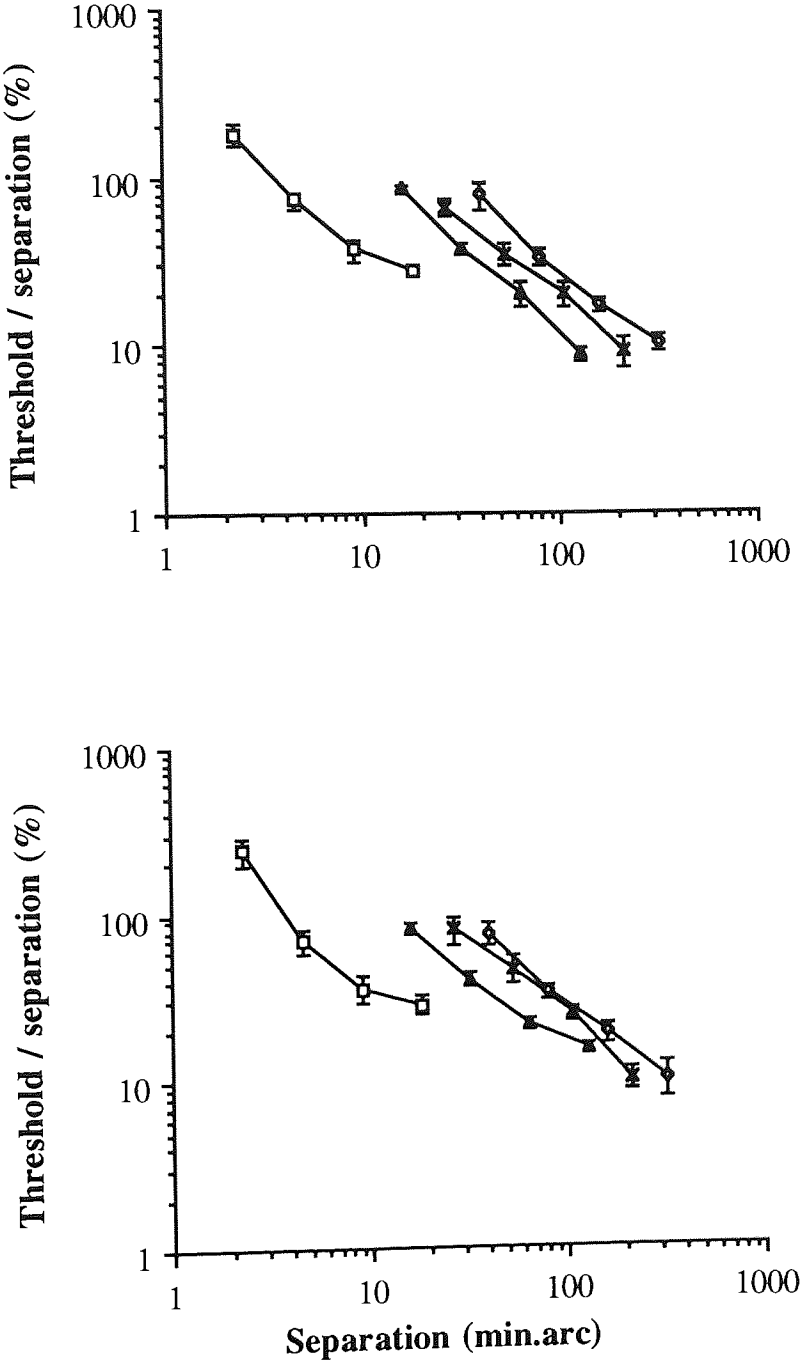

Figure 10.07b: The data replotted with threshold expressed as a percentage of separation.

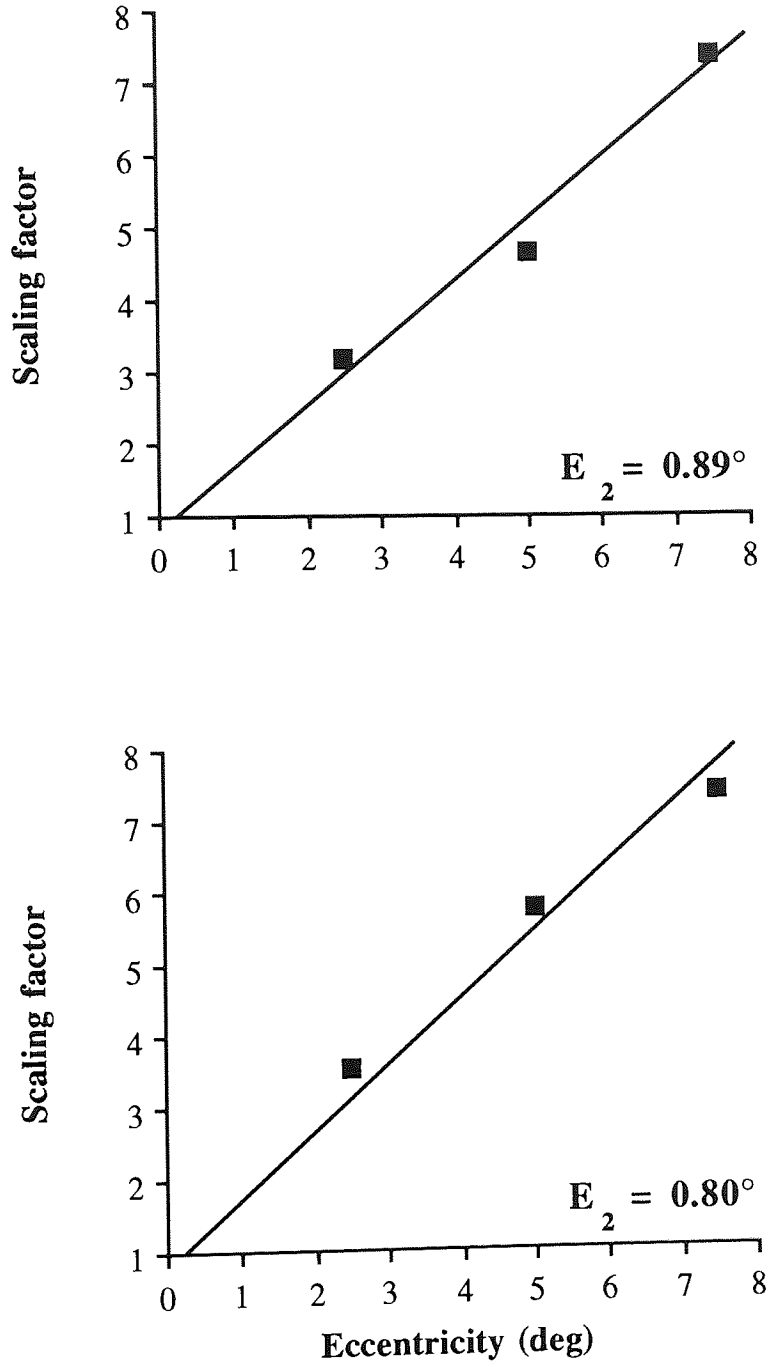

Figure 10.07c: Scaling factors obtained at each eccentricity relative to the smallest eccentricity of 0.267 deg.

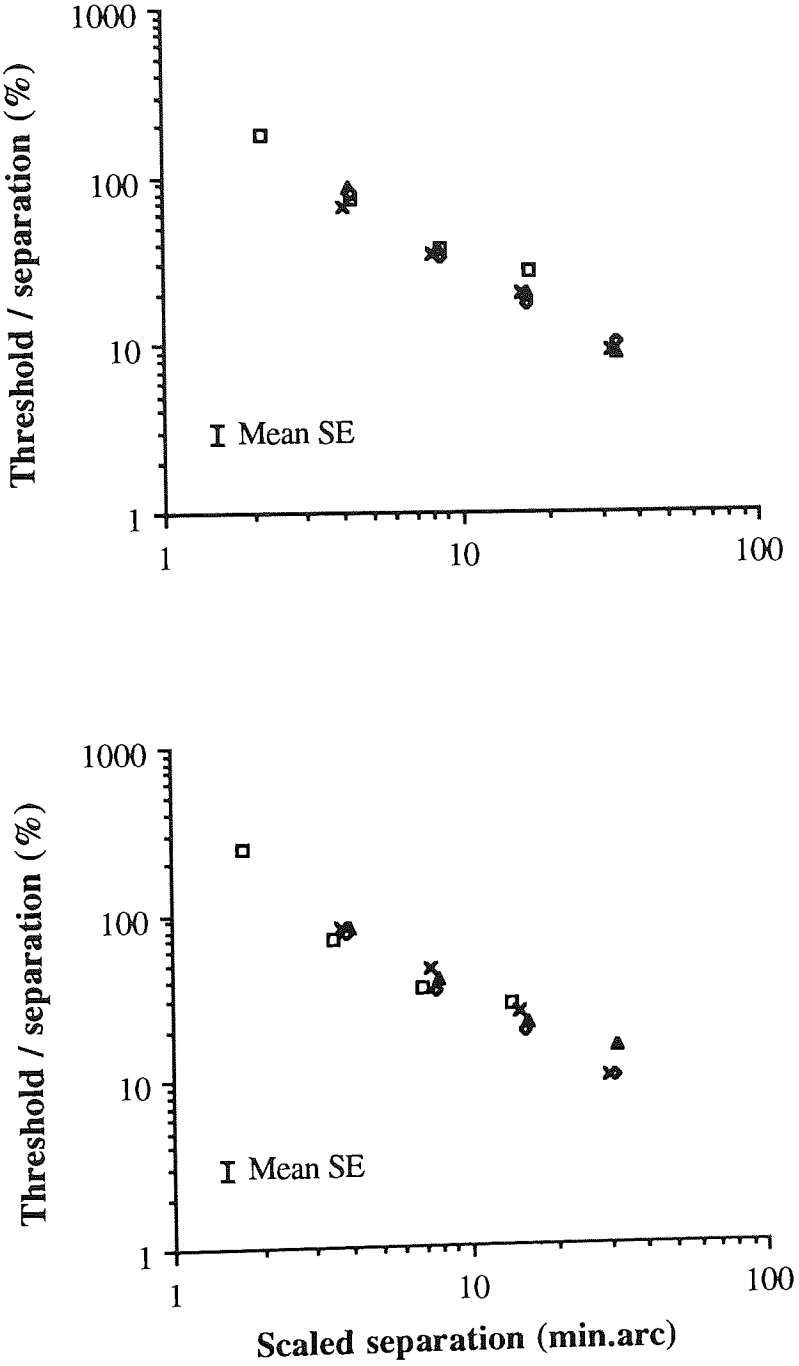

Figure 10.07d: The data of *Figure 10.07b* with the separations at each eccentricity having been scaled along the size (x-) axis.

10.4: Discussion

The experimental data suggest that changes in neural allocation are not the reason for the differences in eccentricity dependence between different tasks. Two tasks were chosen which, individually, had quite different E_2 values but, when the observers performed the two tasks simultaneously, the E_2 values remained the same, as did the differences between these values for the two tasks. However, despite the short 50 msec exposure duration chosen for the latter part of the experiment, the possibility that the allocation process could still take place extremely rapidly, is not completely excluded. It is very difficult to determine the time period which would be definitely too short for any successive processes. What is shown in this experiment, however, is that simultaneous processing of two tasks is performed equally well in the periphery as it is at the fovea.

An interesting finding is that absolute threshold level for both spatial interval and displacement discrimination tasks shows no dependence on whether the subjects attention is directed solely to the solving of one of these tasks or whether attention is shared between tasks. This finding relates to the dichotomy between tasks which are performed either serially or in parallel (Bergen & Julesz, 1983). This dichotomy usually applies to experiments in which the task is to identify a stimulus containing a certain feature (for example, a difference in orientation, vernier offset, colour, size) in the presence of other "distractor" stimuli which do not share this feature.

The features which define parallel tasks are those which are identified quickly and effortlessly in the presence of distractors, and show little dependence on the number of distractor stimuli. Serial tasks, on the other hand, require each stimulus to be examined seprately in order to identify the required feature, and show therefore a strong dependence on the number of distractors. Fahle (1991) has shown that relative position judgements (in the form of vernier offsets) represent a parallel task and can be identified almost immediately in the presence of distractors which either have no vernier offset or have an offset in the opposite direction.

The present experiment has some similarities with the parallel behaviour demonstrated by the tasks above. The data show that the ability to identify one stimulus feature (either separation or displacement) can be performed to the same level of accuracy as when two feature identifications need to be made. Thus, it appears that changes in separation or position are detected almost immediately by the visual system. This is no doubt beneficial in the real world where one can never be sure in what dimensions objects of interest are going to change from one moment to the next. For example, objects may suddenly change either in luminance (due to shading), in size (due to looming or receding), in orientation (due to tilt) or

in position (due to displacement), or all of these changes may occur simultaneously. It is clearly important to be able to identify each of these changes independently without contamination from variations in other features. It would be interesting to continue along these lines and design experiments in which a higher number object feature changes were required to be detected simultaneously. This might reveal at which stage performance begins to suffer.

The reason for the vast differences in E_2 values for different tasks still remains unclear. The present results suggest that the differences are unlikely to be due to variations in neural allocation according to a knowledge of the task involved. This finding is actually not too surprising because, if shifts in neural allocation were possible, they would be of little value in the real world where one is rarely confident of the feature dimension to which one should be attending. Further, aiming attention specifically to one feature dimension would perhaps degrade sensitivity to changes in other features which possessed quite different types of eccentricity dependence.

Chapter 11: Homogeneous flicker and the effect of pure temporal noise

11.1: Introduction

Human flicker sensitivity can be studied by using uniform spots flickering at various temporal frequencies. Flicker sensitivity refers to the inverse of temporal luminance modulation at threshold. This study only deals with flicker sensitivity, all references to critical flicker frequency (CFF) studies have been deliberately excluded.

For foveally fixated spots the dependence of flicker sensitivity on spot size is affected by flicker rate. At low temporal frequencies flicker sensitivity first increases (Raninen & Rovamo, 1987) and then decreases with increasing spot size (Kelly, 1964; Tulunay-Keesey, 1970). Thus, flicker sensitivity has an optimal stimulus size. At medium temporal frequencies flicker sensitivity first increases (Raninen & Rovamo, 1987) but then the increase saturates and flicker sensitivity becomes independent of stimulus size (Kelly, 1964, 1969; Tulunay-Keesey, 1970). At high temporal frequencies flicker sensitivity increases monotonically with stimulus size (Kelly, 1964, 1969; Tulunay-Keesey, 1970; Raninen & Rovamo, 1987).

A decrease in light level reduces the flicker sensitivity of foveal vision at all temporal frequencies and stimulus sizes, but sensitivity is reduced more at high than low temporal frequencies (De Lange, 1958; Kelly, 1959, 1961; Roufs, 1974). The magnitude of spatiotemporal quantal noise increases when light level decreases. The reduction of foveal flicker sensitivity with decreasing retinal illuminance is at least partially due to increase in quantal (Rose, 1942; De Vries, 1943) and / or light-dependent neural (e.g. Lillywhite, 1981) noise. Raninen, Lukkarinen and Rovamo (1993) have studied the effect of pure white temporal noise on flicker sensitivity at the fovea. With increasing contrast of temporal noise flicker sensitivity first remains constant but then starts to decrease when the critical spectral density of noise is exceeded.

Foveal flicker sensitivity for a large (65 deg) stimulus field is insensitive to luminance reduction at low temporal frequencies but sensitivity declines with decreasing luminance at medium and high temporal frequencies (Kelly, 1961). Due to the extent of the field, the result also reflects the properties of the peripheral retina (see Tulunay - Keesey, 1970). In agreement, Kelly's (1961) finding was confirmed by Raninen and Rovamo (1987) who used a small flickering spot in the peripheral visual field.

At low and medium temporal frequencies flicker sensitivity for stimuli of constant size and luminance declines towards the retinal periphery (Tyler, 1981; Tyler & Silverman, 1983;

Raninen & Rovamo, 1987), whereas with increasing eccentricity flicker sensitivity at high temporal frequencies remains practically unchanged when stimulus size is small (Tyler & Silverman, 1983; Raninen & Rovamo, 1987) but increases at large sizes (Tyler, 1981). In the periphery, increasing the size of a stimulus of constant luminance improves flicker sensitivity at all temporal frequencies (Raninen & Rovamo, 1987).

The neural sampling density of the retina decreases with increasing eccentricity (e.g. Drasdo, 1977; Rovamo & Virsu, 1979). This provides an explanation for the reduction of flicker sensitivity towards the retinal periphery for constant size stimuli. The decrease of sampling density can be compensated for by increasing stimulus size towards the visual periphery (Rovamo, Virsu & Näsänen, 1978). It is possible to equalize foveal and peripheral flicker sensitivity at low and medium temporal frequencies by increasing the stimulus size towards the visual field periphery (Tyler & Silverman, 1983; Kelly, 1984; Tyler, 1985; Raninen & Rovamo, 1987). However, at high temporal frequencies flicker sensitivity for large stimulus sizes increases towards the retinal periphery so that the sole increase in size with eccentricity cannot compensate for the differences in flicker sensitivity across the visual field (Tyler & Silverman, 1983; Kelly, 1984; Tyler, 1985; Raninen & Rovamo, 1987). Raninen and Rovamo (1987) have shown that reduction of the luminance of M-scaled targets towards the visual field periphery in order to compensate for the differences in summation of light at the retinal level (flux- or F-scaling) makes flicker sensitivity independent of eccentricity at high temporal frequencies as well.

Studies of peripheral flicker sensitivity with uniform spot stimuli have so far used either constant size stimuli or pre-chosen magnification factors for increasing stimulus size towards the visual periphery. Magnification factors have been based on cone counts of human retina (Tyler, 1987), a combination of cone and ganglion cell distributions (Raninen & Rovamo, 1987), or they have been ad hoc (e.g. Tyler & Silverman, 1983; Kelly, 1984; Tyler, 1985). They all produced roughly the same proportional increase in stimulus size towards the retinal periphery. Foveal stimulus sizes used in the above studies varied between 0.5 and 4 deg, resulting in different series of stimulus sizes across eccentricities. This makes comparison between studies difficult. Further, it is not known whether the result would have been the same if a foveal stimulus size outside the range of 0.5 - 4 deg had been used.

The aim of this experiment was to determine how the dependence of flicker sensitivity on stimulus size is affected by the eccentricity of the stimulus. There are only a few studies concerning the effect of stimulus size on foveal (Kelly, 1969; Tulunay-Keesey, 1970; Raninen & Rovamo, 1987) and peripheral (Raninen & Rovamo, 1987) flicker sensitivity. Until now, comparisons between different studies have been unavoidable if the effect of stimulus size on flicker sensitivity was to be evaluated (e.g. Kelly, 1964). Due to the very

limited number and range of stimulus sizes used at each eccentricity in the previous studies, there is an evident gap in the literature concerning flicker sensitivity for uniform spots. Thus, a systematic study was needed with a wide range of stimulus sizes at each eccentricity in order to produce comprehensive data about the effect of stimulus size on flicker sensitivity at the fovea and in the periphery. In the present experiment flicker sensitivity at various visual field locations was studied at high luminance, at low luminance (with quantal noise), and at high luminance with the addition of pure white temporal noise.

Measuring flicker sensitivity as a function of stimulus size at various eccentricities is equivalent to using spatial scaling. E_2 was used to describe the spatial scale for flicker sensitivity in the human visual system.

11.2: Methods

The apparatus for the flicker experiment is described in the General methods, *Chapter 4.7.3.* The average photopic luminance, measured with a Minolta Luminance Meter LS-110, was set to 50 cd m^{-2}. It corresponded to a scotopic luminance of 110 cd m^{-2}, measured with a Spectra Spot Photometer.

The stimulus was a sinusoidally flickering uniform circular spot with a sharp edge. The horizontal and vertical dimensions of the equiluminous surround were 27.0 and 21.5 cm, respectively. The diameter of the spot varied between 0.5 - 16 cm. The range of viewing distances was 0.43 - 6.88 m, resulting in angular diameters of 2.5 - 1,300 min.arc (0.042 - 21 deg). Control experiments showed that within the viewing distances used the changes in the size of the equiluminous surround had practically no effect on flicker sensitivity.

Michelson contrast of temporal modulation was calculated as $(L_{max} - L_{min}) / (L_{max} + L_{min})$, where L_{max} and L_{min} are the maximum and minimum luminances of the sinusoidal flicker.

White temporal noise was produced by adding to each time pixel (frame) of the stimulus a random number drawn independently from a Gaussian distribution with zero mean and truncation at ± 2.5 SD -units. The r.m.s. contrast of temporal noise was varied by changing the standard deviation of the Gaussian distribution. Luminances of successive temporal noise pixels were uncorrelated. Thus, the one-dimensional temporal noise was white up to a cut-off frequency determined by the frame rate of our display. For the temporal frequencies where noise is white, the spectral density of the noise is calculated (Legge, Kersten & Burgess, 1987) as

$$N_e = c_n^2 \Delta t, \qquad (11.01)$$

where the r.m.s. contrast of noise (c_n) is the standard deviation of the contrast waveform of noise (random luminance increment or decrement divided by the average screen luminance) and (Δt) is the duration of a temporal pixel i.e. the duration of one frame in seconds.

General procedures

Flicker sensitivity was measured by a two-alternative forced-choice (2AFC) algorithm with feedback. The subject's task was to indicate, via the keyboard, which one of the two successive exposures accompanied by similar sound signals contained the stimulus. The stimulus contrast was changed in steps of 0.1 $\log_{10}$ to measure the Michelson contrast of temporal modulation required for the level of 79% correct (Wetherill & Levitt, 1965). Thus, every wrong choice increased contrast by 0.1 $\log_{10}$ units and three consecutive correct responses led to a contrast decrement by the same amount. A smaller number of consecutive correct choices had no effect. The estimate of threshold contrast was an arithmetic mean of the last 8 reversal contrasts of a threshold estimation session and each datapoint shown in the figures is a geometric mean of at least three threshold estimates.

The duration of the flicker stimulus was always 2 sec allowing two complete temporal cycles to be presented even at the lowest temporal frequency studied. The inter-stimulus interval was 600 msec and the delay for the new trial after each response was 250 msec. The beginning phase of the cosine flicker was -90 deg to reduce the visibility of the abrupt appearance and disappearance of the stimulus. Only at 30 Hz was the beginning phase 0 deg because of the 60 Hz frame rate of the display. Technically the apparatus produced a squarewave profile for 30 Hz flicker, but the human visual system is unable to detect its higher harmonics with rapidly decreasing amplitudes at 90 Hz and above.

Flicker sensitivities for a set of stimulus sizes were measured in random order at various eccentricities and temporal frequencies. To avoid adaptation to flicker due to the relatively long presentation time i) the initial modulation amplitude for each threshold measurement was always chosen to be only slightly above threshold and ii) the subjects closed their eyes for the rest of the 2 sec stimulus presentation as soon as the flicker was detected. Adaptation to flicker was fast at 30 Hz in the peripheral visual field and also occurred to a lesser extent at 10 Hz. Therefore, at 10 and 30 Hz the subjects did not trigger off the next presentation immediately, but rested with their eyes open about 15 sec between individual stimulus presentations. Experiments were performed in darkness, the only light coming from the computer display and the fixation target (a dim green LED). It was provided for the peripheral stimuli so that the stimulus was on the horizontal meridian in the nasal visual field. Eccentricity refers to the angular distance between the centre of the stimulus and the point of fixation.

Specific procedures

Experiment 1.

Temporal frequencies of 1, 3, 10, and 30 Hz were used for determining flicker sensitivity at the fovea and at the eccentricities of 5, 10, and 20 deg for stimulus sizes 2.5 - 160 min.arc at 1 and 3 Hz, 2.5 - 320 min.arc at 10 Hz, and 10 - 1,300 min.arc at 30 Hz. The natural pupil diameters were 4.5 - 5.5 mm for the two subjects (PM and KT) studied. Thus, the average retinal illuminance was about 980 phot Td, corresponding to 2,200 scot Td on our display.

Experiment 2.

On the basis of pilot experiments the luminance of the display was lowered to a level that made flicker sensitivities at the two visual field locations studied (fovea and 20 deg eccentricity) similar at large stimulus sizes even for the lowest flicker frequency. The luminance reduction of 3 $\log_{10}$ units (from 50 cd m^{-2} to 0.05 cd m^{-2}) was achieved by placing 5 neutral density filters of 0.6 $\log_{10}$ units in the front of the screen. Dark adaptation time used was 25 minutes. The natural pupil diameters were 5.5 - 6.5 mm. Hence, the average retinal illuminance was 1.4 phot Td, corresponding to 3.1 scot Td. The subjects (PM, OL and HK) confirmed verbally that even in foveal viewing flicker at threshold was only visible on the screen, not reflecting from the surroundings. Stimulus sizes in the experiment were 20 - 640 min.arc at 1 and 3 Hz, 40 - 1,300 min.arc at 10 Hz, and 160 - 1,300 min.arc at 30 Hz.

Experiment 3.

Flicker sensitivity with added temporal white noise was measured at 3 and 30 Hz. The subjects (PM and KT) saw two time windows in succession as before, but this time both windows were flickering, because the previously blank window now contained white temporal noise. Noise was present only within the stimulus area. On the basis of pilot experiments the contrast of noise was increased to a level that at all eccentricities lowered flicker sensitivity for the largest stimulus sizes below the sensitivities measured previously without externally added noise. The average retinal illuminance was about 980 phot Td, corresponding to 2,200 scot Td on our display. Stimulus sizes were 2.5 - 80 min.arc at 3 Hz and 5 - 640 min.arc at 30 Hz.

Subjects

The observers (PM, KT, OL, and HK) performed experiments monocularly using the dominant eye. They were pre-presbyopes. HK was an uncorrected hyperope (0.5 DS) and the others fully corrected myopes (1.0 - 6.0 DS).

Determining the explained variance (r^2)

The goodness of the fit of the least square line to the scaling factor data in *Figure 11.02* was estimated by calculating the variance of the scaling factor values (F) from the predicted estimates (F_{est}) at each flicker rate and expressing this as a proportion of the total variance of the scaling factor values. The proportion was calculated using the following equation:

$$r^2 = 1 - \Sigma(F - F_{est})^2 / \Sigma(F - Z)^2, \qquad (11.02)$$

where $Z = n^{-1}\Sigma F$. The proportion is usually expressed as the percentage of variance explained by multiplying it by 100.

11.3: Results

In the experiments of *Figure 11.01a-d* sensitivity for 1, 3, 10 and 30 Hz flicker was measured at eccentricities of 0, 5, 10, and 20 deg. Subjects were PM and KT. Retinal illuminance was 980 phot Td, corresponding to 2,200 scot Td. At all eccentricities and flicker rates sensitivity first increased with stimulus size up to a critical diameter. In double logarithmic coordinates the slope of the increase in sensitivity with increasing spot diameter was about 1. At large stimulus sizes the increase saturated and flicker sensitivity became independent of area for all flicker rates and eccentricities. The only exception was 30 Hz at the eccentricities of 10 - 20 deg, where sensitivity did not saturate within the range of stimulus sizes used. The critical diameter for summation increased with eccentricity and temporal frequency.

At low temporal frequencies maximum sensitivity was highest at the fovea. The maximum sensitivity of peripheral vision increased with temporal frequency and exceeded the foveal maximum sensitivity at 30 Hz.

The sharp edge of the stimulus affected detection of flicker at large sizes in the periphery. At 1 and 3 Hz flicker was detected at the foveal edge of the stimulus whereas at 30 Hz detection took place at the further edge of the stimulus. This phenomenon is of minor significance, because the scaling procedure was based on the smaller stimulus sizes, which are more accurately localized.

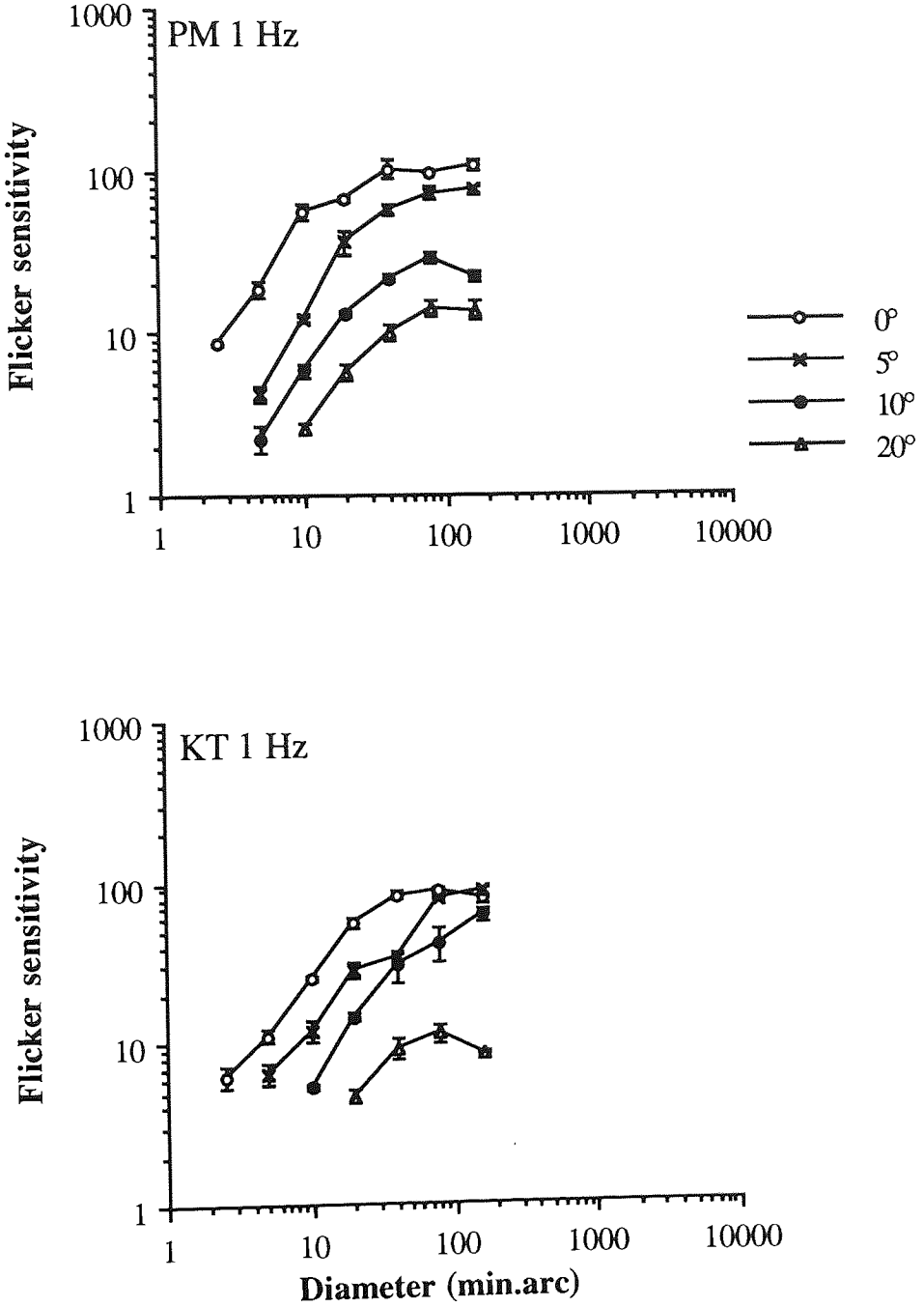

Figure 11.01a: Flicker sensitivity at high luminance at 1 Hz plotted against stimulus diameter. Error bars indicate standard error. Subjects and symbols are shown.

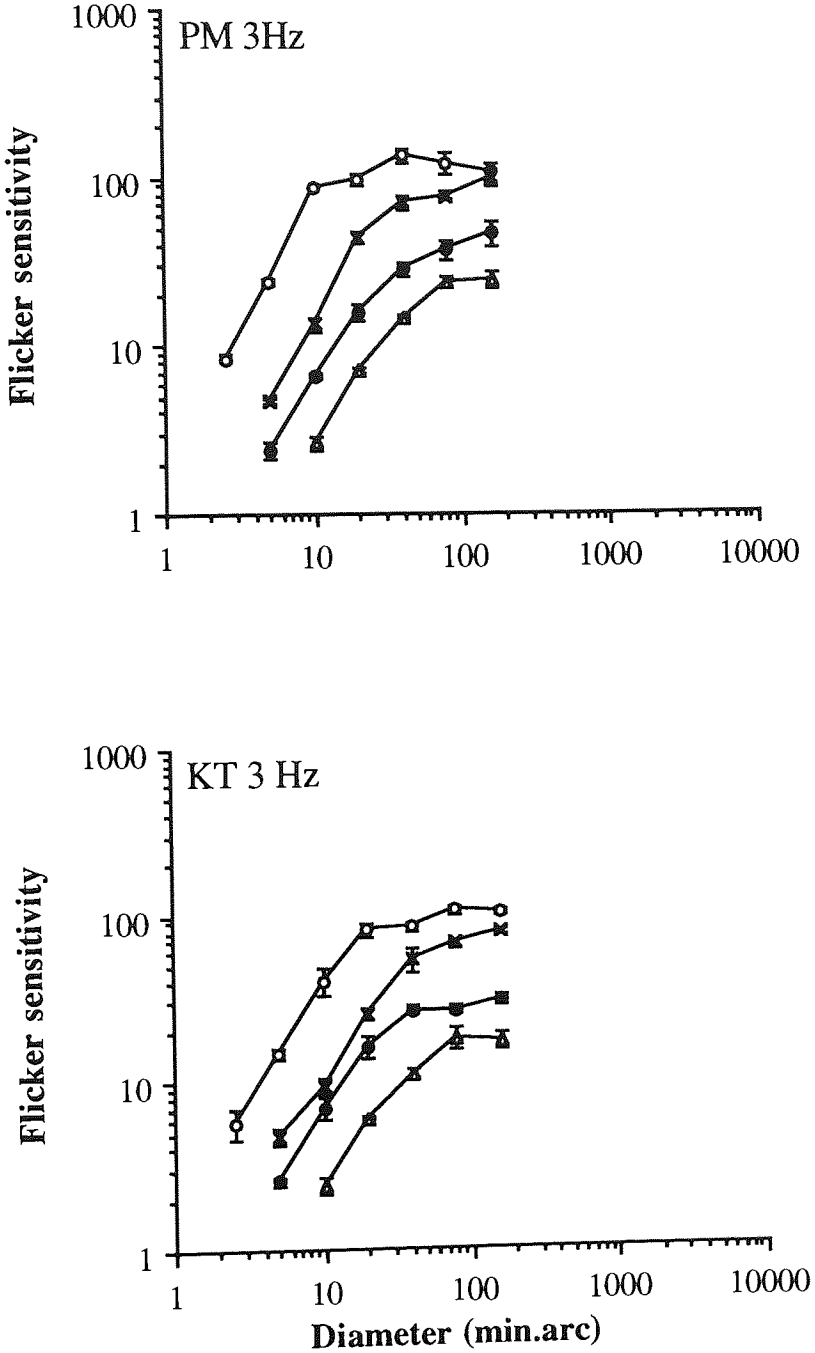

Figure 11.01b: Flicker sensitivity at high luminance at 3 Hz plotted against stimulus diameter.

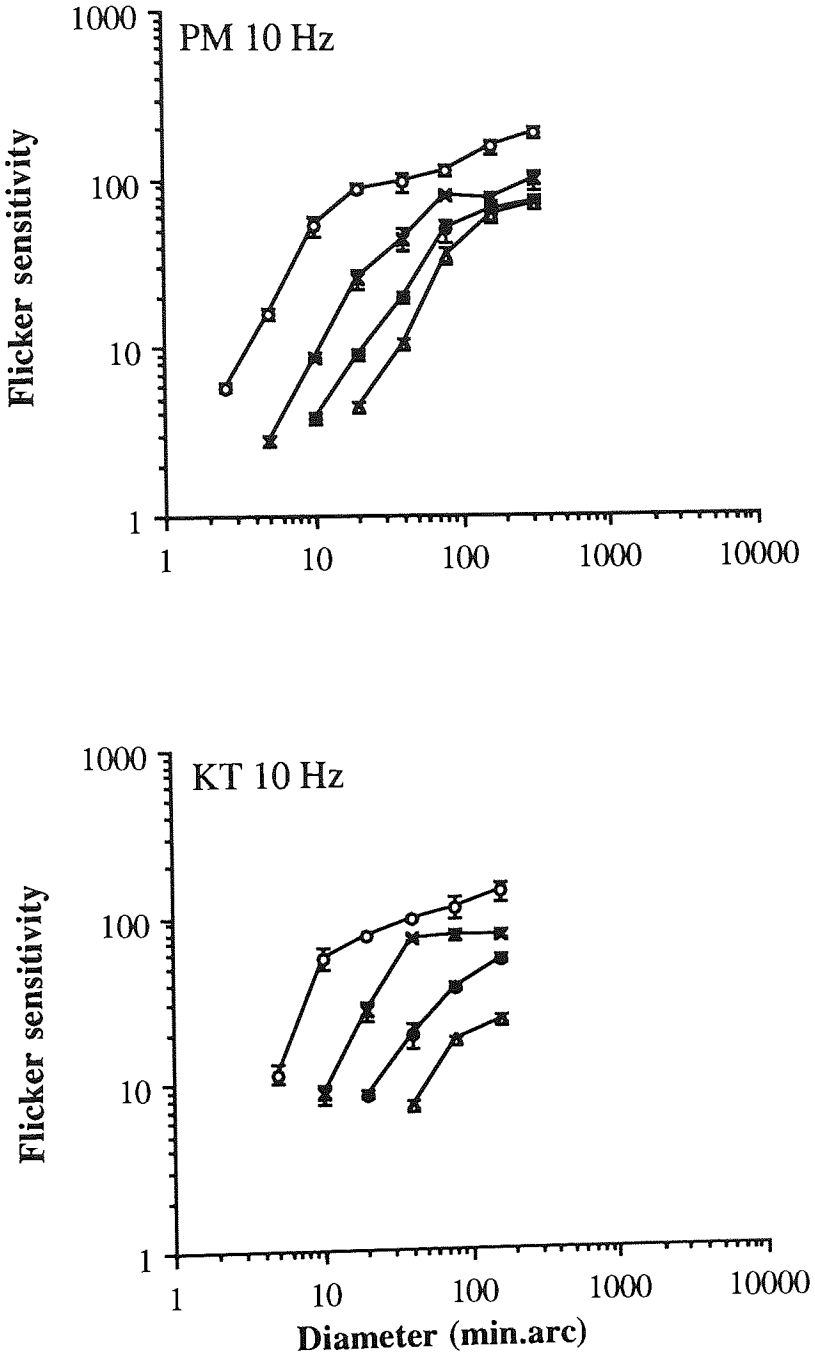

Figure 11.01c: Flicker sensitivity at high luminance at 10 Hz plotted against stimulus diameter.

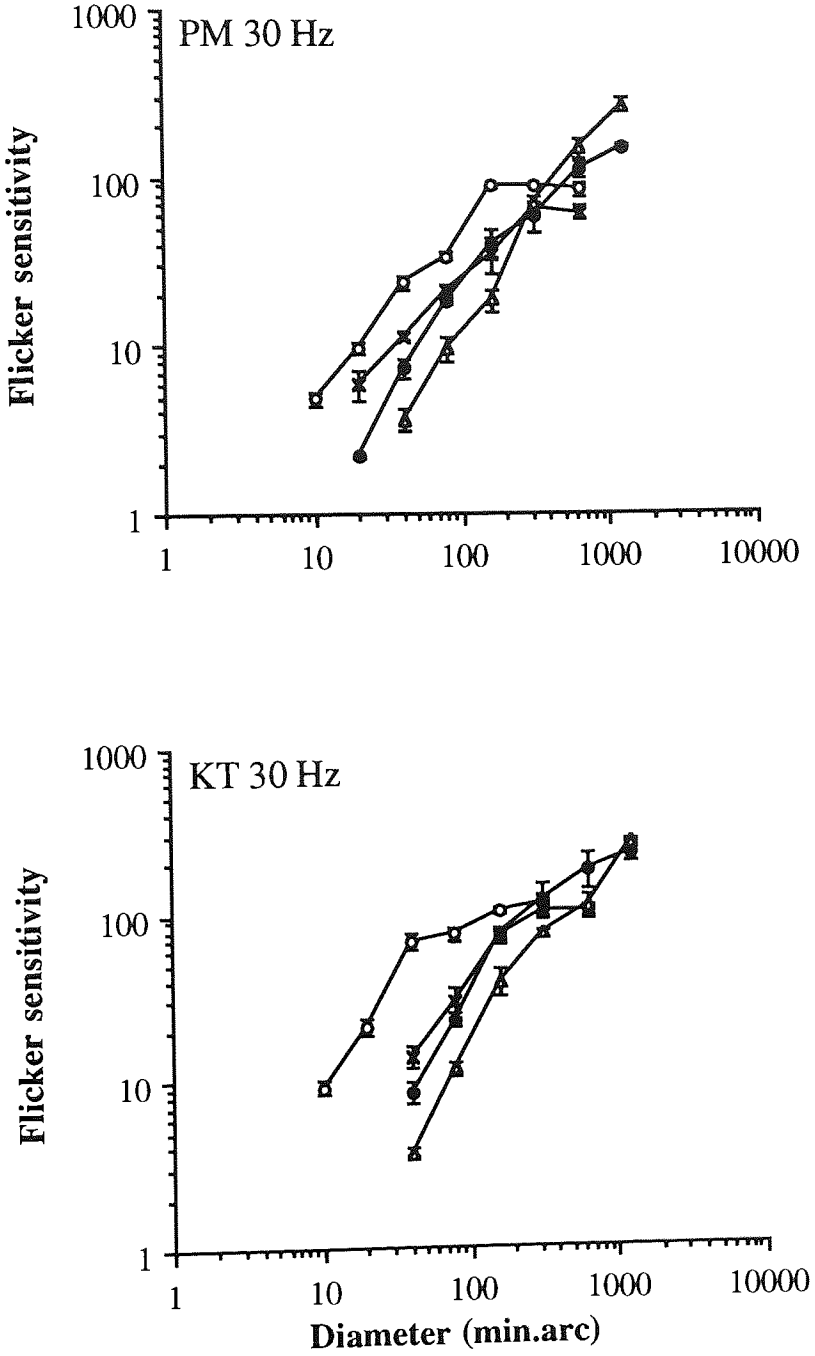

Figure 11.01d: Flicker sensitivity at high luminance at 30 Hz plotted against stimulus diameter.

The amount of the horizontal displacement of the ascending part of each peripheral sensitivity curve from the foveal curve revealed the rate at which stimulus size should be increased with eccentricity in order to keep flicker sensitivity constant across the visual field for small stimulus sizes. A scaling factor for each eccentricity was thus estimated by determining visually the amount by which peripheral data had to be shifted leftwards in order to bring the data points from the periphery into alignment with the foveal data at the ascending parts of the flicker sensitivity curves. This procedure was applied to all frames of *Figure 11.01.*

Figure 11.02a-d shows the scaling factors obtained at each eccentricity for all four temporal frequencies. The increase of scaling factor appeared to be reasonably linear. The foveal scaling factor was constrained to be 1, since the 0 deg data scaled onto itself gives the value of 1. A least squares line constrained to go through (0,1) was fitted to the values of scaling factors of both observers at each temporal frequency. According tho equation *4.04* $E_2 = {}^1/_S$, therefore E_2 (mean ± SE) values were 2.4 (± 0.19), 2.7 (± 0.14), 2.2 (± 0.09), and 4.4 (± 0.41) deg for 1, 3, 10, and 30 Hz, respectively. The explained variance (r^2) for the line of least squares was on average 92%, with a range of 83 - 98%.

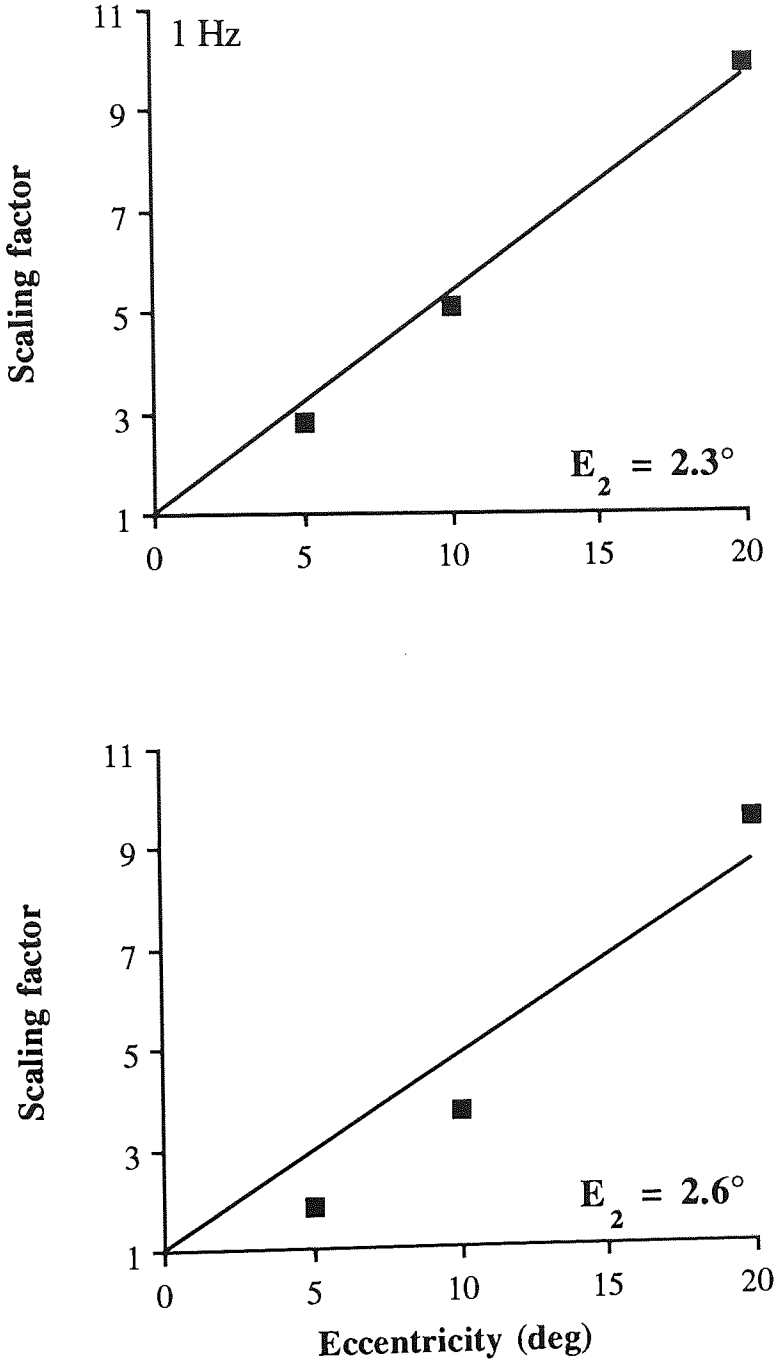

Figure 11.02a: Scaling factors based on flicker sensitivity *vs* stimulus diameter functions at 1 Hz for subjects PM and KT drawn against eccentricity and fitted by least squares lines. The values of E_2 are shown.

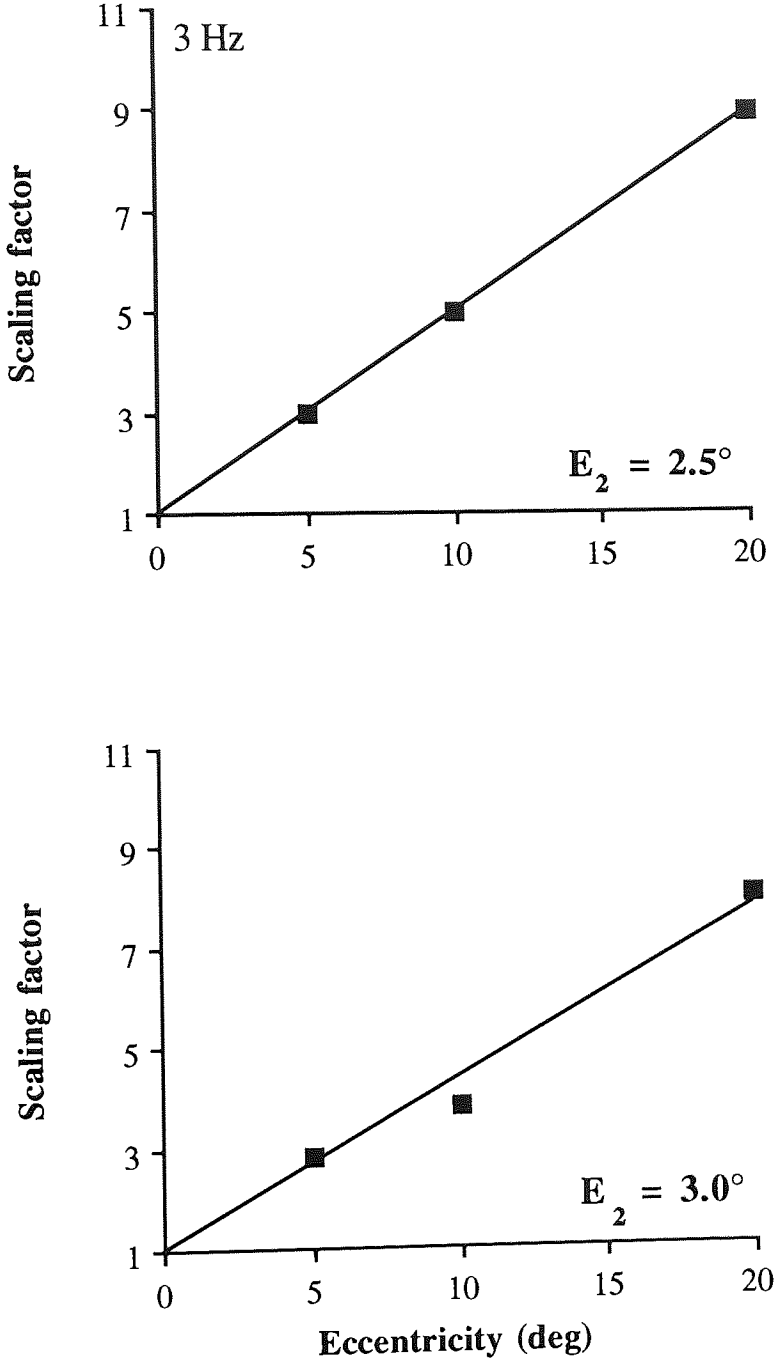

Figure 11.02b: Scaling factors based on flicker sensitivity *vs* stimulus diameter functions at 3 Hz.

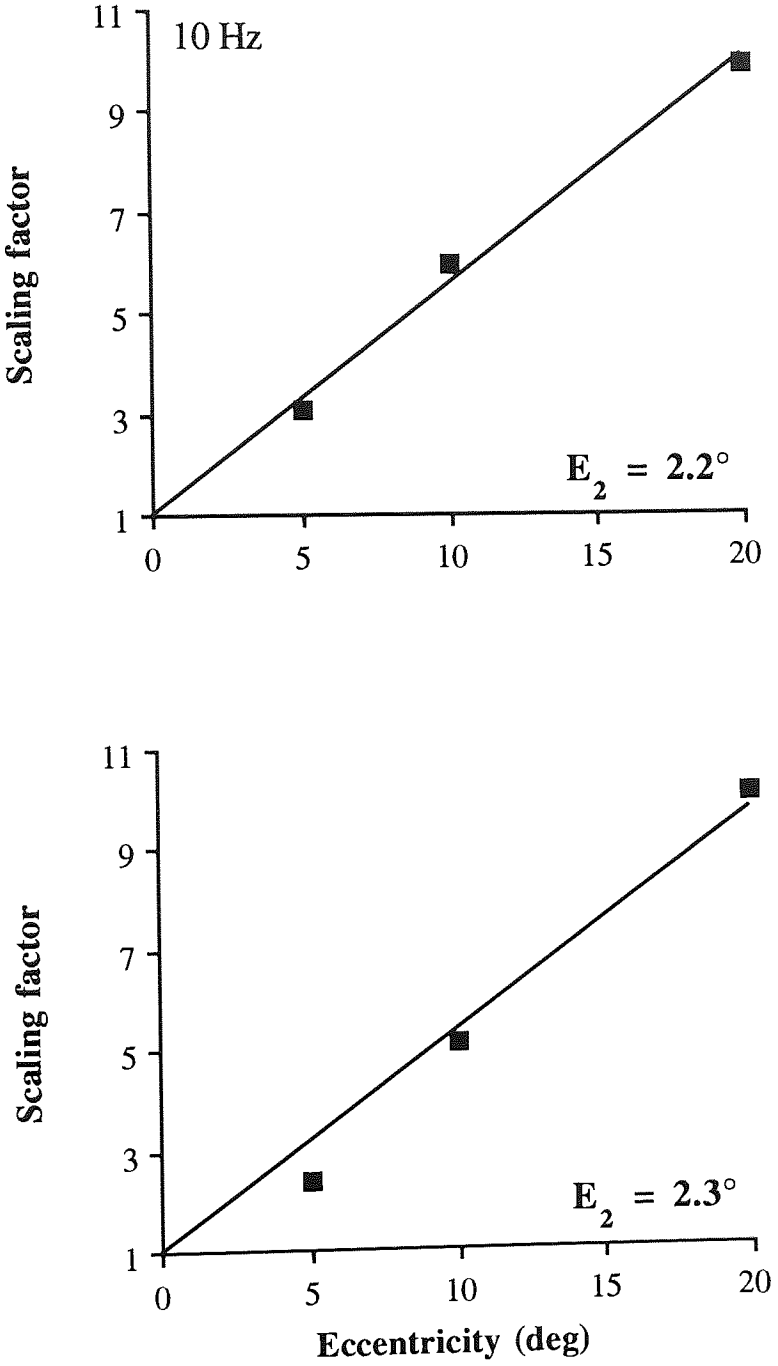

Figure 11.02c: Scaling factors based on flicker sensitivity *vs* stimulus diameter functions at 10 Hz.

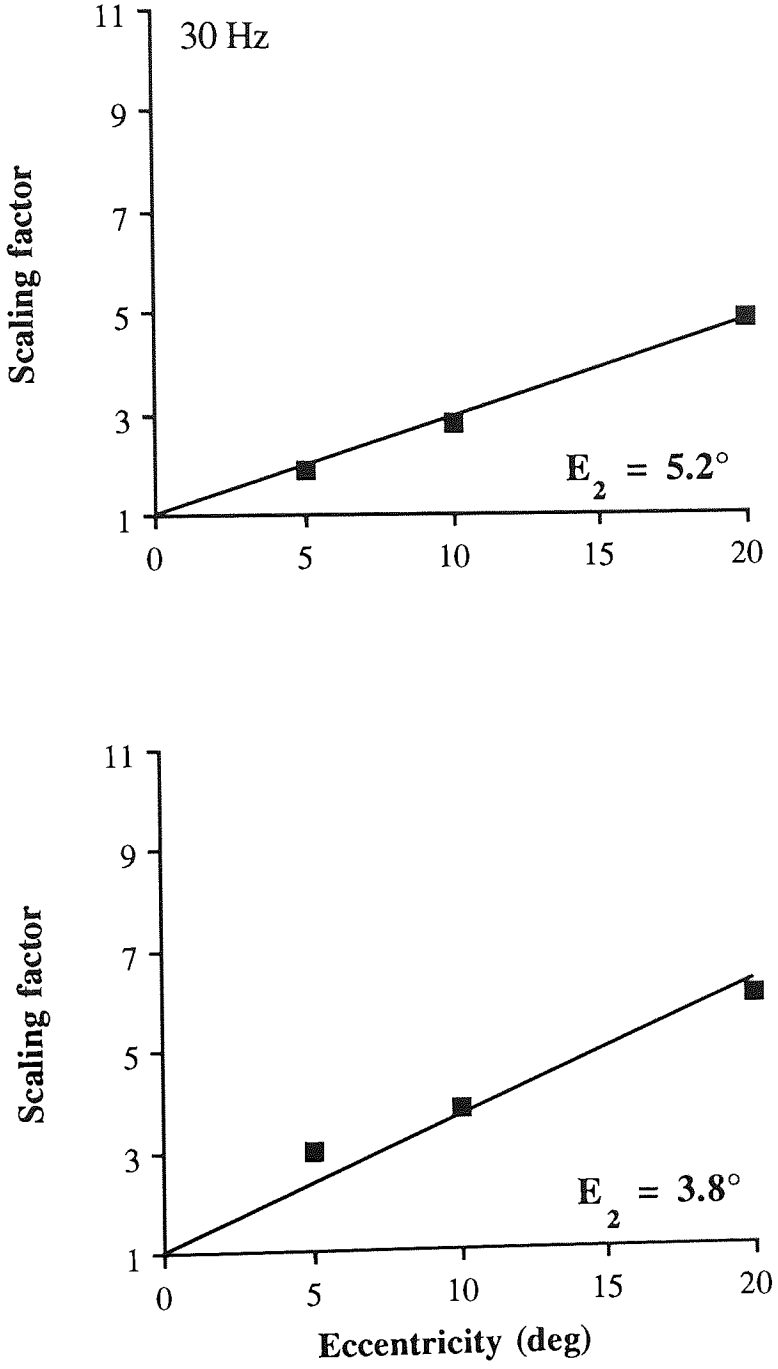

Figure 11.02d: Scaling factors based on flicker sensitivity *vs* stimulus diameter functions at 30 Hz.

According to equation *4.09* $F = 1 + E / E_2$. *Figure 11.03* shows the data from *Figure 11.01* scaled according to equation *4.09* by dividing stimulus diameter by the scaling factor F at each eccentricity.

At 1 - 3 Hz scaling removed eccentricity dependence only for small sizes but at large scaled sizes sensitivity declined steadily towards the retinal periphery.

At 10 Hz spatial scaling removed eccentricity dependence for all stimulus sizes at least for PM, since all data points collapsed together to form a single function. For 30 Hz spatial scaling removed eccentricity dependence at 0 and 5 deg for all sizes but at 10 - 20 deg only for small sizes, since the peripheral flicker sensitivity exceeded the foveal sensitivity at large sizes.

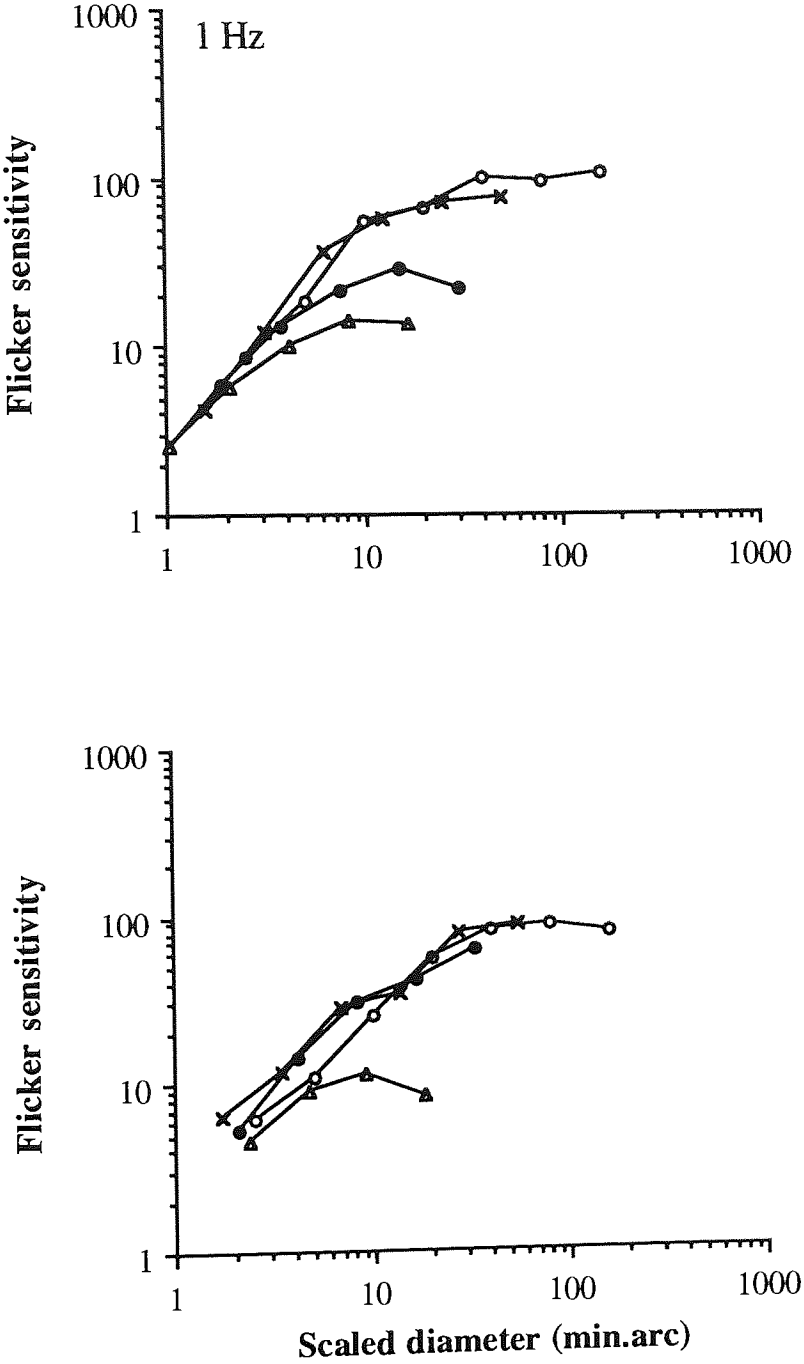

Figure 11.03a: Flicker sensitivity functions at 1 Hz from *Figure 11.01a* plotted against scaled stimulus diameter. Subjecs PM and KT.

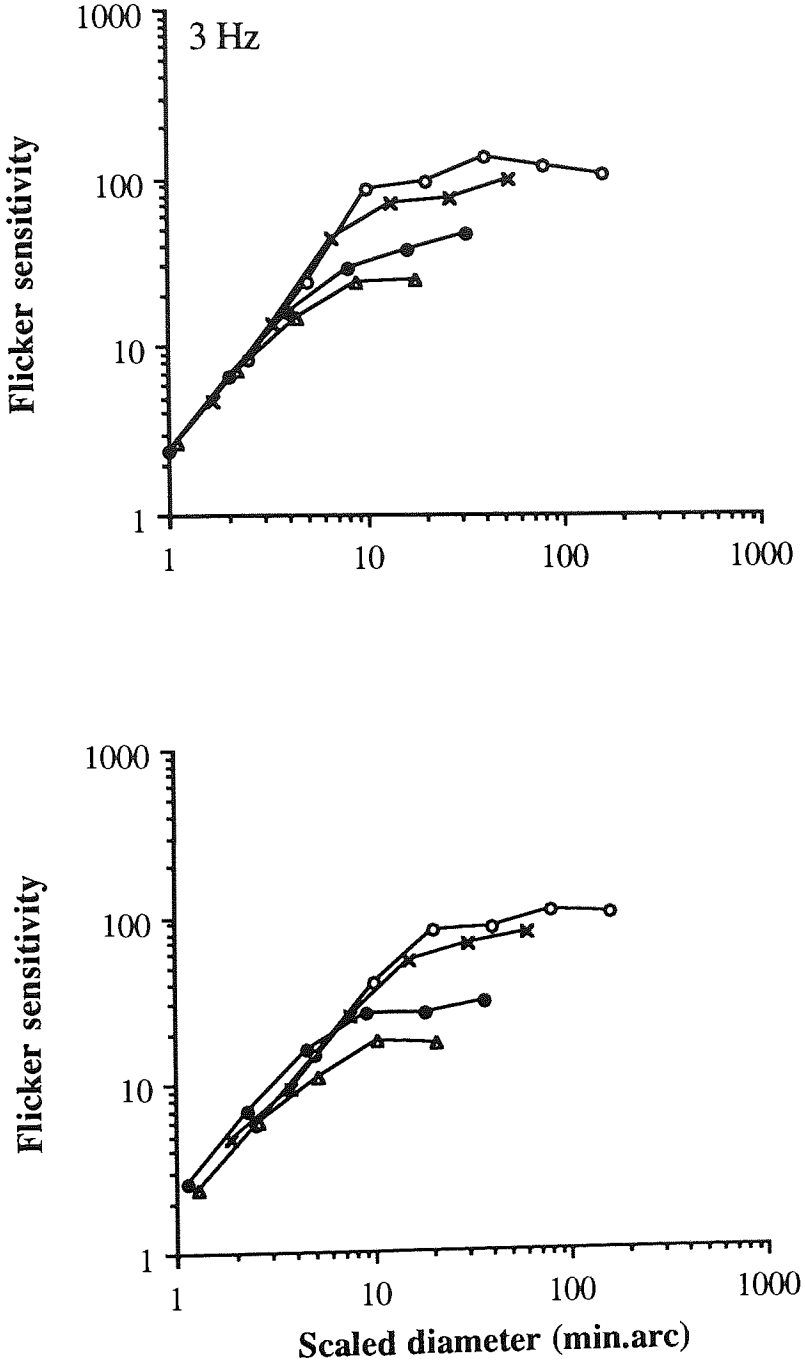

Figure 11.03b: Flicker sensitivity functions at 3 Hz from *Figure 11.01b* plotted against scaled stimulus diameter.

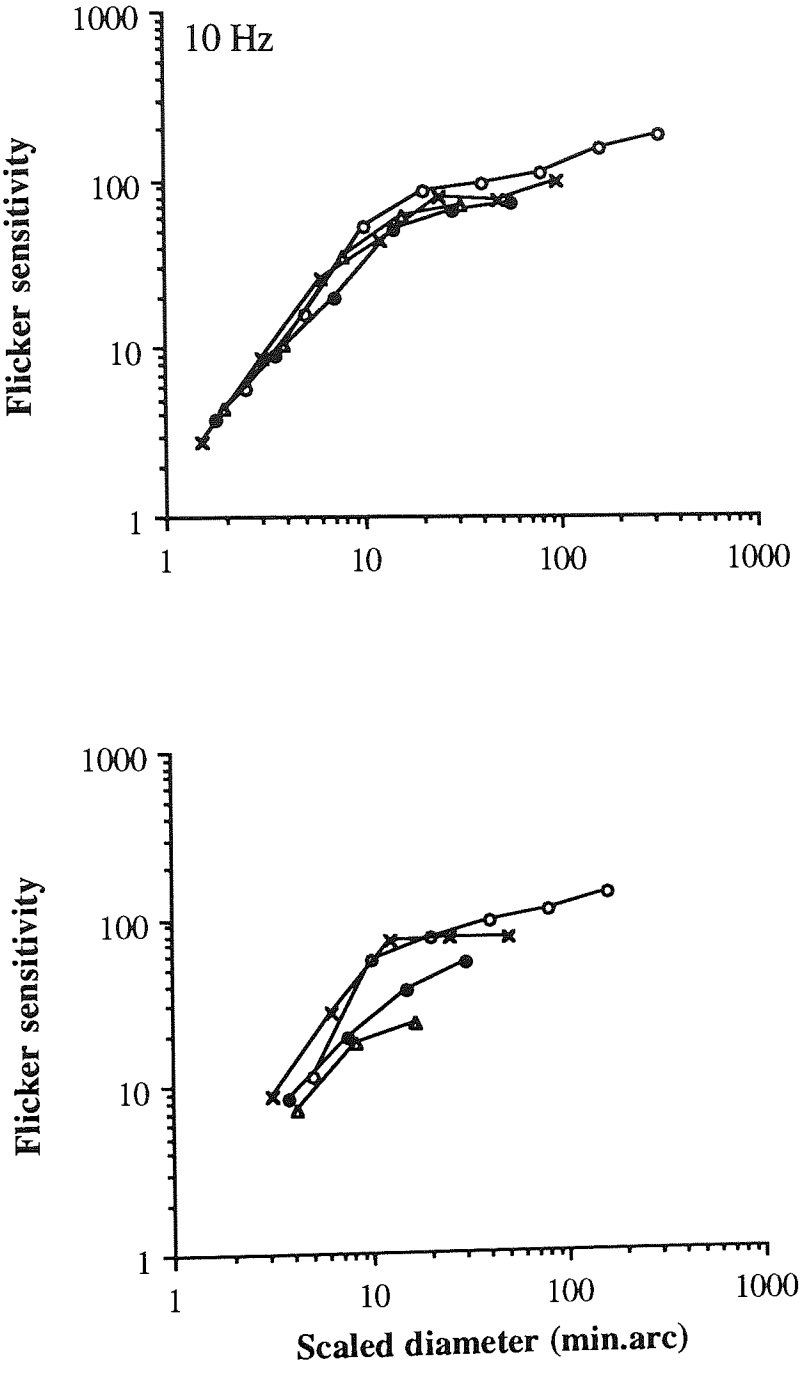

Figure 11.03c: Flicker sensitivity functions at 10 Hz from *Figure 11.01c* plotted against scaled stimulus diameter.

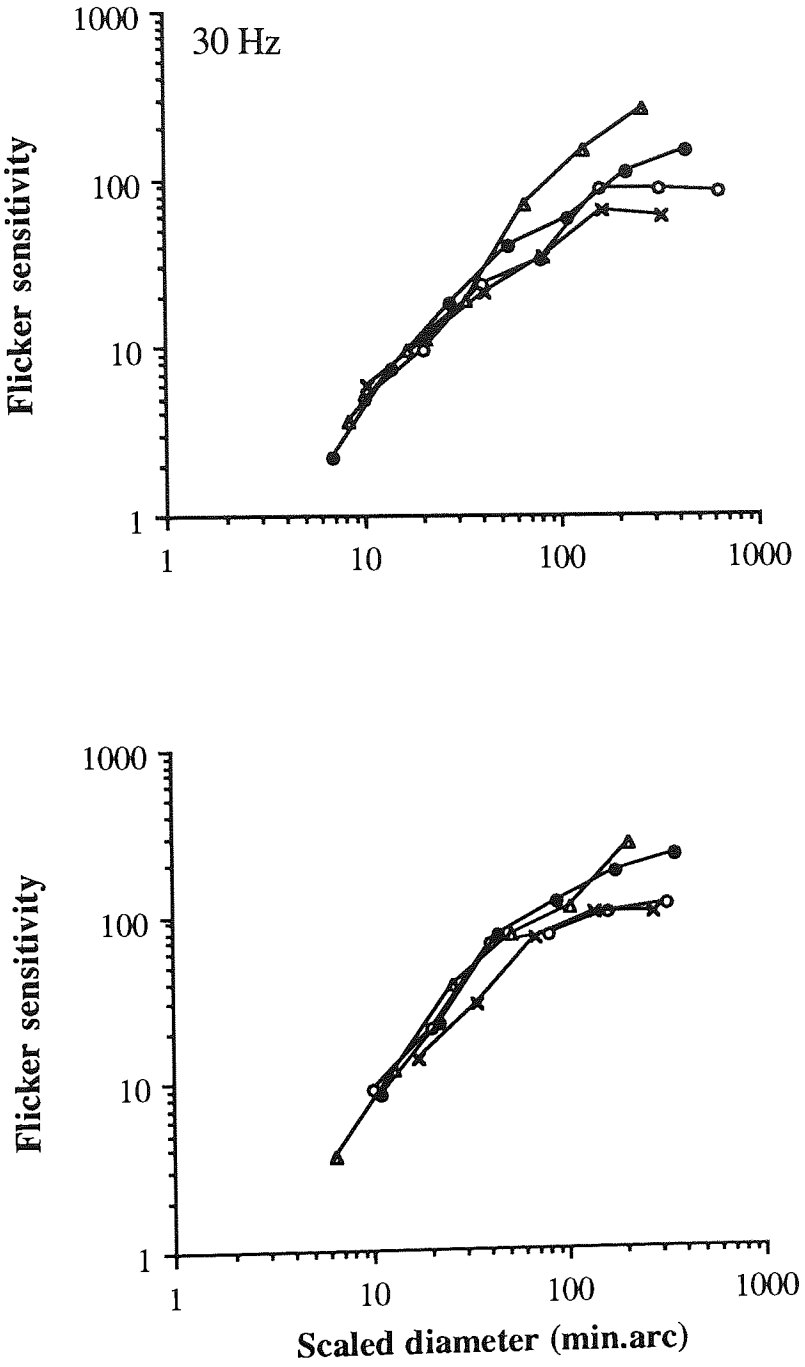

Figure 11.03d: Flicker sensitivity functions at 30 Hz from *Figure 11.01d* plotted against scaled stimulus diameter.

In the experiments of *Figure 11.04* flicker sensitivity was measured at a low light level for 1, 3, 10 and 30 Hz flicker at eccentricities of 0 and 20 deg. Photopic retinal illuminance was 1.4 Td, corresponding to 3.1 scot Td. As *Figure 11.04* shows, flicker sensitivity at all temporal frequencies studied was fairly similar in foveal and peripheral vision. Scaling at small sizes was, however, possible for 1 and 3 Hz data. Due to the small difference between the foveal and peripheral sensitivity curves, the resulting E_2 values were large, about 70 deg for 1 Hz and 22 deg for 3 Hz. At 10 and 30 Hz stimulus size did not have to be increased in the periphery to maintain the foveal performance level. Thus, no spatial scaling was needed when retinal illuminance was 1.4 phot Td. Hence, E_2 was infinite for 10 and 30 Hz.

The data from high and low luminance conditions have been presented in the same scale to allow visualization of the effect of quantal noise on flicker sensitivity. Note that, on average, larger spot sizes were needed to obtain sensitivity *vs* size function at low luminance. Comparison of the data of *Figure 11.04* with the results obtained at high luminance *Figure 11.01* reveals that foveal flicker sensitivity at 1 - 3 Hz decreased almost by 10-fold at all stimulus sizes when retinal illuminance decreased from 980 to 1.4 phot Td. In contrast, peripheral flicker sensitivity decreased only slightly. At 10 Hz flicker both foveal and peripheral sensitivities were clearly reduced from the sensitivities measured in bright light. At 30 Hz there was nearly a 100-fold reduction in sensitivity both at the fovea and in the periphery. Spatial integration in dim light continued at all temporal frequencies and eccentricities to larger stimulus sizes than in bright light and for 10 and 30 Hz saturation did not occur at the stimulus sizes used.

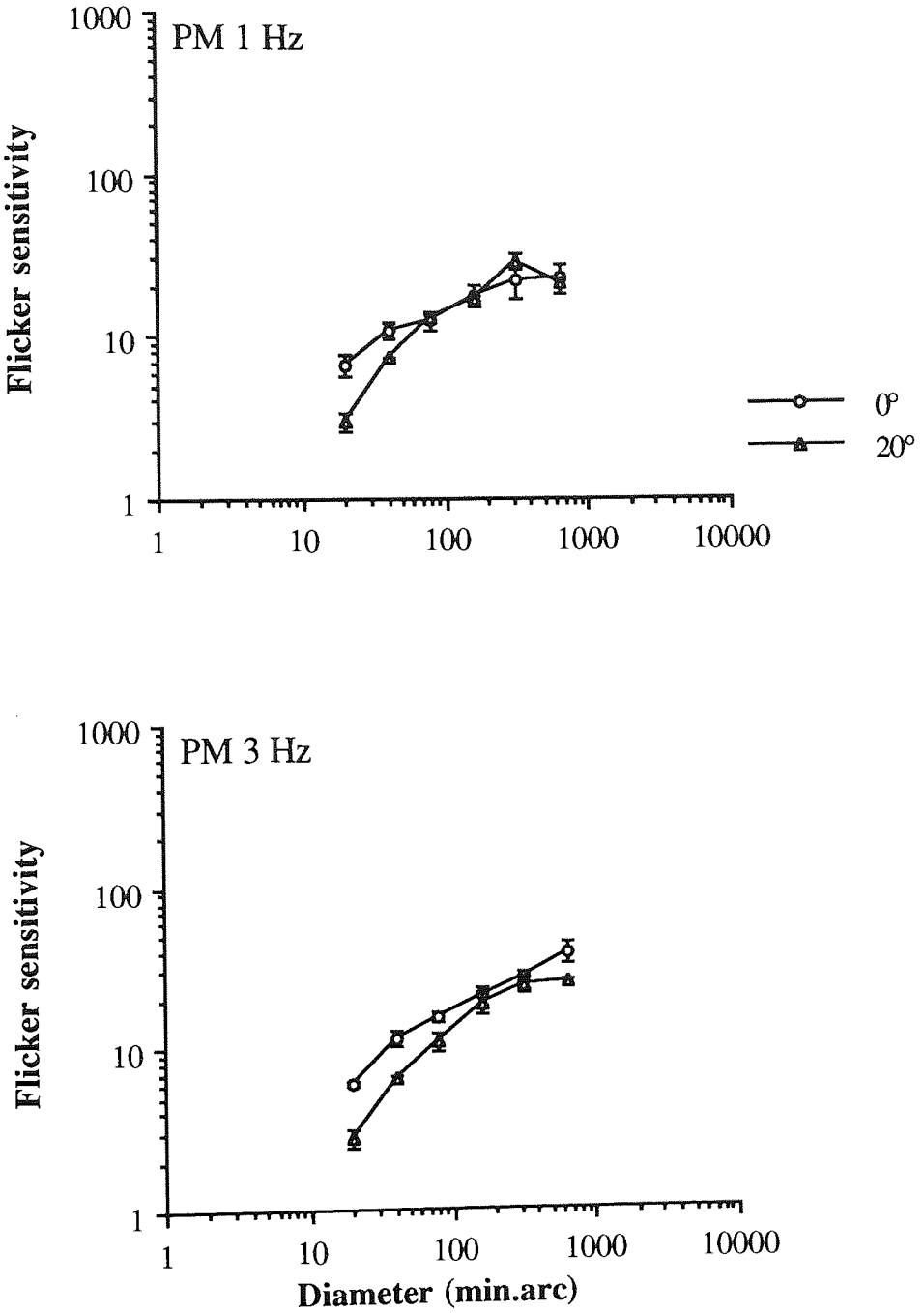

Figure 11.04a, b: Flicker sensitivity at low luminance at 1 Hz (a) and 3 Hz (b) for eccentricities 0 and 20 deg. Subject PM.

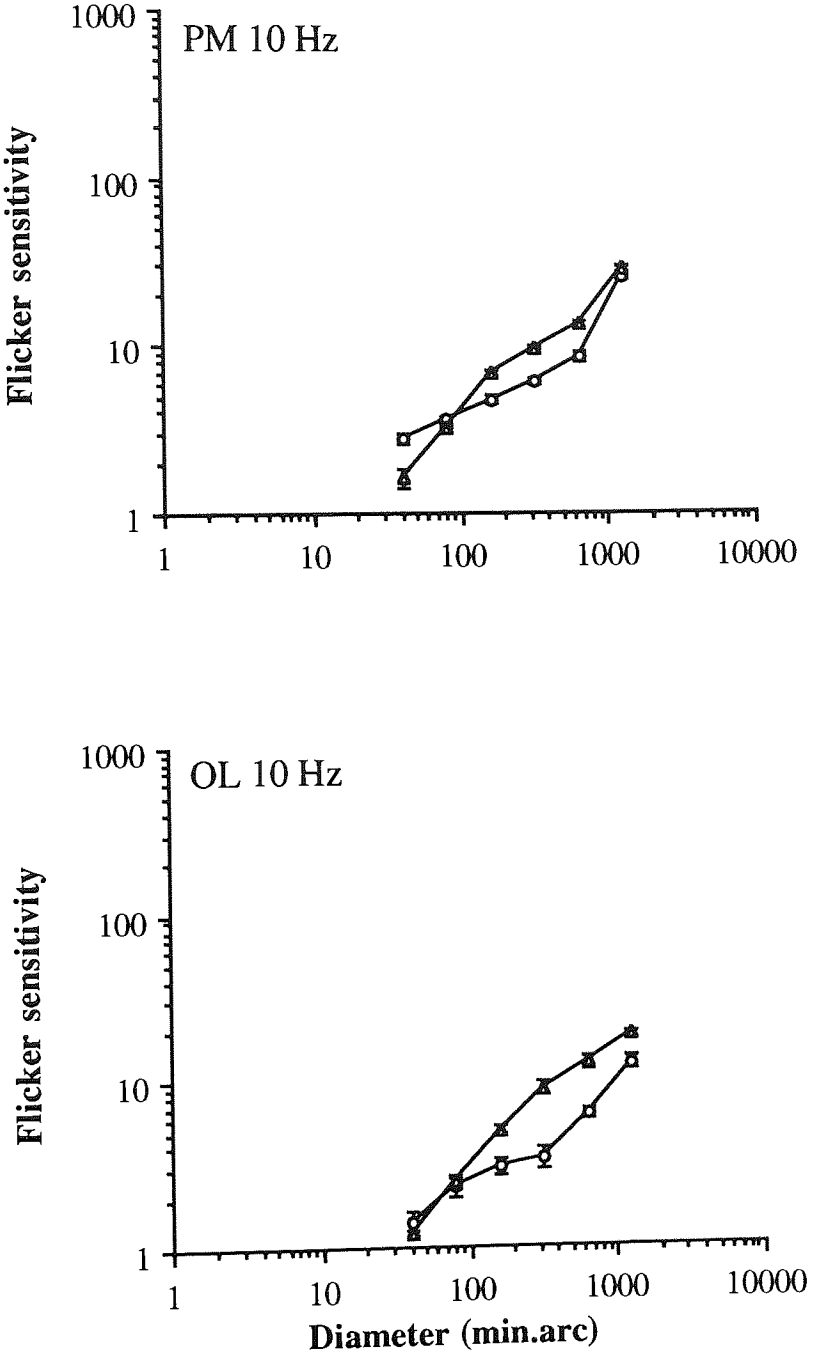

Figure 11.04c: Flicker sensitivity at low luminance at 10 Hz. Subjects PM and OL.

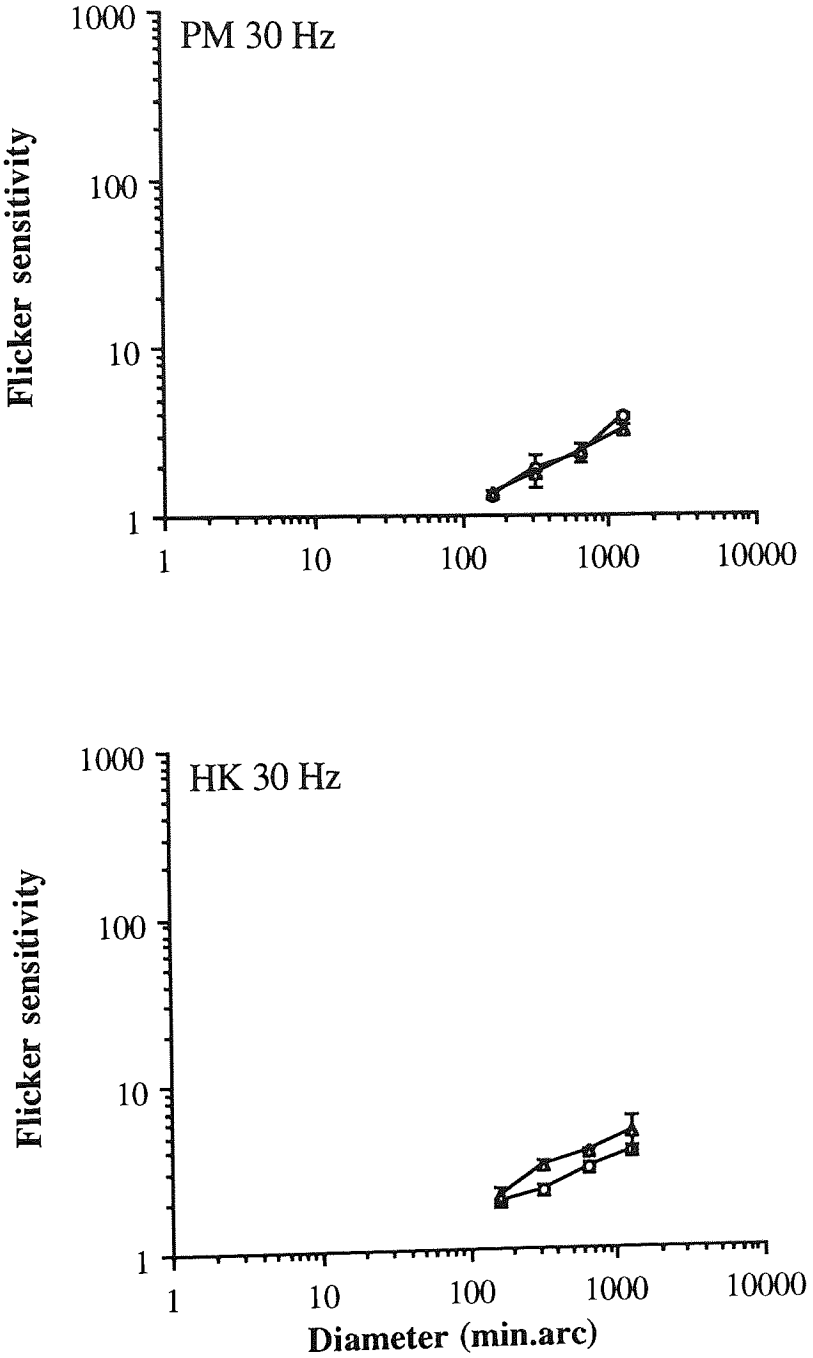

Figure 11.04d: Flicker sensitivity at low luminance at 30 Hz. Subjects PM and HK.

In the experiments of *Figure 11.05 a* and *b* (KT and PM, respectively) flicker sensitivity was measured in white temporal noise for 3 and 30 Hz at the eccentricities of 0, 5, 10 and 20 deg. Retinal illuminance was 980 phot Td. The spectral density of white temporal noise was 167 μsec at 3 Hz and 6.67 μsec at 30 Hz. The corresponding r.m.s. contrasts of noise were 0.1 and 0.02.

At all eccentricities sensitivity first increased with stimulus size but then the increase saturated and flicker sensitivity became independent of stimulus size. The maximum sensitivity was 15 - 23 for 3 Hz and 25 - 50 for 30 Hz at all eccentricities. The critical area for saturation increased with eccentricity and temporal frequency as in *Figures 11.01 b* and *d*. On the basis of comparison with *Figures 11.01 b* and *d*, externally added noise had little effect on flicker sensitivity at small sizes at any eccentricity.

A scaling factor for each eccentricity at each flicker rate was again estimated visually by determining the amount by which peripheral data had to be shifted leftwards in order to bring the data points from the periphery into alignment with the foveal data at the ascending parts of the flicker sensitivity curves. *Figures 11.05 c* and *d* show the scaling factors obtained at each eccentricity for both temporal frequencies. A least squares line constrained to go through (0,1) was fitted to the values of scaling factors at each temporal frequency. The explained variance for the line of least squares calculated by equation *11.02* was 98% for 3 Hz, and 96% for 30 Hz. E_2 values (mean ± SE) of 4.1 (± 0.27) and 7.2 (± 0.78) deg were found for 3 and 30 Hz, respectively. Thus, there was a small, but statistically significant increase in E_2 from the values (2.7 ± 0.14 deg at 3 Hz and 4.4 ± 0.41 deg at 30 Hz) measured without external added temporal noise.

For *Figures 11.05 e* and *f* the data at both temporal frequencies from *Figures 5 a* and *b* were scaled according to equation *4.09* by dividing stimulus diameter by the scaling factor F at each eccentricity. The flicker sensitivity curves now collapsed together at all scaled stimulus sizes as the eccentricity dependence was successfully removed by spatial scaling. Addition of temporal noise reduced the maximum flicker sensitivity at large stimulus sizes to the same level for all eccentricities. Thus, externally added temporal noise abolished the differences in maximum sensitivity, which was the reason for the partial failure of spatial scaling in *Figure 11.03.*

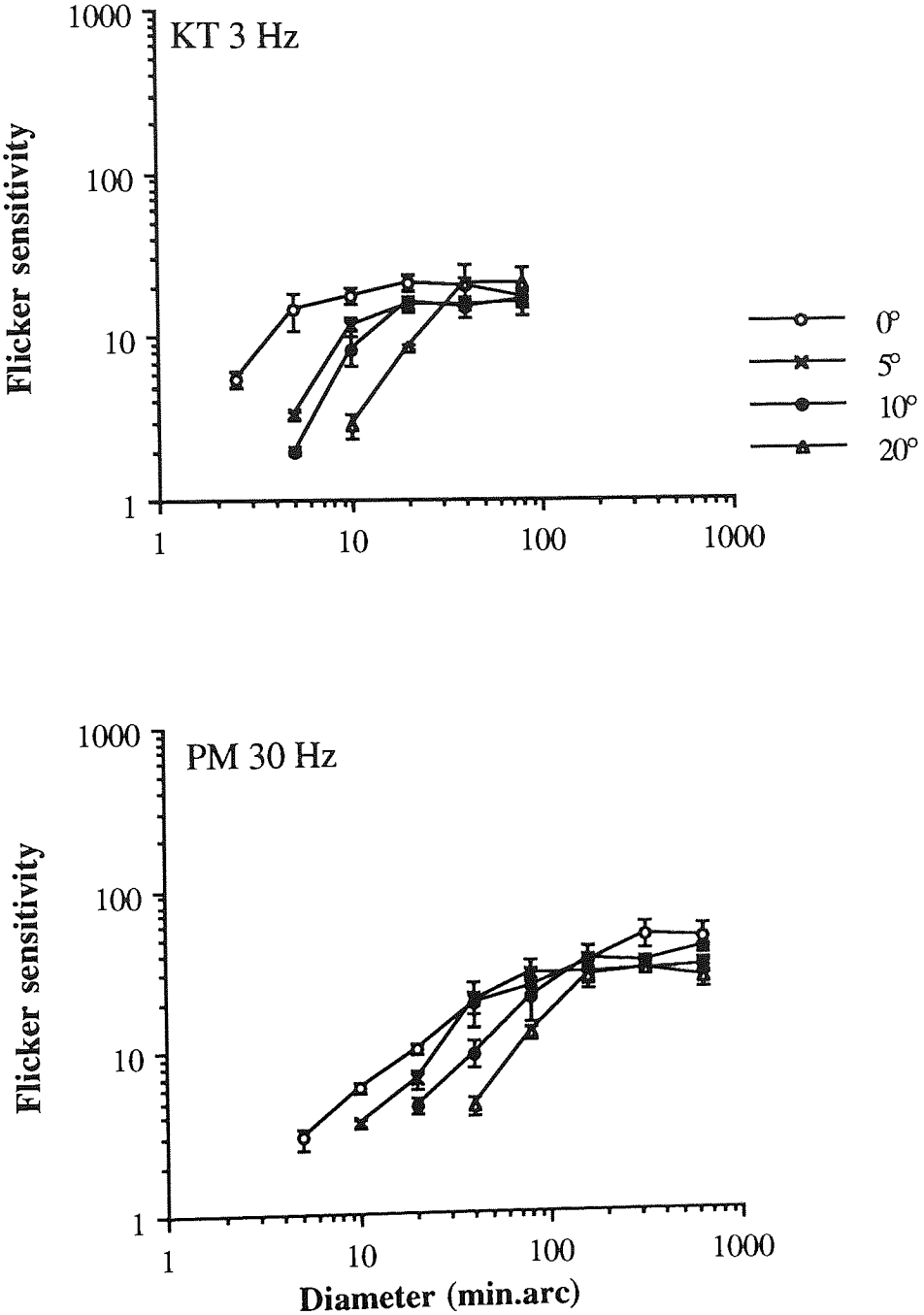

Figure 11.05a,b: Flicker sensitivity at high luminance with added external white temporal noise. Flicker sensitivity plotted against stimulus diameter in (a) for 3 Hz from subject KT and (b) for 30 Hz from subject PM. The r.m.s. contrast of noise was 0.1 at 3 Hz and 0.02 at 30 Hz.

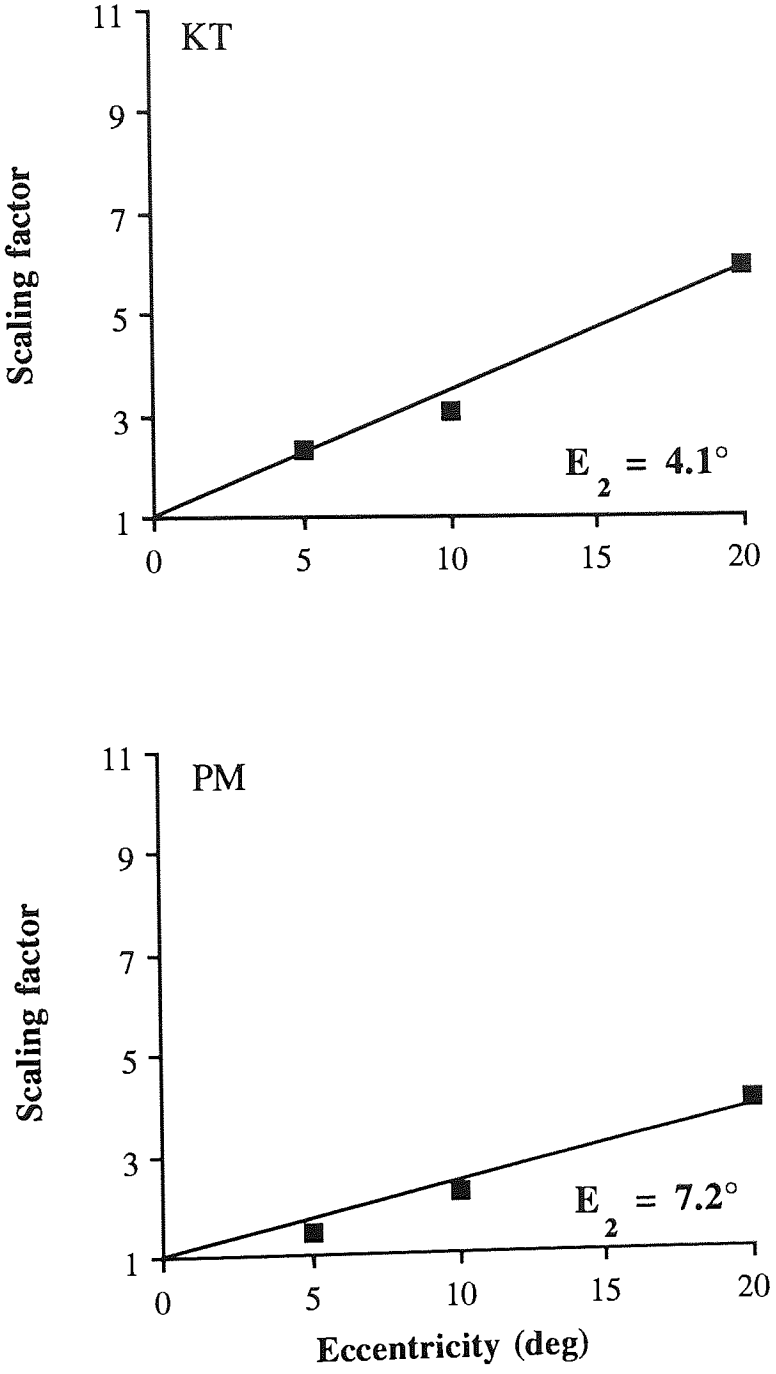

Figure 11.05c,d: Panels (c) and (d) show the corresponding scaling factors from *Figure 11.05* panels *a* and *b* plotted against eccentricity. The values of E_2 are shown.

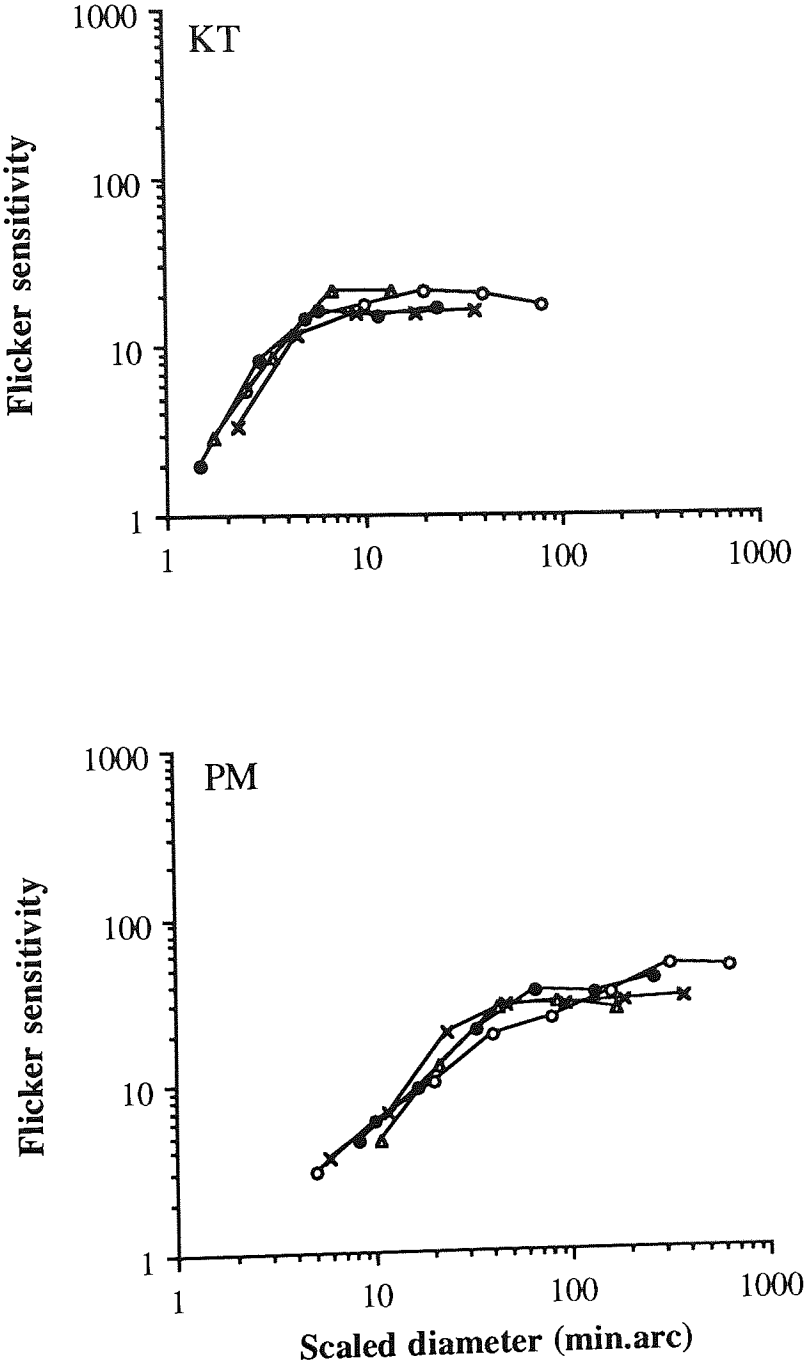

Figure 11.05e,f: Panels (e) and (f) show the flicker sensitivity functions from (a) and (b), respectively, plotted against scaled stimulus diameter.

11.4: Discussion

The present experiments using a flicker detection task showed that at high luminance flicker sensitivity at 1 - 30 Hz first increased with increasing stimulus size until reaching a plateau. At each temporal frequency the ascending parts of the curves from eccentricities of 0 - 20 deg could be superimposed by size scaling. E_2 was found to be 2.2 (± 0.09) - 2.7 (± 0.14) deg for 1 - 10 Hz but 4.4 (± 0.41) deg for 30 Hz. At low temporal frequencies the maximum sensitivity was much higher at the fovea than in the periphery. At 30 Hz this situation reversed. With pure white temporal noise visual performance could be made independent of eccentricity by spatial scaling also at large stimulus sizes, since the added temporal noise had practically no effect at the smallest stimulus sizes, but reduced maximum sensitivities at large sizes to the same level at all eccentricities. With added temporal noise E_2 was 4.1 (± 0.28) for 3 Hz and 7.2 (± 0.78) deg for 30 Hz. When retinal illuminance was reduced from 980 to 1.4 phot Td, the foveal and peripheral flicker sensitivity functions at 1 - 30 Hz were reduced to the same level at all spot sizes studied. E_2 was found to be 70 deg at 1 Hz and 22 deg at 3 Hz but infinite at 10 and 30 Hz.

These results are in agreement with the earlier foveal findings that the dependence of flicker sensitivity on stimulus size is affected by flicker rate (Kelly, 1964, 1969; Tulunay-Keesey, 1970; Raninen & Rovamo, 1987). However, at 1 Hz flicker sensitivity did not start to decrease in the present experiments probably because the spot sizes did not extend to very large sizes. In addition, at 30 Hz the foveal sensitivity saturated probably because the spots used were large enough to reveal saturation. The rapid reduction of the foveal flicker sensitivity at high temporal frequencies with decreasing light level (De Lange, 1958; Kelly, 1959, 1961; Roufs, 1974) as well as the finding (Raninen, Lukkarinen & Rovamo, 1993) that foveal flicker sensitivity is reduced by added temporal white noise were confirmed by the present study.

The present results also agree with the previous findings that in peripheral vision flicker sensitivity at small and medium stimulus sizes increases with size at all temporal frequencies (Raninen & Rovamo, 1987) and that at low and medium temporal frequencies sensitivity for a stimulus of constant size and luminance declines towards the retinal periphery (Tyler, 1981; Tyler & Silverman, 1983; Raninen & Rovamo, 1987) whereas at high temporal frequencies flicker sensitivity remains practically unchanged with small stimulus sizes but increases with eccentricity when stimulus size is large (Tyler, 1981; Tyler & Silverman, 1983). In fact, we found that at 30 Hz flicker sensitivity decreased with increasing eccentricity when the stimulus was small in size, remained constant at medium sizes, and increased with eccentricity at large stimulus sizes.

For most tasks it is necessary to increase the size of the stimulus with increasing eccentricity in order to keep visual performance at the foveal level. The amount of this increase is stimulus and task dependent, as has been shown in the previous chapters and previously suggested by e.g. Drasdo (1991). The E_2 values have ranged from 0.075 deg for bisection acuity (*Chapter 7*) through 0.7 - 1.6 deg for vernier acuity (Levi, Klein & Aitsebaomo, 1985; *Chapter 5,* average) and 2.7 deg for grating acuity (Virsu, Näsänen & Osmoviita, 1987) to 16 deg for gradual unreferenced movement (*Chapter 8,* average). According to the present results E_2 was 70 and 22 deg at 1 and 3 Hz but infinite at 10 and 30 Hz in the flicker detection task when retinal illuminance was low.

In earlier studies the same scaling factors were used for all flicker rates corresponding to E_2 values of 3 deg (Tyler & Silverman, 1983; Tyler, 1985), 3.4 deg (Raninen & Rovamo, 1987), and 5.7 deg (Kelly, 1984). These factors were largely successful since they provide a good compromise to the present E_2 values for flicker without externally added noise (2.2 - 2.7 deg at 1 - 10 Hz and 4.4 deg at 30 Hz).

In the present experiments flicker sensitivity for a uniform spot in bright light could not be equalised across the visual field at large stimulus sizes, in agreement with Tyler (1981, 1985). Similarly, studies using a series of minified or magnified gratings at each eccentricity have shown that contrast sensitivity in the spatial domain, analogous to flicker sensitivity in the temporal domain, could not be equated across the visual field at large stimulus sizes when using stationary (Watson, 1987; Johnston, 1987) or moving gratings (Wright, 1987; Allen & Hess, 1992).

The slope of the increase in flicker sensitivity with increasing stimulus size was about 1. The increase thus obeyed Piper's (1903) law, since the parameter on the horizontal axis is diameter (instead of area, which would render the slope to 0.5). Similarly, contrast sensitivity for small gratings grows with a slope of 0.5 as a function of area in double logarithmic coordinates (Rovamo, Luntinen & Näsänen, 1993). Flicker sensitivity decreases with increasing eccentricity so slowly that it hardly affects the increase of sensitivity with size and is, therefore, not the reason for the saturation of spatial integration.

It is generally asssumed that signal-to-noise ratio is constant at detection threshold. In bright light the principal source of noise is white internal spatiotemporal neural noise because the spectral density (Pelli, 1990) of quantal noise is negligible. The effect of neural noise decreases with increasing stimulus size because the signal-to-noise ratio of a flickering spot with constant temporal modulation is improved by averaging across space in spatiotemporal noise. This leads to the increase in flicker sensitivity with increasing stimulus size because the signal-to-noise ratio remains constant at threshold.

Flicker sensitivity was found to saturate at large stimulus sizes. The saturation can be explained by assuming that detection is mediated by a matched filter the efficiency of which decreases with increasing stimulus size (see Rovamo, Kukkonen, Tiippana & Näsänen, 1993). The reason for better maximum sensitivity at the fovea for 1 - 3 Hz and in eccentric vision for 30 Hz can be explained by assuming either that the efficiency of detection is better or the spectral density of neural noise is lower for 1 - 3 Hz at the fovea and for 30 Hz in the periphery.

At the smallest stimulus sizes the effect of white internal spatiotemporal neural noise is so strong that it predominantly determines flicker sensitivity, which was therefore identical with and without added external temporal noise. With increasing stimulus size the effect of the internal spatiotemporal neural noise is reduced by averaging across space. At medium stimulus sizes the external white temporal noise has a small effect on flicker sensitivity. This reduces flicker sensitivity only slightly, but enough to change E_2. At large stimulus sizes, when the relative effect of the internal spatiotemporal neural noise is reduced so much that the external white temporal noise becomes the principal source of noise, the signal-to-noise ratio of a flickering spot remains constant because it can no longer be improved by averaging across space in pure temporal noise, which by definition is the same at each spatial location. This explains why in the present experiments flicker sensitivity in external temporal noise was independent of stimulus size when flicker sensitivity was lower with external noise than without, in agreement with the hypothesis of Rovamo, Kukkonen, Tiippana & Näsänen (1993).

External temporal noise made it possible to equate entirely flicker sensitivity across eccentricities by spatial scaling. After adding a significant amount of noise, the maximum sensitivities achieved with large stimulus sizes were reduced and flicker sensitivity curves saturated at the same level. Saturation occurred at smaller stimulus sizes in external temporal noise than without noise, because spatial integration became useless when the relative magnitude of internal spatiotemporal neural noise was so much reduced that pure external temporal noise became the principal determinant of flicker sensitivity.

The spectral density of externally added temporal noise that was needed to reduce maximum flicker sensitivity at 3 Hz by a factor of about 5 was 167 μsec, but the spectral density needed to reduce maximum flicker sensitivity at 30 Hz by a factor of about 8 was clearly less, being only 6.67 μsec. In a similar way, the equivalent spatiotemporal noise decreases with increasing spatial frequency (Pelli, 1990).

Quantal and externally added temporal noise had quite a different effect on flicker sensitivity.

Pure temporal noise was obtained by adding random luminance changes to the flicker signal whereas spatiotemporal quantal noise was increased by reducing the average retinal illuminance. Externally added temporal noise reduced flicker sensitivity only at medium and large stimulus sizes whereas quantal noise (caused by decreasing luminance) reduced sensitivity at all stimulus sizes, in comparison with flicker sensitivities obtained in bright light. The reason for this difference is the fact that quantal noise varies across space and time whereas temporal noise varies only across time and therefore its effect cannot be reduced by averaging across space. Flicker sensitivity saturated at larger stimulus sizes in dim light than in bright light. This implies that the spatial extent of the detection filter increases with decreasing light level.

According to the present results an adequate reduction in luminance resulted in practically equal performance at the fovea and in periphery. In agreement, Mandelbaum and Sloan (1947) studied the effect of reducing luminance on visual acuity using Landolt rings and concluded that there was no significant difference between the fovea and periphery at very low light levels. Quantal noise affected flicker sensitivity less in the periphery probably because the signal was averaged from a larger retinal area than at the fovea. This is in agreement with the finding that decreasing light level reduces contrast sensitivity and visual acuity (spatial resolution) more in foveal than peripheral vision (e.g. Koenderink, Bouman, Bueno de Mesquita & Slappendel, 1978d; Rovamo & Raninen, 1990).

Chapter 12: Face discrimination at various eccentricities

12.1: Introduction

Face recognition and discrimination tasks can be performed by comparing the faces of two individuals or comparing two images of the same face when one of the images has been changed or distorted in some way. A natural face can be modified by displacing the features within the face (Haig, 1984), exchanging the features from another face (e.g. Bradshaw & Wallace, 1971), or changing the facial expression in a series of photographs (Bullimore, Bailey & Wacker, 1991). The images of two different faces can also be combined by means of beam-splitter or by digital image processing. Hübner, Rentschler and Encke (1985) used the latter method to fuse the images of W. C. Fields (actor) and S. Dali (painter).

When the task is to recognize individuals or expressions, thresholds can be recorded as percentages of correct answers (Fiorentini, Maffei & Sandini, 1983; Peli, Goldstein, Trempe & Arend, 1989; Rubin & Schuchard, 1989; Hellige, Corwin & Jonsson, 1984) or as reaction times (Hellige *et al.*, 1984; Glass, Bradshaw, Day & Umiltà, 1985). When the locations of facial features (the eyes, nose, or mouth) have been varied, the threshold of dislocation has been estimated by recording how many pixels a feature can be displaced before the displacement is noticed (Haig, 1984). For mixed faces used by Hübner *et al.* (1985), the thresholds were rated according to a preference score. The observer's task was to indicate in each trial which of the two faces presented, comprising different percentages of information from the two original faces, resembled more the face of Fields, for instance.

Face perception ability can further be assessed by determining the contrast threshold for face recognition. This has been done, for instance, when investigating the effect of age (Owsley, Sekuler & Boldt, 1981) or low vision (Rubin & Schuchard, 1989) on face recognition, as well as when comparing contrast thresholds for the detection and discrimination of "real world" targets with visual acuity and contrast sensitivity for vertical, sinusoidal gratings of selected spatial frequencies (Owsley & Sloane, 1987). Individuals with deficits in the central visual field frequently complain about the difficulty in recognizing faces (Bullimore *et al.*, 1991). Bullimore *et al.* investigated face recognition by presenting the subjects (monocularly) with various sizes of faces. The observers included four normal subjects. The smallest face for which the expression and identity could be distinguished at 50 % probability represented threshold (expressed in terms of viewing distance). During an experimental session, Kolers, Duchnicky and Sundstroem (1985) presented a large number (300) of different faces, each in 2 different sizes, in succession. The sizes were randomly chosen from 5 available sizes ranging from 2 to 10 deg of visual angle in the vertical direction. The task was to indicate whether the face (of whichever size) had appeared before in the sequence. The effect of size

on face recognition was determined, and thresholds were expressed as percentage correct as a function of time lag or size ratio between the presentations.

Few studies have investigated face discrimination specifically in the peripheral visual field, although increasing the stimulus size or presenting the images in two different visual field locations for comparison actually extends the stimuli into the peripheral visual field. Anderson and Parkin (1985) positioned the comparison image at the fovea and the test image in a peripheral location, and the task was to identify whether the second image shown in the periphery (at 4 deg eccentricity) was the "same" or "different" face as the first one shown at the fovea. These type of studies usually investigate hemispheral asymmetry, i.e whether the left or right cerebral hemisphere would show superiority in recognizing faces under different experimental conditions and eccentricity itself is not the subject of interest. Hübner *et al.* (1985) compared performance at the fovea and 2 deg eccentricity with a mixture of two faces or a face mixed with a checkerboard texture. By "M-scaling" the images in the periphery, i.e by increasing the peripheral image size a predetermined amount, the face + checkerboard combination became equally distinguishable at the fovea and in the periphery, whereas a two-face combination was more difficult in the periphery than in the fovea despite the size-scaling.

In the periphery, the visibility of complex stimulus patterns is degraded by spatial interference of adjacent contours (Bouma, 1970; Andriessen & Bouma, 1976; Levi, Klein & Aitsebaomo, 1985; Toet & Levi, 1992). The extent of this crowding effect has been found to be up to 0.5 times the eccentricity studied (eccentricity expressed in degrees of the visual field) in a letter recogniton task (Bouma, 1970). Similar results have been presented for orientational judgments (Andriessen & Bouma, 1976). In a line-vernier task the crowding area has been found to increase approximately at the same rate as vernier thresholds (i.e. with an E_2 of about 0.7 deg, Levi *et al.*, 1985) and when the task is to recognize the orientation of a T - shaped target, the crowding area increases even faster (with an E_2 of 0.2 - 0.4 deg, Toet & Levi, 1992). It would be conceivable that crowding would also degrade peripheral face recognition, because a face consists of a collection of features packed closely together.

Human ability to recognize faces has been suggested to decline with increasing eccentricity (e.g. Hellige *et al.*, 1984) and there has been some difficulty in equating foveal and peripheral performance (Hübner *et al.*, 1985). Since visual performance in many other tasks can be made equal across the visual field simply by an appropriate change of scale, it was interesting to see if this would also be the case with face discriminaton, a spatially complex task, when an appropriate scaling procedure was used. A novel method by which a desired amount of geometrical distortion is introduced into an image was used. An image of a face was distorted by various amounts and the smallest distortion recognized was determined

using a two-alternative forced-choice method. This was done at several eccentricities for a series of face stimuli, all of which were simply magnified or minified versions of one another. Eccentricity dependence was determined by using the method of spatial scaling.

12.2: Methods

Apparatus

The apparatus for the experiment is partly described in the General methods, *Chapter 4.7.3.* The average photopic luminance of the CRT was measured with a Minolta Luminance Meter LS-110, and it was set to 50 cd m^{-2}.

The original image was a photograph of a female face (see *Figure 12.01*) transformed to digital form by means of a scanner (HP Scanjet IIc). In the computer the image was presented as an 242 × 261 -size matrix. A distortion matrix of the same size was obtained by first performing a discrete Fourier transform of the original face image and then band-pass filtering the face image with a circularly symmetric log-Gaussian transfer function:

$$MTF(f) = e^{-\ln^2(f/f_c) / (b^2 \ln 2)}, \qquad (12.01)$$

where f = radial spatial frequency [$f = (f_x^2 + f_y^2)^{0.5}$], f_c = radial centre frequency and b = half of the spectral bandwidth at half-height in octaves. Centre frequency for the filter was 4 cycles per image and bandwidth at half-height of the filter was 1 octave. The inverse Fourier transforms then produced the distortion matrix.

The values in the matrix indicate the amount by which the image will be increased or decreased at each location in the image. Thus, the distortion matrix m(u,v) consists of magnification factors that are used to magnify (m > 1) and minify (m < 1) the image locally. The maximum and minimum values of the distortion matrix m(u,v), which determines the extent at which the details are distorted, were 0.5 (minimum) and 1.5 (maximum). The mean of the values in the distortion matrix m(u,v) was 1. Hence, the distorted image was of the same size as the original.

d

Figure 12.01:
(a) The undistorted face stimulus,
(b) the largest distortion used in the experiment,
(c) a strongly distorted test stimulus corresponding to a correlation sensitivity of 10,
(d) a moderately distorted test stimulus corresponding to a correlation sensitivity of 26,
(e) a slightly distorted test stimulus corresponding to a correlation sensitivity of 70, i.e. about the smallest detectable distortion. Note that the images on this page are not photographs. The differences between (a) and (e) are extremely difficult, if not impossible, to detect due to the printing quality of the images.

Point (x,y) in the *original* image corresponding to location (u,v) in the *distorted* image was determined by calculating the cumulative sum of the magnification matrix m(u,v) horizontally and vertically starting always from the top left corner, which represented the point (0,0):

$$x(u,v) = \sum_{i=0}^{u} m(i,v) \qquad (12.02)$$

$$y(u,v) = \sum_{j=0}^{v} m(u,j) \qquad (12.03)$$

The distorted image is then created by placing a grey-scale value from the original image (G) at the location (x,y) calculated above to the distorted image (G') at the location (u,v): G'(u,v) = G(x,y). The values calculated by the above equations for x and y are usually not integers. Thus, they are rounded to the closest integer. The distortion algorithm above was developed by Dr R. Näsänen. When distorted in this manner, the image retains its sharpness and continuity of features, only the shapes within the image change. The amount of distortion can be adjusted in infinitely small steps by changing the magnification matrix m(u,v). In this case it was obtained by multiplying m(u,v) by a decreasing series of constants spaced equidistantly on a logarithmic scale (step size 0.1 $\log_{10}$ units corresponding to a factor of 1.26). For the present experiment a total of 23 test images were created comprising a decreasing series of distortions (see *Figure 12.01*).

Correlation sensitivity (S_r) is calculated as $S_r = (1 - r)^{-1}$, where r is the correlation coefficient between the undistorted image (*Figure 12.1a*) and the distorted image that allows discrimination between them at the level of 84 % of correct. Correlation coefficient $r = \Sigma\Sigma I_d(x,y)I_o(x,y)/\{\Sigma\Sigma I_d^2(x,y)\Sigma\Sigma I_o^2(x,y)\}^{0.5}$, where I_d is the distorted image and I_o is the original image.

The least distorted image that still could be discriminated from the undistorted image was determined by a two-alternative forced-choice algorithm with feedback. The subject's task was to indicate, via the keyboard, which one of the two successive exposures accompanied by similar sound signals contained the distorted stimulus. The estimation of threshold distortion took place in two consecutive staircases. The first staircase started from the most distorted image and distortion was changed image by image within the image series. A random subthreshold starting point was established using this first staircase with one correct - down, one wrong - up -rule. The *second* wrong choice initiated the second staircase, which measured the distortion required for the level of 84 % correct (Wetherill & Levitt, 1965). The

estimate of threshold contrast was an arithmetic mean of the last 8 reversals of a threshold estimation session and each datapoint shown in the figures is a median of at least three threshold estimates.

Stimulus

The stimulus was a distorted photograph of a female face (see *Figure 12.01*), which was presented at 90 % Michelson contrast. The horizontal and vertical dimensions of the equiluminous surround were 26.3 and 19.5 cm, respectively. On the CRT, three image sizes were used in the experiment. The largest image size was 9.9 × 10.7 cm, the medium size was 5.0 × 5.4 cm, and the smallest size 3.0 × 3.2 cm in horizontal (width) and vertical (height) dimensions, respectively. The range of viewing distances was 0.14 - 4.91 m, resulting in angular image widths of 0.35 - 35 deg. Control experiments showed that equal thresholds were obtained whichever stimulus size was used, as long as its angular size in the visual field was held constant.

Procedure

Sensitivity for face discrimination was measured with a set of stimulus sizes in random order at the fovea and eccentricities of 5, 10 and 20 deg. The duration of the stimulus was 1000 msec. The inter-stimulus interval was 600 msec and the delay for the new trial after each response was 250 msec. To avoid adaptation, which was strong at 10 and 20 deg eccentricities, the subjects fixated above or below the fixation point during the first presentations showing the most distorted images, as long as they were easily discernable from the original image. Further, the subjects did not start the next presentation immediately, but rested with their eyes open for a short period of about 10 sec between individual stimulus presentations.

The room was dimly illuminated so that just enough indirect light was available for the fixation target (a black dot on a white background) to be seen. No reflections were visible on the CRT and the surround of the CRT was always of lower luminance than the screen itself. For the foveal presentation the fixation target was positioned in the middle of the right hand edge of the image. Thus, as the both observers used their right eye, the whole image was always positioned in the nasal visual field. For the peripheral stimuli the fixation target was placed so that the stimulus was on the horizontal meridian further in the nasal visual field. Eccentricity therefore refers to the angular distance between the nearest (right) edge of the stimulus and the point of fixation.

Subjects

The results of two observers, PM and SU, are shown. SU, albeit well trained in this specific task was naïve as to the purpose of the experiment. Both observers were fully corrected moderate myopes (PM -2.25 DS; SU -4.00 DS) with no ocular abnormality. Viewing was monocular using the dominant eye, which by coincidence was the right eye for both PM and SU.

The purpose of the experiment was, by utilizing a novel method of image distortion, to measure the smallest detectable amount of geometrical distortion of a human face at several eccentricities. The results would reveal whether this presumably spatially complex task can be made equal across the visual field simply by an appropriate change of scale.

12.3: Results

In *Figure 12.02* correlation sensitivity is shown as a function of the horizontal image size for subjects PM and SU at the fovea and at 5, 10 and 20 deg eccentricities. At all eccentricities thresholds first increased with a stimulus size up to a critical size. In double logarithmic coordinates the slope of this increase in sensitivity with increasing size was about 1. A deviation from this linear increase of the sensitivity function is seen only at the smallest stimulus sizes of PM at 5, 10, and 20 deg eccentricity, where sensitivity was independent of stimulus size. At large stimulus sizes the increase saturated and correlation sensitivity became independent of size at all eccentricities. The critical stimulus size for spatial summation increased with eccentricity.

The shapes of the sensitivity curves at different eccentricities are similar - they are simply displaced along the horizontal axis relative to one another. The amount of this displacement reveals the rate at which magnification needs to increase with increasing eccentricity. Scaling factors, which were required to shift the peripheral data leftwards along the x-axis in order to bring the data points into alignment with the foveal data, were then found for each eccentricity. An initial scaling factor determined visually was used to divide the size values of the peripheral data points at a chosen eccentricity. To assess how well this estimated factor minimised variance between the foveal and eccentric data points, a second-order polynomial regression curve was fitted to the combination of the two data sets. All the parameters of this curve were allowed to float freely in order to obtain the best possible fit. The sum of squares of residual deviations around this curve was calculated. The process was then repeated with other estimates around the initial value until finding a scaling factor which minimised the sum of squares of residual deviations. This factor was then accepted as the final scaling factor for the eccentricity in question. Scaling factors for other eccentricities were determined in the same way.

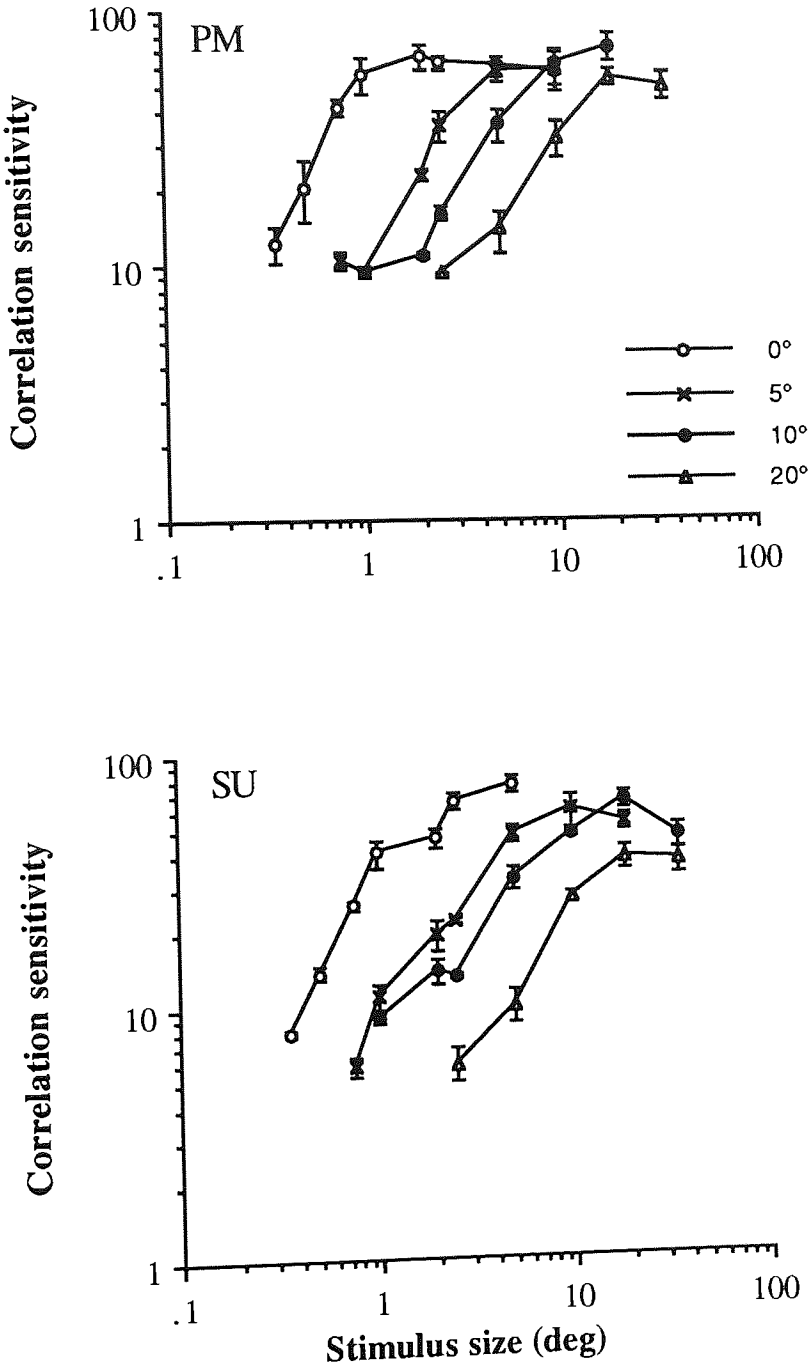

Figure 12.02a: Correlation sensitivity for subjects PM and SU plotted against horizontal stimulus sizes (in deg). Symbols and standard errors are shown.

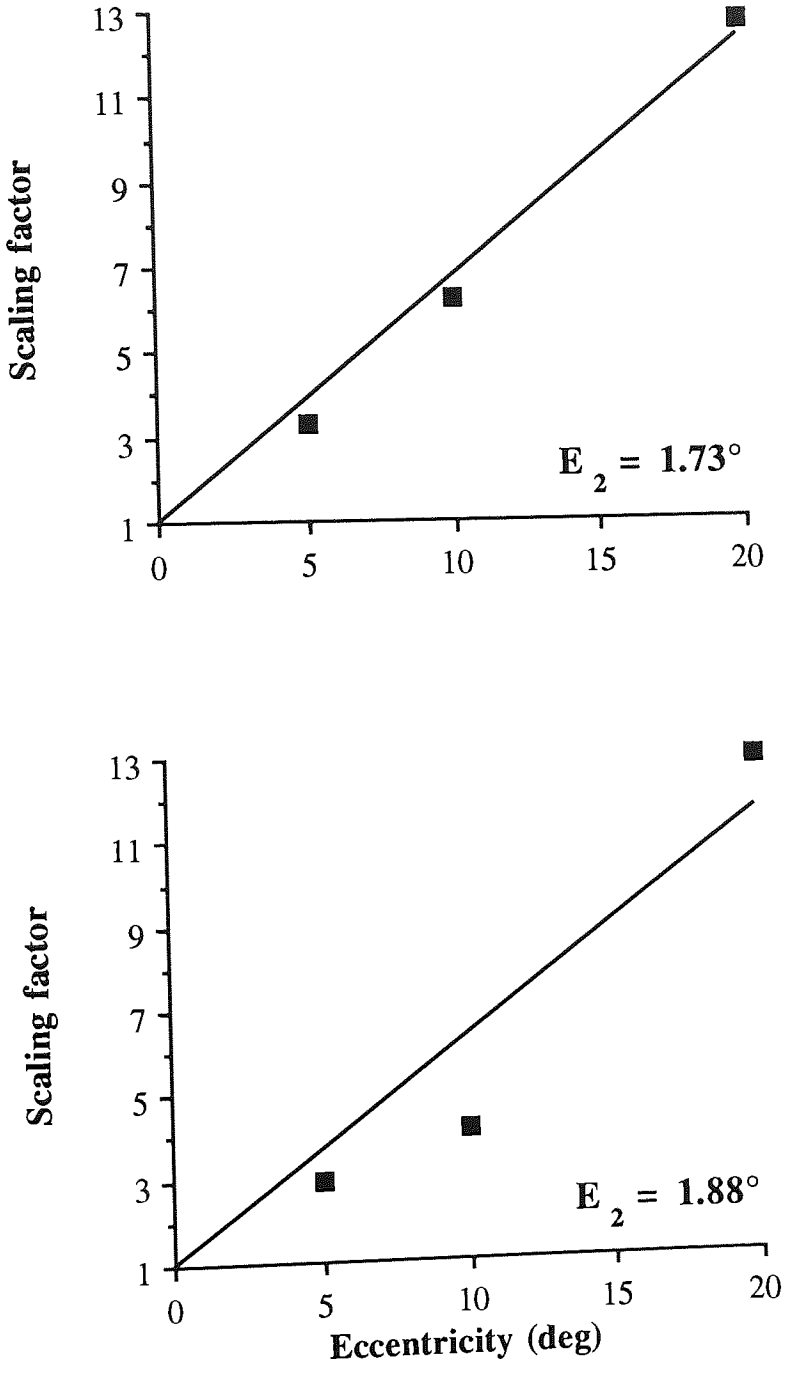

Figure 12.02b: Scaling factors plotted against eccentricity, E_2 values are shown. Subjects as in (a).

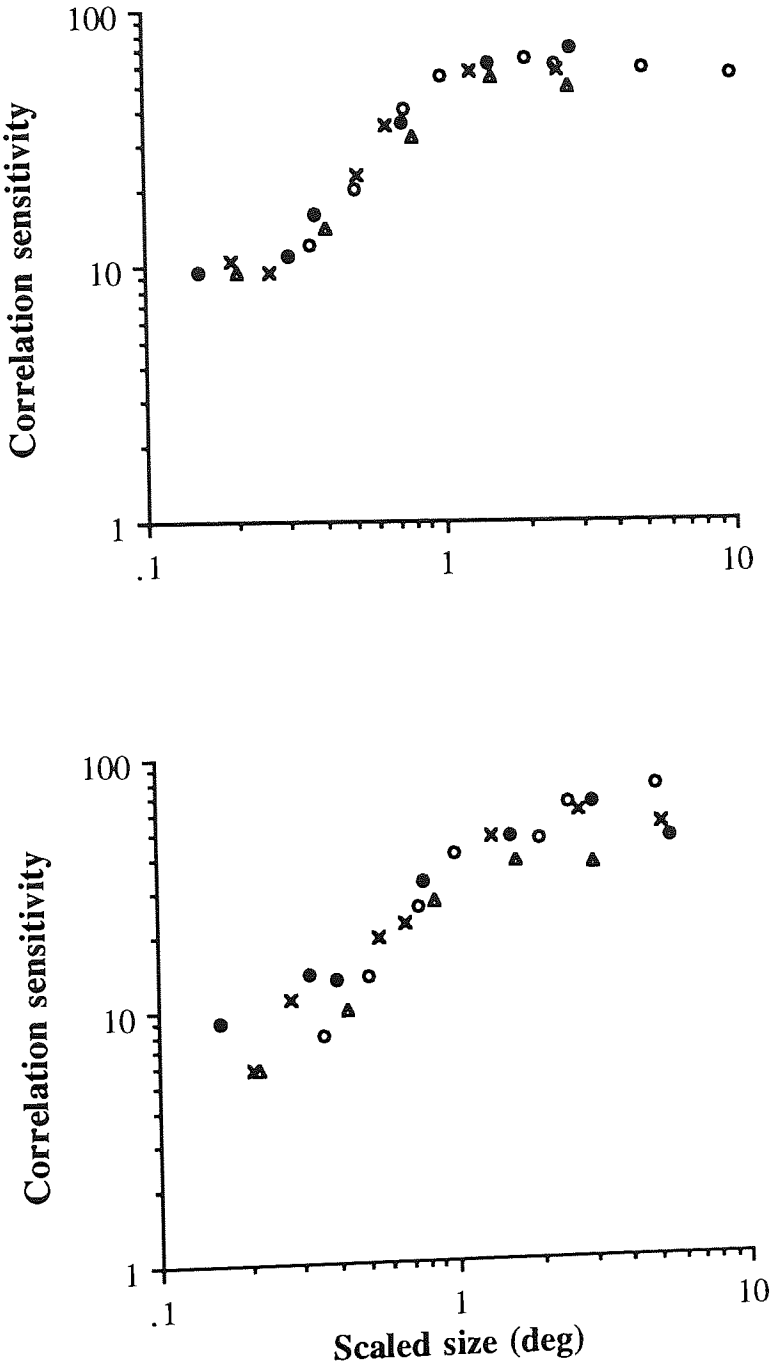

Figure 12.02c: Correlation sensitivity plotted against the scaled stimulus sizes. Symbols and subjects as in (a).

Figure 12.02b shows the scaling factors obtained at each eccentricity for both subjects. The factors are plotted against eccentricity and the data has been fitted with a linear regression line. The foveal scaling factor is constrained to be 1, since the foveal data scaled onto itself gives the value of 1. According to equation *4.04*, $E_2 = {}^1/_S$. The gradient of the linear regression, S, was transformed to E_2, which was found to be 1.73° (± 0.11) deg for PM and 1.88° (± 0.41) deg for SU. The explained variance (r^2) for the line of least squares was 98.5% and 88.1% for PM and SU, respectively.

In *Figure 12.02c* the data of both observers from *Figure 12.02a* has been scaled according to equation *4.09*, $F = 1 + {}^E/E_2$. The scaled data of both subjects have been replotted as a function of scaled stimulus size in *Figure 12.02c*. Correlation sensitivity for face discrimination increases with increasing scaled stimulus size until at large sizes performance tends to become independent of size.

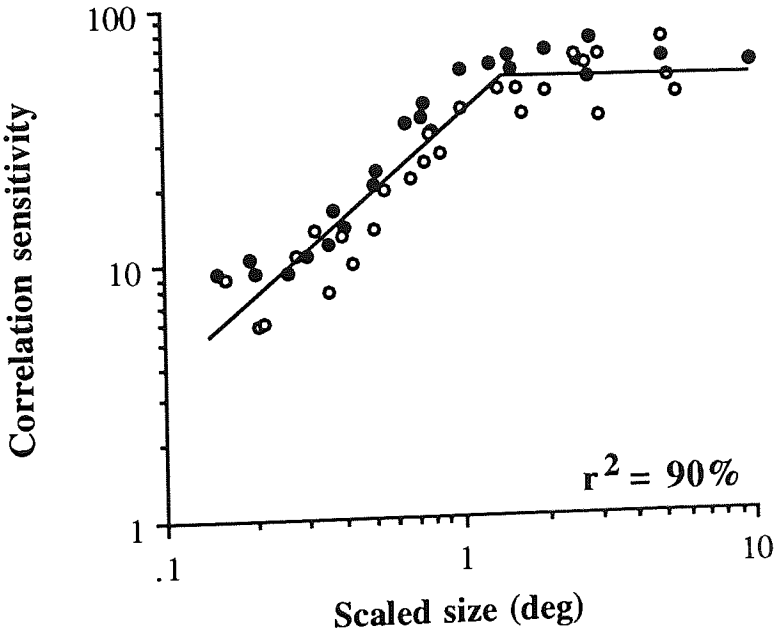

Figure 12.03: Correlation sensitivity for both subjects plotted against the scaled stimulus sizes. Filled circles, PM; open circles, SU.

A single parameter E_2 is clearly successful in removing the eccentricity dependent variance from the data, since all data points collapsed together to form a single function. To further evaluate the data, the explained variance for the scaled data was estimated. The scaled data of two subjects were combined (from *Figure 12.2c*). The variance of the observed data from the predicted data was calculated (the least square line with a slope of 1 and its horizontal extension drawn through the data represents the predicted data in *Figure 12.03*) and this was expressed as a proportion of total variance. This is usually expressed as the percentage of

variance explained by multiplying it by 100. The proportion was calculated using the following equation:

$$r^2 = 1 - \Sigma(\log S - \log S_{est})^2 / \Sigma(\log S - Z)^2 \qquad (12.04),$$

where S = correlation sensitivity, S_{est} = the predicted sensitivity, and $Z = n^{-1}\Sigma\log S$. It is necessary to use logS rather than S, because sensitivities are plotted on a logarithmic scale. The values of S_{est} were calculated separately for the increasing and the saturated portions of the data. For the saturated portion S_{est} was simply the geometric mean of the datapoints. For the increasing portion the thresholds were first divided by the scaled stimulus sizes. Then their geometric mean was used as a constant for determining S_{est} by using the formula S_{est} = constant × scaled size. Explained variance (r^2) was found to be 90 %

12.4: Discussion

In this study the spatial scaling method was used successfully to equate foveal and peripheral performance for face discrimination. E_2 values for face discrimination were found to be 1.73° (± 0.11) deg for PM and 1.88° (± 0.41) deg for SU. These values correspond roughly to the E_2 values for vernier acuity, orientation discrimination and curvature detection which are 1.06 - 1.96 (*Chapter 5*), 1.95 (*Chapter 9*) and 1.84 - 1.96 deg (Whitaker, Latham, Mäkelä & Rovamo, 1993), respectively. Direct comparison of the values is possible, since the same method of spatial scaling has been used in all experiments.

When scrutinizing the distorted facial test images (*Figure 12.01*), it can be seen that the distortion is most detectable at the mouth area. This is quite coincidential, and is due to the distortion matrix used. The observers confirmed that at each location in the visual field it was actually the distortion of the mouth that could be seen just above threshold, so that feature was specifically attended to. This type of selective observation of the test image reduces the task to one of simple shape discrimination, where combinations of spatial offset (vernier acuity), curvature and orientation discrimination are likely to determine performance. The assumption that vernier, curvature and orientation discrimination mechanisms were used when performing this specific experiment is supported by the similarity of the E_2 values in the tasks. It is a very interesting finding that an apparently complex task such as face discrimination can be equated across the visual field to performance in simple positional tasks.

Of the previous studies on face discrimination, that of Haig (1984) is one of just two which are comparable with the present study. Unfortunately, however, he did not extend his investigation into the visual periphery. Haig found that the vertical positioning of the mouth was most important when judging which of the two pictures presented was the original and

which one was modified. Sensitivity for displacement of the eyes and nose was not as good. Note however, that in the present experiment it was not the location of the mouth which varied, but it's shape.

Hübner *et al.* (1985) presented mixed-face stimuli in the peripheral visual field, albeit only at 2 deg eccentricity. The images were produced digitally. A test image containing, for instance, 30 % of target face and 70 % of masking image (another face or a checkerboard texture) was formed by adding up the intensity values of corresponding pixels in the two images; 30% of the intensity value in the target face pixel and 70 % of the intensity value in the masking image pixel. The peripheral image size was M-scaled approximately according to the estimates of Rovamo and Virsu (1979) so, that the viewing distance was decreased from the foveal 1 m to 1.7 m at 2 deg eccentricity. This increase in size corresponds to using an E_2 of 2.86 deg, which is not very different from the present values 1.73 - 1.88 deg, but indicates that the image was probably somewhat smaller than optimum at the peripheral location. Two mixture images containing different intensities of the target face were presented sequentially. The task was to decide in which of the two images the target face was seen more clearly. Increasing target energy predictably led to an increase in the proportion of correct responses. This trend of detection with increasing target energy was similar at the fovea and at 2 deg eccentricity when the target face was mixed with the checkerboard texture. However, when two faces were fused, detecting the target face at 2 deg eccentricity was more difficult than at the fovea. Thus, according to the findings, M-scaling was successful in equating foveal and peripheral performance when a face was fused with a checkerboard pattern, whereas peripheral recognition remained poorer than at the fovea, when two faces were fused. The authors suggested that the masking effect is stronger in extrafoveal than in foveal vision in the presence of spectrally adjacent noise energy.

The great advantage of the present image distortion method is that the amount of distortion can be quantified accurately. The method can be used both in natural images (scanned photographs) and artificially produced images. Practical applications include evaluation of the ability to recognize faces for i) people who may need to identify individuals in their profession (e.g. police) and ii) for patients with central visual field losses (due to e.g. macular degeneration), amblyopia or other visual deficits.

13. Conclusion

The present results show that, irrespective of the particular foveal stimulus size chosen, the performance in vernier acuity, spatial interval discrimination, bisection acuity, displacement detection, orientation discrimination, flicker sensitivity, and face discrimination can be made independent of visual field location at eccentricities of 0 - 15 deg (0 - 20 deg for face discrimination) by properly magnifying the stimulus with increasing eccentricity. In certain tasks this independence of eccentricity was critically dependent on the segregation of the confounding effects of eccentricity and separation between stimulus parts. The amount of magnification needed increased approximately linearly with eccentricity but the slope of increase depended on the task. These findings agree with the general magnification theory (Virsu, Näsänen & Osmoviita, 1987) stating that the detectability of any foveal stimulus can be matched in peripheral vision by a suitable magnification of the stimulus in every spatial dimension.

13.1: Differences between tasks

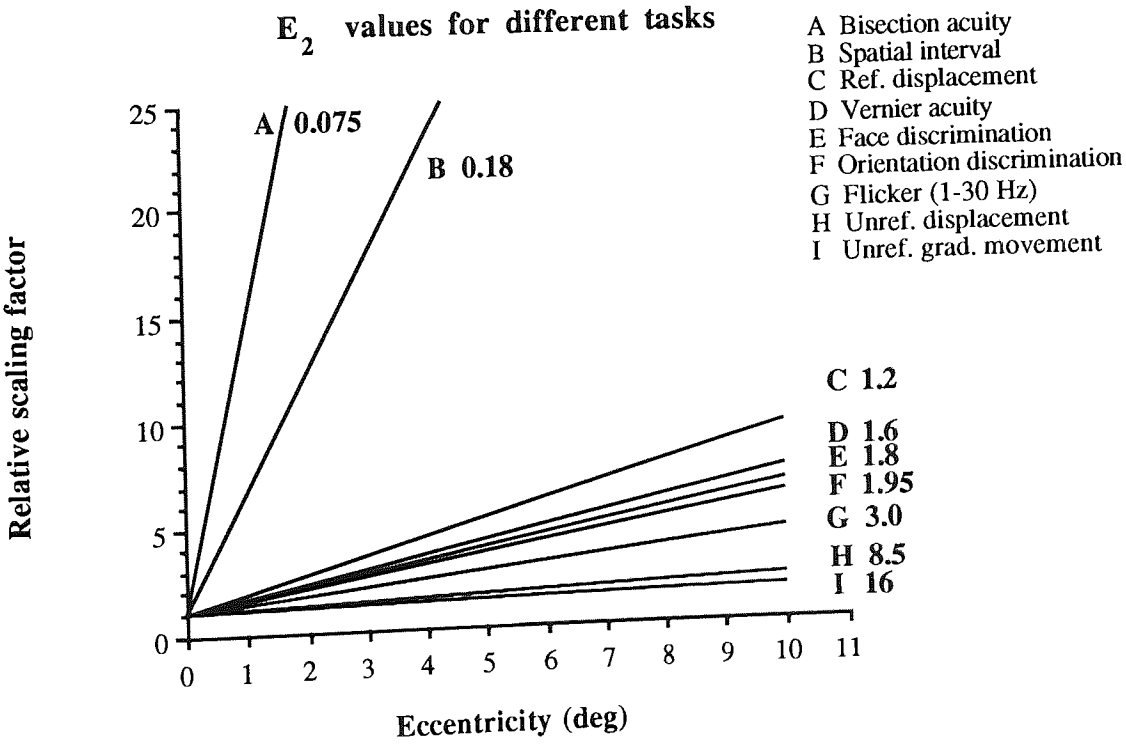

Figure 13.01: Normalized gradients (relative to 0 deg eccentricity) corresponding to the E_2 values in all the tasks investigated in the present thesis.

In *Figure 13.01* the normalized gradients corresponding to the present E_2 values have been plotted in the same graph for comparison. According to the present results E_2 for bisection acuity is about 200 times smaller than for discrimination of unreferenced gradual displacement. In addition, even between the hyperacuities E_2 varies 26 -fold.

The primary cortex is only one of the areas on which the visual field is mapped. If different aspects (colour, motion, texture) of a stimulus are processed at different locations possessing unequal cortical magnifications, thresholds may be unevenly affected by their relative influence with increasing eccentricity. However, according to Gattass, Sousa and Covey (1985) the increase of $1/M$ with eccentricity is fairly similar in many visual areas. The lowest slope occurs in the parieto-occipital area PO and steepest in V4 of the macaque monkey. On the basis of Figure 6 of Gattass *et al.* these slopes correspond roughly to E_2 values of 4 deg for PO and 1.7 for V4. A greater degree of foveal emphasis may be present in the non-topological representation of the temporal lobe (Drasdo, 1991). Thus, it is not easy to explain the widely differing E_2 values with differences in magnification factors between various cortical areas. Further, it seems unlikely that the hyperacuity stimuli consisting of 2 - 3 squares in a purely spatial task (bisection acuity, spatial interval discrimination, and vernier acuity with a 21 -fold difference in E_2) would be processed in different cortical areas.

It has been suggested that the discrepancies in gradients amongst different tasks may be determined by the relative activity within separate processing channels, each having their own magnification factor (Connolly & Van Essen, 1984; Drasdo, 1989, 1991), the relative contributions of which depend upon the spatio-temporal characteristics of the task. If these two channels possess dramatically different distributions across the visual field, one being highly specialized for foveal vision, the other more evenly distributed across all eccentricities, the rate of threshold increase with eccentricity in any given task would then depend upon the extent to which visual processing was mediated by one channel or the other. This could mean that, for instance, performance in tasks requiring recognition or colour discrimination would decline faster with eccentricity than contrast detection for a flickering grating. However, whether there is a difference in the sampling densities of the two channels (de Monasterio, 1978; Harwerth & Levi, 1978; Connolly & Van Essen, 1984; Schein & de Monasterio, 1987; Drasdo, 1989, 1991), or not (Livingstone & Hubel, 1988a; Perry & Silveira, 1988), the difference is all too small to account for the differences in threshold gradients observed in the present study. It does not seem possible to explain the 200 -fold differences in the present E_2 values by different sampling densities of M- and P-cell populations, since E_2 has been estimated to be 4.8 deg for M-cells and 1.2 deg for P-cells, providing only a four-fold difference in E_2 (Drasdo, 1991). By suitably weighting the contribution from M- and P-cell populations it would be possible to obtain E_2 values between 1.2 and 4.8 deg, but this range is still too narrow to cover all the E_2 values obtained in this

thesis.

Deeley and Drasdo (1987) and Toet, Snippe and Koenderink (1988b) suggest that the difference in the rate of decline in acuity tasks and relative localization tasks is due to optical effects. Aberrations and the structures of the media of the human eye degrade the image as would a low pass filter, reducing visibility at high spatial frequencies. This filtering is useful because at the fovea it reduces aliasing resulting from moiré patterns formed between a periodic stimulus and the regular mosaic of receptors and improves hyperacuity performance by allowing interpolation (Snyder, 1982). Filtering has no significant effect in peripheral vision due to the faster increase in neural sampling interval compared with optical degradation (Charman, 1983). Therefore, the blur of the peripheral point spread function is small compared to neural sampling density, hence depriving the periphery of the multiple samples required for hyperacuity performance. These factors would lead to an artificially high rate of decline in hyperacuity with increasing eccentricity by increasing sensitivity only at the fovea.

Spatial undersampling and positional irregularity have been proposed to occur in the periphery (Wilson, 1991), which would in turn selectively degrade peripheral performance, specifically at small stimulus sizes. The present magnification method using a series of stimuli that were magnified versions of each other guaranteed, however, that multiple samples were available at each eccentricity. Peripheral undersampling is, perhaps, one of the reasons why the stimuli in tasks such as spatial interval discrimination and bisection need to be increased in size so rapidly with eccentricity. However, the similarity of the shape of the functions at different eccentricities reinforces the view that scale invariance can be demonstrated for many different tasks despite the abovementioned qualitative differences between foveal and peripheral vision (blur, undersampling and positional irregularity).

In essence, whichever single scaling factor is chosen, whether the choice has been based on anatomically or psychophysically acquired information, no single factor can be successfully applied to all tasks, because in different tasks and by using different stimuli changes in visual performance with increasing eccentricity are very different (Weymouth, 1958; Rovamo & Virsu, 1979; Levi, Klein & Aitsebaomo, 1984, 1985; Saarinen, Rovamo & Virsu, 1989; Drasdo, 1991).

13.2: Possible explanations for differences in E_2 values

One explanation for the 200 -fold difference in E_2 values could have been a dynamic, task and eccentricity dependent allocation of neural information processing resources suggested by Van Essen and Anderson (1990). This type of allocation of neural resources has been

demonstrated in the primate (Richmond, Wurtz & Sato, 1983). When testing this possibility in an experiment in which eccentricity dependent performance was measured simultaneously in two tasks, each possessing markedly different E_2 values, it became clear that there were no changes in E_2 values whether the attention was directed in one task or divided between two tasks. Therefore, task-dependent variation in neural allocation does not seem to be the mechanism responsible for the variation in E_2 values, at least not in the tasks investigated.

Another explanation for the variation in the E_2 values could be based on the receptive field sizes of the neural elements. Large receptive fields are known to be evenly distributed across the visual field, whereas the small fields only reside at the fovea, the minimum receptive field size increasing with eccentricity (see *Figure 13.02*). It has been suggested (e.g. Tolhurst, 1973) that movement is detected by large receptive fields having preference to low spatial frequencies even at the fovea, whereas pattern analysis would be performed using small receptive fields sensitive to relatively high spatial frequencies. For tasks where, at the fovea, high resolution is needed and where blurring the stimulus deteriorates performance (e.g. resolution), small receptive fields are used for optimum performance. Doubling of this receptive field size therefore occurs at a small eccentricity (*Figure 13.02*). For tasks where large receptive fields are utilized even at the fovea, the doubling of receptive field size occurs at larger eccentricities and this results in a larger E_2 value. This type of arrangement may be the reason for the differences in E_2 values between certain tasks, although the only difference it could account for would be between resolution tasks (E_2 ~ 2 deg) and tasks with larger E_2 values than this.

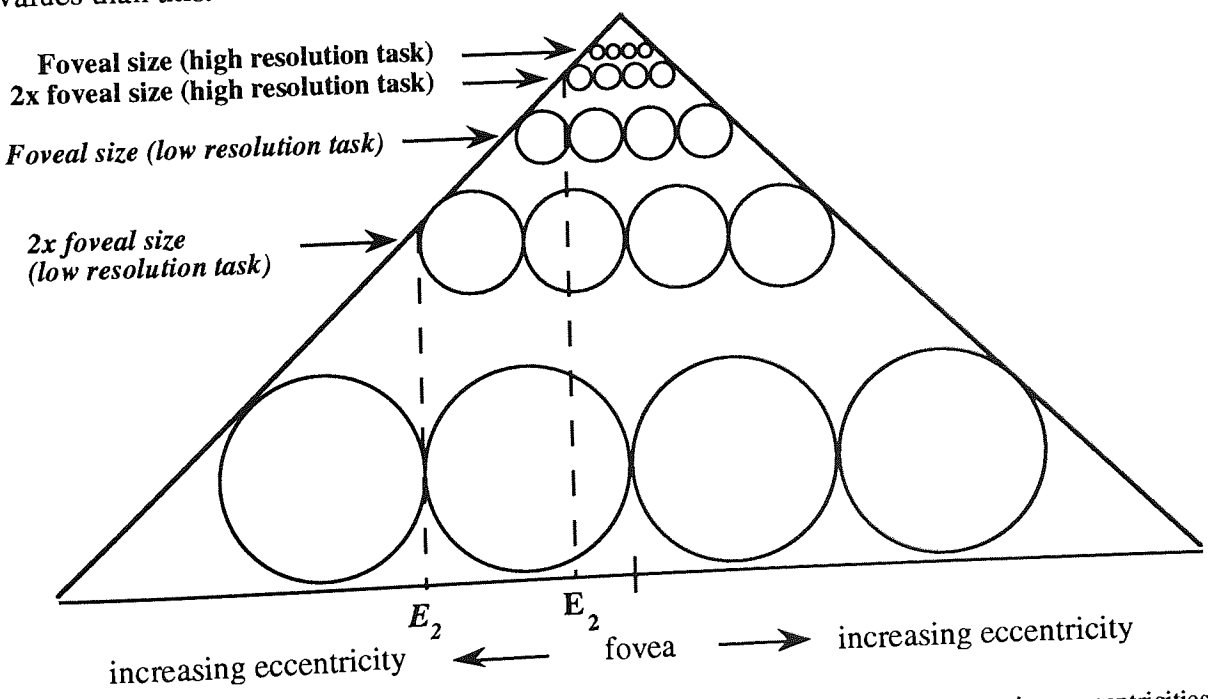

Figure 13.02: A schematic drawing of the receptive fields of the neural elements at various eccentricities and a theory on why the E_2 value becomes different in two different tasks.

It has become clear that psychophysical E_2 values should not be used for *predicting* the E_2 values of cortical visual areas, because by choosing the task and stimuli appropriately it seems possible to obtain virtually any E_2. In *Table 13.01* E_2 values for several psychophysical tasks are shown. The values obtained in the present study have been included.

Table 13.01: Some estimates of E_2 in psychophysical tasks

(Values other than acquired in the present experiments, and marked with (*) have been determined by the present author)

Task / Investigators	E_2 (deg)	Eccentricity range (deg)	Specific features
VERNIER ACUITY			
present study	1.23-1.78	0-15	lines
	1.06-1.96	0.267-15	isoeccentric dots
Levi, Klein & Aitsebaomo (1985)	0.6-0.8		
Virsu, Näsänen & Osmoviita (1987)	1.88*	0-20	scaled by the present method
Westheimer (1982)	1.14*	0-10	based on optimum thresholds
Klein & Levi (1987)	0.19	0-20	3-dot stimulus
Toet, Snippe & Koenderink (1988a)	0.19	0-20	3-dot stimulus
SPATIAL INTERVAL DISCRIMINATION			
present study	0.17-0.19	0.267-7.5	ISI 50 msec
	0.07-0.22	0.267-7.5	ISI 500 msec
Levi & Klein (1990a)	-0.03*	1.25-10	isoeccentric
McKee, Welch, Taylor & Bowne (1990)	0.04*	0.15-2.4	non-isoeccentric
Yap, Levi & Klein (1989)	0.6-0.8	0-10	non-isoeccentric
Levi & Klein (1990b)	0.68-0.83	0-10	non-isoeccentric
BISECTION			
present study	0.07-0.08	0.267-7.5	configuration (a)
	-0.10- -0.03	0.267-7.5	configuration (b)
Levi & Klein (1990a)	0.31*	0.625-10	isoeccentric
	0.44-0.47		Levi & Klein's own estimate
Yap, Levi & Klein, (1987a)	0.55-0.59	0-10	non-isoeccentric
Klein & Levi (1987)	0.15-0.31	0-10	non-isoeccentric
DISPLACEMENT			
present study	1.06-1.35	0.533-10	ref. instantaneous
	6.3-11.1	0-10	unref. instantaneous
	13.5-18.5	0-10	unref. gradual (1 sec)
Leibowitz, Johnson & Isabelle (1972)	12*	0, 10, 20	unref. gradual (1 sec)
Johnson & Scobey (1980)	12*	0, 18	unref. gradual (1 sec)
Post & Leibowitz (1981)	13*	0, 30	unref. gradual (0.1-1 sec)
Johnson & Leibowitz (1976)	10*	0, 30	unref. gradual (0.1-1 sec)
Post, Scobey & Johnson (1984)	12*	0-17	unref. (2.5-80 msec)
Johnson & Scobey (1980)	9*	0, 18	unref. (50 msec)
Levi, Klein & Aitsebaomo (1984)	5.6-13.9	0-30	unref.instantaneous
McKee & Nakayama (1984)	1.7*	0-40	rel. (52 msec) motion detection
Levi, Klein & Aitsebaomo (1984)	1.3	0-10	ref. motion discrimination (grating)
Levi, Klein & Aitsebaomo (1984)	1.05	0-10	ref. motion detection (grating)

ORIENTATION			
present study	1.95	0-15	
Westheimer (1982)	1.85*, 2.28*	0-10	
Paradiso & Carney (1988)	2.4*	0-20	
VISUAL ACUITY			
Yap, Levi & Klein (1989)	1.7-2.0	0-10	resolution, dots
Levi & Klein (1990b)	2.1-2.5	0-10	resolution, lines
McKee & Nakayama (1984)	2.7*	0-40	grating acuity
Virsu *et al.* (1987)	2.4*	0-20	grating acuity
Westheimer (1967)	0.9*	0-10	Snellen E acuity
Virsu *et al.* (1987)	1.7*	0-20	Snellen E acuity
Westheimer (1979)	2.8*	0-10	Snellen E acuity
Virsu *et al.* (1987)	1.0*	0-20	Landolt C acuity
Weymouth (1958)	1.4*	0-20	Landolt C acuity
CONTRAST SENSITIVITY			
Watson (1987)	4.2*	0, 3	contrast sensitivity
Johnston (1987)	5.4*	0-20	contrast sensitivity
Rovamo & Virsu (1979)	2.38-3.45	0-30	contr. sens. at four principal meridians (see *Table 3.02*)
OTHERS			
Lie (1980)	9.35*	0-25	detection
Johnston & Wright (1986)	3.77*	0-25	lower threshold of motion
Kelly (1984)	5.7*	0-12	flicker sensitivity (0.5 Hz)
Fendick & Westheimer (1983)	0.63*	0-10	stereoscopic acuity
Levi *et al.* (1985)	~0.7	0-10	crowding
Toet & Levi (1992)	0.2-0.4	0-10	crowding

In *Table 3.03* the values for cortical magnification varied between 0.68 - 3.45 deg. The data of Curcio *et al.* (1987) suggest an E_2 value of 3.0 deg within 0 - 7.1 deg eccentricity for retinal cones. In addition, Drasdo (1991) has determined the following E_2 values: M-cells, 4.76 deg; P-cells, 1.29 deg; all retinal ganglion cells, 1.36 deg; cortical magnification (V1), 1.14 deg. These values have been mentioned in *Chapter 3*.

The ultimate reason for the diverse differences in the rate at which performance falls with eccentricity in different tasks remains uncertain. The points discussed above may all contribute to these differences, and there are probably other contributory factors which have been overlooked. The reasons why such diverse peripheral gradients have developed is clear. Predators prefer to attack their prey from behind and it is obviously crucial for survival to detect movement of the approaching enemy in the peripheral visual field as early as possible. Static tasks, on the other hand, usually represent little or no threat, and allow time to direct gaze at the target for closer scrutiny. Due to the limited transmission capacity of the visual system, especially of the optic nerve, it is necessary to restrict the information flow from the retina to the cortex. Therefore, movement sensitivity is not concentrated at the central fovea, but is evenly distributed throughout the visual field. The ability to perform extremely precise

spatial judgements is fovea-centered and declines rapidly away from central vision. The need for central precision can be explained by the importance of, for instance, being able to detect prey or a pond of water large distances away. Although one can conceive the reasons why the visual system is specialized is such useful manner, the precise physiological mechanisms by which this is achieved still remain to be unveiled.

Whereas the experimental results of this thesis were not expected to explain the entire processes of peripheral vision, they have been able to confirm in several tasks the quantitative nature of the differences between foveal and peripheral vision. The unexpectedly large diversity of peripheral gradients, all obtained using the same methodology, represents the main outcome of this work.

Publications and Presentations

Full papers

Whitaker, D., Rovamo, J., MacVeigh, D. and **Mäkelä, P.** (1992) Spatial scaling of vernier acuity tasks. *Vision Research*, 32, 1481-1491.

Whitaker, D., **Mäkelä, P.**, Rovamo, J. and Latham, K. (1992) The influence of eccentricity on position and movement acuities as revealed by spatial scaling. *Vision Research*, 32, 1913-1930.

Mäkelä, P., Whitaker, D. and Rovamo, J. (1993) Modelling of orientation discrimination across the visual field. *Vision Research*, 33, 723-730.

Whitaker, D., Latham, K., **Mäkelä, P.** and Rovamo, J. (1993) Detection and discrimination of curvature in foveal and peripheral vision. *Vision Research*, 33, 2215-2224.

Mäkelä, P., Rovamo, J. and Whitaker, D. (1994) Effects of luminance and temporal noise on flicker sensitivity as a function of stimulus size at various eccentricities. *Vision Research*, in press.

Book chapter

Rovamo, J., **Mäkelä, P.** and Whitaker, D. (1993) Models of the visual cortex on the basis of psychophysical observations. In *Functional organisation of the human visual system*, Wenner-Gren Center International Symposium series, Basingstoke, Macmillan, pp.241-254.

Manuscripts under preparation

The effect of eccentricity on simultaneous performance in two separate tasks

Face discrimination at various eccentricities

Abstracts

Mäkelä, P., Rovamo, J. and Whitaker, D. (1991) The effect of spatial scaling on positional acuities in foveal and peripheral vision. *The Abstract Collection of ScanVision '91 Congress* in Copenhagen, Denmark 12-14 April 1991.

Mäkelä, P., Rovamo, J. and Whitaker, D. (1991) Vernier line and two-dot vernier acuities in peripheral vision. *Ophthalmic and Physiological Optics*, 11, p.396.

Mäkelä, P., Rovamo, J. and Whitaker, D. (1991) Spatial scaling of vernier and bisection acuity in foveal and peripheral vision. *Perception*, 20, p.74.

Mäkelä, P., Rovamo, J. and Whitaker, D. (1991) Spatial scaling of positional acuities across the visual field. *European Journal of Neuroscience*, Suppl.4, p.177.

Mäkelä, P., Whitaker, D. and Rovamo, J. (1991) Spatial scaling of absolute and relative movement discrimination. *Optics and Photonics News*, Suppl.2, p.73, and *OSA Technical Digest Series*, 17, p.123.

Mäkelä, P., Whitaker, D. and Rovamo, J. (1992) An example of the enormous task-dependent variations in peripheral visual performance. *Investigative Ophthalmology and Visual Science*, 33, p.825.

Mäkelä, P., Whitaker, D. and Rovamo, J. (1992) Modelling of orientation discrimination at various eccentricities. *Perception*, 21, Suppl.2, p.99.

Mäkelä, P., Whitaker, D. and Rovamo, J. (1993) Dependence of flicker sensitivity on size, luminance and eccentricity. *Perception*, 22, Suppl., p.132

Mäkelä, P., Rovamo, J. and Whitaker, D. (1994) Face perception at various eccentricities. *Perception*, submitted.

Presentations

Oral presentations

Mäkelä, P., Rovamo, J. and Whitaker, D. (1991) Spatial scaling of positional acuities across the visual field. *European Neuroscience Association* (ENA), United Kingdom. September 8 - 12.

Mäkelä, P., Whitaker, D. and Rovamo, J. (1992) An example of the enormous task-dependent variations in peripheral visual performance. *Association for Research in Vision and Ophthalmology* (ARVO), U.S.A. May 3 - 8.

Mäkelä, P. (1992) Task-dependent performance in peripheral vision. Internal seminar, University of Aston. November 8.

Posters

Mäkelä, P., Rovamo, J. and Whitaker, D. (1991) The effect of spatial scaling on positional acuities in foveal and peripheral vision. *ScanVision'91* -congress, Denmark. April 12 - 14.

Mäkelä, P., Rovamo, J. and Whitaker, D. (1991) Vernier line and two-dot vernier acuities in peripheral vision. *Society of Experimental Optometry* (SEO), United Kingdom. July 15 - 16.

Mäkelä, P., Whitaker, D. and Rovamo, J. (1992) Modelling of orientation discrimination at various eccentricities. *15th European Conference on Visual Perception* (ECVP), Italy. August 30 - September 3.

List of references

Abramov, I., Gordon, J. & Chan, H. (1991) Color appearance in the peripheral retina: effects of stimulus size. *Journal of the Optical Society of America A*, 8, 404-414.

Allen, D. & Hess, R. F. (1992) Is the visual field temporally homogeneous? *Vision Research*, 32, 1075-1084.

Anderson, S. J., Mullen, K. T. & Hess, R. F. (1991) Human peripheral spatial resolution for achromatic and chromatic stimuli: limits imposed by optical and retinal factors. *Journal of Physiology*, 442, 47-64.

Anderson, E. & Parkin, A. J. (1985) On the nature of the left visual field advantage for faces. *Cortex*, 21, 453-459.

Andrews, D. P. (1967) Perception of contour orientation in the central fovea., Part II: spatial integration. *Vision Research*, 7, 998-1013.

Andrews, D. P., Miller, D. T. (1978) Acuity for spatial separation as a function of stimulus size. *Vision Research*, 18, 615-619.

Andrews, D. P., Butcher, A. K. & Buckley, B. R. (1973) Acuities for spatial arrangement in line figures: human and ideal observers compared. *Vision Research*, 13, 599-620.

Andriessen, J. J. & Bouma, H. (1976) Eccentric vision: adverse interactions between line segments. *Vision Research*, 16, 71-78.

Aubert, B. (1886) Die Bewegungsempfindung. *Pflügers Archiv für die gesamte Physiologie*, 39, 347-370.

Baker, C. L. & Braddick, O. J. (1985) Eccentricity-dependent scaling of the limits for short-range apparent motion perception. *Vision Research*, 25, 803-812.

Beck, J. & Ambler, B. (1973) The effects of concentrated and distributed attention on peripheral acuity. *Perception & Psychophysics*, 14, 225-230.

Beck, J. & Halloran, T. (1985). Effects of spatial separation and retinal eccentricity on two-dot vernier acuity. *Vision Research*, 25, 1105-1111.

Bergen, J. R. & Julesz, B. (1983) Parallel versus serial processing in rapid pattern discrimination. *Nature,* 303, 696-698.

Berry, R. N. (1948) Quantitative relations among vernier, real depth, and stereoscopic depth acuities. *Journal of Experimental Psychology,* 38, 708-721.

Bouma, H. (1970) Interaction effects in parafoveal letter-recognition. *Nature,* 266, 177-178.

Bourdon, B. (1902) *La Perception Visuelle de l'Espace,* p.146. Schleicher, Paris.

Boyce, P. R. (1965) The visual perception of movement in the absence of an external frame of reference. *Optica Acta,* 12, 47-54.

Bradley, A. & Freeman, R. D. (1985) Is reduced vernier acuity in amblyopia due to position, contrast or fixation deficits? *Vision Research,* 25, 55-66.

Bradley, A. & Skottun, B. C. (1987) Effects of contrast and spatial frequency on vernier acuity. *Vision Research* 27, 1817-1824.

Bradshaw, J. L. & Wallace, G. (1971) Models of the processing and identification of faces. *Perception & Psychophysics,* 9, 443-448.

Brindley, G. S. & Lewin, W. S. (1968) The sensations produced by electrical stimulation of the visual cortex. *Journal of Physiology,* 196, 479-493.

Bullimore, M. A., Bailey, I. L. & Wacker, R. T. (1991) Face recognition in age-related maculopathy. *Investigative Ophthalmology and Visual Science,* 32, 2020-2029.

Burbeck, C. A. (1981) Criterion-free pattern and flicker thresholds. *Journal of the Optical Society of America,* 71, 1343-1350.

Burbeck, C. A. (1986) Exposure-duration effects in localization judgments. *Journal of the Optical Society of America A* , 3, 1983-1988.

Burbeck, C. A. & Regan, D. (1983) Independence of orientation and size in spatial discriminations. *Journal of the Optical Society of America,* 73, 1691-1694.

Burbeck, C. A. & Yap, Y. L. (1990a) Spatial filter selection in large-scale spatial-interval discrimination. *Vision Research* 30, 263-272.

Burbeck, C. A. & Yap, Y. L. (1990b) Two mechanisms for localization? Evidence for separation-dependent and separation-independent processing of position information. *Vision Research*, 30, 739-750.

Burbeck, C. A. & Yap, Y. L. (1990c) Spatiotemporal limitations in bisection and separation discrimination. *Vision Research*, 30, 1573-1586.

Campbell, F. W. & Gubisch, R. W. (1966) Optical quality of the human eye. *Journal of Physiology*, 186, 558-578.

Celesia, G. G. & Meredith, J. T. (1982) Visual evoked responses and retinal eccentricity. *Annals of the New York Academy of Sciences*, 388, 648-650.

Charman, W.N. (1983) The retinal image of the human eye. In *Progress in Retinal Research*, 2. Osborne, N. & Chader, G. (Eds.) Pergamon Press, Oxford. pp. 1-50.

Coletta, N. J., Williams, D. R. & Tiana, C. L. M. (1990) Consequences of spatial sampling for human motion perception. *Vision Research*, 30, 1631-1648.

Connolly, M. & Van Essen, D. (1984) The representation of the visual field in parvocellular and magnocellular layers of the lateral geniculate nucleus in the macaque monkey. *Journal of Comparative Neurology*, 226, 544-564.

Cornsweet, T. N. (1962) The staircase-method in psychophysics. *American Journal of Psychology*, 75, 485-491.

Cowey, A. & Rolls, E. T. (1974) Human cortical magnification and its relation to visual acuity. *Experimental Brain Research*, 21, 447-454.

Curcio, C. A. & Allen, K. A. (1990) Topography of ganglion cells in human retina. *Journal of Comparative Neurology*, 300, 5-25.

Curcio, C. A., Sloan, K. R., Kalina, R. E. & Hendrickson, A. E. (1990) Human photoreceptor topography. *Journal of Comparative Neurology*, 292, 497-523.

Curcio, C. A., Sloan, K. R., Packer, O., Hendrickson, A. E. and Kalina, R. E. (1987) Distribution of cones in human and monkey retina: individual variability and radial asymmetry. *Science*, 236, 579-582.

Daniel, P. M. & Whitteridge D. (1961) The representation of the visual field on the cerebral cortex in monkeys. *Journal of Physiology*, 159, 203-221.

Deeley, R. J. & Drasdo, N. (1987) The effect of optical degradation on the contrast sensitivity function measured at the fovea and in the periphery. *Vision Research*, 27, 1179-1186.

De Lange, H. (1958) Research into the dynamic nature of the human fovea -> cortex systems with intermittent and modulated light. I. Attenuation characteristics with white and colored light. *Journal of the Optical Society of America*, 48, 777-789.

de Monasterio, F. M (1978) Properties of concentrically organized X and Y ganglion cells of macaque retina. *Journal of Neurophysiology*, 41, 1394-1417.

Derrington, A. M. & Lennie, P. (1984) Spatial and temporal contrast sensitivities of neurones in lateral geniculate nucleus of macaque. *Journal of Physiology*, 357, 219-240.

De Vries, H. L. (1943) The quantum character of light and its bearing upon threshold of vision, the differential sensitivity and visual acuity of the eye. *Physica*, 10, 553-564.

DeYoe, E. A. & Van Essen, D. C. (1988) Concurrent processing streams in monkey visual cortex. *Trends in Neurosciences*, 11, 219-226.

Dixon, W. J. & Mood, A. M. (1948) A method for obtaining and analyzing sensitivity data. *Journal of the American Statistical Association*, 43, 109-126.

Dobelle, W. H., Turkel, J., Henderson, D. C. & Evans, J. R. (1979) Mapping representation of the visual field by electrical stimulation of human visual cortex. *American Journal of Ophthalmology*, 88, 727-735.

Dow, B. M., Snyder, A. Z., Vautin, R. G. & Bauer, R. (1981) Magnification factor and receptive field size in foveal striate cortex of the monkey. *Experimental Brain Research*, 44, 213-228.

Dow, B. M., Vautin, R. G. & Bauer, R. (1985) The mapping of visual space onto foveal striate cortex in the macaque monkey. *Journal of Neuroscience*, 5, 890-902.

Drasdo, N. (1977) The neural representation of visual space. *Nature*, 266, 554-556.

Drasdo, N. (1989) Receptive field densities of the ganglion cells of the human retina. *Vision Research*, 29, 985-988.

Drasdo, N. (1991) Neural substrates and threshold gradients in peripheral vision. In Kulikowski, J. J., Walsh, V. & Murray, I. J. (Eds.) *Vision and visual dysfunction*, Vol. 5, Ch. 19, pp. 250-264. London: Macmillan Press.

Elliot, P. (1964) Forced choice tables (Appendix 1). In Swets, J. A. (Ed.) *Signal Detection and Recognition by Human Observers*, pp. 679-684. New York, Wiley.

Enroth-Cugell, C. & Robson, J. G. (1966) The contrast sensitivity of retinal ganglion cells of the cat. *Journal of Physiology*, 187, 517-552.

Exner, S. (1875) Über das Sehen von Bewegungen und die Theorie des zusammengesetzen Auges. *Sitzungsberichte der Kaiserlichen Akademie der Wissenschaften*, 72, 156-190.

Fahle, M. (1986) Curvature detection in the visual field and a possible physiological correlate. *Experimental Brain Research*, 63, 113-124.

Fahle, M. (1991) Parallel perception of vernier offsets, curvature, and chevrons in humans. *Vision Research*, 31, 2149-2184.

Fendick, M. & Westheimer, G. (1983) Effects of practice and the separation of test targets on foveal and peripheral stereoacuity. *Vision Research*, 23, 145-150.

Filimonoff, I. N. (1932) Über die Variabilität der Grosshirnrindenstruktur. Mitteilung II: Regio occipitalis beim erwachsenen Menschen. *Journal für Psychologie und Neurologie*, 44, 1-96.

Findlay, J. M. (1978) Estimates on probability functions: a more virulent PEST. *Perception & Psychophysics*, 23, 181-185.

Fiorentini, A., Maffei, L. & Sandini, G. (1983) The role of high spatial frequencies in face perception. *Perception*, 12, 195-201.

Foster, D. H., Thorson, J., McIlwain, J. T. & Biederman-Thorson, M. (1981) The fine-grain movement illusion: a perceptual probe of neuronal connectivity in the human visual system. *Vision Research*, 21, 1123-1128.

Fox, P. T., Miezin, F. M., Allman, J. M., Van Essen, D. C. & Raichle, M. E. (1987) Retinotopic organization of human visual cortex mapped with positron-emission tomography. *Journal of Neuroscience*, 7, 913-922.

Gattass, R., Sousa, A. P. B. & Covey, E. (1985) Cortical visual areas of the macaque: possible substrates for pattern recognition mechanisms. *Experimental Brain Research*, Suppl. 11, 1-20.

Glass, C., Bradshaw, J. L., Hay, R. H. & Umiltà, C. (1985) Familiarity, spatial frequency, and task determinants in processing laterally presented representations of faces. *Cortex*, 21, 513-531.

Gordon, J. & Abramov, I. (1977) Color vision in the peripheral retina. II Hue and saturation. *Journal of the Optical Society of America*, 67, 202-207.

Haig, N. D. (1984) The effect of feature displacement on face recognition. *Perception*, 13, 505-512.

Hampton, D. R. & Kertesz, A. E. (1983a) The extent of Panum's area and the human cortical magnification factor. *Perception*, 12, 161-165.

Hampton, D. R. & Kertesz, A. E. (1983b) Fusional vergence response to local peripheral stimulation. *Journal of the Optical Society of America*, 73, 7-10.

Harter, M. R. (1970) Evoked cortical responses to checkerboard patterns: effect of check size as a function of retinal eccentricity. *Vision Research*, 10, 1365-1376.

Harvey, L. O. Jr & Pöppel, E. (1972) Contrast sensitivity of the human retina. *American Journal of Optometry*, 49, 748-753.

Harwerth, R. S. & Levi, D. M. (1978) Reaction time as a measure of suprathreshold grating detection. *Vision Research*, 18, 1579-1586.

Hecht, S. & Mintz, E. V. (1939) The visibility of single lines at various illuminations and the retinal basis of visual resolution. *Journal of General Physiology*, 22, 593-612.

Heeley, D.W. & Buchanan-Smith, H. M. (1990) Recognition of stimulus orientation. *Vision Research*, 30, 1429-1437.

Hellige, J. B., Corwin,W. H. & Jonsson, J. E. (1984) Effects of perceptual quality on the processing of human faces presented to the left and right cerebral hemispheres. *Journal of Experimental Psychology: Human perception and performance*, 10, 90-107.

Hering, E. (1899) Über die Grenzen der Sehschärfe. *Berichte über die mathematisch - physikalische Classe der Königliche Sächsische Gesellschaft Wissenschaften, Leipzig Naturwiss.Teil.* pp.16-24.

Hess, R. F. & Watt, R. J. (1990) Regional distribution of the mechanisms that underlie spatial localization. *Vision Research*, 30, 1021-1031.

Hirsch, J. & Hylton, R. (1982) Limits of spatial frequency discrimination as evidence of neural interpolation. *Journal of the Optical Society of America*, 72, 1367-1374.

Hirsch, J. & Hylton, R. (1985) Spatial frequency discrimination at low frequencies: evidence for position quantization by receptive fields. *Journal of the Optical Society of America A*, 2, 128-135.

Hood, D. C. & Finkelstein, M. A. (1986) Visual sensitivity. In Boff, K. R., Kaufman, L. & Thomas J. P. (Eds), *Handbook of Perception and Human Performance*, Vol.1, Ch. 5, pp.1-66. Wiley, New York.

Hubel, D. H. & Wiesel, T. N. (1962) Receptive fields, binocular interaction and functional architecture in the cat's visual cortex. *Journal of Physiology*, 160, 106-154.

Hubel, D. H. & Wiesel, T. N. (1968) Receptive fields and functional architecture of monkey striate cortex. *Journal of Physiology*, 195, 215-243.

Hubel, D. H. & Wiesel, T. N. (1972) Laminar and columnar distribution of geniculo-cortical fibers in macaque monkey. *Journal of Comparative Neurology*, 146, 421-450.

Hubel, D. H. & Wiesel, T. N. (1974) Uniformity of monkey striate cortex: a parallel relationship between field size, scatter, and magnification factor. *Journal of Comparative Neurology*, 158, 295-306.

Hubel, D. H. & Wiesel, T. N. (1977) Functional architecture of macaque monkey visual cortex. *Proceedings of the Royal Society of London, Series B*, 198, 1-59.

Hübner, M., Rentschler, I. & Encke, W. (1985) Hidden-face recognition: comparing foveal and extrafoveal performance. *Human Neurobiology*, 4, 1-7.

Jamar, J. H. T., Kwakman L. F. Tz. & Koenderink, J. J. (1984) The sensitivity of the peripheral visual system to amplitude modulation and frequency modulation of sine wave patterns. *Vision Research*, 24, 243-249.

Jennings, J. A. M. & Charman, W. N. (1978) Optical image quality in the peripheral retina. *American Journal of Optometry & Physiological Optics*, 55, 582-590.

Johnson, C.A. & Leibowitz, H.W. (1976) Velocity-time reciprocity in the perception of motion: foveal and peripheral determinations. *Vision Research*, 16, 177-180.

Johnson, C. A. & Scobey, R. P. (1980) Foveal and peripheral displacement thresholds as a function of stimulus luminance, line length and duration of movement. *Vision Research*, 20, 709-715.

Johnson, C.A. & Scobey, R.P. (1982) Effects of reference lines on displacement thresholds at various durations of movement. *Vision Research*, 22, 819-821.

Johnston, A. (1987) Spatial scaling of central and peripheral contrast sensitivity functions. *Journal of the Optical Society of America A*, 4, 1583-1593.

Johnston, A. & Wright, M. J. (1985) Lower thresholds of motion for gratings as a function of eccentricity and contrast. *Vision Research*, 25, 179-185.

Johnston, A. & Wright, M. J. (1986) Matching velocity in central and peripheral vision. *Vision Research*, 26, 1099-1109.

Kaplan, E. & Shapley, R. M. (1982) X and Y cells in the lateral geniculate nucleus of macaque monkeys. *Journal of Physiology*, 330, 125-143.

Kelly, D. H. (1959) Effects of sharp edges in a flickering field. *Journal of the Optical Society of America*, 49, 730-732.

Kelly, D. H. (1961) Visual responses to time-dependent stimuli. I. Amplitude sensitivity measurements. *Journal of the Optical Society of America*, 51, 422-429.

Kelly, D. H. (1964) Sine waves and flicker fusion. *Documenta Ophthalmologica*, 18, 16-35.

Kelly, D. H. (1969) Flickering patterns and lateral inhibition. *Journal of the Optical Society of America*, 59, 1361-1370.

Kelly, D. H. (1984) Retinal inhomogeneity. I. Spatiotemporal contrast sensitivity. *Journal of the Optical Society of America A*, 1, 107-113.

Klein, S.A. & Levi, D.M. (1985) Hyperacuity thresholds of 1 sec: theoretical predictions and empirical validation. *Journal of the Optical Society of America A*, 2, 1170-1190.

Klein, S. A. & Levi, D. M. (1987) Position sense of the peripheral retina. *Journal of the Optical Society of America A*, 4, 1543-1553.

Koenderink, J.J., Bouman, M. A., Bueno de Mesquita, A. E. & Slappendel, S. (1978a) Perimetry of contrast detection thresholds of moving spatial sine wave patterns. I. The near peripheral visual field (eccentricity 0°-8°). *Journal of the Optical Society of America*, 68, 845-849.

Koenderink, J.J., Bouman, M. A., Bueno de Mesquita, A. E. & Slappendel, S. (1978b) Perimetry of contrast detection thresholds of moving spatial sine wave patterns. II. The far peripheral visual field (eccentricity 0°-50°). *Journal of the Optical Society of America*, 68, 850-854.

Koenderink, J.J., Bouman, M. A., Bueno de Mesquita, A. E. & Slappendel, S. (1978c) Perimetry of contrast detection thresholds of moving spatial sine wave patterns. III. The target extent as a sensitivity controlling parameter. *Journal of the Optical Society of America*, 68, 854-860.

Koenderink, J.J., Bouman, M. A., Bueno de Mesquita, A. E. & Slappendel, S. (1978d) Perimetry of contrast detection thresholds of moving spatial sine wave patterns. IV. The influence of the mean retinal illuminance. *Journal of the Optical Society of America*, 68, 860-865.

Kolers, P. A., Duchnicky, R. L. & Sundstroem, G. (1985) Size in the visual processing of faces and words. *Journal of Experimental Psychology*, 11, 726-751.

Kröse, B. J. A. & Julesz, B. (1989) The control and speed of shifts of attention. *Vision Research*, 29, 1607-1619.

Kulikowski, J. J. & Tolhurst, D. J. (1973) Psychophysical evidence for sustained and transient detectors in human vision. *Journal of Physiology*, 232, 149-162.

Legge, G.E. & Campbell, F.W. (1981) Displacement detection in human vision. *Vision Research*, 21, 205-213.

Legge, G.E., Kersten, D. & Burgess, A. E. (1987) Contrast discrimination in noise. *Journal of the Optical Society of America A*, 4, 391-404.

Le Grand, Y. (1967) *Form and space vision*, pp.127-145. Indiana University Press, Bloomington.

Leibowitz, H. W. (1955) Effect of reference lines on the discrimination of movement. *Journal of the Optical Society of America*, 45, 829-830.

Leibowitz, H. W., Johnson, C. A. & Isabelle, E. (1972) Peripheral motion detection and refractive error. *Science*, 177, 1207-1208.

Levi, D. M. & Klein, S. A. (1989) Both separation and eccentricity can limit precise position judgements: a reply to Morgan and Watt. *Vision Research*, 29, 1463-1469.

Levi, D. M. & Klein, S. A. (1990a) The role of separation and eccentricity in encoding position. *Vision Research*, 30, 557-585.

Levi, D. M. & Klein, S. A. (1990b) Equivalent intrinsic blur in spatial vision. *Vision Research*, 30, 1971-1993.

Levi, D. M. & Westheimer, G. (1987) Spatial-interval discrimination in the human fovea: what delimits the interval? *Journal of the Optical Society of America A*, 4, 1304-1313.

Levi, D. M., Klein, S. A. & Aitsebaomo, A. P. (1984) Detection and discrimination of the direction of motion in central and peripheral vision of normal and amblyopic observers. *Vision Research*, 24, 789-800.

Levi, D. M., Klein, S. A. & Aitsebaomo, A. P. (1985) Vernier acuity, crowding and cortical magnification. *Vision Research*, 25, 963-977.

Levi, D. M. & Klein, S. A., Yap, Y. L. (1988) "Weber's law" for position: unconfounding the role of separation and eccentricity. *Vision Research*, 28, 597-603.

Lie, I. (1980) Visual detection and resolution as a function of retinal locus. *Vision Research*, 20, 967-974.

Lillywhite, P. G. (1981) Multiplicative intrinsic noise and the limits to visual performance. *Vision Research*, 21, 291-296.

Livingstone, M. S. & Hubel, D. H. (1988a) Do the relative mapping densities of the magno- and parvocellular systems vary with eccentricity? *Journal of Neuroscience*, 8, 4334-4339.

Livingstone, M. S. & Hubel, D. H. (1988b) Segregation of form, color, movement, and depth: anatomy, physiology, and perception. *Science*, 240, 740-749.

Ludvigh, E. (1953) Direction sense of the eye. *American Journal of Ophthalmology*, 36, 139-143.

Mandelbaum, J. & Sloan, L. L. (1947) Peripheral visual acuity with special reference to scotopic illumination. *American Journal of Ophthalmology*, 30, 581-588.

McKee, S.P. & Nakayama, K. (1984) The detection of motion in the peripheral visual field. *Vision Research*, 24, 25-32.

McKee, S. P., Welch, L., Taylor, D. G. & Bowne, S. F. (1990) Finding the common bond: stereoacuity and the other hyperacuities. *Vision Research*, 30, 879-891.

McKee, S. P. & Westheimer, G. (1978) Improvement in vernier acuity with practice. *Perception & Psychophysics*, 24, 258-262.

Meredith, J. T. & Celesia, G. G. (1982) Pattern-reversal visual evoked potentials and retinal eccentricity. *Electroencephalography and Clinical Neurophysiology*, 53, 243-253.

Millodot, M. (1966) Foveal and extra-foveal acuity with and without stabilized retinal images. *British Journal of Physiological Optics*, 23, 75-106.

Millodot, M. (1990) *Dictionary of Optometry*, 2nd Ed., London, Butterworths.

Millodot, M., Johnson, C. A., Lamont, A. & Leibowitz, H. W. (1975) Effect of dioptrics on peripheral visual acuity. *Vision Research*, 15, 1357-1362.

Moreland, J. D. & Cruz, A. (1959) Colour perception with the peripheral retina. *Optica Acta,* 6, 117-151.

Morgan, M. J. (1986) The detection of spatial discontinuities: interactions between contrast and spatial contiguity. *Spatial Vision,* 1, 291-303.

Morgan, M. J. & Aiba, T. S. (1985) Vernier acuity predicted from the changes in the light distribution of the retinal image. *Spatial Vision,* 1, 151-161.

Morgan, M.J. & Regan, D. (1987) Opponent model for line interval discrimination: interval and vernier performance compared. *Vision Research,* 27, 107-118.

Morgan, M.J. & Watt, R.J. (1989) The Weber relation for position is not an artefact of eccentricity. *Vision Research,* 29, 1457-1462.

Noorlander, C., Koenderink, J. J., Den Ouden, R. J. & Edens, B. W. (1983) Sensitivity to spatiotemporal colour contrast in the peripheral visual field. *Vision Research,* 23, 1-11.

Nothdurft, H. C. (1985) Orientation sensitivity and texture segmentation in patterns with different line orientation. *Vision Research,* 25, 551-560.

Østerberg, G. (1935) Topography of the layer of rods and cones in the human retina. *Acta Ophthalmologica* (Suppl.), 6, 1-102.

Owsley, C., Sekuler, R. & Boldt, C. (1981) Aging and low contrast vision: face perception. *Investigative Ophthalmology and Visual Science,* 21, 362-364.

Owsley, C. & Sloane, M. E. (1987) Contrast sensitivity, acuity, and the perception of "real-world" targets. *British Journal of Ophthalmology,* 17, 791-796.

Paradiso, M. A. & Carney, T. (1988) Orientation discrimination as a function of stimulus eccentricity and size: nasal/temporal retinal asymmetry. *Vision Research,* 28, 867-874.

Peli, E., Goldstein, R. B., Trempe, C. L & Arend, L. E. (1989) Image enhancement improves face recognition. In *Noninvasive Assessment of the Visual System, 1989 Technical Digest Series,* 7, 64-67.

Pelli, D. G. & Zhang, L. (1991) Accurate control of contrast on microcomputer displays. *Vision Research,* 31, 1337-1350.

Pelli, D. G. (1990) The quantum efficiency of vision. In Blakemore, C. (Ed) *Vision : Coding and efficiency*. Cambridge: Cambridge University Press.

Pentland, A. (1980) Maximum likelihood estimation: the best PEST. *Perception & Psychophysics,* 28, 377-379.

Perry, V. H. & Cowey, A. (1984) Retinal ganglion cells that project to the superior colliculus and pretectum in the macaque monkey. *Neuroscience,* 12, 1125-1137.

Perry, V. H. & Cowey, A. (1985) The ganglion cell and cone distributions in the monkey's retina: implications for central magnification factors. *Vision Research,* 25, 1795-1810.

Perry, V. H. & Cowey, A. (1988) The lengths of the fibres of Henle in the retina of macaque monkeys: implications for vision. *Neuroscience,* 25, 225-236.

Perry, V. H, Oehler, R. & Cowey, A. (1984) Retinal ganglion cells that project to the dorsal lateral geniculate nucleus in the macaque monkey. *Neuroscience,* 12, 1101-1123.

Perry, V. H. & Silveira, L. C. L. (1988) Functional lamination in the ganglion cell layer of the macaque's retina. *Neuroscience,* 25, 217-223.

Piper, H. (1903) Über die Abhängigkeite des Reizwertes leuchten der Objekte von ihrer Flächenbezw. Winkelgrösse. *Zeitschrift für Psychologie und Physiologie der Sinnesorgane,* 32, 92-112.

Polyak, S. L. (1932) *Localization of Function in the Cerebral Cortex*, Vol.13, Association for Research into Nervous and Mental Disorders. Williams & Wilkins company, Baltimore.

Polyak, S. L. (1941) *The retina.* University of Chicago Press, Chicago.

Polyak, S. L. (1957) *The vertebrate visual system.* University of Chicago Press, Chicago.

Post, R. B. & Leibowitz, H. W. (1981) The effect of refractive error on central and peripheral motion sensitivity at various exposure durations. *Perception & Psychophysics,* 29, 91-94.

Post, R.B., Scobey, R.P. & Johnson, C.A. (1984) Effects of retinal eccentricity on displacement thresholds for unidirectional and oscillatory stimuli. *Vision Research,* 24, 835-839.

Purkinje, J. E. (1825) *Neue Beiträge zur Kenntnis des Sehens*, Reimer, Berlin.

Raninen, A. N., Lukkarinen, T. S. & Rovamo, J. M. (1993) Modelling flicker sensitivity with and without noise. *Investigative Ophthalmology and Visual Science,* 34/4, p.780.

Raninen, A. & Rovamo, J. (1987) Retinal ganglion-cell density and receptive-field size as determinants of photopic flicker sensitivity across the human visual field. *Journal of the Optical Society of America*, 4, 1620-1626.

Ransom-Hogg, A. & Spillmann, L. (1980) Perceptive field size in fovea and periphery of the light and dark adapted retina. *Vision Research,* 20, 221-228.

Regan, D. (1989) Orientation discrimination for objects defined by relative motion and objects defined by luminance contrast. *Vision Research,* 29, 1389-1400.

Rentschler, I. & Treutwein, B. (1985) Loss of spatial phase relationship in extrafoveal vision. *Nature,* 313, 308-310.

Richards, W. (1971) The fortification illusions of migraines. *Scientific American,* 224, 88-96.

Richmond, B. J., Wurtz, R. H. & Sato, T. (1983) Visual responses of inferior temporal neurons in awake rhesus monkey. *Journal of Neurophysiology,* 50, 1415-1432.

Rolls, E. T. & Cowey, A. (1970) Topography of the retina and striate cortex and its relationship to visual acuity in rhesus monkeys and squirrel monkeys. *Experimental Brain Research,* 10, 298-310.

Rose, R. (1942) The relative sensitivities of television pickup tubes, photographic film, and the human eye. *Proceedings of the Institute of Radio Engineers (I.R.E),* 30, 293-300.

Roufs, J. A. J. (1974) Dynamic properties of vision. -V. Perception lag and reaction time in relation to flicker and flash thresholds, 853-869.

Rovamo, J., Kukkonen, H., Tiippana, K. & Näsänen, R. (1993) Effects of luminance and exposure time on contrast sensitivity in spatial noise. *Vision Research,* 33, 1123-1129.

Rovamo, J., Luntinen, O. & Näsänen, R. (1993) Modelling the dependence of contrast sensitivity on grating area and spatial frequency. *Vision Research,* 33, 2773-2788.

Rovamo, J. & Raninen, A. (1984) Critical flicker frequency and M-scaling of stimulus size and retinal illuminance. *Vision Research*, 24, 1127-1131.

Rovamo, J. & Raninen, A. (1990) Cortical acuity and the luminous flux collected by retinal ganglion cells at various eccentricities in human rod and cone vision.*Vision Research*, 30, 11-21.

Rovamo, J. & Virsu, V. (1979) An estimation and application of the human cortical magnification factor. *Experimental Brain Research*, 37, 495-510.

Rovamo, J. & Virsu, V., Laurinen, P. & Hyvärinen, L. (1982) Resolution of gratings oriented along and across meridians in peripheral vision. *Investigative Ophthalmology and Visual Science*, 23, 666-670.

Rovamo, J., Virsu, V. & Näsänen, R. (1978) Cortical magnification factor predicts the photopic contrast sensitivity of peripheral vision. *Nature*, 271, 54-56.

Rubin, G. S. & Schuchard, R. A. (1989) Does contrast sensitivity predict face recognition performance in low vision observers? In *Noninvasive Assessment of the Visual System, 1989, Technical Digest Series*, 3, 130-133.

Saarinen, J. (1988) Detection of mirror symmetry in random dot patterns at different eccentricities. *Vision Research*, 28, 755-759.

Saarinen, J. (1993a) Shifts of visual attention at fixation and away from fixation. *Vision Research*, 33, 1113-1117.

Saarinen, J. (1993b) Focal visual attention and pattern discrimination. *Perception*, 22, 509-515.

Saarinen, J., Rovamo, J. & Virsu, V. (1987) Texture discrimination at different eccentricities. *Journal of the Optical Society of America A*, 4, 1699-1703.

Saarinen, J., Rovamo, J. & Virsu, V. (1989) Analysis of spatial structure in eccentric vision. *Investigative Ophthalmology & Visual Science*, 30, 293-296.

Schein, S. J. (1988) Anatomy of macaque fovea and spatial densities of neurons in foveal representation. *Journal of Comparative Neurology*, 269, 479-505.

Schein, S. J. & de Monasterio, F. M. (1987) Mapping of retinal and geniculate neurons onto striate cortex of macaque. *Journal of Neuroscience*, 7, 996-1009.

Scobey, R. P. (1982) Human visual orientation discrimination. *Journal of Neurophysiology*, 48, 18-26.

Shapley, R. & Perry, V.H. (1986) Cat and monkey retinal ganglion cells and their visual functional roles. *Trends in Neurosciences*, 229-235.

Skottun, B. C., Bradley, A. & Freeman, R. D. (1986) Orientation discrimination in amblyopia. *Investigative Ophthalmology and Visual Science,* 27, 532-537.

Snyder A. W. (1982) Hyperacuity and interpolation by the visual pathways. *Vision Research*, 22, 1219-1220.

Spinelli, D., Bazzeo, A. & Vicario, G. B. (1984) Orientation sensitivity in the peripheral visual field. *Perception*, 13, 41-47.

Stensaas, S. S., Eddington, D. K. & Dobelle, W. H. (1974) The topography and variability of the primary visual cortex in man. *Journal of Neurosurgery*, 40, 747-755.

Stephenson, C. M. E. & Braddick, O. J. (1983) Discrimination of relative spatial phase in fovea and periphery. *Investigative Ophthalmology and Visual Science*, Suppl. 24, 146.

Stephenson, C. M. E., Knapp, A. J. & Braddick, O. J. (1991) Discrimination of spatial phase shows a qualitative difference between foveal and peripheral processing. *Vision Research*, 31, 1315-1326.

Stigmar, G. (1971) Blurred visual stimuli. *Acta Ophthalmologica,* 49, 364-379.

Sullivan, G. D., Oatley, K. & Sutherland, N. S. (1972) Vernier acuity as affected by target length and separation. *Perception & Psychophysics*, 12, 438-444.

Swanson, W. H. & Wilson, H. R. (1985) Eccentricity dependence of contrast matching and oblique masking. *Vision Research*, 25, 1285-1295.

Talbot, S. A. & Marshall, W. H. (1941) Physiological studies on neural mechanisms of visual localization and discrimination. *American Journal of Ophthalmology,* 24, 1255-1264.

Taylor, M. M. & Creelman, C. D. (1967) PEST; efficient estimates on probability functions. *Journal of the Acoustical Society of America,* 41, 782-787.

Toet, A. & Levi, D. M. (1992) The two-dimensional shape of spatial interaction zones in the parafovea. *Vision Research,* 32, 1349-1357.

Toet, A., Snippe, H. P. & Koenderink, J. J. (1988a) Local spatial scale for three-dot alignment acuity. *Biological Cybernetics*, 59, 319-323.

Toet, A., Snippe, H. P. & Koenderink, J. J. (1988b) Effects of blur and eccentricity on differential spatial displacement discrimination. *Vision Research,* 28, 535-553.

Tolhurst, D. J. & Ling L. (1988) Magnification factors and the organization of the human striate cortex. *Human Neurobiology,* 6, 247-254.

Tootell, R. B., Switkes, E., Silverman, M. S. & Hamilton, S. L. (1988) Functional anatomy of macaque striate cortex. II. Retinotopic organization. *Journal of Neuroscience,* 8, 1531-1568.

Tootell, R. B., Silverman, M. S., Switkes, E. & De Valois, R. L. (1982) Deoxyglucose analysis of retinotopic organization in primate striate cortex. *Science,* 218, 902-904.

Treisman, A. M. & Gelade, G. (1980) A feature-integration theory of attention. *Cognitive Psychology*, 12, 97-136.

Tsal, Y. (1983) Movements of attention across the visual field. *Journal of Experimental Psychology and Human Performance*, 9, 523-530.

Tulunay-Keesey, U. (1970) Variables determining flicker sensitivity in small fields. *Journal of the Optical Society of America*, 60, 390-398.

Tulunay-Keesey, U. (1972) Flicker and pattern recognition: a comparison of thresholds. *Journal of the Optical Society of America*, 62, 446-448.

Tyler, C. W. (1981) Specific deficits of flicker sensitivity in glaucoma and ocular hypertension. *Investigative Ophthalmology and Visual Science*, 20, 204-212.

Tyler, C. W. (1985) Analysis of visual modulation sensitivity. II. Peripheral retina and the role of photoreceptor dimensions. *Journal of the Optical Society of America*, 2, 393-398.

Tyler, C. W. (1987) Analysis of visual modulation sensitivity. III. Meridional variations in peripheral flicker sensitivity. *Journal of the Optical Society of America*, 4, 1612-1619.

Tyler, C.W. & Silverman, G. (1983) Mechanisms of flicker sensitivity in peripheral retina. *Investigative Ophthalmology and Visual Science*, Suppl.24, p.145.

Tyler, C.W. & Torres, J. (1972) Frequency response characteristics for sinusoidal movement in the fovea and periphery. *Perception & Psychophysics*, 12, 232-236.

van de Grind, W. A., van Doorn, A. J. & Koenderink, J. J. (1983) Detection of coherent movement in peripherally viewed random-dot patterns. *Journal of the Optical Society of America*, 73, 1674-1683.

Vandenbussche, E., Vogels, R. & Orban, G. A. (1986) Human orientation discrimination: changes with eccentricity in normal and amblyopic vision. *Investigative Ophthalmology and Visual Science*, 17, 237-245.

van Esch, J. A., Koldenhof, E. E., Doorn, A. J. & Koenderink, J. J. (1984) Spectral sensitivity and wavelength discrimination of the human peripheral visual field. *Journal of the Optical Society of America*, 1, 443-450.

Van Essen, D. C. & Anderson, C. H. (1990) Information processing strategies and pathways in the primate retina and visual cortex. In *An Introduction to Neural and Electronic Networks*, Zornetzer, S. F., Davis, J. L., Lau, C. (Eds), pp.43-72. Academic Press, Orlando.

Van Essen, D. C., Newsome, W. T. & Maunsell, J. H. R. (1984) The visual field representation in striate cortex of the macaque monkey: asymmetries, anisotropies and individual variability. *Vision Research*, 24, 429-448.

Virsu, V., Näsänen, R. & Osmoviita, K. (1987) Cortical magnification and peripheral vision. *Journal of the Optical Society of America A*, 4, 1568-1578.

Virsu, V. & Rovamo, J. (1979) Visual resolution, contrast sensitivity and the cortical magnification factor. *Experimental Brain Research*, 37, 475-494.

Virsu, V., Rovamo, J., Laurinen, P. & Näsänen, R. (1982) Temporal contrast sensitivity and cortical magnification. *Vision Research*, 22, 1211-1217.

von Graefe, A. (1856) Über die Untersuchung des Gesichtsfeldes bei amblyopishchen Affectionen. *Graefes Archiv für Ophthalmologie,* 2, 258-298.

Ward, R. M., Casco, C. & Watt, R. J. (1985) The location of noisy visual stimuli. *Canadian Journal of Psychology,* 39, 387-399.

Wässle, H., Grünert, U., Röhrenbeck, J. & Boycott, B. B. (1989) Cortical magnification factor and the ganglion cell density of the primate retina. *Nature,* 341, 643-646.

Wässle, H., Grünert, U., Röhrenbeck, J. & Boycott, B. B. (1990) Retinal ganglion cell density and cortical magnification factor in the primate. *Vision Research,* 30, 1897-1911.

Watson, A. B. (1987) Estimation of local spatial scale. *Journal of the Optical Society of America A,* 4, 1579-1582.

Watt, R. J. (1984) Towards a general theory of the visual acuities for shape and spatial arrangement. *Vision Research,* 24, 1377-1386.

Watt, R. J. (1987) Scanning from coarse to fine spatial scales in the human visual system after the onset of a stimulus. *Journal of the Optical Society of America A,* 4, 2006-2021.

Watt, R. J. & Andrews, D. P. (1982) Contour curvature analysis: hyperacuities in the discrimination of detailed shape. *Vision Research,* 22, 449-460.

Watt, R. J. & Morgan, M. J. (1983) The recognition and representation of edge blur: evidence for spatial primitives in human vision. *Vision Research,* 23, 1465-1477.

Waugh, S. J. & Levi, D. M. (1993) Visibility, timing and vernier acuity. *Vision Research,* 33, 505-526.

Weber, E. H. (1834) D3 Pulsu, Resorpitione, Auditu et Tactu: *Annotationes Anatomicae at Physiologicae.* Leipzig, Koelor.

Wertheim, Th. (1891; translated by Dunsky, I.L., 1980) Peripheral visual acuity. *American Journal of Optometry and Physiological Optics,* 57, 915-924.

Westheimer, G. (1965) Spatial interaction in the human retina during scotopic vision. *Journal of Physiology,* 181, 881-894.

Westheimer, G. (1967) Spatial interaction in human cone vision. *Journal of Physiology*, 190, 139-154.

Westheimer, G. (1975) Visual acuity and hyperacuity. *Investigative Ophthalmology and Visual Science*, 14, 570-572.

Westheimer, G. (1979) The spatial sense of the eye. *Investigative Ophthalmology and Visual Science*, 18, 893-912.

Westheimer, G. (1981) Visual hyperacuity. In *Progress in Sensory Physiology*, Vol.1, pp. 1-30. New York, Springer.

Westheimer, G. (1982) The spatial grain of the perifoveal visual field. *Vision Research*, 22, 157-162.

Westheimer, G. (1983) Temporal order detection for foveal and peripheral visual stimuli. *Vision Research*, 23, 759-763.

Westheimer, G. & Hauske, G. (1975) Temporal and spatial interference with vernier acuity. *Vision Research*, 15, 1137-1141.

Westheimer, G. & McKee, S. P. (1977a) Integration regions for visual hyperacuity. *Vision Research*, 17, 89-93.

Westheimer, G. & McKee, S. P. (1977b) Spatial configurations for visual hyperacuity. *Vision Research*, 17, 941-947.

Westheimer, G. & McKee, S. P. (1979) What prior uniocular processing is necessary for stereopsis? *Investigative Ophthalmology and Visual Science*, 18, 614-621.

Westheimer, G., Shimamura, K. & McKee, S. P. (1976) Interference with line-orientation sensitivity. *Journal of the Optical Society of America*, 66, 332-338.

Wetherill, G. B. & Levitt, H. (1965) Sequential estimation of points on a psychometric functon. *British Journal of Mathematical and Statistical Psychology*, 18, 1-10.

Weymouth, F.W. (1958) Visual sensory units and the minimal angle of resolution. *American Journal of Ophthalmology*, 46, 102-112.

Whitaker, D. & MacVeigh, D. (1990) Displacement thresholds for various types of movement: effect of spatial and temporal reference proximity. *Vision Research*, 30, 1499-1506.

Whitaker, D. & MacVeigh, D. (1991) Interaction of spatial frequency and separation in vernier acuity. *Vision Research*, 31, 1205-1212.

Whitaker, D., Latham, K., Mäkelä, P. & Rovamo, J. (1993) Detection and discrimination of curvature in foveal and peripheral vision. *Vision Research*, 33, 2215-2224.

Whitaker, D. & Walker, H. (1988) Centroid evaluation in the vernier alignment of random dot clusters. *Vision Research*, 28, 777-784.

Williams, D. R. (1986) Seeing through the photoreceptor mosaic. *Trends in Neurosciences*, 9, 193-198.

Williams, R. A., Enoch, J. M. & Essock, E. A. (1984) The resistance of selected hyperacuity configurations to retinal image degradation. *Investigative Ophthalmology and Visual Science*, 25, 389-399.

Wilson, H. R. (1986) Responses of spatial mechanisms can explain hyperacuity. *Vision Research*, 26, 453-469.

Wilson, H. R. (1991) Model of peripheral and amblyopic hyperacuity. *Vision Research*, 31, 967-982.

Wilson , M. E. (1970) Invariant features of spatial summation with changing locus in the visual field. *Journal of Physiology*, 207, 611-622.

Wooten, B. R. & Wald, G. (1973) Color vision mechanisms in the peripheral retinas of normal and dichromatic observers. *Journal of General Physiology*, 61, 125-145.

Wright M. J. (1987) Spatiotemporal properties of grating motion detection in the center and the periphery of the visual field. *Journal of the Optical Society of America A*, 4, 1627-1633.

Wright, M. J. & Johnston, A. (1985a) The relationship of displacement thresholds for oscillating gratings to cortical magnification, spatiotemporal frequency and contrast. *Vision Research*, 25, 187-193.

Wright, M. J. & Johnston, A. (1985b) Invariant tuning of motion aftereffect. *Vision Research*, 25, 1947-1955.

Yap, L. Y., Levi, D. M. & Klein, S. A. (1987a) Peripheral hyperacuity: 3-dot bisection scales to a single factor from 0 to 10 degrees. *Journal of the Optical Society of America A*, 4, 1554-1561.

Yap, Y. L., Levi, D. M. & Klein, S. A. (1987b) Peripheral hyperacuity: isoeccentric bisection is better than radial bisection. *Journal of the Optical Society of America A*, 4, 1562-1567.

Yap, Y. L., Levi, D. M. & Klein, S. A. (1989) Peripheral positional acuity: retinal and cortical constraints on 2-dot separation discrimination under photopic and scotopic conditions. *Vision Research*, 29, 789-802.

Zeki, S. M. & Shipp, S. (1988) The functional logic of cortical connections. *Nature*, 335, 311-317.